



**Monitoring Food Quality using  
Sensor Technology from  
“Harvest to Home”**

**By**

**June Frisby B.Sc.**

**Thesis submitted for the degree of Doctor of Philosophy**

**Supervisor: Prof. Dermot Diamond**

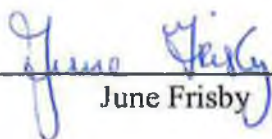
**Dublin City University**

**July 2005**

**Declaration:**

I hereby certify that this material, which I now submit for assessment on the programme of study leading to the award of Doctor of Philosophy is entirely my own work and has not been taken from the work of others save and to the extent that such work has been cited and acknowledged within the text of my work.

**Signed:**

  
\_\_\_\_\_  
June Frisby

**I.D. Number: 51187795**

**Date:**

16<sup>th</sup> September 2005

## List of Publications and Presentations

### Posters Presentations

#### **ADLEC 2001 (Analog Devices Limerick Engineering Conference)**

Analog Devices, Limerick, Ireland, 14<sup>th</sup> November 2001

*Title: Autonomous Temperature Sensing*

#### **WEFTA 2002 (Western European Fishing Technologists Association)**

Galway, Ireland, May 2002

*Title: Autonomous Temperature Sensing*

### Oral Presentations

#### **WEFTA 2002 (Western European Fishing Technologists Association)**

Galway, Ireland, 13<sup>th</sup>-15<sup>th</sup> May 2002

*Title: Autonomous Temperature Sensing*

#### **32<sup>nd</sup> Annual Food Science and Technology Research Conference 2002**

University College Cork, Ireland, 12<sup>th</sup>-13<sup>th</sup> September 2002

*Title: Wireless pH/Temperature Sensing of Pig Carcasses*

#### **Recent Advances in Irish Pig Meat Quality**

University College Cork, Ireland 30<sup>th</sup> January 2003

*Title: Autonomous pH and Temperature Sensing of Pig Carcasses*

#### **Dublin City University School of Chemical Sciences Research Day**

Dublin, Ireland, 26<sup>th</sup> March 2003

*Title: On-line Meat Quality Monitoring*

#### **National Centre for Sensor Research Sensor Short Series**

NCSR, Dublin, Ireland, 23<sup>rd</sup> May 2003

*Title: Applications of Wireless Sensing in the Food Industry*

**TAFT 2003 (Trans Atlantic Fisheries Technology Conference)**

Reykjavik, Iceland, 10<sup>th</sup>-14<sup>th</sup> June 2003

*Title: Development of Temperature Logging Technology for the Fishing Industry*

Papers

**‘Development of an autonomous, wireless pH and temperature sensing system for monitoring pig meat quality’**, June Frisby, Declan Raftery, Joseph P. Kerry and Dermot Diamond. *Meat Science*, 70, 329 (2005).

**‘Web-based real-time temperature monitoring of shellfish catches using a wireless sensor network Crowley’**, Karl Crowley, June Frisby, Seamus Murphy, Mark Roantree and Dermot Diamond, *Sensors and Actuators* (In press).

## Acknowledgements

I would like to take this opportunity to thank Prof. Dermot Diamond, an excellent mentor and a true friend, for his outstanding generosity and support over the past four years.

I would also like to extend my gratitude to Dr. Gillian M<sup>c</sup>Mahon and Dr. Sonia Ramirez-Garcia for their continued guidance and friendship during my post-graduate studies.

For the members of Dermot's research group past and present, thank you for all your kindness. My time at DCU has been a wonderful experience and is full of memories I will always cherish.

I would like to thank the members of the NCSR and the technicians in the School of Chemical Sciences for their support during my PhD studies.

I would also like to express my appreciation for the expertise and financial contribution from our partners, industrial collaborators and funding bodies.

To my close friends, all of you have helped me in your own special way when I needed it the most. Thank you...

To Mam and Dad, George, Irene, Abi, Andrew, Paul and Lisa, thank you for all your love and support through the years.

Finally, to Eddy, I cannot express my thanks and appreciation through words alone so to you I dedicated this thesis.

## Table of Contents

<b>Title Page</b>	<b>I</b>
<b>Declaration</b>	<b>II</b>
<b>List of Publications</b>	<b>III</b>
<b>Acknowledgements</b>	<b>V</b>
<b>Table of Contents</b>	<b>VII</b>
<b>Abstract</b>	<b>XII</b>
<b>Abbreviations</b>	<b>XIII</b>

### CHAPTER 1

<b>1</b>	<b>THEORY AND BACKGROUND .....</b>	<b>1</b>
1.1	PROJECT 1: DEVELOPMENT OF AN AUTONOMOUS, WIRELESS PH AND TEMPERATURE SENSING SYSTEM FOR MONITORING PIG MEAT QUALITY	2
1.1.1	<i>Introduction.....</i>	2
1.1.2	<i>Background Project Information.....</i>	3
1.1.3	<i>Post-mortem Changes in Muscle Tissue.....</i>	4
1.1.4	<i>Preventing PSE .....</i>	5
1.1.5	<i>Temperature Measurements of Pig Carcasses .....</i>	7
1.1.6	<i>pH Measurements.....</i>	9
1.1.7	<i>Legislation for Temperature Monitoring in the Food Industry .....</i>	19
1.1.8	<i>Autonomous (Wireless) Sensing .....</i>	19
1.1.9	<i>Wireless pH and Temperature Monitoring of Pig Carcasses.....</i>	21
1.2	PROJECT 2: DEVELOPMENT OF A WEB-BASED WIRELESS TEMPERATURE SENSING SYSTEM FOR THE FISHING INDUSTRY .....	22
1.2.1	<i>Introduction.....</i>	22
1.2.2	<i>Temperature Monitoring Devices.....</i>	23
1.2.3	<i>Shelf life Prediction.....</i>	28
1.2.4	<i>Traceability .....</i>	28
1.3	PROJECT 3: DEVELOPMENT OF AN ON-PACKAGE SENSOR FOR DETECTING SHELLFISH SPOILAGE.....	30
1.3.1	<i>Introduction.....</i>	31
1.3.2	<i>Methods to Evaluate the Freshness and Quality of Fish.....</i>	31
1.3.3	<i>pH Indicators and Optical Sensors .....</i>	37
1.3.4	<i>Spectroscopy – Properties of Electromagnetic Radiation.....</i>	38
1.3.5	<i>Absorbance.....</i>	40
1.3.6	<i>Beer-Lambert Law.....</i>	41
1.3.7	<i>Chromophores.....</i>	42
1.3.8	<i>Optically Responsive Polymer Films.....</i>	44

## CHAPTER 2

### 2 DEVELOPMENT OF AN AUTONOMOUS, WIRELESS PH AND TEMPERATURE SENSING SYSTEM FOR MONITORING PIG MEAT QUALITY..... 49

2.1	INTRODUCTION .....	50
2.1.1	<i>RF Temperature Monitoring System .....</i>	<i>50</i>
2.1.2	<i>pH and Temperature Correlation.....</i>	<i>54</i>
2.1.3	<i>Wireless pH/Temperature Monitoring System.....</i>	<i>55</i>
2.2	EXPERIMENTAL.....	57
2.2.1	<i>Measuring the Sensor Response Time of the RF Temperature Monitoring System.....</i>	<i>57</i>
2.2.2	<i>Monitoring the Chilling Rates of Pig Carcasses .....</i>	<i>58</i>
2.2.3	<i>Calibration of the Wireless pH/Temperature Monitoring system .....</i>	<i>59</i>
2.2.4	<i>Measuring the Temperature Response Time of the Wireless pH/Temperature Monitoring System.....</i>	<i>60</i>
2.2.5	<i>RF Loggers and Base Station Set-up.....</i>	<i>60</i>
2.3	RESULTS AND DISCUSSION .....	62
2.3.1	<i>Measuring the Sensor Response Time of the RF Temperature Monitoring System.....</i>	<i>62</i>
2.3.2	<i>Monitoring the Chilling Rates of Pig Carcasses .....</i>	<i>63</i>
2.3.3	<i>Measuring the Temperature Response Time of the Wireless pH/Temperature Monitoring System.....</i>	<i>66</i>
2.3.4	<i>Calibration of the Wireless pH/Temperature Monitoring System .....</i>	<i>67</i>
2.3.5	<i>Repeat Calibration Studies.....</i>	<i>71</i>
2.3.6	<i>pH and Temperature Monitoring of Pig Carcasses .....</i>	<i>74</i>
2.4	CONCLUSION.....	80

## CHAPTER 3

### 3 DEVELOPMENT OF A WEB-BASED WIRELESS TEMPERATURE SENSING SYSTEM FOR THE FISHING INDUSTRY..... 84

3.1	INTRODUCTION .....	85
3.2	PRELIMINARY TEMPERATURE MONITORING FIELD TRIALS USING THE RF TEMPERATURE LOGGING SYSTEM .....	85
3.3	RF-GSM TEMPERATURE MONITORING FIELD TRIALS .....	86
3.3.1	<i>RF-GSM Temperature Monitoring System.....</i>	<i>86</i>
3.4	RF-GSM TEMPERATURE MONITORING HARDWARE SPECIFICATION .....	89
3.4.1	<i>Logger Description and Operating Method.....</i>	<i>89</i>

3.4.2	<i>Base Station Description and Operating Method</i> .....	90
3.5	EXPERIMENTAL.....	91
3.5.1	<i>Preliminary Temperature Monitoring Field Trials using the RF Temperature Logging System</i> .....	91
3.5.2	<i>Sensor Response Time of the RF-GSM Temperature Monitoring System</i> .....	92
3.5.3	<i>Temperature Monitoring Field Trials using the RF-GSM Temperature Monitoring System</i> .....	92
3.5.4	<i>RF-GSM Temperature Monitoring System Set-up on-board the Fishing Vessel</i> .....	94
3.6	RESULTS AND DISCUSSION.....	96
3.6.1	<i>Preliminary Temperature Monitoring Field Trials using the RF Temperature Logging System</i> .....	96
3.6.2	<i>Sensor Response Time of the RF-GSM Temperature Monitoring System</i> .....	98
3.6.3	<i>Temperature Monitoring Field Trials using the RF-GSM Temperature Monitoring System</i> .....	99
3.7	CONCLUSION.....	110

## CHAPTER 4

### **4 FABRICATION AND CHARACTERISATION OF PH SENSITIVE MEMBRANES AND THEIR RESPONSE TO SPOILAGE VOLATILES RELEASED BY COOKED SHELLFISH..... 112**

4.1	INTRODUCTION.....	113
4.1.1	<i>Fabrication and Characterisation of pH Sensitive Membranes</i> .....	113
4.1.2	<i>Monitoring of Headspace Spoilage Volatiles Released from Cooked Whelk in Different Storage Conditions using the pH Sensitive Membranes</i> .....	116
4.2	EXPERIMENTAL.....	117
4.2.1	<i>Fabrication and Characterisation of pH Sensitive Membranes</i> .....	117
4.2.2	<i>Monitoring of Headspace Spoilage Volatiles Released from Cooked Whelk in Different Storage Conditions using the pH Sensitive Membranes</i> .....	128
4.3	RESULTS AND DISCUSSION.....	133
4.3.1	<i>Fabrication and Characterisation of pH Sensitive Membranes</i> .....	133
4.3.2	<i>Monitoring of Headspace Spoilage Volatiles Released from Cooked Whelk in Different Storage Conditions using the pH Sensitive Membranes</i> .....	150
4.4	CONCLUSION.....	157

## CHAPTER 5

### **5 TRANSFER OF THE SENSOR TECHNOLOGY TO THE SEAFOOD PROCESSING INDUSTRY..... 160**



5.1	INTRODUCTION .....	161
5.1.1	<i>Correlation of the Sensor Response to Microbial Spoilage of Cooked Whelk Stored at Different Temperatures</i> .....	161
5.2	EXPERIMENTAL.....	162
5.2.1	<i>Materials</i> .....	162
5.2.2	<i>Preparation of Sensors</i> .....	162
5.2.3	<i>Equipment</i> .....	162
5.2.4	<i>History of the Whelk Samples</i> .....	162
5.2.5	<i>Experimental Set-up</i> .....	163
5.2.6	<i>Pasteurisation Process</i> .....	165
5.2.7	<i>Microbial Testing</i> .....	165
5.2.8	<i>Total Volatile Base Nitrogen (TVB-N)</i> .....	166
5.3	RESULTS AND DISCUSSION .....	167
5.3.1	<i>Cooked Whelk-On-Shell</i> .....	167
5.3.2	<i>Cooked Whelk-No-Shell</i> .....	174
5.4	CONCLUSION.....	179

## CHAPTER 6

### **6 OPTIMISATION OF THE SENSOR DESIGN AND CORRELATION OF THE SENSOR RESPONSE TO MICROBIAL SPOILAGE OF COOKED WHELK..... 180**

6.1	INTRODUCTION .....	181
6.1.1	<i>Modification of the Sensor Design</i> .....	181
6.2	EXPERIMENTAL.....	182
6.2.1	<i>Materials</i> .....	182
6.2.2	<i>Sensor Fabrication</i> .....	183
6.2.3	<i>Mechanical Transformation of the PTFE Gas Permeable Membrane Using Stretching Operations</i> .....	183
6.2.4	<i>Observation</i> .....	183
6.2.5	<i>Sensor Response to Water Vapour</i> .....	185
6.2.6	<i>Sensor Response to Microbial Spoilage of Cooked Whelk</i> .....	185
6.2.7	<i>Microbial Testing</i> .....	186
6.2.8	<i>TVB-N</i> .....	186
6.3	RESULTS AND DISCUSSION .....	186
6.3.1	<i>Mechanical Transformation of the PTFE Gas Permeable Membrane Using Stretching Operations</i> .....	186
6.3.2	<i>Sensor Response to Water Vapour</i> .....	187
6.3.3	<i>Sensor Response to Microbial Spoilage of Cooked Whelk</i> .....	190

6.4 CONCLUSION.....197

**CHAPTER 7**

**7 OVERVIEW, ONGOING ACTIVITIES AND FUTURE WORK ..... 198**

**APPENDIX 1..... 207**

**APPENDIX 2..... 214**

**APPENDIX 3..... 216**

**APPENDIX 4..... 221**

## Abstract

A food quality sensor is a device that responds to some property associated with food quality and transforms the response into a signal <sup>(1)</sup>. This signal may provide direct information about the quality factor to be measured or may have a known relationship to the quality factor. On-line food quality sensors operate directly in the process stream, giving a real-time signal that relates to the quality factor in question. Therefore, an on-line sensor has the advantage of giving an immediate measurement allowing processes to be adjusted if necessary (1). This thesis is based on 3 projects describing the design and development of on-line food quality sensor systems for specific food applications as outlined below:

- Project 1: Development of an autonomous, wireless pH and temperature sensing system for monitoring pig meat quality
- Project 2: Development of a web-based wireless temperature sensing system for the fishing industry
- Project 3: Development of on-package sensors to detect shellfish spoilage

Projects 1 & 2 describe pH and temperature sensors which are coupled with wireless communications to create autonomous, wireless sensing devices capable of delivering data in real-time to a remote PC where the data can be analysed or automatically uploaded onto the internet via specifically designed web-enabled software. Project 3 focuses on the development of pH sensitive polymer membranes that change colour in response to spoilage volatiles released by shellfish packed in sealed containers. Field trials performed with the aid of Irish food industries and collaborating Irish research institutes played a major role in obtaining the results for each of the mentioned projects. These include the Department of Food and Nutritional Sciences, University College Cork; Galtee Meats, Mitchelstown, Co. Cork; Bord Iascaigh Mhara (BIM) coastal staff and Errigal Iasc, Carrick, Co. Donegal. The following thesis gives a detailed account of the recent challenges faced by the Irish food sector including the detection of poor quality pig meat, traceability and temperature control within the fishing industry and methods to evaluate seafood spoilage. The research activities carried out to overcome such challenges are discussed including the potential impact on the Irish food industry.

---

<sup>(1)</sup> Holm, F., Food Quality Sensors, in Flair-Flow 4 Report, FoodGroup Denmark, (2003)

## List of Abbreviations

<b>AQI</b>	Artificial Quality Index
<b>BCG</b>	Bromocresol Green
<b>BTB</b>	Bromothymol Blue
<b>CTABr</b>	Cetyltrimethylammonium Bromide
<b>DBS</b>	Dibutyl Sebacate
<b>DFD</b>	Dark, Firm, Dry
<b>DMA</b>	Dimethylamine
<b>GSM</b>	Global System for Mobile
<b>HACCP</b>	Hazard Analysis Critical Control Points
<b>IR</b>	Infrared
<b>IUPAC</b>	International Union of Pure and Applied Chemistry
<b>LED</b>	Light Emitting Diode
<b>LPWN</b>	Low Power Wireless Network
<b>m-CP</b>	m-Cresol Purple
<b>NIST</b>	National Institute of Standards and Technology
<b>OCTABr</b>	Octadecyltrimethylammonium Bromide
<b>PH<sub>45</sub></b>	pH taken at 45 minutes post-mortem
<b>PH<sub>u</sub></b>	Ultimate pH
<b>PSE</b>	Pale, Soft, Exudative
<b>PTFE</b>	Polytetrafluoroethylene
<b>QIM</b>	Quality Index Method
<b>RF</b>	Radio Frequency
<b>RFID</b>	Radio Frequency Identification
<b>RFN</b>	Red, Firm, Non-exudative
<b>SEM</b>	Scanning Electron Microscope
<b>SSO</b>	Specific Spoilage Organism
<b>SSP</b>	Seafood Spoilage Prediction
<b>TI</b>	Temperature Indicator
<b>TOABr</b>	Tetraoctylammonium Bromide
<b>TMA</b>	Trimethylamine
<b>TMAO</b>	Trimethylamine Oxide
<b>TOABr</b>	Tetraoctylammonium Bromide
<b>TVA</b>	Total Volatile Acids
<b>TVB-N</b>	Total Volatile Basic Nitrogen
<b>TVC</b>	Total Viable Count
<b>TTI</b>	Time Temperature Indicator
<b>WLAN</b>	Wireless Local Area Network

## **Abstract**

A food quality sensor is a device that responds to some property associated with food quality and transforms the response into a signal (1). This signal may provide direct information about the quality factor to be measured or may have a known relationship to the quality factor. On-line food quality sensors operate directly in the process stream, giving a real-time signal that relates to the quality factor in question. Therefore, an on-line sensor has the advantage of giving an immediate measurement allowing processes to be adjusted if necessary (1). This thesis is based on 3 projects describing the design and development of on-line food quality sensor systems for specific food applications as outlined below:

- Project 1: Development of an autonomous, wireless pH and temperature sensing system for monitoring pig meat quality
- Project 2: Development of a web-based wireless temperature sensing system for the fishing industry
- Project 3: Development of on-package sensors to detect shellfish spoilage

Projects 1 & 2 describe pH and temperature sensors which are coupled with wireless communications to create autonomous, wireless sensing devices capable of delivering data in real-time to a remote PC where the data can be analysed or automatically uploaded onto the internet via specifically designed web-enabled software. Project 3 focuses on the development of pH sensitive polymer membranes that change colour in response to spoilage volatiles released by shellfish packed in sealed containers. Field trials performed with the aid of Irish food industries and collaborating Irish research institutes played a major role in obtaining the results for each of the mentioned projects. These include the Department of Food and Nutritional Sciences, University College Cork; Galtee Meats, Mitchelstown, Co. Cork; Bord Iascaigh Mhara (BIM) coastal staff and Errigal Iasc, Carrick, Co. Donegal. The following thesis gives a detailed account of the recent challenges faced by the Irish food sector including the detection of poor quality pig meat, traceability and temperature control within the fishing industry and methods to evaluate seafood spoilage. The research activities carried out to overcome such challenges are discussed including the potential impact on the Irish food industry.

---

<sup>(1)</sup> Holm, F., Food Quality Sensors, in Flair-Flow 4 Report, FoodGroup Denmark, (2003)

# **1 Theory and Background**

## **1.1 Project 1: Development of an Autonomous, Wireless pH and Temperature Sensing System for Monitoring Pig Meat Quality**

### **1.1.1 Introduction**

This project focuses on the development of a unique wireless pH & temperature monitoring system to assess pig meat quality. PSE (pale, soft and exudative) pig meat continues to be a major problem in the pig meat industry today. The PSE condition in pork is related to a number of factors including genetics, pre-slaughter stress and insufficient chilling of pig carcasses, which cause a rapid rate of glycolysis post-mortem (<1hr). As a result the pH drops to low levels while the muscle temperature is still high. A wireless dual channel system that monitors pH & temperature simultaneously has been developed to provide pH and temperature data of the carcass during the first 24 hours after slaughter. It has been demonstrated that this approach can distinguish in real time, pH and temperature profiles that are 'non-normal', and identify carcasses that are PSE positive quickly and easily. The results from this project have been published in the international journal *Meat Science* (1).

### **1.1.2 Background Project Information**

This sub-project is part of a larger project designed to assess the incidences of PSE in pig meat within Irish slaughtering plants. There are four partners involved: The Department of Food and Nutritional Sciences, University College Cork, Ireland; Teagasc, The National Food Centre, Castleknock, Dublin 15, Ireland; The National Microelectronics Centre (NMRC), Co. Cork, Ireland and The National Centre for Sensor Research (NCSR) at Dublin City University.

One of the biggest challenges confronting the pork manufacturing industry today is the demand for high quality meat products. PSE pig meat is a major problem causing huge financial costs within meat processing industries. A recent study carried out in Ireland indicated that cooked hams manufactured from severe PSE pork had an estimated financial loss of 50% in comparison to those manufactured from normal pork (2). The results from this study indicate that PSE muscles are difficult to process into high quality products. Pre-slaughter handling, method of slaughter and chilling at the processing plant are all factors that influence pork quality (3-7). It is difficult to establish standard procedures for measuring the quality of pork within the industry as

pork quality characteristics change dramatically with time. In recent years many novel techniques have been assessed for their ability to measure the quality of meat in the early post-mortem period (8-10). These include measurement of muscle electrical properties, colour, pH and reflectance using fibre optic probes (10-12). Muscle has certain electrical characteristics such as impedance and conductivity, which change with time post-mortem (12). If these complex electrical changes are correlated with muscle pH decline, they may be of value in the assessment of meat quality. However at the critical time (45 minutes post-mortem), neither optical nor electrical methods are yet sufficiently reliable for accurate diagnosis of PSE (13). pH has been repeatedly shown to be the best among the known predictors of technological yield and the accuracy and precision is better than that of any other examined technique (14). The results of recent studies suggest that the potential sources of error arising from unrecognised temperature-related pH effects should be taken into consideration (15). It is also advised that industries establish an agreed temperature at which meat pH is reported so that valid comparisons of different pH measurements may be made (16). As the output signal from a pH combination electrode is temperature dependent, for accurate measurements and compensation for temperature effects, the temperature must be simultaneously measured. This is especially important when using pH measurements for the prediction of meat quality or when measurements from different sources are compared. Therefore, it would be far more effective to improve the existing pH measuring system to meet the specific demands and requirements of the meat industry by facilitating pH/temperature measurements at point-of-need in the production line. The following section explains how the integration of wireless communications and sensor technology to form a Wireless pH/Temperature Monitoring System can assist the pork industry in assessing pork quality before it enters the processing stream thereby increasing the overall yield and value of the pork.

### 1.1.3 Post-mortem Changes in Muscle Tissue

There are three pork quality categories discussed in this project; RFN (red, firm and non-exudative), DFD (dark, firm and dry), and PSE (pale, soft and exudative). After an animal is slaughtered, the circulatory system shuts down depriving the muscle tissue of oxygen, which causes the metabolic processes to shift from aerobic metabolism to anaerobic metabolism (17). Lactic acid is a by-product of anaerobic metabolism and builds up in the muscle. As lactic acid accumulates, the pH of the muscle drops from



approximately 7.2 in living tissue to approximately 5.6 in meat within about 24 hours after slaughter (18). As the carcass is chilled, a moderate rate of pH decline over a prolonged time period gives rise to high-quality meat that is red in colour, firm in texture and non-exudative (RFN), Figure 1-1a. Alternatively, a rapid rate in pH decline early post-mortem (<1 hour) creates an acidic environment while the carcass temperature is still high, denaturing muscle proteins and reducing their ability to hold water. The resulting meat is pale, soft and exudative (PSE), Figure 1-1b. The development of PSE muscle may be influenced by a number of factors including genetics and improper handling of the animal prior to slaughter (5, 6, 19, 20). On the other hand, muscles destined for DFD meat have low levels of glycogen at the time of slaughter that confines the amount of acid that can be produced, and limits pH fall, Figure 1-1c. While both RFN and PSE muscle end up with similar ultimate pH values of approximately 5.6 or 5.7, DFD muscle usually has an ultimate pH value above 6.0. This reduced acidity provides increased water-holding ability in the muscle, tightly binding water to muscle proteins, which contributes to the firm texture. A period of extended stress on the pig, caused by factors such as severe weather, long transport or unfavourable holding conditions, can deplete the muscle glycogen and triggers the DFD condition in pork muscle.



**Figure 1-1 Quality variations in pork tissue a. (Red, Firm and Non-exudative) RFN or Normal b. (Pale, Soft and Exudative) PSE c. (Dark, Firm and Dry) DFD**

#### 1.1.4 Preventing PSE

Chilling meat as soon as possible after slaughter lowers the temperature of the meat and slows down metabolic processes, reducing the rate of pH decline (21-23). By slowing down the rate of pH decline, the denaturation of proteins is reduced and the colour and the water-holding capacity of the meat may be improved. Therefore, intensive and early chilling may prevent mild cases of PSE by avoiding the combination of both high temperature and low pH (24). In severe cases of PSE, the rapid pH drop makes it difficult to lower the muscle temperature fast enough to prevent protein denaturation. In

muscle with normal post-mortem metabolism, if the temperature is dropped too rapidly, the ATP concentrations (needed to provide energy for the contraction cycle) may still be high. In this scenario, once the muscle drops below 15°C calcium is released from the sarcoplasmic reticulum. This calcium, together with the remaining ATP, can trigger severe muscle contraction and shortening. Once the ATP is depleted, this contraction is irreversible, causing the meat to be tougher and lose moisture (17).

#### *1.1.4.1 Chilling and Chilling Systems*

The purpose of any chilling system is to remove the heat from the carcass as quickly as possible after slaughter. This affects pork quality and is important to prevent microbial growth. Chilling can reduce the adverse effects of mild forms of PSE because as temperature decline is accelerated, the rate of pH decline will decrease. High post-mortem temperatures accelerate glycolysis (measured as the drop in pH), whereas low temperatures retard glycolysis. This is not surprising since higher temperatures are known to speed up the rate of chemical reactions, and therefore their effects in speeding up glycolysis in post-mortem muscle would be expected (17). Therefore, efficient chilling systems should aid in reducing the occurrence of PSE. However, this reduction in PSE is only apparent in some carcasses (24, 25).

At the time of death, muscle tissue is flaccid and highly extensible. Within a few hours it becomes inextensible and relatively rigid, a phenomenon known as rigor mortis (rigor). A number of factors can influence the time of onset of rigor mortis such as temperature, stimulation of respiration, or struggling at the time death. Offer (25) generated a model for the formation of PSE meat, reporting that the normal rate of pH fall in pork carcasses is about 0.01 pH units/min. This corresponds to a rigor time of about 150 minutes (assuming a linear pH decline). A marginal case of PSE is usually considered to correspond to a pH of 6.0 at 45 min, or about 0.02 units/min. In an extreme case, rigor is achieved in only 15 min corresponding to a rate of 0.1 units/min. Protein denaturation in a carcass with a relatively moderate pH decline and a prolonged period of temperature abuse may be greater than in a carcass experiencing more severe conditions (elevated temperature and rapid pH decline) for a shorter period duration. It was reported, when the rate of pH decline occurred at the normal rate of 0.01 pH units/min, increasing the length of time to reach carcass half-cooling from 100 minutes to 700 minutes, produced an 18 fold increase in the fraction of denatured protein. A rate of pH decline of 0.02 units/min (marginal PSE) would increase the fraction of denatured proteins 7-fold. At a rate of pH fall of 0.1 units/min (severe PSE), this would only

increase the fraction of denatured proteins by a factor of 1.7. It is apparent that more rapid chilling has greater benefits for carcasses experiencing slower and intermediate pH declines. The reason for this is that at very high rates of pH fall, rigor is attained very quickly before the carcass has cooled appreciably and the speed of chilling has little influence on the carcass temperature in the critical pre-rigor period.

Van der Wal *et al.* (26) tested three different chilling regimes. A moderate conventional chilling regime (0-4 °C; air velocity 0.5 m/s) served as a control and two forced chilling regimes; moderate rapid chilling (-5 °C) for 2h or ultra rapid chilling (-30 °C) for 30 minutes with a downward air velocity of 1, 2 or 4 m/s. After forced chilling, the carcasses were delivered to the cooler for equalisation chilling (0-4 °C, 0.5 m/s) till 24h post-mortem. The authors found a significant effect on muscle temperature compared to control samples however meat quality parameters were not affected by the chilling regime. Maribo *et al.* (22) stated that the benefits of rapid chilling was acknowledged by the Danish Pig Industry, leading to the introduction of tunnel chilling operating at a temperature of approximately -20 °C. The authors reported that lowering of the muscle temperature early post-mortem resulted in a reduced rate of the pH fall and a higher pH from 2 to 6 hrs in the cooled carcasses. Taylor (27) found no difference in quality associated with different cooling rates. It can be clearly seen that the literature has conflicting recommendations on the conditions for different chilling systems to reduce the incidence of PSE.

#### *1.1.4.2 Pre-Slaughter Conditions*

It is also reported that pre-slaughter conditions can affect the quality of the meat (4). Grandin reports that gentle handling, rest, and showering before slaughter helps lower body temperature (5). Monin *et al.* (28) reported that the control of muscle temperature is less important before than after the death of animals from the point of view of meat quality. However, in practice, the muscle temperature of pigs should be kept as low as possible before killing, as it determines directly the muscle temperature in the immediate post-mortem period (28).

### 1.1.5 Temperature Measurements of Pig Carcasses

Continuous research through the years and the evolution of technology allows temperature measurements to be made very easily. Some research in the earlier years devised theoretical models to predict the cooling curves of pig carcasses. Theoretically calculated temperatures during slaughter and chilling were comparable with the measured values indicating that a finite-element calculation method in combination with a cylindrical model for heat transport could be used to predict muscle temperatures for various chilling regimes (26). Today, temperature data loggers allow continuous logging of carcass temperature from the moment of death. There's a wide variety of temperature data loggers commercially available ranging from spear probes to tiny button type temperature data loggers that can be completely immersed into the carcass allowing the temperature to be monitored under severe conditions. A description of the temperature data loggers available on the market is discussed in greater detail in section 1.2.

The merging of radio frequency communications and temperature sensing devices to form 'wireless temperature monitoring systems' allows the carcass temperature to be measured in real time at point-of-need. The benefit of such a system is that temperature data can be accessed in real time via a PC, a laptop or a palm computer, signalling 'out-of-control' situations where early intervention may allow corrective actions to be taken, ultimately ensuring successful carcass chilling and improving final meat quality.

The type and the design of temperature sensors are very important when taking temperature readings. Specially designed sensors may be necessary for specific applications. For example a temperature sensor incorporated into a stainless steel spear type probe is needed to monitor the internal temperature of pig carcasses, see Chapter 2. To accurately read a temperature it is important to understand what happens during the reading. When two bodies with different temperatures are connected to each other, heat will flow from the warmer body to the colder body. After some time they will both reach the same temperature. This is called thermal equilibrium. This process has important consequences that can strongly influence the reading, both positively and negatively (29):

- Close contact between the measuring probe and the substance to be measured accelerates the heat transfer. The thermal resistance of the surface layer is very important.

- The thermal capacity of the reading instrument needs to be small enough compared to the body being measured so that the temperature of the body is not influenced by the measuring instrument, and that the temperature changes are accurately detected.
- The measuring instrument and the body to be measured needs to be sufficiently separated from the external surroundings. Heat transfer from and to the external surroundings can influence the reading.

All of the above need to be taken into consideration when designing a temperature sensor for a specific application. Once again, referring to the stainless steel spear type probe designed for meat pH measurements, close contact with the muscle is achieved by completely immersing the temperature sensitive part of the probe into the carcass. The probe design eliminates the temperature effects from external environments. The size of the probe is very important. It must be long enough to reach deep into the carcass muscle so a true value of the muscle temperature is obtained. The probe must have a narrow diameter to minimise destructive sampling. Chapter 2 describes in detail the benefits of using a spear-type probe compared to other temperature sensors for monitoring internal carcass temperatures.

## 1.1.6 pH Measurements

### *1.1.6.1 The Importance of pH*

pH is one of the most common laboratory measurements because many chemical processes are dependent on pH. Changing the pH of the solution can often significantly alter the speed or rate of chemical reactions. The solubility of many chemicals in solution is dependent on pH. The physiological chemistry of living organisms has very specific pH boundaries. The quality of meat depends on the rate and extent of post-mortem pH decline, for example in pig carcasses, a moderate rate of pH decline over a prolonged time period results in good quality pork. In our modern lives, virtually everything we use has been tested for pH at one time – from the tap water we drink, the food we eat, the medicines we take. The list is endless.

### 1.1.6.2 The Definition of pH

pH is an abbreviation of “pondus hydrogenii” and was proposed by the Danish scientist S.P.L. Sorensen in 1909, and is defined as the negative log of the activity of hydrogen ions ( $a_{\text{H}^+}$ );

$$\text{pH} = -\log_{10} a_{\text{H}^+} \quad \text{Equation 1-1}$$

pH represents the ‘activity’ of hydrogen ions in a solution, at a given temperature. The term *activity* is used because pH reflects the amount of available hydrogen ions not the concentration of hydrogen ions. The activity of an ion  $a_i$  is defined by:

$$a_i = \alpha_i C_i \quad \text{Equation 1-2}$$

Where  $C_i$  is the concentration of the ion  $i$  and  $\alpha_i$  is its activity coefficient.  $\alpha_i$  is a function of ionic strength (30), and consequently for accurate measurements of pH with an electrode, ionic strength is often buffered to ensure  $\alpha_i$  remains constant, e.g. by adding a large excess of an ‘indifferent electrolyte’ to which the electrode is insensitive. This allows electrodes to be calibrated directly in terms of concentration.

### 1.1.6.3 Measuring pH

pH is measured using two electrodes: the indicator (sensing) electrode and the reference electrode. These two electrodes are often combined into one body – a combination electrode. When the two electrodes are immersed in a solution, a galvanic cell is established, whose potential is dependent on both electrodes. Ideal measuring conditions exist when only the potential of the indicator electrode changes in response to varying pH, while the potential of the reference electrode remains constant, see section 1.1.6.5.

### 1.1.6.4 The Electrochemical Measuring System

The reference electrode in Figure 1-2 is a half-cell with an accurately known electrode potential  $E_{ref}$  that is ideally independent of the analyte concentration or any other ions in the solution under study. Examples of reference electrodes include the silver/silver chloride electrode (Ag/AgCl, KCl) and Calomel electrode (Hg/Hg<sub>2</sub>Cl<sub>2</sub>, KCl).

#### 1.1.6.4.1 Silver/Silver Chloride Electrode

The silver/silver chloride electrode is prepared, e.g. by coating a silver wire anode with silver chloride electrolytically in 0.1mol/L chloride solution. The silver chloride coated wire is immersed in KCl solution of known concentration, usually saturated, i.e. >3 mol/L. The response of the silver/silver chloride electrode is based on the following reaction:

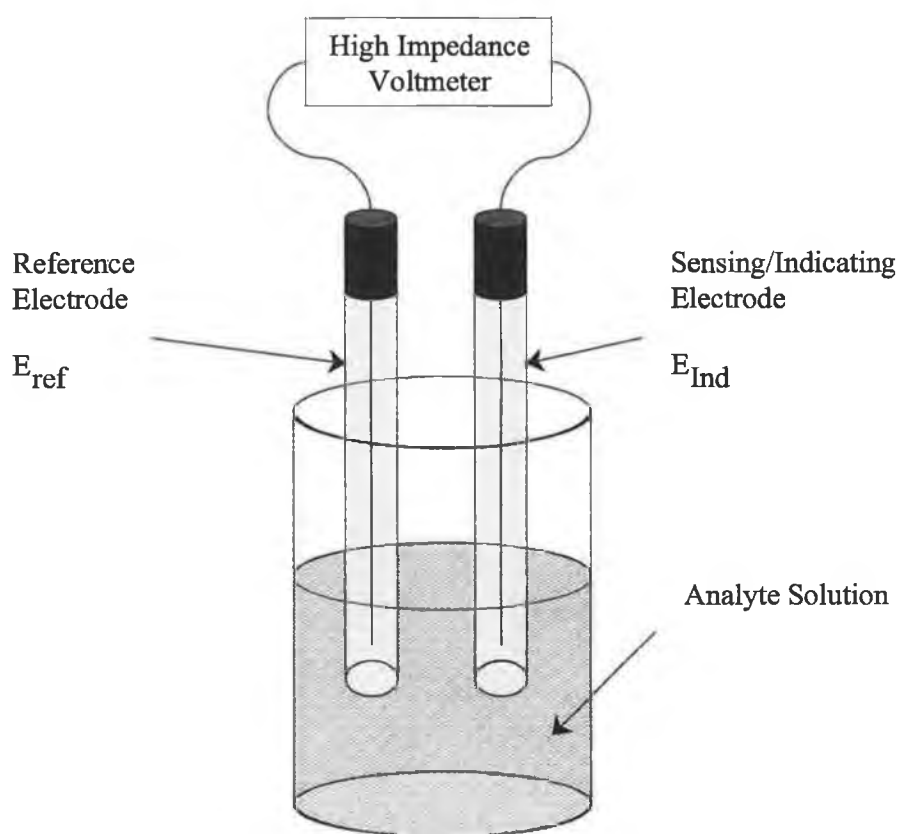
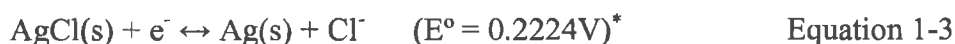


**Figure 1-2 Electrochemical measurement System**

The silver/silver chloride electrode is the most reproducible reference half-cell, with good electrical and chemical stability at 25°C. All the constituents that alter the silver ion concentration affect the potential of the electrode. Thus, the electrode cannot be used directly (without an additional salt bridge) in solutions that contain proteins, bromide, iodide or sulphide ions that form insoluble compounds (precipitates) with the silver ions. The temperature hysteresis effect is very small with the silver/silver chloride

---

\*  $E^\circ$  is the standard electrode potential – see section 1.1.6.7

reference electrode. For this reason it is recommended for applications in which the temperature cannot always be held constant. The *indicator electrode*, which is immersed in the analyte solution, develops a potential  $E_{ind}$  that depends upon analyte activity. Most indicator electrodes used in potentiometry are highly selective in their responses i.e. pH electrodes are selective for  $H^+$ . The high impedance voltmeter refers to the pH meter that measures the potential between the pH-indicating electrode  $E_{ind}$  and the reference electrode  $E_{ref}$ .

### 1.1.6.5 pH electrodes

The majority of pH electrodes available are combination electrodes. They combine the reference and pH sensing elements into a single electrode. When the combination electrode in Figure 1-3 is placed in a solution the potential of the cell is as follows:

$$E_{cell} = E_{ind} - E_{ref}^* \quad \text{Equation 1-4}$$

Where  $E_{ref}^* = E_{ref} + E_j$  ( $E_j$  is the liquid junction potential)

(Ideally constant due to non-contact with the sample)

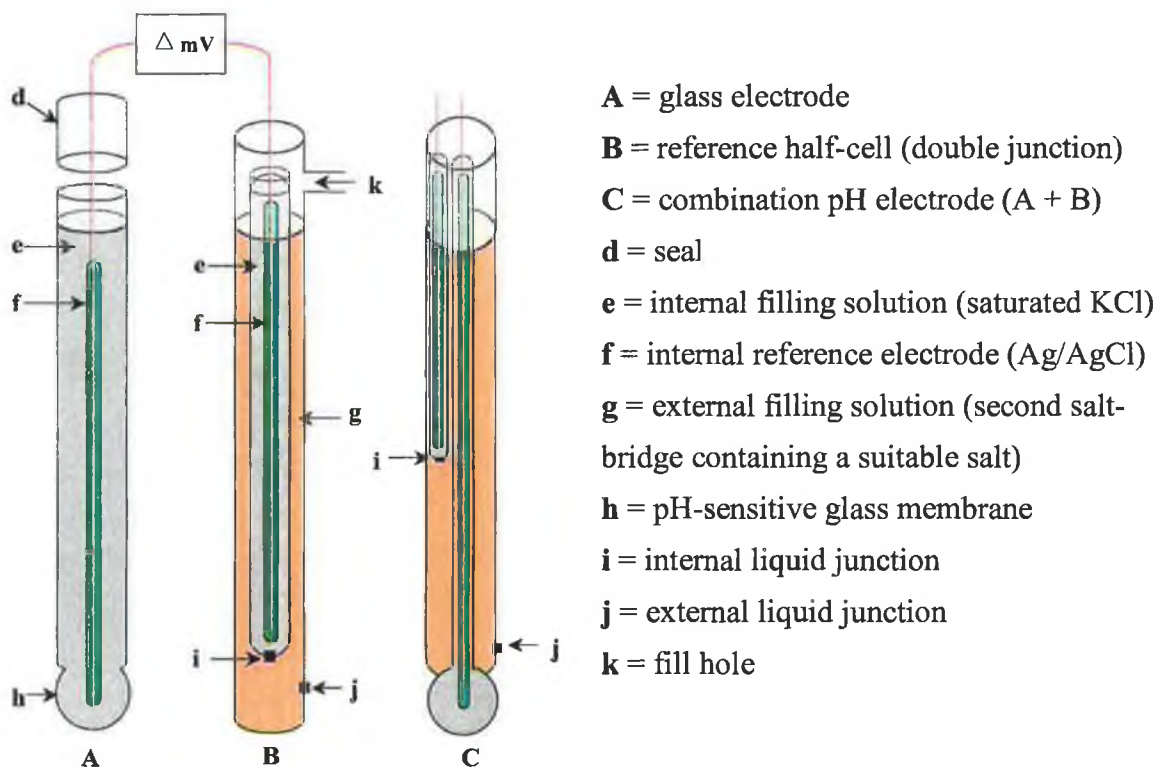


Figure 1-3 Typical electrode construction



### 1.1.6.5.1 Liquid Junction Potentials

In a potentiometric cell, the reference electrode is connected to the sample via a salt bridge electrolyte. The salt bridge ensures electrical contact between the two half-cells of the electrochemical cell through free diffusion of ions. However, bulk mixing of the bridge and sample solutions must be avoided. This is achieved by ensuring the area of contact is minimised, by using for example, capillary contact or a ceramic frit. A liquid junction potential develops across the boundary between two electrolyte solutions that have different compositions, usually the reference electrode assembly and the sample (30). Figure 1-4 shows a very simple liquid junction consisting of a 1 M HCl solution in contact with a 0.01 M HCl solution. A porous ceramic frit prevents the two solutions from mixing. At the junction zone a concentration gradient is established, and this is the driving force for diffusion. Both  $H^+$  and  $Cl^-$  ions diffuse across the boundary from the more concentrated solution to the dilute solution.  $H^+$  ions are more mobile than  $Cl^-$  ions, thus, the  $H^+$  ions diffuse more rapidly than the  $Cl^-$  ions resulting in a charge separation i.e. a boundary potential. The charge developed counteracts the differences in diffusion rates of the two ions and a steady state equilibrium is achieved. The steady state potential developed is called the liquid junction or diffusion potential.

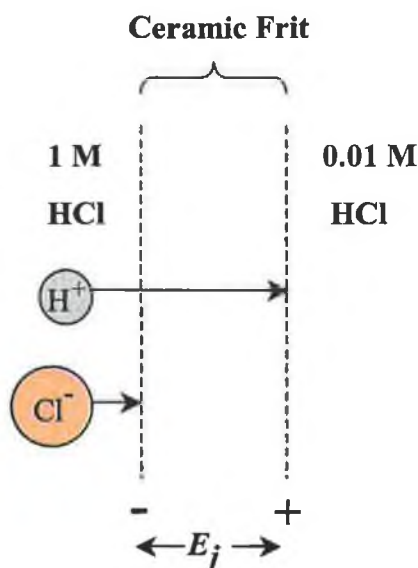


Figure 1-4 Schematic representation of a liquid junction potential  $E_j$ . The length of the arrows corresponds to the relative mobility of the two ions (30).

The value of the liquid junction potential is, in the majority of cases, unknown, and sets a limit on the accuracy of direct potentiometric measurements. The magnitude of the liquid junction potential can be minimised by ensuring the salt bridge between the

reference electrode and the analyte solution is saturated with ions of almost equal mobility i.e. saturated  $K^+Cl^-$ .

In direct potentiometry it is essential that the differences in the liquid junction potentials between the calibration solutions and the sample solutions are minimal as a voltage change due to the liquid junction potential is misinterpreted as a pH change. In meat pH measurements there is a difference between the buffer solution matrix and the sample matrix that creates a liquid junction potential error. It is not recommended to use standard silver/silver chloride electrodes for meat pH measurements as the sample matrix contains proteins that react with the silver ions in solution to form an insoluble precipitate on the electrode junction resulting in unstable and inaccurate readings. The following section addresses the errors associated with standard silver/silver chloride electrodes when used to measure samples containing proteins.

#### *1.1.6.6 Glass electrodes*

Both the composition of the glass electrode's pH sensitive glass and the composition of the glass electrode's inner solution have an influence on the potential that will develop. The response of the electrode is the voltage developed between the inside and outside of the membrane. This voltage is proportional to the difference in pH in the inner solution and the sample. The response is caused by an exchange at both surfaces of the swollen membrane between the ions of the glass and the  $H^+$  ions of the solution – an ion exchange that is controlled by the concentration of  $H^+$  ions in both solutions.

The types shown in Figure 1-5 are examples of glass electrodes. Glass electrodes are available in a number of different shapes and lengths to fit a wide range of applications. The combination pH electrode KCMSW11 available from Thermo Russell, Auchtermuchty, Scotland, Figure 1-5a, is used in this project to measure the pH of pork muscle. The internal half-cell consists of a high electrical resistance glass tube, which has a pH sensitive membrane at the lower end. Within the reference cell is an internal silver/silver chloride reference system held in a high stability gel matrix with an open inner junction, which connects to the sample via the external filling solution (3 M potassium chloride) and the ceramic junction. The inner electrolyte is a viscous solution comprising saturated AgCl and KCl. In standard Ag/AgCl electrodes the inner electrolyte contains  $Ag^+$  ions in solution, which are free to diffuse across the junction and react with proteins in the sample to form insoluble solids that block the junction. In the KCMSW11 double junction pH electrode the viscosity of the electrolyte prevents the  $Ag^+$  ions from diffusing across the junction. A second salt bridge (double junction)

comprising saturated KCl protects the sample further from the internal reference electrolyte. This pH probe was designed specifically for meat applications and addresses many of the problems posed by standard Ag/AgCl electrodes.



Figure 1-5 Different glass electrodes for different applications (Thermo Russell, Russell pH Ltd, UK)

#### 1.1.6.7 The Nernst Equation

The Nernst equation expresses the electrical potential of an electrochemical cell at non-standard state conditions at any time during the electrochemical cell's reaction.

The Nernst Equation is written as:

$$E = E^{\circ} - \frac{2.303RT}{nF} \log (a_{H^{+}}) \quad \text{Equation 1-5}$$

Where;

- **E** is the cell potential measured by the electrodes
- **E°** is the standard potential of the cell at 298.15°K
- **R** is the universal gas constant = 8.3145 J/mol. K (Joule per mol and per Kelvin)
- **T** is the temperature = 298.15°K

- **n** is the number of moles of electrons transferred in the balanced equation or the charge/valency of the ion. Which in the case of the hydrogen ion  $n = 1$
- **F** is the Faraday constant, which is the electrical charge in coulombs (C) for every mole (mol) of reactant involved in the electrochemical cell,  $F = 96485.309$  C/mol.

At a temperature (T) of 298.15 °K (25°C) the Nernst equation can be written as:

$$E = E^\circ + \left( \frac{8.3125 \text{ J/mol} \cdot \text{K} \times 298.15 \text{ K}}{96485.309 \text{ C/mol}} \right) \times 2.303 \text{ pH} \quad \text{Equation 1-6}$$

$$E = E^\circ + 0.059 \text{ VpH} \quad (1 \text{ J/C} = 1 \text{ Volt}) \quad \text{Equation 1-7}$$

That is a change of 59 mV at 25° C per pH unit (the slope of the equation).

Temperature is a key variable in pH measurement, affecting not only the slope of the electrode, but sample and buffer pH values, plus the potential of the electrode (causing electrode drift). Temperature must therefore always be reported with the pH value. The slope of the equation must be determined by calibration in at least two solutions of known concentration. This is used to correct for the variation in the slope factor arising from a number of sources including the temperature factor T in the Nernst slope ( $RT/nF$ ).

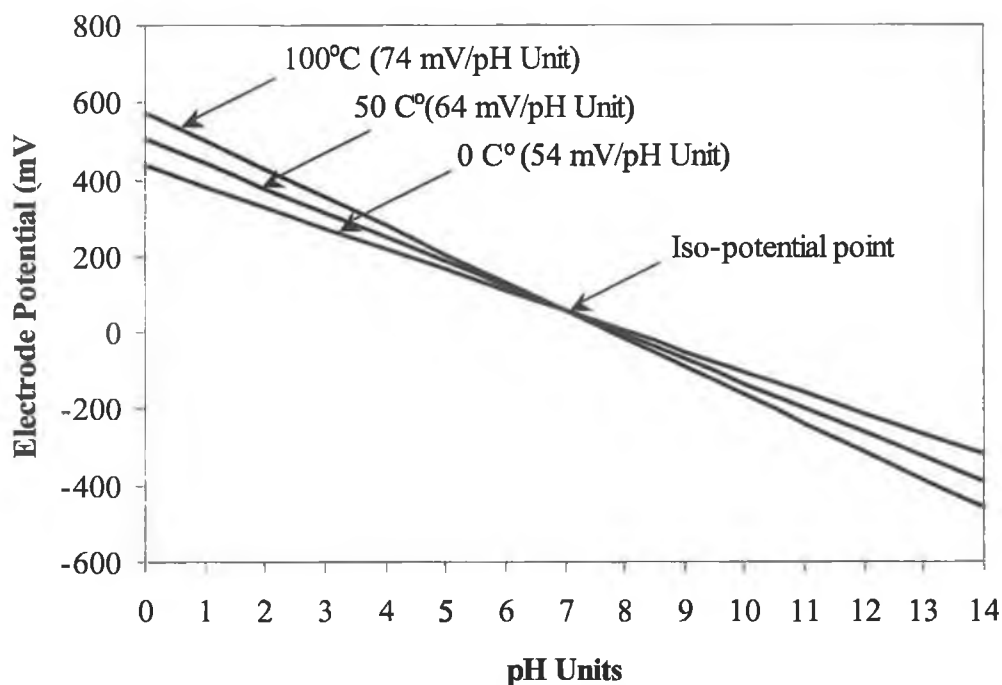


Figure 1-6 Change of electrode slope with temperature

Plotting the pH versus mV at a number of different temperatures will, for most electrodes, reveal that the lines intersect at almost the same point, see Figure 1-6. This point is called the iso-potential point or iso-pH. If, by electrical circuitry or calculation, the pH and iso-pH are made to coincide, compensation is made for the electrode's temperature dependence and measurements in a fairly large temperature range will be possible.

#### 1.1.6.8 Buffers

Calibration is required to allow the potential of the cells in unknown solutions to be converted to pH values. For this purpose a solution with a precisely known pH and which shows a certain degree of insensitivity when lightly contaminated with acid or alkaline species, i.e. it must have a buffering capacity, is used. In buffer solutions, the pH is maintained due to an equilibrium established between weak acids, bases and their salts. Equation 1-9 defines the equilibrium constant for the acid dissociation equilibrium reaction in Equation 1-8.



Equation 1-8

$$K_a = \frac{[H^+][A^-]}{[HA]}$$

Equation 1-9

A strong acid is one that completely dissociates in solution while weak acids only partially dissociate in solution. In weak acids the reaction in Equation 1-8 favours the left hand side of the equation. Adding the salt or conjugate base ( $A^-$ ) of the acid will increase the salt concentration which further pushes the reaction to the left hand side. Therefore, the acid is usually overwhelmingly in the HA form. Looking at Equation 1-9 above, this means there is plenty of  $[A^-]$  and  $[HA]$ . Adding small amounts of acid or alkali will increase or decrease  $[H^+]$ , and Equation 1-8 can shift to compensate and keep  $K_a$  constant. Hence, weak acids and their conjugate bases are used as buffers.

The chemicals used in buffer solutions must be pure and stable and the pH values should be well defined. There are two types of buffer solutions. Technical buffers with a high buffer capacity and IUPAC/NIST\* buffers with a lower buffer capacity. The IUPAC/NIST buffers are directly in accordance with the pH definition thus ensuring better accuracy. IUPAC and NIST address the shifts in buffer pH with temperature. These standards are defined using a hydrogen electrode measuring system and are directly traceable to the hydrogen electrode-measuring set-up at one of the Primary Laboratories (e.g. NIST, IUPAC)

#### 1.1.6.9 pH Electrode Calibration

Electrodes cannot be produced with exactly identical characteristics. Zero pH and slope will vary with time and different manufacturers produce electrodes with different nominal values. The calibration matches the pH meter to the current characteristics of the electrodes. Calibration adjusts the slope and offset of the slope produced using the Nernst equation and is usually expressed as a percentage of a theoretically perfect slope (i.e. 100%). For a properly functioning electrode, the calibration slope should be between 95 – 102% of the theoretical value. The calibration process is generally performed by measuring the pH in two different buffer solutions. This enables both  $pH^0$  (zero pH) and the slope to be determined. Zero pH is defined as the pH value at which the measured potential is zero.

---

\* IUPAC (International Union of Pure and Applied Chemistry, [www.iupac.org](http://www.iupac.org))

NIST (National Institute of standards and Technology, US, [www.nist.gov](http://www.nist.gov))

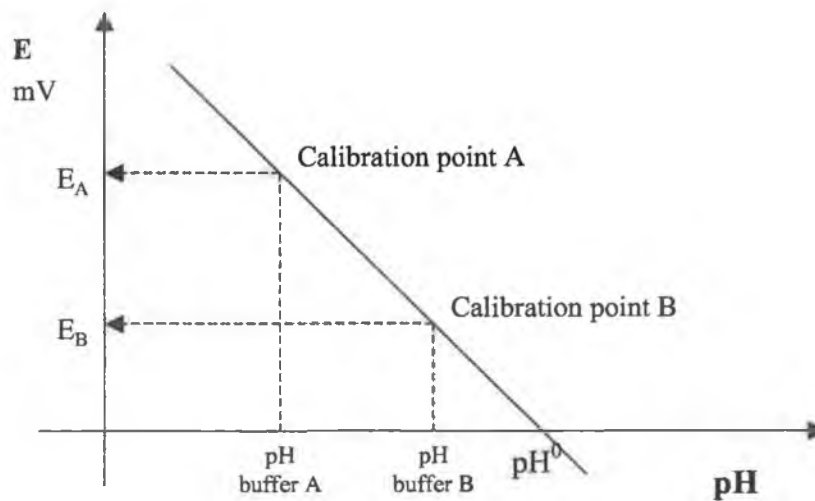


**Figure 1-7 pH calibration curve**

The slope is usually stated as a percentage of the theoretical value and should be independent of temperature. However, as mentioned before, the slope expressed as mV/pH is directly dependent on temperature. As an alternative a slope at 25°C is often used (100% = 59mV/pH). The calibration should be performed in a consistent manner. The two buffers should bracket the measuring interval i.e. for sample measurement between pH 4.5 and 6.7, it would be appropriate to use buffers with pH 4.01 and pH 7.00.

### 1.1.7 Legislation for Temperature Monitoring in the Food Industry

Galtee Meats (Mitchelstown, Ireland) Ltd, processes over half a million pigs annually accounting 20% of the national kill and has developed a significant customer base predominantly in the Irish & UK markets and also in the rest of Europe, USA and Japan. Galtee produces quality pork and bacon cuts in accordance with the standard specifications set out in manuals from the Irish Livestock & Meat Board and to other specifications as agreed with customers. Galtee is at all times concerned about the welfare of its consumers. Galtee operates HACCP (Hazard Analysis Critical Control Points) within the plant to ensure its products are produced to the highest quality standards. HACCP is a preventative system of food control aimed at food safety assurance. HACCP is a documented and verifiable approach for the identification of hazards, preventative measures and Critical Control Points (CCP), and the implementation of a monitoring system. The internationally agreed principles of

HACCP can be applied to all sectors of food and drink manufacturing, distribution and retailing. In the HACCP system there is zero tolerance for exceeding a critical limit.

The HACCP system is comprised of 7 components and the fourth component states that control procedures should be established and implemented to monitor each Critical Control Point (CCP) to check that it is under control (31). Monitoring is the scheduled testing or observation of a CCP and its limits must be documented and determined at the time the production line is in operation. Ideally, the monitoring would be performed by mechanical methods continually during production, such as a temperature-recording device with an alarm system.

Food safety and quality has become an area of intense concern to the general public and because of this the food industry is coming under increased pressure to improve quality standards. The EU and European National legal systems, and the USA are moving towards regulating quality over the entire food chain, from harvesting to the supermarket shelf. It is therefore imperative that accurate monitoring systems are developed. This is where autonomous sensing devices will prove to be extremely useful.

### 1.1.8 Autonomous (Wireless) Sensing

One of the most dynamic areas of research and economic development is communications and computing where data transfer including text, graphics, images, videos and sound are becoming increasingly feasible. The mobile phone industry alone gives a clear indication of the numerous capabilities of computing devices where wireless communications allow motion pictures from one mobile phone to another to be transferred across the world in seconds. With computer devices becoming smaller and smaller, it is clear that these technologies will enable us to ultimately extend the desktop resources (including memory, computation, and communication) to almost anywhere we travel. More importantly, this constant access, augmented by battery powered body mounted sensors, will enable our computers to be sensitive to the activities in which we are engaged, and thus allow the computer to participate in a collaborative and active manner as we perform our tasks (32-34). Researchers at CENS, the Centre for Embedded Networked Sensing are investigating fundamental properties of Embedded Networked Systems that will monitor and collect information on such diverse subjects as plankton colonies, endangered species, soil and air contaminants, medical patients and buildings. At CENS they believe that Embedded Networked Sensing Systems will reveal previously unobservable phenomena (35). A recent publication describes the



principle of Internet scale sensing where every analytical measurement is Internet enabled (36). The widespread adoption of this principle leads to the emergence of 'internet-scale sensing and control systems', in which millions of sensing devices and actuators are linked in a seamless manner with a wide variety of users, ranging from individuals, to Government agencies, industrial users or public service providers, across many application sectors.

The convergence of sensor technologies, communications and computing has made inexpensive, powerful, and ubiquitous sensing a readily achievable reality. This is the world of 'silent technology' in which computing capability becomes an invisible component of everyday items and activities (37). Silent technology refers to the new wave of computing in which everyday objects have embedded computing power that enables them to gather information and interact with other objects without human intervention (37). This ubiquitous sensing capability carries some potentially revolutionary consequences for all types of businesses. Sensors have a pivotal role to play in this world, as they are the primary sources of information about our environment. The revolutions in wireless communications and sensors bring many opportunities in remote sensing. One area of great interest and importance is the evaluation and monitoring of the quality of food we eat. This project explains how the merging of radio frequency communications with sensor technology to form 'autonomous sensing systems' can be used in the pork industry to assess the quality of raw material and to provide scientific information of carcass condition.

### 1.1.9 Wireless pH and Temperature Monitoring of Pig Carcasses

Today, wireless communications greatly facilitate everyday operations such as transferring data and controlling equipment either at home or in the industry. In the past, wires or cables were necessary to carry out these operations but occasionally factors including distance and physical obstructions inhibit the installation of costly cables. Low power wireless network (LPWN) technology such as Radio Frequency (RF) communications would be a practical solution in situations where wires or cables are not suitable or are cumbersome to employ. RF communications can penetrate materials such as concrete and timber (excluding metal). Wireless Local Area Networks (WLANs) based on narrow band RF communications can achieve distances up to 3000 metres depending on the transmission power (38) and a multi-directional radiation pattern does not require line-of-sight (LOS) for operation. The approach offers many

advantages over hard-wired systems and can be particularly useful in many industrial applications where data collection is necessary on a large scale. For example, today abattoirs are becoming highly automated and extensive amounts of data (e.g. origin, carcass weight, breed, grade, temperature, pH etc.) need to be collected and sorted and transmitted to other locations where it can be analysed (39). Traceability is a major driving force for data collection in the food industry especially since the new EU Food Safety Law 178/2002, which took effect on the 1<sup>st</sup> January 2005, which requires traceability of all raw materials. The wireless sensor network system discussed in this thesis therefore offers an excellent means of tracking the pH and temperature history of pig carcasses soon after they have been slaughtered until they leave the chill room for further processing. Furthermore, coupling the pH and temperature monitoring system with RF communications allows the data to be analysed in real time from remote locations, and facilitates data integration within a plant, and at a higher level, both from multiple sources across multiple plants. Access to such information will become increasingly important for quality control, waste reduction and audit tracking within the food-processing sector.

## **1.2 Project 2: Development of a Web-based Wireless Temperature Sensing System for the Fishing Industry**

### **1.2.1 Introduction**

Perishable foods require chilling to retard many of the microbial, physical, chemical and biochemical reactions associated with food spoilage and deterioration. Temperature abuse is one of the main contributors responsible for food spoilage and careful temperature control is of paramount importance for the quality and safety of chilled and frozen foods (40). For example, the relative spoilage of fish increases four times if the temperature is raised from 0°C to 10°C, and approximately 8 times if the temperature is raised from 0°C to 20°C (41). By inhibiting microbial growth, food quality and safety can be preserved for extended periods (42).

For effective chilling the temperature must be controlled all the way from the raw material supply, through production, manufacture or slaughter, to the presentation of the product for final consumption, the '*cold-chain*' (43-47). A breach in the cold-chain can affect the quality and safety of the product and the consequences may be serious for both the producer and the consumer. For this reason, continuous temperature monitoring is a prerequisite for maintaining the quality and safety of perishable foods.

### **1.2.2 Temperature Monitoring Devices**

There is a large variety of temperature monitoring devices available on the market ranging from simple mercury thermometers to more sophisticated temperature data loggers. Glass mercury thermometers are perfectly adequate when, for example, a spot temperature reading of a solution is required during a laboratory experiment, but for safety reasons glass thermometers are not practical when spot temperature measurements of solid food products, i.e. meat and cheese, are required. Where solid food products are concerned, electronic handheld temperature probes with digital displays are more appropriate. These types of temperature measuring devices are perfect for their described applications but are not suitable for permanent recording.

When permanent temperature records are required for traceability purposes, temperature data logging devices are more appropriate, giving the user a time stamped temperature history. Numerous temperature data-logging units exist on the market with varying

temperature ranges and accuracies depending on the application. These units can store large amounts of data, i.e. up to 32,000 time-temperature values, depending on their memory capacity and can have a long battery lifetime i.e. up to 10 years. Internal clocks allow parameters such as sampling frequency and start/end times to be preset in advance. The loggers can be connected to a PC via serial ports (RS232 connections) for configuration and data downloads. These temperature-logging units are rugged, self-sufficient systems that once set up for a mission measure temperature and record the data in a protected memory. Examples of such temperature data-logging units include the DS1921 Thermochron iButton (available from Dallas Semiconductor), the LOGpen-10 (available from Advantech Automation Corporation) and the StowAway® Tidbit® (available from Onset). These are just a few of the vast amount of temperature data loggers available.

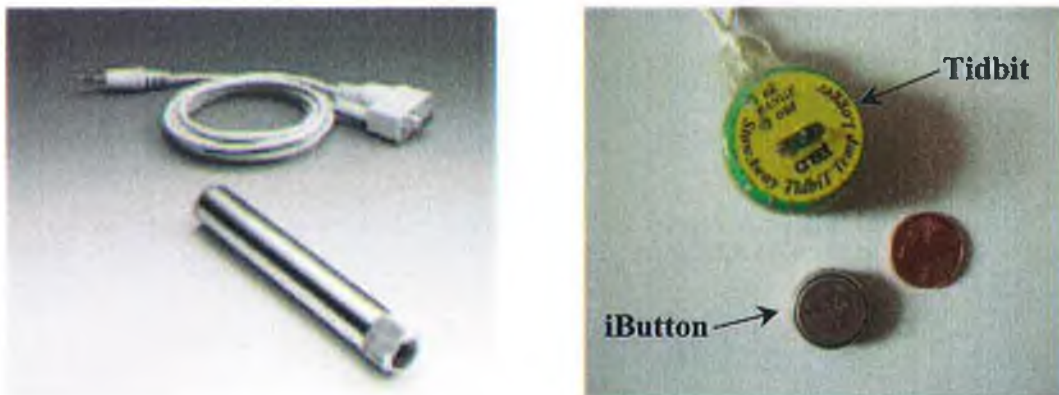


**Figure 1-8 LOGpen-10 (48) (left). StowAway® Tidbit® and the DS1921 Thermochron iButton (right).**

The DS1921 Thermochron iButton is 16mm wide with a stainless steel casing that is robust and waterproof. It measures temperature from  $-40^{\circ}\text{C}$  to  $+85^{\circ}\text{C}$  in  $0.5^{\circ}\text{C}$  increments and has an accuracy of  $\pm 1^{\circ}\text{C}$ . It has a real-time clock and a programmable alarm system that flags temperature values outside a pre-defined range, recording the exact time and how long the temperature stayed outside the permitted range. Up to 2,048 temperature values taken at equidistant intervals ranging from 1 to 255 minutes can be stored. Data is transferred to a PC via a serial connection and the software allows the data to be displayed as a graph or histogram. The recyclable iButton logs data for more than 10 years or up to 1 million temperature measurements.

The LOGpen-10 as its name suggests has a pen-shaped design (19mm diameter  $\times$  130mm length) that's robust, easy to carry and easy to insert any place for temperature

measurement. The housing is made of stainless steel and brass and is chromium plated to provide excellent heat conductivity. It measures temperatures from  $-40^{\circ}\text{C}$  to  $+80^{\circ}\text{C}$  with an accuracy of  $\pm 1^{\circ}\text{C}$  and can record 4,000 temperature readings. A sampling interval between 1 second and 18 hours can be selected and an internal clock allows the user preset the recording start time. When the memory capacity is reached, the device can either overwrite the earliest data or stop recording. The logger has a typical lifetime of 1-2 years depending on the sampling frequency. The logger is configured and the recorded data retrieved via a serial connection to a PC. A two-coloured LED indicates the operating status of the LOGpen-10. When a temperature measurement outside a set limit is recorded, the LED turns from green to red. Users can therefore identify abnormal temperatures at a glance, without the need for downloading data to a PC.

The StowAway<sup>®</sup> Tidbit<sup>®</sup> is a waterproof temperature logger. There are two models available with different temperature ranges i.e.  $-5^{\circ}\text{C}$  to  $37^{\circ}\text{C}$  and  $-20^{\circ}\text{C}$  to  $50^{\circ}\text{C}$ . The unit possesses on-board memory with a memory capacity of up to 32,000 temperature readings. An Optic Shuttle<sup>™</sup> that communicates with the logger via IR communications allows the temperature data to be transported back to a host PC where an Optic Base Station<sup>™</sup> facilitates data transfer.

The three temperature monitoring systems described above are designed to work remotely. Unless the logger is conveniently located, i.e. immediately inside the door of a refrigerated container, the logger must be removed from the product being transported before any stored information can be downloaded. In reality, this means that the temperature profiles can only be analysed at the end of the transport run and not at any stage during the journey.

Disposable temperature indicators (TIs) and time-temperature indicators (TTIs) are an alternative to using conventional electronic temperature monitoring. TIs are small (postage stamp-sized) disposable labels that give a visible response if a predetermined threshold temperature is exceeded. However, for TTIs the extent of the colour migration is dependent on the extent of temperature abuse that has occurred (49). The performance of TIs and TTIs stored under isothermal and non-isothermal conditions was tested in a study performed at the National Food Centre (49). The results from this study indicated that the Chillcheck<sup>™</sup> temperature indicators performed reliably under isothermal conditions. In varying temperature conditions, they responded more to surface/ambient temperature rather than to product core temperatures. In practical use, no colour change would indicate that the temperature control had been satisfactory. However, the authors advise that in the case of a colour change, caution must be exercised when interpreting the result as relatively minor temperature fluctuations may cause a colour change with

little adverse impact on the product quality. In the same study the authors reported that full colour change of the time-temperature indicator, 3M Monitormark™ 51, could equally be obtained by subjecting a product to a temperature of 15°C for 42 hours or 7°C for 48 hours. However, these two temperature conditions could have different quality and safety implications for a perishable product. The study showed that the time-temperature indicators were not sufficiently responsive to accurately integrate the time-temperature history for high-risk perishable food products.

Although the TIs and TTIs give an immediate indication of whether or not the product has been subjected to out-of-limit temperatures, there appears to be a certain amount of ambiguity regarding the colour change. When consumer safety is at stake there is no room for ambiguity.

To ensure maximum safety and temperature control in the food industry real-time temperature monitoring provides an excellent solution that can be achieved through wireless radio frequency transmission systems. Radio frequency systems have become very popular recently with more and more products being released on the market such as the i-Q line of radio frequency identification (RFID) tags available from Identec Solutions and the DigiTrak RF system available from Digitron. With radio frequency systems a contactless transfer of data between the data-carrying device and its reader is far more flexible. This gives the operator the ability to communicate directly with the data-logging device without the need to be connected to a computer.

The i-Q32T RFID tag (131 mm × 28 mm × 21 mm) with a plastic casing (IP 65) provides real-time data collection in wireless applications such as identification, tracking and tracing and temperature monitoring. It has an internal sensor temperature range of -40°C to +85°C and an optional external sensor with a temperature range of -127°C to +127°C. Using advanced UHF (430 to 440 MHz) radio frequency technology the i-Q32T tag transmits and receives data at distances up to 30 meters (open field) from a handheld device or up to 100 meters (open field) from a fixed interrogator. The tag has a 32,000 byte memory and stores user and process information as well as temperature data. This system can work with up to 2,000 tags in the radio frequency range. The i-Q32T tag can be programmed to take readings at user definable intervals from 1 to 255 min and can operate effectively for over 6 years.

The DigiTrak RF system comprises of a DT02 temperature transmitter (165 mm × 90 mm × 26 mm) with a temperature range of -30°C to +93°C. It has radio frequency operating range of 120 meters (open field) operating at 868 MHz. The temperature data is sent wirelessly to the DTBASE base station connected to a PC or networked

computer. The web-based software provides access control and multi user options via a PC or network.



**Figure 1-9 The i-Q32T system (50). A handheld device allows the temperature data to be accessed via radio frequency communications.**

Although the problems associated with previous monitoring systems have been addressed by the use of contactless technology, which eliminates the need to remove the monitoring device from its position to download the recorded data, the system described above must be within the specified range to communicate with the base station/receiver. The base station/receiver must be connected to a PC to allow user access/control and in many situations this may not be very practical i.e. setting up a PC on a cold storage haulage vehicle. The i-Q32T tags can be accessed by an operator via a handheld device, which addresses some of the impracticalities posed by other wireless systems. This system is perfectly adequate for tracking and identification applications where product data is only required at destination terminals. If perishable products were strictly maintained within the specified temperature range for the duration of the journey then the temperature monitoring systems described above would suffice as they would provide a time-temperature history that can be passed onto a potential customer. On the other hand, if the product temperature rises above a threshold value for long periods of time due to a refrigeration malfunction or high temperature setting the consequences could be serious. The temperature history can be retrieved upon arrival at the final

destination where if necessary the products can be discarded without putting the consumer at risk but at a high cost to the producer. If a real-time monitoring system was installed that alerts the operator/driver of an out-of-control temperature situation a simple remedial action such as adjusting the temperature control setting may rectify the situation without posing any risk to the consumer or the producer.

### 1.2.3 Shelf life Prediction

The shelf life of fresh fish may vary from batch to batch and accurate prediction of shelf life is particularly important to ensure product quality. Studies in the past have shown that microbial models can accurately predict the shelf life of specific fish species i.e. cod (51). Seafood Spoilage Prediction (SSP) software has been developed to predict and illustrate the effect of constant and fluctuating temperatures on the growth of specific spoilage organisms (SSOs) and on the remaining shelf life of seafood (52). The inclusion of different types of spoilage models in SSP allowed the software to be applicable for shelf life prediction of many seafoods but each model has a specific range of applicability with respect to product characteristics and storage conditions. The SSP software allows growth of SSO and remaining shelf life to be predicted at constant storage temperatures, for simple temperature profiles entered manually within the software, and for temperature profiles collected by different data loggers. The ability of SSP to read temperature profiles collected by data loggers, and to predict their effect on remaining product shelf life can be applied directly, e.g. in the evaluation of chill chains in industry and within research. Combining shelf life prediction and electronic time-temperature data with information collected from the moment of catch i.e. from traceability systems, will further improve product quality assurance in the seafood sector (52).

### 1.2.4 Traceability

Since the 1980s, concerns about the safety and quality of food have increased at both government and consumer levels (53). According to the Centre for Disease Control and Prevention, 76 million people each year in the United States suffer from food-borne disease, of which 325,000 spend time in hospital and 5,000 die. Many articles have been published highlighting the importance of food traceability for public health and consumer protection and methods to effectively implement traceability systems in the



food industry (53-59). The EU's new food safety regulations, which were enforced on 1<sup>st</sup> January 2005, place huge responsibilities on food and feed business operators to devise a safe system for supplying food. Article 18 of the EU's new food legislation states that the traceability of food, feed, food-producing animals and any other substance intended to be, or expected to be, incorporated into a food or feed shall be established at all stages of production, processing and distribution. A report published by the food and beverage industry application centre at Intenia discusses the details of the new EU food safety regulations stating, "Traceability will become a licence to operate. And from January 1, 2005 all companies will be obliged by law to have adequate traceability systems in place. Because without them companies will be excluded from the food chain."

With the new EU food regulations in place food industries are forced to face the inevitable and implement traceability systems that will allow them compete in the food chain. As data management technologies become more powerful and less costly, product traceability will be easily employed. Take for example the fisheries industry; little information is passed on from the fisherman to the fish processors and they rely heavily on reputation and long-term business relations. Today, information other than the area where the fish was caught cannot be given precisely, and information i.e. days on ice, temperature history of the catch, is not readily available. In order to establish full chain traceability it is necessary to include all players, starting with the fishermen, collectors, auctions and traders, continuing with producers and ending up with retailers (59). Transmission of all the required information physically with the fish products would be impracticable and so the use of information technology is preferable. The EU concerted project Tracefish established agreed specifications for an IT based traceability scheme for the fish industry (60). The Tracefish scheme pragmatically deals with the diversity and complexity of the captured fish distribution chains taking into consideration the commercial needs and sensitivities of the food businesses, whilst enabling whole chain traceability. A simple system for introducing traceability in the fresh fish chain was tested in Denmark (59). The fish were iced and sorted into boxes on-board the fishing vessel according to species. Each box was provided with information on fish species, catch date, vessel number and box number, readable in text and in the form of a bar code on a label. The information was entered into a computer and the data transmitted via a wireless mobile phone to a central database on a computer ashore. The computer used on-board was a laptop unit placed in the wheelhouse of the fishing vessel. A connection was made to a label-printing unit in the hold, where the labels were printed and attached to the boxes, as they were stored. Before the vessel

entered the harbour the collector (an operator who takes care of the fish from when the fishing vessels enter the harbour until the fish is sold at the auction) retrieved the catch information from the vessel via the central database. The information was transferred between all the steps in the chain from the fishing vessel, collector, auction, and wholesaler to the retailer. The final customer received all the information on a printed label of when the fish was caught, which vessel had caught the fish, and how it was handled on the way to the fish market (59).

Tracefish is an excellent traceability system that provides an accessible means of recording and transferring large amounts of data from 'catch to consumer'. Integrating time-temperature information into traceability systems would gain consumers confidence in the product thereby adding value to the catch. Chapter 3 describes how a real-time web-based temperature monitoring system can be easily deployed on-board inshore fishing vessels and its overall potential to improve quality control and traceability within the fishing industry.

## **1.3 Project 3: Development of an On-Package Sensor for Detecting Shellfish Spoilage**

### **1.3.1 Introduction**

The previous project describes a unique temperature monitoring system initially used to monitor the temperature of salmon and mackerel catches onboard small inshore fishing boats off the south coast of Ireland, and was then transferred onto larger inshore fishing trawlers to monitor the temperature of whelk catches caught off the east coast of Ireland. The trials were also extended to include real time temperature monitoring on the refrigerated trucks that delivered the whelk from Howth Harbour, Co. Dublin to Errigal Fish Co. Ltd, Co. Donegal, a distance of approximately 300km. At Errigal Fish Co. Ltd, the whelk are processed and packed into sealed containers which are then exported to their foreign customers i.e. Japan. During long haul journeys abroad the products can easily become temperature abused rendering them 'unsafe' for human consumption. Ultimately, the consequences may be serious for both the customer and for Errigal Fish Co. Ltd. Today, great emphasis is placed on consumer safety and if customers receive goods that are already spoiled as a result of temperature abuse during transit this may reflect badly on the processor i.e. Errigal Fish Co. Ltd, but most importantly the consumers safety is at risk. For this reason, pH sensitive membranes placed inside the sealed containers that change colour in response to spoilage volatiles will give the consumer an immediate indication of whether or not the product is safe to eat. If strict measures have already been enforced to ensure quality and safety then such food quality sensors will benefit both the consumer and the processor as the consumer will be confident that the product they are receiving is safe and the processor will in return reap the rewards.

### **1.3.2 Methods to Evaluate the Freshness and Quality of Fish**

Numerous methods exist to aid the evaluation of fish freshness including sensory, chemical, biochemical, microbial and various other instrumental methods as described below.

### *1.3.2.1 Sensory Evaluation*

Sensory evaluation is defined as the scientific discipline used to evoke, measure, analyse and interpret characteristics of food as perceived by the senses of sight, smell, taste and touch (61). European fisheries research institutes have developed a rapid, objective sensory method for the evaluation of fish freshness called the Quality Index Method (QIM). QIM is based on the significant sensory parameters for raw fish. The scores for all the quality parameters (appearance, odour of skin, eyes, gills and outer slime) are added to give an overall score, the so-called quality index, which can be used to predict storage life (61, 62). QIM is primarily used on whole or gutted fish but the method is difficult to use with fish fillets and schemes for lightly preserved seafood are not yet available (63). Using sensory methods for evaluation of food gives valuable information on the food quality but accurate sensory assessment requires considerable training and skill and its application is time consuming and costly (63).

### *1.3.2.2 Microbial Methods*

Spoilage is characterised by any change in a food product that renders it unacceptable to the consumer from a sensory point of view. The major cause of food spoilage is microbial growth and metabolism resulting in the formation of amines, sulfides, alcohols, aldehydes, ketones and organic acids with unpleasant and unacceptable off-flavours (64). The term 'unacceptable' when applied to food spoilage is product-specific – for example, ammonia odours are part of a desirable odour profile in some dried and fermented fish products, but are not acceptable in most fresh and lightly preserved seafoods (64).

#### *1.3.2.2.1 Total Viable Counts*

The activity of microorganisms is the main factor limiting the shelf life of fresh fish. An estimation of the total number of microorganisms, named total viable counts (TVC), is used as an acceptability index in standards, guidelines and specifications (61). The total count represents, the total number of bacteria that are capable of forming visible colonies on a culture media at a given temperature (65). If a count is made after systematic sampling and a history of the fish is known from catch i.e. temperature conditions, packaging etc., TVCs may give a comparative measure of the overall degree of bacterial contamination and the hygiene applied (65).

#### 1.3.2.2.2 Specific Spoilage Organisms

Spoilage reactions in food are complicated and dynamic in the sense that spoilage reactions and spoilage microorganisms may change as a function of product characteristics and storage conditions (52). It is well known that minor changes in processing and packaging of fish products cause a dramatic change in the development and composition of the spoilage association and a complete different type of spoilage (50). During storage, the microflora changes owing to different abilities of the microorganisms to tolerate the preservation conditions (64). Microbial activity limits the shelf life of packed as well as unpacked fresh fish products (66). Knowledge of the microorganisms involved in spoilage is needed to develop microbiological and chemical methods for evaluation of quality and shelf life (67). Despite the heterogeneity in raw materials and processing conditions, the microflora that develops during storage and in spoiling foods can be predicted based on knowledge of the origin of the food, the substrate base and a few central preservation parameters such as temperature, atmosphere, water activity and pH (67). However, only a few of the microbial community, the specific spoilage organisms (SSO), give rise to the offensive off-flavours associated with seafood spoilage (64). For example, it has been shown that the specific spoilage organism, photobacterium phosphoreum, is responsible for the microbial spoilage of packed cod, (68), and the activity of this SSO in model substrates allows the remaining shelf life of the product to be accurately predicted using the iterative approach (51, 66). The iterative approach is product related and it is based on initial studies with naturally contaminated products, where SSOs, their spoilage domains, and growth kinetics are determined, the data is generated and mathematical models allows the effects of intrinsic and extrinsic parameters to be quantified, and finally the model is validated by comparing it to data from storage experiments (51). Seafood Spoilage Predictor (SSP) software, discussed in section 4.1.2, has been developed to predict and illustrate the effect of constant and fluctuating temperatures on the growth of SSOs and on the remaining shelf life of seafood (52). However, to benefit from this property of kinetic models the initial level of SSOs in a batch needs to be determined by a rapid microbiological method (52). Traditional microbiological methods are laborious, time consuming, costly and require skill in execution and interpretation of results (65).

### 1.3.2.3 Chemical Methods

An alternative or supplementary method to microbial analyses involves the measurement of chemical changes associated with microbial growth processes in foods (69). Volatile compounds including amines, sulphides, alcohols, aldehydes, ketones and organic acids are released from fish flesh as it deteriorates and the composition and concentration of the volatile compounds change depending on the freshness of the fish (48). Therefore, measurements of characteristic volatile compounds can be used to monitor the freshness or spoilage stage of fish (61). Total volatile basic nitrogen (TVB-N) is one of the most widely used measurements of seafood quality (65). In seafood, TVB-N primarily includes trimethylamine (TMA), ammonia, and dimethylamine (DMA) (63). Each of these compounds, as well as levels of TVB-N, are useful indices of spoilage in different fresh and lightly preserved seafood. The European Commission (Council Regulation No. 95/145/EEC of March 1995) specified that TVB-N should be used if sensory evaluation indicates doubt about freshness of different fish species (63).

#### 1.3.2.3.1 Volatile Amines

Fish flesh naturally contains very low levels of carbohydrate, which is depleted during the struggle prior to death. This has two important consequences for spoilage. The absence of carbohydrate means that bacteria present on the fish will immediately resort to using the readily available nitrogenous materials, producing off-odours and flavours. Trimethylamine oxide (TMAO) occurs in appreciable quantities in marine fish as part of the osmoregulatory system and is reduced to TMA during microbial spoilage an important component in the characteristic odour of fish (70). Ammonia is formed by the bacterial degradation/deamination of proteins and amino acids, which are present in high quantities in seafood. The enzymatic decomposition of TMAO generates DMA at sub-zero temperatures and is therefore useful as a frozen storage index (63, 71-73).

Numerous techniques have been developed over the years to aid the analysis of the volatile compounds released as a result of microbial spoilage. Headspace methods for the analysis of volatile compounds involve the collection and concentration of the volatiles for subsequent chromatographic separation to identify and quantify the separated compounds (74). Due to the complexity, cost and lengthiness of chromatographic methods for the analysis of volatile compounds these techniques are suitable only for specialised research and analytical laboratories (61). There is an increased interest in the use of gas sensor array systems, so-called electronic noses, for

the rapid assessment of volatile compounds in food (61, 63, 75-79). Electronic noses are the common name for sensors responding to odour (volatiles) using an array of simple and non-specific sensors and a pattern recognition software system. Essentially, each odour leaves a characteristic pattern or fingerprint on the sensor array, and an artificial neural network is trained to distinguish and recognise the odours (80). A study was carried out by the Icelandic Fisheries Laboratory to evaluate the quality of cod using two electronic noses, *LibraNose* and *FreshSense* (81, 82). The two electronic noses are based on different sampling procedures and sensor technologies. *LibraNose* is based on an array of eight thickness shear mode resonators coated with metalloporphyrins and a small metal capsule that is put on the surface of fish for sampling volatiles. *FreshSense* is based on four electrochemical sensors (CO, H<sub>2</sub>S, SO<sub>2</sub>, and NH<sub>3</sub>) and a larger sampling container allowing the analysis of the whole fillet (48, 82). The study showed that better performance is achieved when the data from both electronic noses are combined (81). The responses of electronic noses have been shown to correlate with objective measures of quality in fresh seafood. However, none of the electronic nose instruments which are available commercially have been implemented in the fish industry (82) as the stability of correlation between sensory data and electronic nose response still represents a problem for practical applications of gas sensors in seafood shelf life evaluation (63).

#### *1.3.2.4 Multi-Sensor-Devices*

Recently, multi-sensor-devices based on visible light spectroscopy, electrical properties, image analysis, colour, electronic noses and texture have been calibrated with sensory scores of QIM for attributes like appearance, smell and texture to give an Artificial Quality Index (AQI) that can be as accurate and precise as the QIM sensory scores. With the costs of labour and training of assessors set to increase and the cost of instrumentation set to decrease dramatically, it is believed that multi-sensor-devices will be adopted by the fishing industry in the future but that remains to be seen (48, 83).

#### *1.3.2.5 Visible Spoilage Indicators*

With more and more seafood products being sold in sealed containers on display cabinets, it is difficult for the customers to use their sense of smell to detect off-odours at the moment of purchase. For this reason, use-by-dates are helpful but only if the correct storage conditions have been maintained.

Recently, the advent of visual spoilage indicators that respond to volatile compounds released by fish into the headspace of sealed containers proves promising for determining the spoilage of packaged fish (84-86). The concept was first patented under the title of "Food Quality Indicator Device", United States patent application no. 20020044891, (35), and has been licensed by COX Technologies, USA, under the trade name of Fresh Tag<sup>TM</sup>. The patent gives a general description of a food quality indicator comprising of an indicator compound that changes colour due to the presence of volatile compounds, such as volatile bases, in spoiled food.

It has been demonstrated that increasing TVB-N levels in the confined headspace associated with packaged fish (i.e. cod and whiting) are possible to detect by monitoring changes in the colour of paper discs impregnated with an acidochromic dye using UV-Vis reflectance spectroscopy (84). The dye does not distinguish between the various bases (NH<sub>3</sub>, TMA, DMA) but rather responds to any volatile base capable of deprotonating it. The authors found that fresh whiting produced larger, and more rapid colour changes than fresh cod, suggesting that the rate of release of volatile bases from whiting is faster. It was also suggested that a more reproducible result could be obtained if an automated approach was adopted (e.g. screen printing, spin coating) to deposit very precise amounts of the dye onto the substrate surface. Such materials may therefore play a role in the development of 'intelligent packaging' that conveys some idea of the freshness of the packaged food to the consumer (84). Recently, another method was developed using a pH indicator dye, cresol red, physically entrapped in a cellulose polymer film to respond to headspace TVB-N released from selected fish species (i.e. cod and orange roughy) during spoilage (85, 86). The authors approach was based on a study that describes the entrapment of a pH indicator dye into a plasticised cellulose acetate matrix to form a fast response pH indicator optode that was tested in a flow-cell for on-line monitoring of pH. Cellulose acetate was chosen as the polymer matrix due to its high permeability to basic gases and its excellent long-term stability (86). Once again the volatile amines released were monitored over time by measuring the response of the pH indicator dye using UV-Vis reflectance spectroscopy. It was also reported that the pK<sub>a</sub> of the dye in the polymer matrix did not vary significantly from that in free solution and there was a linear relationship between the colour intensity of the dye and the log of the NH<sub>3</sub> concentration in the headspace (86). The results from these studies showed that there was a significant increase in the TVB-N content in the headspace of fish samples after an incubation period of 8-12 hours for cod and 12-15 hours for orange roughy (85). Whiting obtained from a local supermarket and stored at room temperature, showed a definite and measurable increase in TVB-N levels between



24 and 30 hours and the TVB-N levels of deepwater fish, orange roughy and black scabbard, increased between 30 and 45 hours when stored at room temperature (86).

The major difference between the approaches adopted by Loughran *et al.* and Byrne *et al.*, apart from the type of indicator dye used, is the technique employed to immobilise the dye onto a solid substrate. Loughran *et al.* describes a simple technique whereby the paper discs were impregnated with the dye by soaking them in the dye solution followed by a short drying process (84) whereas Byrne *et al.* employed a widely used technique in sensor applications whereby the indicator dye is physically entrapped into a cellulose acetate membrane (85, 86).

### 1.3.3 pH Indicators and Optical Sensors

Acid-base indicators (i.e. pH indicators) are dyes whose acid form has one colour and whose base form has another colour (87). The appearance of colour arises from the property of the coloured material to absorb selectively within the visible region of the electromagnetic spectrum (88). Optical sensors for acidic (HCL, SO<sub>2</sub>, CO<sub>2</sub>, acetic acid) or basic gases (NH<sub>3</sub>, amines) often make use of pH indicator dyes immobilised in polymers (89). Trinkel *et al.* describes the development of an aqueous based optical sensor for detecting ammonia whereby a pH-sensitive dye (bromophenol blue) was immobilised as an ion pair with cetyltrimethylammonium in a silicone matrix (90). The colour of the bromophenol blue dye changed reversibly from yellow (protonated dye:  $\lambda_{\max} = 426$  nm) to blue (deprotonated dye:  $\lambda_{\max} = 608$  nm) with increasing concentration of ammonia in solution. The concentration of ammonia was determined by measuring the transmittance at a given wavelength. This study was based on work previously carried out by Werner *et al.* (91) where a **lipophilic ion pair**, see section 4.1, was obtained by reacting the indicator dye (bromophenol blue or bromocresol green) with the lipophilic salt cetyltrimethylammonium bromide (CTABr) as follows:

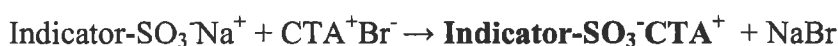


Figure 1-10 shows the protonated and deprotonated forms of the bromocresol green dye when exposed to ammonia in solution.

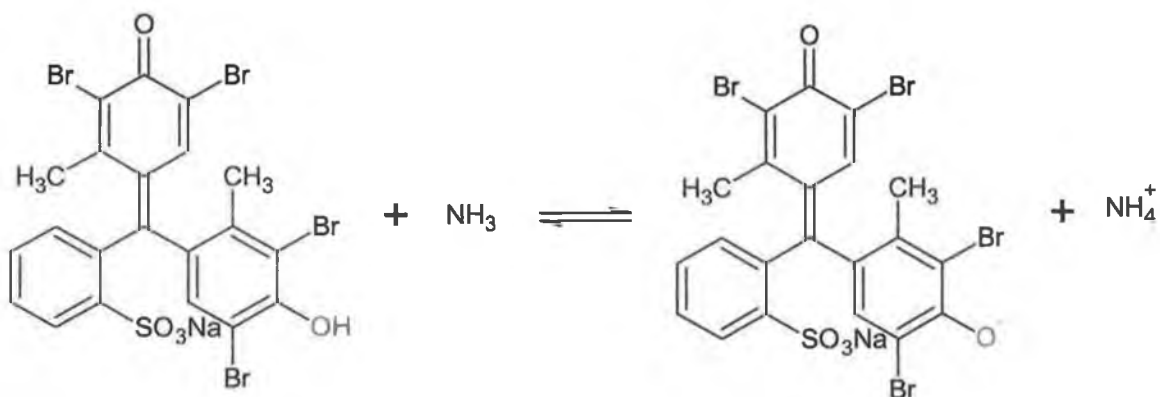


Figure 1-10 The yellow acidic form of the bromocresol green dye is deprotonated by ammonia to give a blue-green basic form.

The sensors described so far are based on the detection of dissolved ammonia. For ammonia gas detection the ammonia must first be solvated in water before reacting with the dye. The reaction scheme is illustrated in Figure 1-11. The overall reaction is similar to the reaction shown in Figure 1-10.

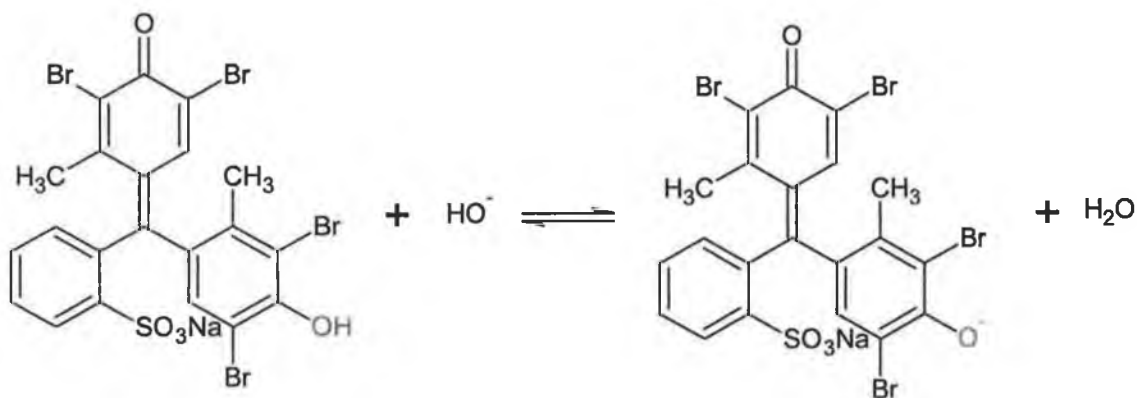


Figure 1-11 Ammonia reacts with water to produce the hydroxide ion  $\text{OH}^-$  which deprotonates the dye to its basic form. The overall reaction is similar to the reaction in Figure 1-10.

### 1.3.4 Spectroscopy – Properties of Electromagnetic Radiation

Spectroscopy is the study of electromagnetic radiation and its interaction with matter (30, 92). The electromagnetic spectrum ranges from  $\gamma$ -ray, X-ray, ultraviolet, visible, infrared, and microwave to radio frequency radiation. Electromagnetic radiation is commonly treated as a wave phenomenon, an electric field that undergoes sinusoidal oscillations as it moves through space characterised by a wavelength ( $\lambda$ ) or frequency ( $\nu$ ). Figure 1-12 represents a two-dimensional representation of a beam of monochromatic (i.e. single wave-length), plane-polarised radiation (oscillations of the electric field are in a single plane). The wavelength ( $\lambda$ ) is defined as the distance between adjacent peaks of the sinusoidal wave (usually expressed in meters, see Table 1-1) and the amplitude  $A$  is the height of the wave. The frequency ( $\nu$ ) is the number of wave cycles that travel past a fixed point per unit of time, and is usually given in cycles per second, or hertz (Hz).

Region	Unit	Definition
X-ray	Angstrom, Å	$10^{-10}$ m
Ultraviolet/visible	Nanometer, nm	$10^{-9}$ m
Infrared	Micrometer, $\mu\text{m}$	$10^{-6}$ m

Table 1-1 Wavelength units for various spectral regions

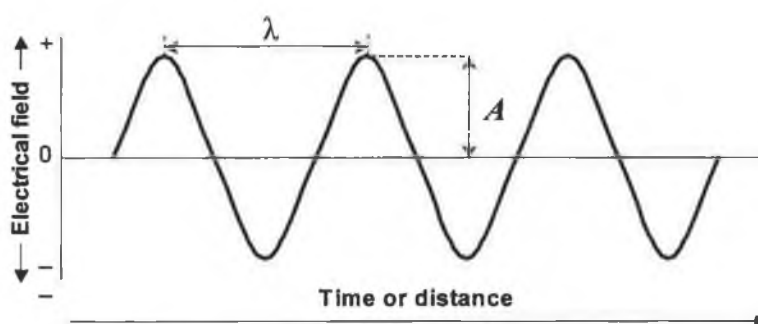


Figure 1-12 Representation of a beam of monochromatic radiation of wavelength  $\lambda$  and amplitude  $A$  (adapted from Skoog, D.A, D.M. West, and F.J. Holler, Fundamentals of Analytical Chemistry. Sixth Edition, 1992, p509)

All electromagnetic radiation travels through space at a velocity ( $c$ ) of  $3.00 \times 10^8 \text{ ms}^{-1}$  (88). The relationship between wavelength, frequency and velocity is expressed as follows (88):

$$c = \nu\lambda = 3.00 \times 10^8 \text{ ms}^{-1} \quad \text{Equation 1-10}$$

The rate of propagation of the electromagnetic radiation through a medium containing matter is slowed down as the electromagnetic field of the radiation interacts with the electrons in the atoms or molecules of the medium (30). To understand many of the interactions between radiation and matter, it is necessary to postulate that electromagnetic radiation is made up of packets of energy called photons or radiation quanta (30, 92). The energy of a photon depends upon the frequency of the radiation and is given by the equation:

$$E = h\nu \quad \text{Equation 1-11}$$

Where  $h$  is Planck's constant ( $6.63 \times 10^{-34} \text{ J.s}$ ). When molecules absorb radiation the energy absorbed is quantised and only certain frequencies (and wavelengths) are affected. The molecule is promoted from an initial energy state ( $E^I$ ) to a higher energy state ( $E^{II}$ ) (92). The change in energy is expressed in the equation below:

$$\Delta E = E^{II} - E^I = h\nu \quad \text{Equation 1-12}$$

This is the Bohr frequency rule and is the basis of all quantitative spectroscopy (92). In terms of wavelength and wavenumber ( $\bar{\nu}$ ), where the wavenumber is defined as the reciprocal of the wavelength in centimeters ( $1/\lambda$ ), the equation is as follows:

$$E = \frac{hc}{\lambda} = hc\bar{\nu} \quad \text{Equation 1-13}$$

### 1.3.5 Absorbance

Absorption is a process in which a chemical species in a transparent medium selectively attenuates certain frequencies of electromagnetic radiation (30), as mentioned previously. Every elementary particle (atoms, ions or molecules) has a unique set of energy states, and at room temperature most of these particles are in their ground state,

the lowest energy state. When an elementary particle is subjected to a photon of electromagnetic radiation, absorption occurs if the energy of the photon matches exactly the energy difference between the ground state and one of the higher energy states of the particle. The energy of the photon is transferred to the atom, ion, or molecule, converting it to the higher energy state, an excited state (see section 1.3.7).

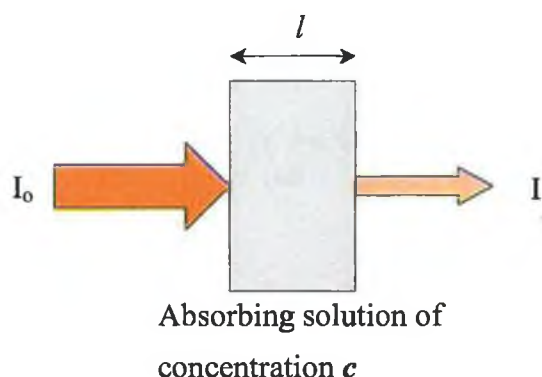


**Figure 1-13 Attenuation of a beam of radiation by an absorbing solution (adapted from Skoog, D.A, D.M. West, and F.J. Holler, Fundamentals of Analytical Chemistry. Sixth Edition, 1992, p519)**

Figure 1-13 illustrates a beam of parallel monochromatic radiation passing through an absorbing solution with a concentration  $c$  and a path length  $l$ , (measured in cm). Interactions between the photons and the absorbing species decrease the intensity of the beam from  $I_0$  to  $I$ . The transmittance  $T$  of the solution is defined as the fraction of incident radiation transmitted by the solution and is often expressed as a percentage.

$$T = \frac{I}{I_0}$$

**Equation 1-14**

The absorbance  $A$  of the solution can be defined by the following equation:

$$A = -\log_{10} T = \log\left(\frac{I_0}{I}\right)$$

**Equation 1-15**

### 1.3.6 Beer-Lambert Law

The Beer-Lambert law states that the absorbance of a solution is directly proportional to the path length and to the concentration of the absorbing species (88) defined as follows:

$$A = \log\left(\frac{I_o}{I}\right) = \epsilon cl \quad \text{Equation 1-16}$$

$A$  = absorbance

$\epsilon$  = molar absorptivity ( $\text{L}\cdot\text{cm}^{-1}\cdot\text{mol}^{-1}$ ), defined as the probability of an electronic transmission from the ground state to an excited state

$c$  = concentration of the analyte ( $\text{mol}\cdot\text{L}^{-1}$ )

$l$  = path length (cm)

Deviations from the linear relationship between absorbance and concentration occur at high analyte concentrations (usually  $> 0.01\text{M}$ ) where the average distance between absorbing species is reduced affecting the charge distribution of neighbouring particles. This interaction can alter the ability of the particles to absorb a given wavelength of radiation (30).

### 1.3.7 Chromophores

pH indicators are weak organic acids with unsaturated functional groups, termed chromophores, which absorb in the visible region of the electromagnetic spectrum (30). Table 1-2 below presents a number of organic chromophores containing unsaturated double or triple bonds. To understand why chromophores are responsible for absorption it is necessary to describe the electronic transitions that occur within a molecule when it is subjected to electromagnetic radiation. Two types of electrons are responsible for the absorption of ultraviolet and visible radiation by organic molecules. These include shared electrons that participate directly in bond formation and are thus associated with more than one atom, and unshared outer electrons (i.e. non-bonding) that are localised about atoms such as oxygen and nitrogen (30). The wavelength at which organic molecules absorb depends upon the strength of the bonds within the molecule. For

instance, the electrons may be in strong  $\sigma$  bonds (covalent bond formed between two nuclei), in weaker  $\pi$  bonds (bond formed by the sideways overlap of two parallel  $p$  orbitals) or non-bonding  $n$  (molecular orbitals that do not participate in bonding) (93). When energy is absorbed all these types of electrons can be elevated to excited antibonding states that can be represented diagrammatically as in Figure 1-14, the antibonding states represented as  $\sigma^*$  and  $\pi^*$  (88).

Chromophore	Example	$\lambda_{\max}$ (nm)	$\epsilon_{\max}$
Alkene	$C_6H_{13}CH=CH_2$	177	13,000
Conjugated alkene	$CH_2=CHCH=CH_2$	217	21,000
Alkyne	$C_5H_{11}C\equiv C-CH_2$	178	10,000
		196	2,000
		225	160
Carbonyl	$CH_3COCH_3$	186	1000
		280	16
Carboxyl	$CH_3COOH$	204	41
Azo	$CH_3N=NCH_3$	339	5
Nitro	$CH_3NO_2$	280	22
Nitrate	$C_2H_5ONO_2$	270	12
Aromatic	Benzene	204	7,900
		256	200

Table 1-2 Absorption characteristics of some common organic chromophores (30)

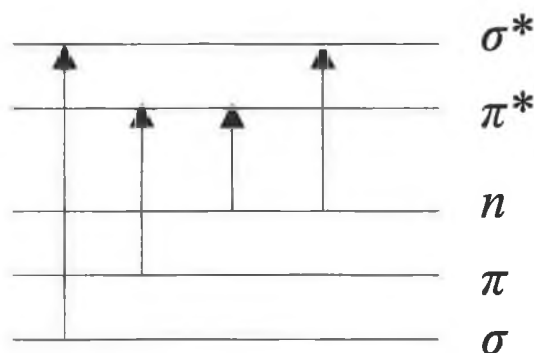


Figure 1-14 Bonding and antibonding energy transitions

The shared electrons in single bonds such as C-C and C-H are so firmly held that their excitation requires energies corresponding to wavelengths below 200nm in the vacuum ultraviolet region ( $\sigma \rightarrow \sigma^*$  transitions) (30, 88).  $\pi \rightarrow \pi^*$  and  $n \rightarrow \pi^*$  absorptions occur in the near ultraviolet and visible region and result from the presence of chromophores (i.e. functional groups containing double or triple bonds) where the electrons are relatively loosely held and thus easily excited (30, 88). Chromophores have characteristic molar absorptivities  $\epsilon$  and absorb at fairly well defined wavelengths. The wavelengths of these characteristic absorptions and their molar absorptivities are often greatly changed due to the presence of other chemical groups in the molecular structure. It has been found that groups such as  $-\text{OH}$ ,  $-\text{NH}_3$  and halogens, which all possess unshared electrons, cause the normal chromophore absorptions to occur at longer wavelengths (i.e. displaced towards the red end of the spectrum, known as a Red Shift) with an increase in the molar absorptivity. Groups that cause this shift are known as auxochromes (88).

### 1.3.8 Optically Responsive Polymer Films

Optically responsive polymer films typically consist of ~33 wt% polymer (e.g. polyvinylchloride (PVC), cellulose acetate), ~64 wt% plasticiser (e.g. dibutyl sebacate), ~1-5 wt% host compound (e.g. pH indicator dye), and additives (e.g. lipophilic salts) (94). Polymers such as PVC and cellulose acetate have a high glass transition temperature ( $T_g$ ) and are very brittle (89). Plasticisers are materials that are added to polymers to increase their flexibility (95). Without plasticisers, the high density of the polymer chains hinders diffusion of ions and gases in the polymer matrix. The immobilisation of the pH indicator dye and the role of lipophilic salts in the polymer membranes are discussed in detail in Chapter 4.



## References

1. Frisby, J., Raftery, D., Kerry, J. P., and Diamond, D., Development of an autonomous, wireless pH and temperature sensing system for monitoring pig meat quality, *Meat Science*, *70*, 329 (2005).
2. O'Neill, D. J., Lynch, P. B., Troy, D. J., Buckley, D. J., and Kerry, J. P., Effects of PSE on the quality of cooked hams, *Meat Science*, *64*, 113 (2003).
3. Lynch, P. B., Lawlor, P. G., Davis, D., Kerry, J. P., Buckley, D. J., and Walsh, L., Studies on Pre-Slaughter Handling of Pigs and its Relationship to Meat Quality, Teagasc Pig Production Department Moorepark Research Centre, pp. 1 (1998).
4. Van der Wal, P. g., Engel, B., and Hulsegge, B., Causes for variation in pork quality, *Meat Science*, *46*, 319 (1997).
5. Grandin, T., Methods to reduce bloodsplash, in *Allen D, Leman Swine Conference*, Vol. 21, Veterinary Outreach Programs, University of Minnesota, pp. 206 (1994).
6. Grandin, T., Assessment of Stress During Handling and Transport, *Journal of Animal Sciences*, *75*, 249 (1997).
7. Rosenvold, K., and Andersen, H. J., The significance of pre-slaughter stress and diet on colour stability of pork, *Meat Science*, *63*, 199 (1997).
8. Forrest, J. C., Line speed implementation of various pork quality measures, Animal Sciences Department, Purdue University, West Lafayette, IN (1998).
9. van Laack, R. L. J. M., Kauffman, R. G., and Polidori, P., Evaluating Pork Carcasses for Quality, in *National Swine Improvement Federation Annual Meeting*, University, Clive, Iowa (1998).
10. Mullen, A. M., McDonagh, C., and Troy, D., Technologies for Detecting PSE in Pork, Teagasc, The National Food Centre, Ashtown, Dublin 15 (2003).
11. Geesink, G. H., Schreutelkamp, F. H., Frankhuizenc, R., Vedderb, H. W., Faberb, N. M., Kranena, R. W., and Gerritzena, M. A., Prediction of pork quality attributes from near infrared reflectance spectra, *Meat Science*, *65*, 661 (2003).
12. Byrne, C. E., Troy, D. J., and Buckley, D. J., Postmortem changes in muscle electrical properties of Bovine M. longissimus dorsi and their relationship to meat quality attributes and pH fall, *Meat Science*, *54*, 23 (2001).
13. Swatland, H. J., On-Line Assessment of Pork Muscle Quality and Marbling, in *National Swine Improvement Federation Conference and Annual Meeting* (1996).
14. Monin, G., Recent methods for predicting quality of whole meat, *Meat Science*, *62*, S231 (1998).
15. Jansen, M. L., Determination of meat pH – temperature relationship using ISFET and glass electrode instruments, *Meat Science*, *58* (2001).
16. Karlsson, A. H., and Rosenvold, K., The calibration temperature of pH-glass electrodes: significance for meat quality classification, *Meat Science*, *62* (2002).
17. Pearson, A. M., and Young, R. B., *Muscle and Meat Biochemistry. Food Science and Technology. A series of Monographs*, Elsevier Science & Technology Books (1989).
18. Lawrie, R. A., *Meat Science. Fourth Edition.*, Pergamon International Library (1985).

19. Warriss, P. D., and Brown, S. N., Pig welfare and meat quality: A United Kingdom view., in *1st Conference Virtual Internacional sobre Qualidade de Cairne Suina* (2000).
20. Driessen, B., and Geers, R., Stress during transport and quality of pork. A European View., in *1st Conference Virtual Internacional sobre Qualidade de Cairne Suina* (2000).
21. Gregory, N., *Processing Factors Influencing pH Values*, American Meat Science Association (2000).
22. Maribo, H., Olsen, E. V., Barton-Gade, P., Moller, A. J., and Karlsson, A. H., Effect of Early Post-Mortem Cooling on Temperature, pH fall and Meat Quality in Pigs, *Meat Science*, 50 (1998).
23. Grandin, T., *Animal Handling Troubleshooting Guide: Tips for Solving Common Animal Handling Problems* (2000).
24. Russell, R., Meat (pork) Quality/ A total overview: Practical Meat Quality Technology, What is Meat Quality?, in *National Swine Improvement Federation Conference and Annual Meeting* (1997).
25. Offer, G., Modelling of the formation of pale, soft and exudative meat: Effects of chilling regime and rate and extent of glycolysis, *Meat Science*, 10, 155 (1984).
26. van der Wal, P. G., Engel, B., van Beek, G., and Veerkamp, C. H., Chilling pig carcasses: Effects on temperature, weight loss and ultimate meat quality, *Meat Science*, 40, 193 (1995).
27. Taylor, A., Nute, G. R., and Warkup, C. C., The effect of chilling, electrical stimulation, and conditioning on pork eating quality, *Meat Science*, 39, 333 (1995).
28. Monin, G., Lambooy, E., and Klont, R., Influence of temperature variation on the metabolism in situ and after excision, *Meat Science*, 40, 149 (1995).
29. Peters, F., and Peetermans, M., *Temperature Sensors*, Vol. Master Module 8.
30. Skoog, D. A., West, D. M., and Holler, F. J., *Fundamentals of Analytical Chemistry*, Saunders College Publishing (1992).
31. HACCP User Guide, in *Managing the Cold Chain for Quality and Safety. FLAIR-FLOW EUROPE RETUER workshop*, Gormley, R., Ed., The National Food Centre, Dunsinea, Castleknock, Dublin 15, Ireland (1998).
32. Korteum, G., Segall, Z., and Bauer, M., Context-Aware, adaptive wearable computers as remote interfaces to 'intelligent' environments, in *The Second International Symposium on Wearable Computers*, Pittsburgh, Pennsylvania (1998).
33. Bauer, M., Heiber, T., Korteum, G., and Segall, Z., A collaborative wearable system with remote sensing, in *The Second International Symposium on Wearable Computers*, Pittsburgh, Pennsylvania (1998).
34. DeVaul, R. W., Schwartz, S. J., and Pentland, A., MITHril: Context-aware computing for daily life., The Media Laboratory Massachusetts Institute of Technology (2001).
35. Miller, D. W., Wilkes, J. G., and Conte, E. D., Food Quality Indicator Device, in *United States Patent and Trademark Office*, The Government of the United States of America, as represented by the Secretary, Department of Health and Human Services (2002).
36. Diamond, D., Internet-Scale Sensing, *Analytical Chemistry*, 279 (2004).
37. Hunter, D., Silent Technology - The Next Wave. Accenture Insights, Issue No. 5 (2001).

38. LXE, RF/Wireless Basics. An Intro to Wireless Data Collection Networks, Products, Standards and Solutions, LXE Inc. (2003).
39. Madec, F., Geers, R., Vesseur, P., Kjeldsen, N., and Blaha, T., Traceability in the pig production chain, *OIE*, 20, 526 (2001).
40. Gormley, R., Safe Temperature Control for Food, *Food Ireland*, 35 (February 1990).
41. Gormley, R., Fish Chilling and Marketing, *Food Ireland*, 34 (November 1988).
42. Gormley, R., Safety of Chilled Foods, *Food Ireland*, 43 (October 1990).
43. George, M., Managing the Cold Chain for Quality and Safety, Flair-Flow Europe Technical Manual (2000).
44. Gormley, R., The Chill Chain, *Food Ireland* (April 1995).
45. Gormley, R., Temperature Control in the Distribution and Retailing of Chilled Foods, *Food Ireland*, 13 (January 1989).
46. Gormley, R., Chilled Foods in Catering, *Food Ireland*, 42 (March 1989).
47. Gormley, R., Chilled Foods at Retail Level, *Food Ireland*, 43 (September 1989).
48. Olafsdottir, G., Nesvadba, P., Di Natale, C., Careche, M., Oehlenschlager, J., Tryggvadottir, S. V., Schubring, R., Kroeger, M., Heia, K., and Esaiassen, M., Multisensor for fish quality determination, *Trends in Food Science & Technology*, 15, 86 (2004).
49. Gormley, R., Brennan, M., and Butler, F., Upgrading the Cold Chain for Consumer Food Products, Teagasc, The National Food Centre, Dunsinea, Castleknock, Dublin 15 (2000).
50. Gram, L., and Huss, H. H., Microbiological spoilage of fish and fish products, *International Journal of Food Microbiology*, 33, 121 (1996).
51. Dalgaard, P., Mejlholm, O., and Huss, H. H., Application of an iterative approach for development of a microbial model predicting the shelf-life of packed fish, *International Journal of Food Microbiology*, 38, 169 (1997).
52. Dalgaard, P., Buch, P., and Silberg, S., Seafood Spoilage Predictor--development and distribution of a product specific application software, *International Journal of Food Microbiology*, 73, 343 (2002).
53. McKean, J., The importance of traceability for public health and consumer protection, *Revue Scientifique et Technique de l'Office International des Epizooties*, 20, 363 (2001).
54. Moe, T., Perspectives on Traceability in Food Manufacture, *Trends in Food Science & Technology*, 9, 211 (1998).
55. Bonbled, P., Traceability in the food industry: an overview of legal requirements and regulations, and how they affect those working in the industry, *OCL-Oleagineux Corps Gras Lipides*, 7, 406 (2000).
56. Opara, L., and Mazaud, F., Food traceability from field to fork, *Outlook in Agriculture*, 30, 239 (2001).
57. Gac, A., and Durand, M., The cold chain - The traceability concept - Practical applications, *Bulletin de L'Academie Nationale de Medecine*, 185, 301 (2001).
58. Borresen, T., Traceability in the fishery chain to increase consumer confidence in fish products - Application of molecular biology techniques, in *First Joint Trans Atlantic Fisheries Technology Conference. TAFT 2003*, The Icelandic Fisheries Laboratories, Reykjavik, Iceland (2003).
59. Borresen, T., Freideriksen, M., and Larsen, E., Traceability of catch to consumer in Denmark, in *Quality of Fish from Catch to Consumer*, Lutten, J. B., Oehlenschlager, J., and Olafsdottir, G., Eds., Wageningen: Academic Publishers, pp. 93 (2003).

60. Denton, W., Tracefish: the development of a traceability scheme for the fish industry, in *Quality of Fish from Catch to Consumer*, Lutén, J. B., Oehlenschläger, J., and Olafsdóttir, G., Eds., Wageningen Academic Publishers (2003).
61. Olafsdóttir, G., Martinsdóttir, E., Oehlenschläger, J., Dalgaard, P., Jensen, B., Undeland, I., Mackie, I. M., Henehan, G., Nielsen, J., and Nilsen, H., Methods to evaluate fish freshness in research and industry, *Trends in Food Science & Technology*, 8, 258 (1997).
62. Martinsdóttir, E., Lutén, J. B., Schelvis-Smit, A. A. M., and Hyldig, G., Developments of QIM - past and future, in *Quality of Fish from Catch to Consumer*, Lutén, J. B., Oehlenschläger, J., and Olafsdóttir, G., Eds., pp. p265.
63. Dalgaard, P., Freshness, Quality and Safety in Seafoods, Flair-Flow Europe Technical Manual, pp. p 6 (2000).
64. Gram, L., and Dalgaard, P., Fish spoilage bacteria - problems and solutions, *Current Opinion in Biotechnology*, 13, 262 (2002).
65. Huss, H. H., Assessment of Fish Quality, in *Quality and Quality Changes in Fresh Fish. FAO Fisheries Technical Paper - 348* (1995).
66. Dalgaard, P., Modelling of microbial activity and prediction of shelf life for packed fresh fish, *International Journal of Food Microbiology*, 26, 305 (1995a).
67. Gram, L., Ravn, L., Rasch, M., Bruhn, J. B., Christensen, A. B., and Givskov, M., Food spoilage--interactions between food spoilage bacteria, *International Journal of Food Microbiology*, 78, 79 (2002).
68. Dalgaard, P., Qualitative and quantitative characterization of spoilage bacteria from packed fish, *International Journal of Food Microbiology*, 26, 319 (1995b).
69. Dainty, R. H., Chemical/biochemical detection of spoilage, *International Journal of Food Microbiology*, 33, 19 (1996).
70. Adams, M. R., and Moss, M. O., *Food Microbiology*, The Royal Society of Chemistry (1995).
71. Baixas-Nogueras, S., Bover-Cid, S., Vidal-Carou, M., and Veciana-Nogues, M., Volatile and nonvolatile amines in Mediterranean hake as a function of their storage temperature, *Journal of Food Science*, 66, 83 (2001).
72. Timm, M., and Jørgensen, B. M., Simultaneous determination of ammonia, dimethylamine, trimethylamine and trimethylamine--oxide in fish extracts by capillary electrophoresis with indirect UV-detection, *Food Chemistry*, 76, 509 (2002).
73. Baixas-Nogueras, S., Bover-Cid, S., Veciana-Nogues, M., and Vidal-Carou, M., Suitability of volatile amines as freshness indexes for iced Mediterranean hake, *Journal of Food Science*, 68, 1607 (2003).
74. Wilkes, J. G., Review: Sample Preparation for the Analysis of Flavours and Off-Flavours in Foods, *Journal of Chromatography, A*, 3 (2000).
75. Schweizer-Berberich, P.-M., Vaihinger, S., and Gopel, W., Characterisation of food freshness with sensor arrays, *Sensors and Actuators B: Chemical*, 18, 282 (1994).
76. Mielle, P., 'Electronic noses': Towards the objective instrumental characterization of food aroma, *Trends in Food Science & Technology*, 7, 432 (1996).
77. O'Connell, M., Valdora, G., Peltzer, G., and Martin Negri, R., A practical approach for fish freshness determinations using a portable electronic nose, *Sensors and Actuators B: Chemical*, 80, 149 (2001).

78. Haugen, J., Electronic noses in food analysis, *Headspace Analysis of Foods and Flavours Advances in Experimental Medicine and Biology*, 488, 43 (2001).
79. Gelman, A., Drabkin, V., and Glatman, L., A rapid non-destructive method for fish quality control by determination of smell intensity, *Journal of the Science of Food and Agriculture*, 83, 580 (2003).
80. Holm, F., Food Quality Sensors, in *Flair-Flow 4 Report*, FoodGroup Denmark, Denmark (2003).
81. Di Natale, C., Olafsdottir, G., Einarsson, S., Martinelli, E., Paolesse, R., and D'Amico, A., Comparison and Integration of Different Electronic Noses for Freshness Evaluation of Cod-Fish Fillets, *Sensors and Actuators B: Chemical*, 77, 572 (2001).
82. Olafsdottir, G., Di Natale, C., and Macagnano, A., Measurements of Quality of Cod by Electronic Noses, in *Quality of Fish from Catch to Consumer*, Luten, J. B., Oehlenschlager, J., and Olafsdottir, G., Eds., Wageningen Academic (2003).
83. Nesvadba, P., Introduction to and outcome of the project "Multi-sensor techniques for monitoring the equality of fish", in *Quality of Fish from Catch to Consumer - Labelling, Monitoring and Traceability*, Luten, J. B., Oehlenschlager, J., and Olafsdottir, G., Eds.
84. Loughran, M., and Diamond, D., Monitoring of volatile bases in fish sample headspace using an acidochromic dye, *Food Chemistry*, 69, 97 (2000).
85. Byrne, L., Lau, K. T., and Diamond, D., Monitoring of headspace total volatile basic nitrogen from selected fish species using reflectance spectroscopic measurements of pH sensitive films, *The Analyst*, 127, 1338 (2002).
86. Byrne, L., Lau, K. T., and Diamond, D., Development of pH sensitive films for monitoring spoilage volatiles released into packaged fish headspace, *Irish Journal of Agriculture and Food Research*, 42, 119 (2003).
87. Ebbing, D. D., and Gannon, S. D., *General Chemistry*, Houghton Mifflin Company, Boston, New York.
88. Denney, R. C., and Sinclair, R., *Visible and Ultraviolet Spectroscopy - Analytical Chemistry by Open Learning*, John Wiley & Sons.
89. Mohr, G. J., *Materials and Polymers in Optical Sensing*, Centre for Chemical Sensors/Biosensors and BioAnalytical Chemistry (2000).
90. Trinkel, M., Trettnak, W., Reininger, F., Benes, R., O'Leary, P., and Wolfbeis, O. S., Study of the performance of an optochemical sensor for ammonia, *Analytica Chimica Acta*, 320, 235 (1996).
91. Werner, T., Klimant, I., and Wolfbeis, O. S., *Analyst*, 120, 1627 (1995).
92. Whiffen, D. H., *Spectroscopy*, Longman Group Limited, London (1996).
93. Atkins, P. W., *Physical Chemistry* (1994).
94. Spichiger-keller, U. E., *Chemical Sensors and Biosensors for Medical and Biological Applications*, Wiley-VCH (1998).
95. Sears, J. K., and Darby, J. R., *The Technology of Plasticisers*, John Wiley & Sons (1982).

## **2 Development of an Autonomous, Wireless pH and Temperature Sensing System for Monitoring Pig Meat Quality**

## 2.1 Introduction

Despite many efforts over the years, there is still very little consensus regarding methods of measuring the physical characteristics of meat and meat products. Many methods have been published but only one procedure to date has been agreed upon internationally, and that is for beef (1). Standardisation of methods is essential if investigations carried out by different groups are to be directly comparable. Thus some agreement should be made regarding methods of measuring the physical quality characteristics of meat and meat products. In an attempt to standardise methods it has been reported that the rate of pH and temperature decline post-mortem, together with the final pH of the muscle along with other conditions at the slaughter plant such as chilling regimes should all be documented (1). As previously discussed, the rate of post-mortem lactic acid production in pig carcasses is closely associated with carcass temperature. In this section, the initial work on capturing pig carcass chilling profiles using self-contained, autonomous temperature sensing units is described. The continual carcass temperature monitoring attempts to show how closely poor carcass chilling rates (affected by chill type, chill location of carcasses, chill density, and chill filling rates etc.) are linked to incidences of PSE in pigs. During the field trials it was soon realised that in order to establish an accurate relationship between carcass chilling rates and the incidence of PSE, detailed analytical data on the rate of pH and temperature decline is needed. This requirement has led to the development of a new wireless battery powered data collection system for monitoring pH and temperature.

### 2.1.1 RF Temperature Monitoring System

The RF Temperature Monitoring System consists of a RF logger unit, a base unit, a 9-volt power supply module, a 9-pin RS232 cable for PC/laptop interface and RF Temperature Logger Control Software (RfTempLogV06), Figure 2-1 and Figure 2-3. The RF temperature logger unit is controlled via the software through the RF base unit, which attaches to the PC/Laptop through the RS-232 port. A 9-volt power pack is included to power the RF base unit, Figure 2-1. The battery lifetime of the RF logger unit depends on the sampling frequency i.e. 1 year with hourly RF communication with the base Unit. The RF transmission frequency is 433MHz and the maximum RF operating range or maximum distance between the base unit and the logger unit for data transfer is approximately 10 metres in free space. The RF logger unit has the memory

capacity to store 32,000 temperature readings. The operating range of the temperature sensor is from  $-18$  to  $85^{\circ}\text{C}$ , resolution  $0.5^{\circ}\text{C}$  and accuracy  $2^{\circ}\text{C}$ .

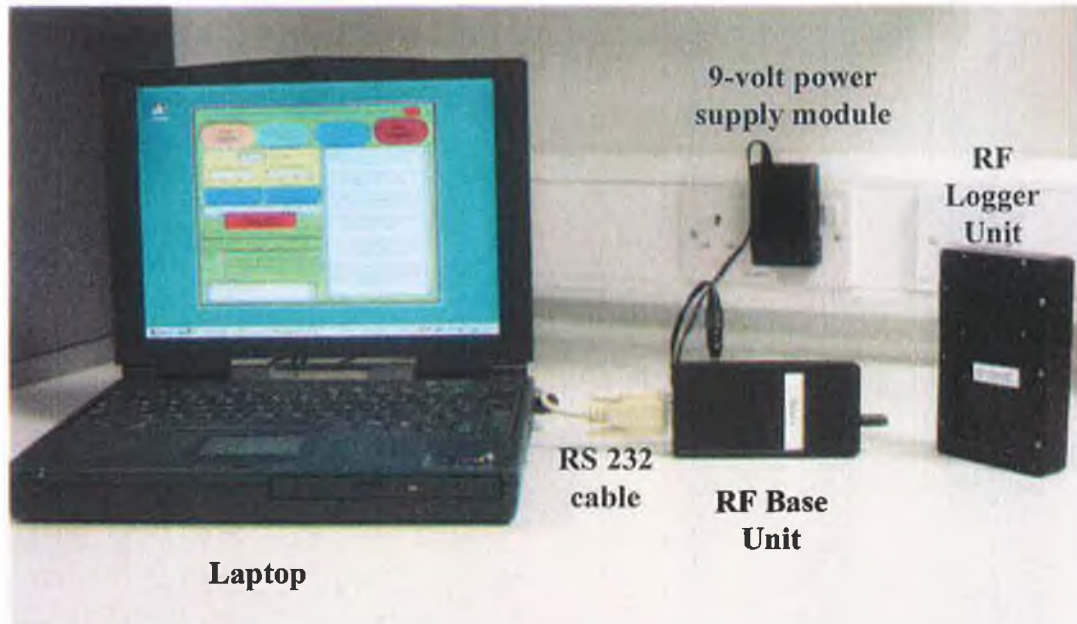


Figure 2-1 The RF Temperature Monitoring System

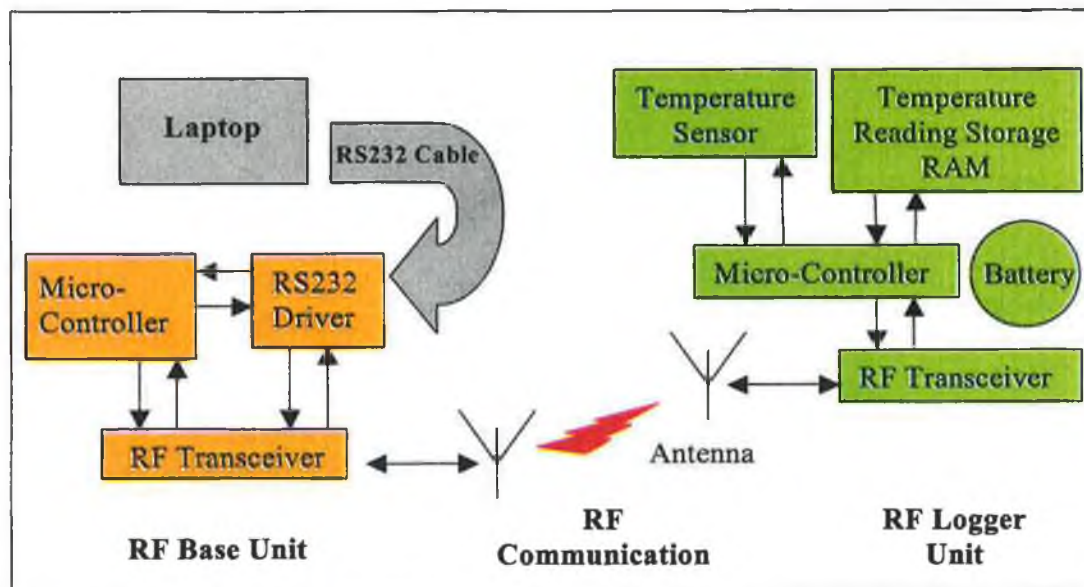


Figure 2-2 Block Diagram of the RF Temperature Monitoring System



### 2.1.1.1 Software and Operating Procedure

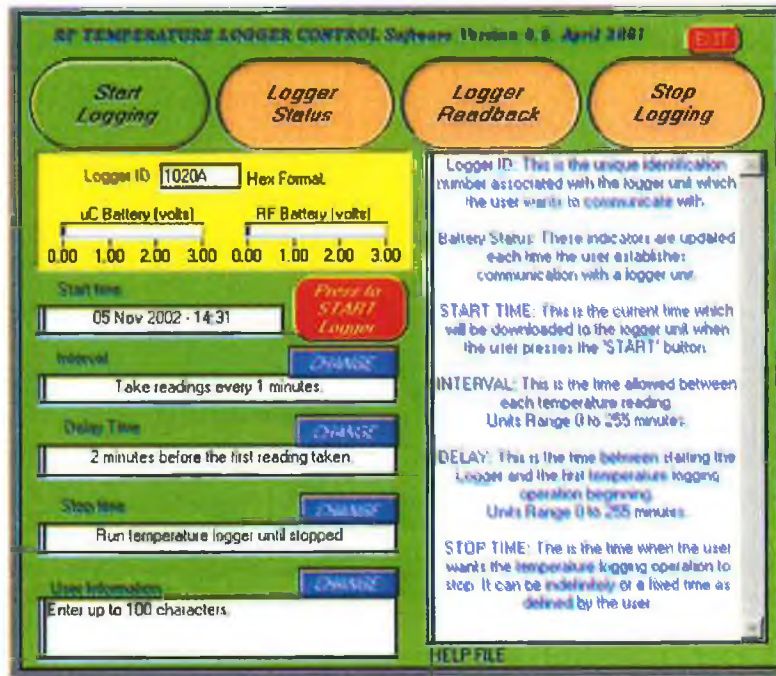


Figure 2-3 The RF Temperature Logger Control Software

Once the software is installed selecting 'Start', 'Programs', 'rftlv06', may access it. A front panel window will open with 4 selection buttons across the top allowing the user to choose the operation required.

'Start logging' operation begins a logging operation in one of two modes, Mode 1 logging for a predefined duration, or Mode 2 logging indefinitely until stopped by the user.

'Logger Status' Mode 3 allows the user get an update on a loggers current operating mode without interfering with the current operation of the logger.

'Logger Readback' Mode 4 allows the user get a more complete update on a loggers current operating mode without interfering with the current operation of the logger. This mode will return a graph of all temperatures recorded to date and allows the user the option to save an ASCII text file of this data for entry into a data analysis package.

'Stop Logging' Mode 5 allows the user stop an active logging session. This will stop both modes 1 or 2 operation regardless of the current status.

### 2.1.1.2 RF Temperature Logger Design

Robust packaging is one of the most important requirements of the RF temperature logger unit. The unit must be sealed (in accordance with IP67 or IP68 rating (2)) able to function in hostile environments whether it is completely submerged in water or is submitted to very moist conditions as in cold storage. As a result a number of methods and different types of packaging were tested.

Initially the circuit boards and power supply (2 AA Batteries) were placed in Datec-Pocket Boxes (Part No: A9072119) with sealing IP65 (protection against spraying water), Figure 2-4a. IP65 rating is not sufficient protection for very wet conditions. To ensure maximum protection these boxes were then sealed with translucent sealant, Figure 2-4b, and finally with black insulating tape Figure 2-4c. Although the boxes are completely sealed, this method will only suffice for short-term use. For applications that require temperature monitoring over a longer period of time i.e. up to 1 year, a more robust package is required. For this reason a new completely waterproof box was specifically designed Figure 2-5. As the temperature sensor chip (AD7814) is integrated onto the circuit board inside the box, it is important to design a robust box that sufficiently seals the circuit without compromising the temperature response time.



**Figure 2-4 Illustrates complete sealing of the Datec-Pocket boxes (6.5 × 12.0 × 2.2 cm) a. OKW enclosure with seal b. silicon used to completely seal the box c. tape ensures maximum protection**

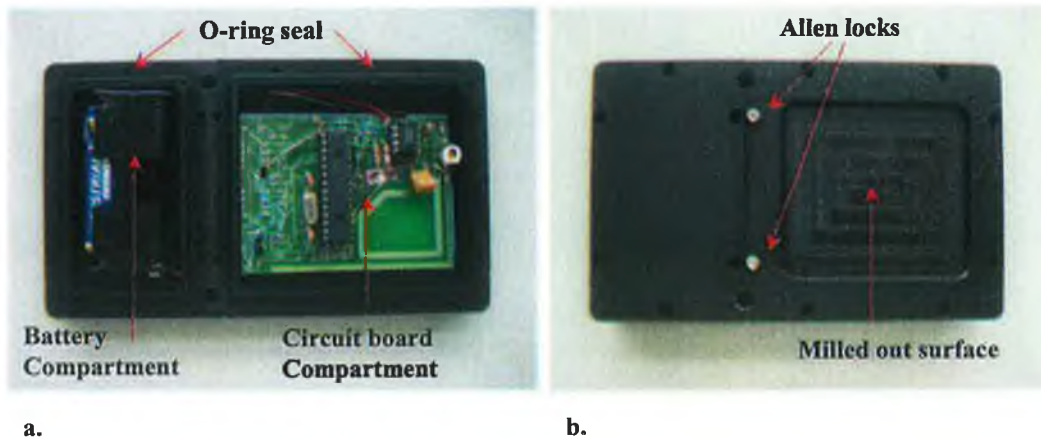


**Figure 2-5** The specially designed waterproof box ( $8.4 \times 14.2 \times 2.5$  cm) with an o-ring seal a. robust box with two separate compartments b. 14 allen locks secure the lid in place and exerts pressure on the o-ring to form a tight seal. The temperature sensor is integrated onto the circuit board so the surface of the box was milled out to reduce the thickness of the box to maximise temperature response times

### 2.1.2 pH and Temperature Correlation

pH measurements are highly temperature dependent and this is especially important when pH is used to predict meat quality. For accurate pH measurements, electrodes must be carefully calibrated and the sample temperature noted. Today, most electrodes have a temperature sensor (thermistor) embedded in the body. The signal from the thermistor is fed back into the meter electronics to provide temperature compensation for changes in the Nernst slope factor. However, this feature is unfortunately not included in the spear type electrode sourced for this project to perform pH measurements in meat and penetrable solids (KCMSW11/KNIPHE; Thermo Russell, Auchtermuchty, Fife, Scotland), Figure 2-7. A specialist logger was designed specifically for this application, Figure 2-6, and has several input channels allowing the pH and temperature of the sample (meat) to be accurately recorded. It also has an additional temperature input channel that records ambient temperature changes. For example, this unique feature allows the effects of the surrounding temperature environment (i.e. chill room temperature) on the carcass to be evaluated while simultaneously measuring the core carcass temperature near the site of the pH measurements. Finally, commercially available pH meters do not have RF (Radio Frequency) wireless communications and networking capabilities. In contrast, the multi channel pH/temperature logger developed specifically for this project enables real-time temperature profiles to be captured in multiple carcasses from almost immediately after slaughter, through out the various processing stages, and particularly in cold storage. The use of a localised Low Power Wireless Network (LPWN) of sensing devices allows

this to happen without cumbersome and awkward wiring, and facilitates remote access to the information e.g. via web links web-enabled databases of real-time and archived data.

### 2.1.3 Wireless pH/Temperature Monitoring System

The prototype Wireless pH/Temperature Monitoring System was developed in collaboration with Whistonbrook Technologies, London, UK, specifically for this project. The system includes 2 logger units, a base station and an RS232 cable (links the base station to the PC), Figure 2-6. Each logger unit is powered by 3 AA batteries and comprises a PIC microprocessor, EEPROM memory, a RF transmission module (RF transmission Frequency 433MHz), two temperature sensors (10K3A1 thermistor with a resistance of 10k at 25°C ± 2%, a 5K thermistor with a resistance of 5K at 25°C ± 1%) integrated into two stainless steel probes, and a pH sensor. The combination pH glass electrode fits securely inside a stainless steel knife allowing safe penetration of semi-solid materials, Figure 2-7. The integrated temperature and pH sensors take measurements at one-second intervals (Mode 1 for testing and calibration) or at five-minute intervals (Mode 2 for standard operations).

The base station is powered by 4 AA batteries and comprises a PIC microprocessor, EEPROM memory, a RF receiver module (receiver frequency 433MHz), an RS232 transceiver and a real time clock. When the logging unit is within range of the base station (up to 10 meters) the logger transmits the pH & temperature measurements simultaneously to a base station via the low power RF communications. Each logger has a unique identification code that enables the base station to recognise the incoming data from each logger. Data is received by the RF receiver from the logger as a string of values. The base station then sorts the data by logger id and stores the values on the EEPROM memory chips. The values are also transmitted via the RS232 cable to a PC/Laptop. Visual Basic software is used for data capture and real time traces are displayed. The sensors are designed to monitor the external ambient temperature and the internal muscle pH and temperature of the carcass from the moment it enters the chill room, (see Appendix 1 for circuit board diagrams and software flow charts for both the RF logger and the base station).

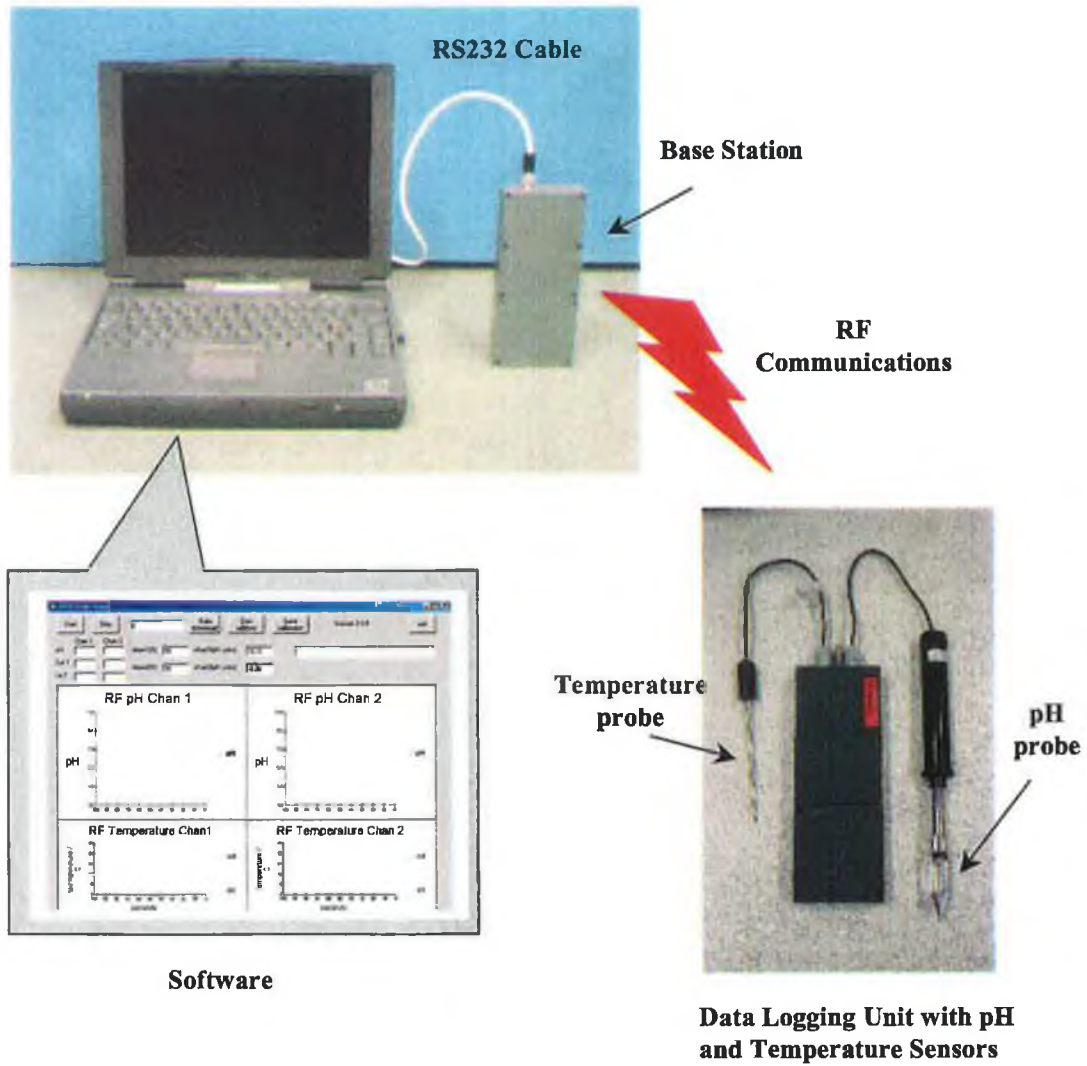


**Figure 2-6 Wireless pH/Temperature Monitoring System consists of a pH probe and 2 temperature probes attached to an RF data logging unit which transmits the pH and temperature data to the RF base station via low power radio frequency communications. An RS232 cable connects the RF base station to a laptop where the pH and temperature data are displayed in Visual Basic software.**

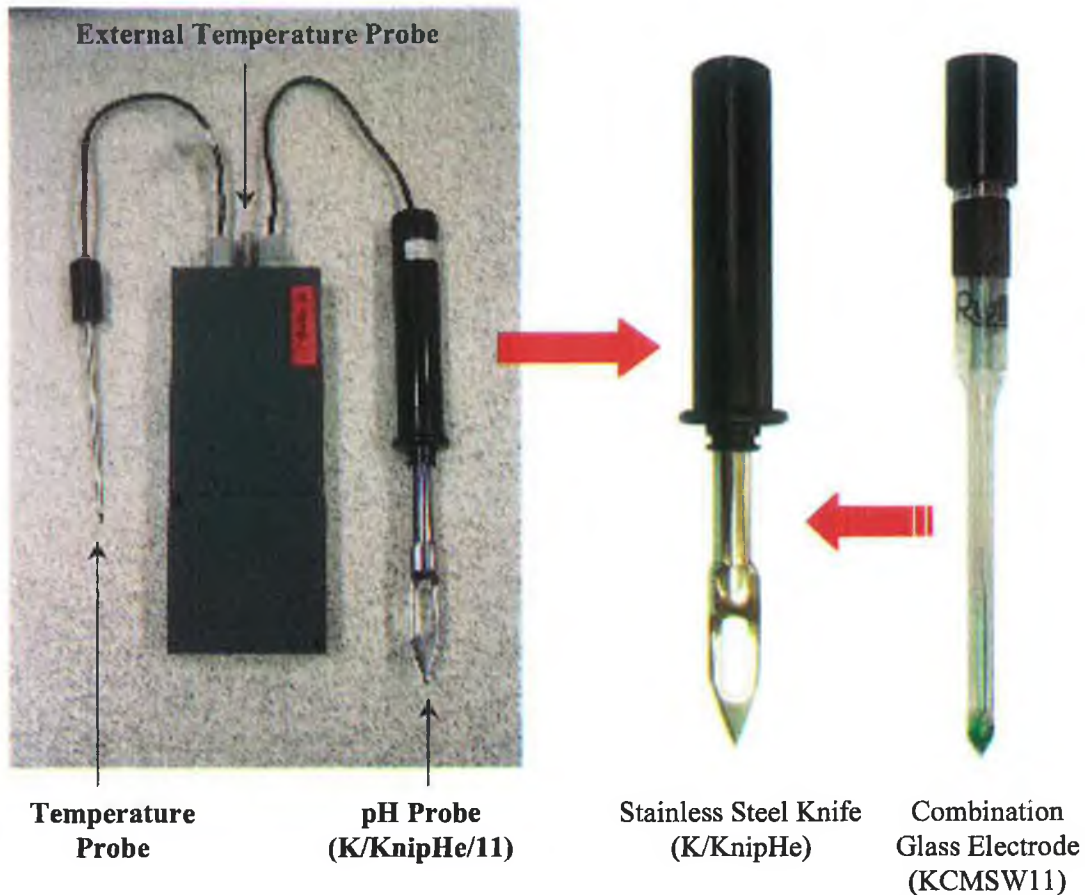


**Figure 2-7 Data logger with pH and temperature probes. The combination glass electrode (KCMSW11) fits securely inside a stainless steel knife (K/KnipHe) allowing safe penetration of semi-solid products i.e. meat products**

## 2.2 Experimental

### 2.2.1 Measuring the Sensor Response Time of the RF Temperature Monitoring System

The RF Temperature Monitoring System was programmed to operate in Mode 2 and the sampling frequency was set to 1 minute. The loggers were allowed to equilibrate at room temperature before they were completely submerged into a polystyrene container of ice and water. The time taken for the temperature to reach 90% of the step change was used to determine the response time.

## 2.2.2 Monitoring the Chilling Rates of Pig Carcasses

The Radio Frequency Temperature Monitoring System, Figure 2-1, was used to monitor the chilling rates of the pig carcasses. The accompanying software enables various logger parameters to be set prior to commencing a run (start time, end time, delay). A Gateway Laptop PC was used to collect the experimental data. Post-run data processing was performed using MS-EXCEL '97. Field trials using the RF Temperature Monitoring System were performed with the assistance of the staff at Galtee Meats, Mitchelstown, Co. Cork. The chilling rates of pig carcasses were monitored both directly (complete contact with the meat) and indirectly (measuring the environment i.e. ambient temperature of the chill rooms). The RF Temperature Monitoring System was programmed to operate in Mode 2 and the sampling frequency was set to 1 minute.

### 2.2.2.1 Indirect Temperature Sampling

Sampling points chosen were as follows:

- **1<sup>st</sup> method:** Loggers were placed at various points in the selected chill room i.e. in the centre and outer edge of the chill room. The loggers were placed before the carcasses began entering the chill room.
- **2<sup>nd</sup> method:** Loggers were strapped to the surface of carcasses at selected areas in the chill room, Figure 2-8a. The loggers were attached immediately as the carcass entered the chill room at 45min post-mortem (the time taken for the carcass to reach the chill room after slaughter).

### 2.2.2.2 Direct Temperature Sampling

The loggers were inserted to a depth sufficient to immerse completely the temperature-sensitive part of the logger and to minimise errors due to heat conduction from other areas, Figure 2-8a & Figure 2-8b.

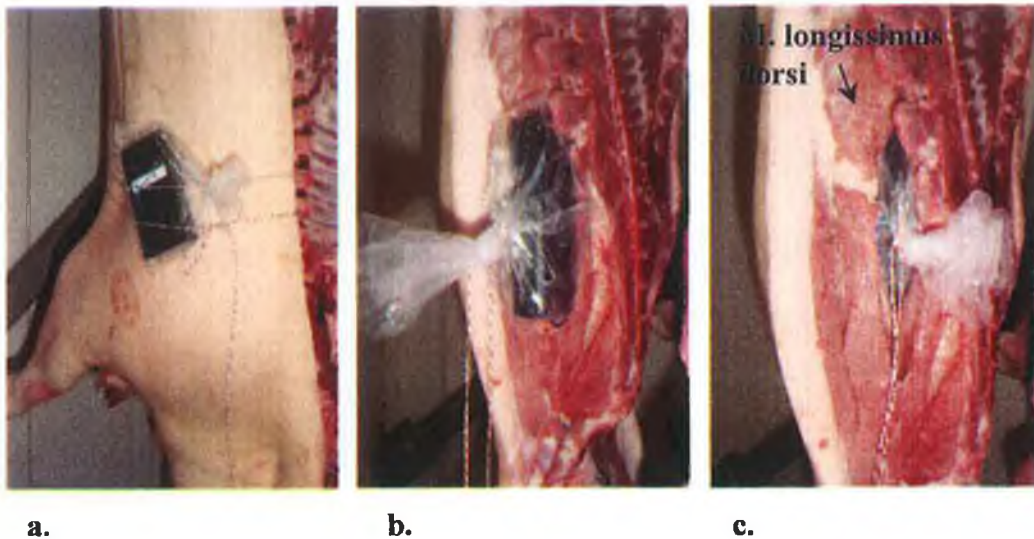


Figure 2-8a. Illustrates the temperature logger strapped to the carcass (indirect sampling). Figure 2-8b & 2-8c show the temperature logger inside the longissimus dorsi muscle (direct sampling)

### 2.2.3 Calibration of the Wireless pH/Temperature Monitoring system

The buffers (pH 4.01 buffer capsules, Product Code BC54, and pH 7.00 buffer capsules, Product Code BC57, Thermo Russell) used in the calibration were traceable to the IUPAC/NIST pH scale. The pH electrodes were supplied with specified pH and temperature values for the pH 4.01 and pH 7.00 buffers used.

#### 2.2.3.1 Slope and Offset Calibration

The pH and temperature probes for both RF data-logging units were placed in the pH 7.00 buffer solution at 25°C. The pH and temperature values of the buffer solution were transmitted every second (Mode 1) via radio frequency communications to the base station connected to the laptop where the Visual Basic software displayed the data in real time. The **offset** was adjusted manually in the software until a pH value equal to 7.00 was displayed on the screen. The same procedure was repeated using the pH 4.01 buffer solution but this time the **slope** was manually adjusted to give a pH value equal



to 4.01. This solution was replaced by the pH 7.00 buffer solution. If the software displayed a pH value equal to 7.00 then the pH probe was calibrated correctly.

#### *2.2.3.2 Temperature Calibration*

The pH 7.00 buffer solution was raised to 50°C. The solution was slowly cooled (approximately 4°C per minute) to 2°C. As the temperature decreased, a pH and temperature reading was transmitted every second (Mode 1) to the laptop where the data was plotted in real-time. The above procedure was carried out for each logger. The change in pH with temperature for the pH 7.00 buffer solution was then compared to the IUPAC specified values for the pH 7.00 buffer solution and the accuracy of the pH probes was determined. This procedure was repeated (n=2) for both loggers 8 months later as a stability study.

#### 2.2.4 Measuring the Temperature Response Time of the Wireless pH/Temperature Monitoring System

The Wireless pH/Temperature Monitoring System was set up in Mode 1 (pH and temperature readings taken every second). The temperature probe was completely submerged in a mixture of ice and water contained in a polystyrene cup. The time/temperature data was recorded and processed.

#### 2.2.5 RF Loggers and Base Station Set-up

The trials took place in selected chill rooms at the Galtee Meats abattoir, Mitchelstown, Co. Cork. Before commencing each trial run the pH and temperature probes of loggers 1 & 2 were calibrated in Mode 1 as per section 2.2.3.1 above. The loggers were then set to the standard operating mode (Mode 2) where the pH and temperature inputs were sampled at 5-minute intervals. For each trial run two carcasses were selected as the carcasses entered the chill room, approximately 45 minutes post-mortem (this is the approximate time taken for the carcasses to reach the chill following slaughter) using an independent pH probe (Description: SenTix SP pH penetration probe). The probe was calibrated in buffers pH 4.01 and pH 7.00 (pH 4 buffer, BC54: pH 7 buffer, BC57: Thermo Russell) before taking measurements. The criteria for selecting carcasses were as follows: PSE carcass – pH<5.8 at 45 minutes post-mortem; Normal or DFD carcass –

pH > 6.0 at 45 minutes post-mortem. The pH electrode was inserted ~10cm into the longissimus dorsi muscle at the height of the 10<sup>th</sup> dorsal vertebrae, near the fat layer. When the pH probe equilibrated a pH reading was recorded.

The position of the base station in the chill room relative to the loggers was very important. In these trials the distance between the loggers and the base station was kept to a minimum i.e. ~ 1 meter. The base station was secured to the wall of the chill room at an equal height from the ground (or slightly higher/lower) to that of the loggers, which were attached to carcasses, Figure 2-9. The carcasses were placed side by side in the chill room (on the outer edge) directly in front of the base station with no interfering carcasses. The pH and temperature probes were inserted ~ 10cm into the longissimus dorsi muscle. A LED on the base station indicated that both loggers were transmitting data. The loggers remained attached until they were removed the next day (up to 24 hours later) as the carcasses left the chill room for further processing.

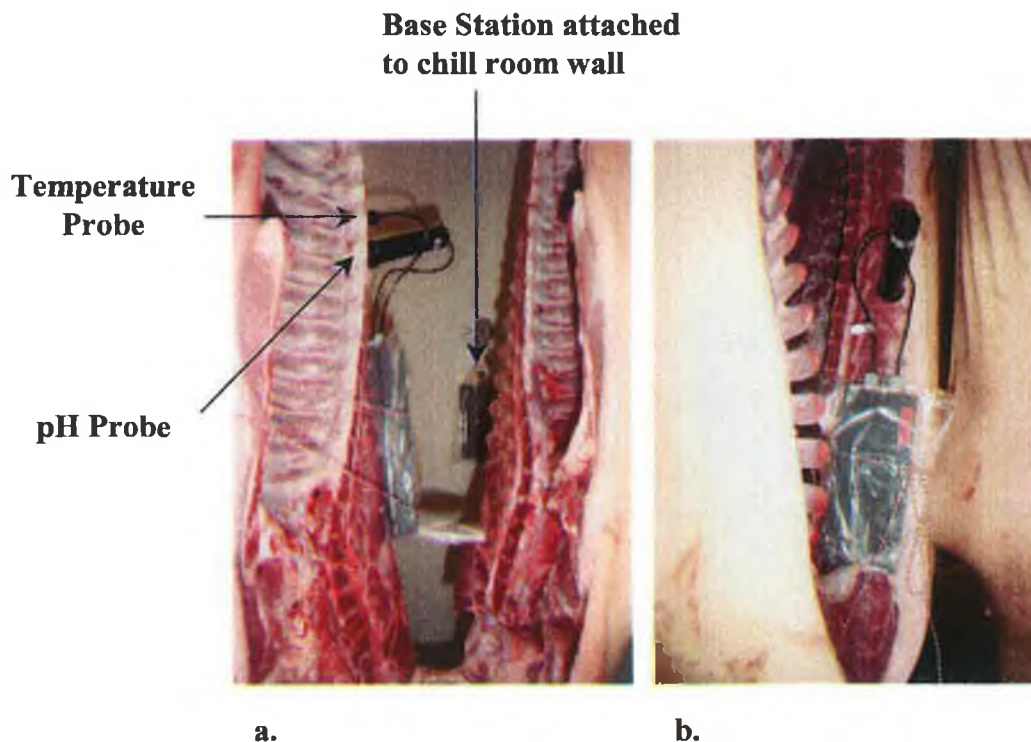


**Figure 2-9** Illustrates the pH and temperature monitoring system in operation. The pH probes are inserted to a depth of ~10cm into the longissimus dorsi muscle. The RF logger takes a pH and temperature reading every 5 min and transmits this data to the RF base station on the wall.

## 2.3 Results and Discussion

### 2.3.1 Measuring the Sensor Response Time of the RF Temperature Monitoring System

Figure 2-10 indicates that when the RF temperature logger was submerged in a polystyrene container of iced water it reached 90% of the step change in ~8 minutes. The initial temperature ( $T_i$ ) was taken as 20.5°C and the final temperature ( $T_f$ ) was 0°C, the temperature of iced water. Therefore, a step change of 90% ( $T_{90}$ ) is equivalent to 2.1°C.

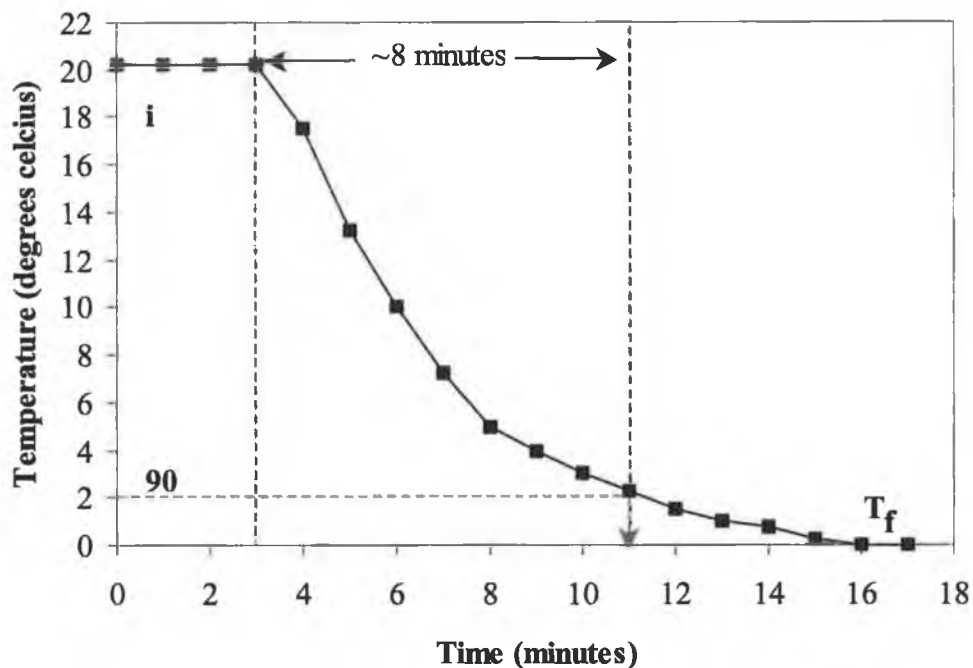


Figure 2-10 Illustrates the temperature response time for the RF Temperature Monitoring System. The temperature reached 90% of the step change ( $T_{90}$ ) in ~ 8 minutes.  $T_i = 20.5^\circ\text{C}$ ,  $T_f = 0^\circ\text{C}$  (iced water), therefore  $T_{90} = 2.1^\circ\text{C}$ .

## 2.3.2 Monitoring the Chilling Rates of Pig Carcasses

### 2.3.2.1 Indirect Temperature Sampling

The loggers were placed in the chill rooms to monitor the ambient temperature and to compare the ambient temperatures of different chill rooms. The ambient temperatures of three different chill rooms on three different days were compared, Figure 2-11. The graph clearly shows the variability of the ambient temperatures between the different chill rooms. All three loggers were placed in similar positions i.e. on the wall of the chill room. During the initial period there are large temperature fluctuations in all three chill rooms. There are two reasons for this. Firstly, the temperature increases as warm carcasses fill the chill room. Secondly, an initial defrost-freeze-defrost process slowly chills the carcasses. During the blast freeze process the ambient temperature can fall below  $-5^{\circ}\text{C}$  and during the defrost period the ambient temperature rises to approximately  $10^{\circ}\text{C}$ . Loggers were strapped to carcasses as another indirect approach to monitoring the cooling system. Figure 2-12 shows how the ambient/carcass temperature can vary within a chill room. This graph indicates that the ambient temperature in the centre of the chill room is lower than the ambient temperature on the outer region.

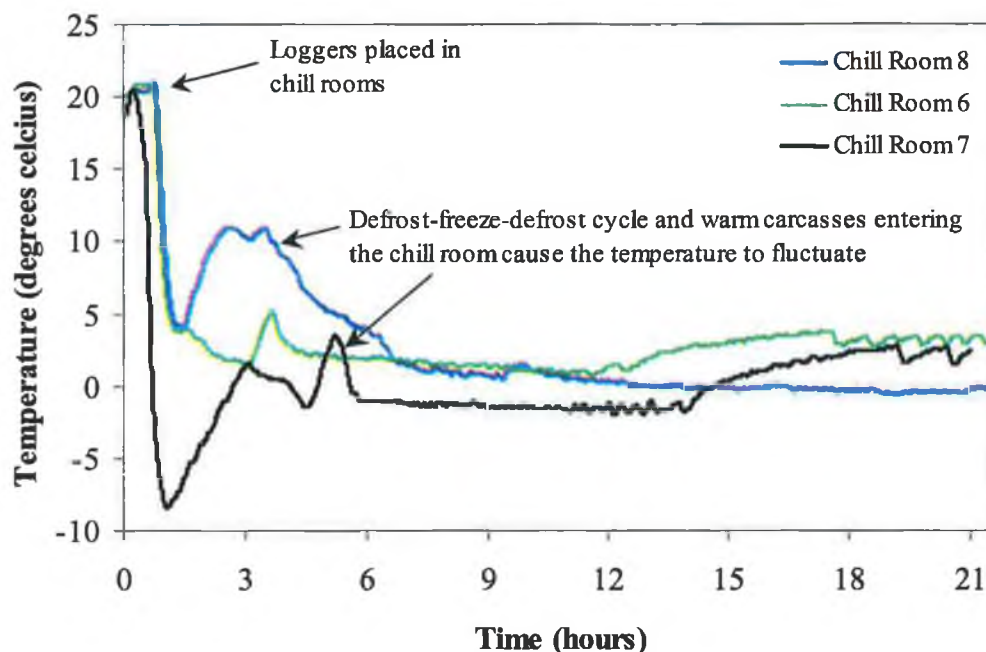


Figure 2-11 Comparison of ambient temperature of 3 different chill rooms on 3 different days

Once again, the temperature fluctuations due to the initial defrost-freeze-defrost process can be seen. The ambient temperature finally equilibrates between 3 and  $4^{\circ}\text{C}$ . The

ambient air temperature is also monitored by Galtee Meats using a temperature probe, which is fixed close to the vents where the freezing air is expelled. The temperature loggers were attached to the warm carcasses. Therefore, this explains the temperature difference in the profiles obtained from the temperature loggers and the Galtee Meats temperature probe.

### 2.3.2.2 Direct Temperature Sampling

The direct sampling approach indicates that the carcass temperature decreases exponentially over time. Figure 2-13 shows the relationship between the ambient temperature and the chilling rates of 2 adjacent carcasses in the same chill. The maximum internal carcass temperature registered by the loggers was  $\sim 35^{\circ}\text{C}$  almost 20 minutes after the loggers were placed inside the carcasses.

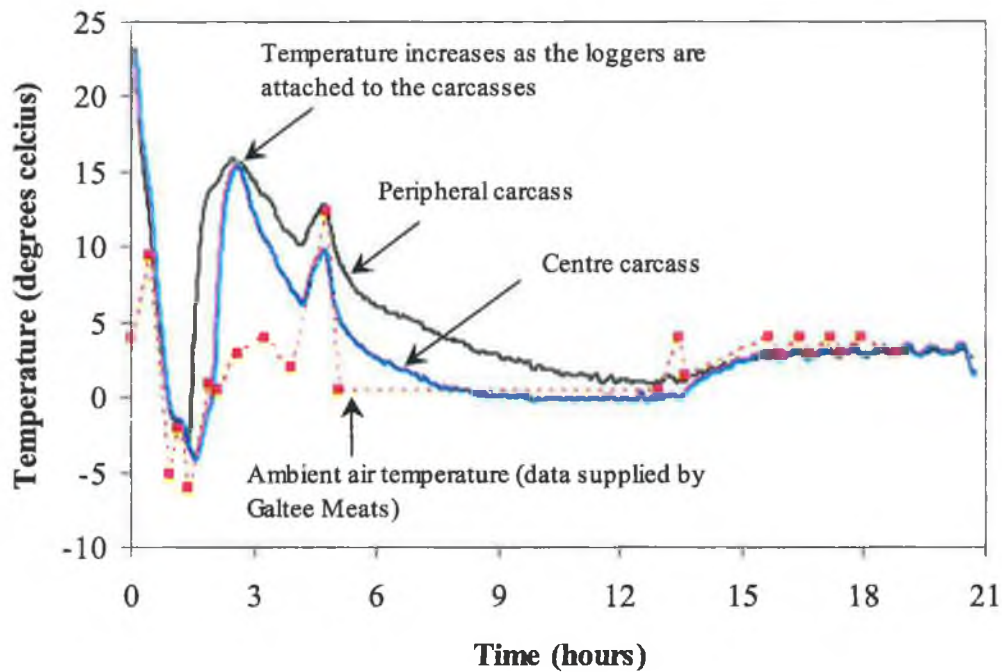
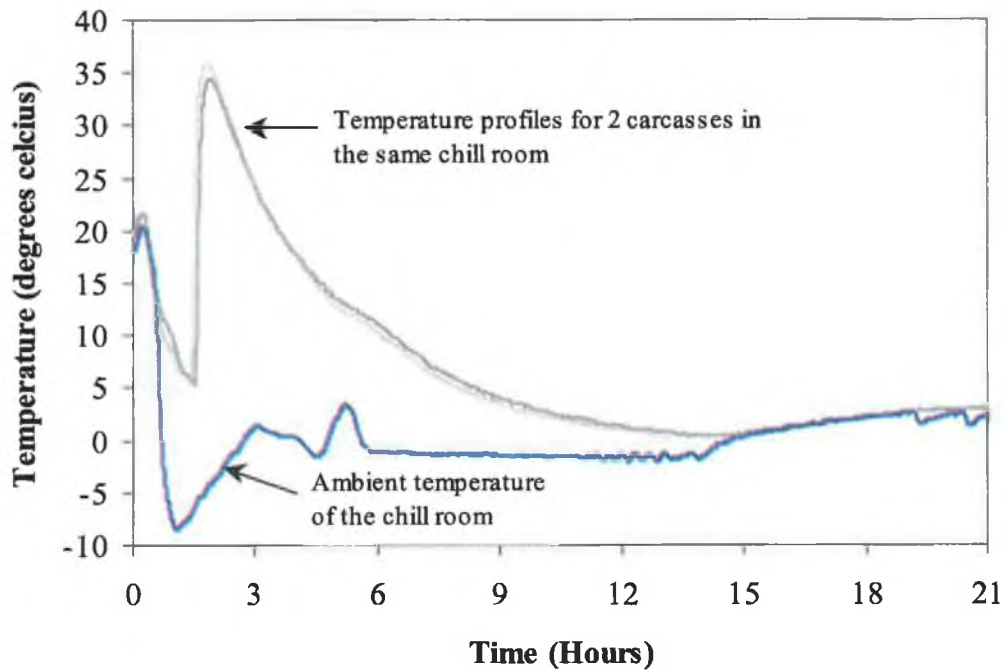


Figure 2-12 Illustrates the variation in ambient/carcass temperature within a single chill room



**Figure 2-13 Shows the cooling curves for 2 carcasses in the same chill room**

Poor chilling at the slaughter plant will increase PSE because the internal temperature of the meat is lowered too slowly. In this project, the autonomous temperature sensors, monitoring time and temperature give an indication of how chill type and carcass location within the chill may have an affect on the chilling rates of carcasses. Temperature can be measured directly (complete contact with the meat) or indirectly (measuring the environment i.e. ambient temperature of the chill rooms). The indirect approach is an easy method and there is no sample destruction. However, measuring ambient temperature alone will not give an accurate internal carcass temperature profile. Furthermore, the ambient temperature varies in a chill room, Figure 2-12. This is due to an uneven distribution of cold air, which will therefore cause the internal temperature of the carcasses to cool down at different rates. Poor air-circulation in specific locations in a chill room will therefore increase the amount of PSE carcasses. Normal carcasses can eventually become PSE if the internal carcass temperature is lowered too slowly.

Figure 2-11 gives the ambient temperatures of three different chill rooms obtained with loggers placed in similar positions i.e. on the walls. The results vary greatly. The ambient temperature for chills 6 & 7 follow similar trends from the beginning where the carcasses enter the chill room to the end where the carcasses leave the chill room. The graph shows that chill room 7 is a few degrees lower during the entire temperature

trace. On the other hand, the temperature profile for chill room 8 varies dramatically with ambient temperatures as high as 11°C at the beginning while the chill room is being filled to below 0°C for the last 9-10 hours. During the last 9-10 hours of the temperature trace for chill rooms 6 & 7 the temperature equilibrates between 3 & 4°C. The varying ambient temperature for all three chill rooms indicates a lack of accurate and precise temperature control. Slower cooling rates allow a longer period for lactic acid production, and can result in PSE where previously there may not have been any. The other extreme, very rapid chilling may reduce PSE incidence to a certain degree but other aspects of meat quality would be compromised, see section 1.1.4. Therefore, there is a need for temperature control in the chill rooms.

By inserting the loggers into the carcass to a depth sufficient to immerse completely the temperature-sensitive part of the logger, a more accurate temperature profile of the internal carcass temperature can be obtained, Figure 2-13. The RF Temperature Logger is relatively large (12cm × 6.5cm × 2.2cm) and the temperature sensor is embedded on the circuit board inside the protective box. The air pocket inside the box must first be heated to the temperature of the carcass resulting in a sluggish response time. The response time for this particular application is too slow as it took almost 20 minutes for the logger to register the internal carcass temperature, Figure 2-13. This method of sampling is destructive and unappealing to the meat industry.

The internal carcass-chilling rate has been measured using an autonomous temperature monitoring system designed and developed by the NCSR and Analog Devices, Limerick. Limitations and challenges presented by the RF Temperature Monitoring System have been identified during the field trials. To overcome the limitations a unique Wireless pH/Temperature Sensing System has been developed that not only monitors internal carcass chilling rates with excellent temperature response times and minimum sample destruction it also monitors intramuscular pH. The results obtained by the Wireless pH/Temperature Sensing System are displayed in the following section.

### 2.3.3 Measuring the Temperature Response Time of the Wireless pH/Temperature Monitoring System

Figure 2-14 shows that when the temperature probe was submerged in a polystyrene container of iced water it reached 90% of the step change in 5 seconds. This is a dramatic improvement in the temperature response time compared to ~8 minutes for the RF Temperature Monitoring System Figure 2-10.

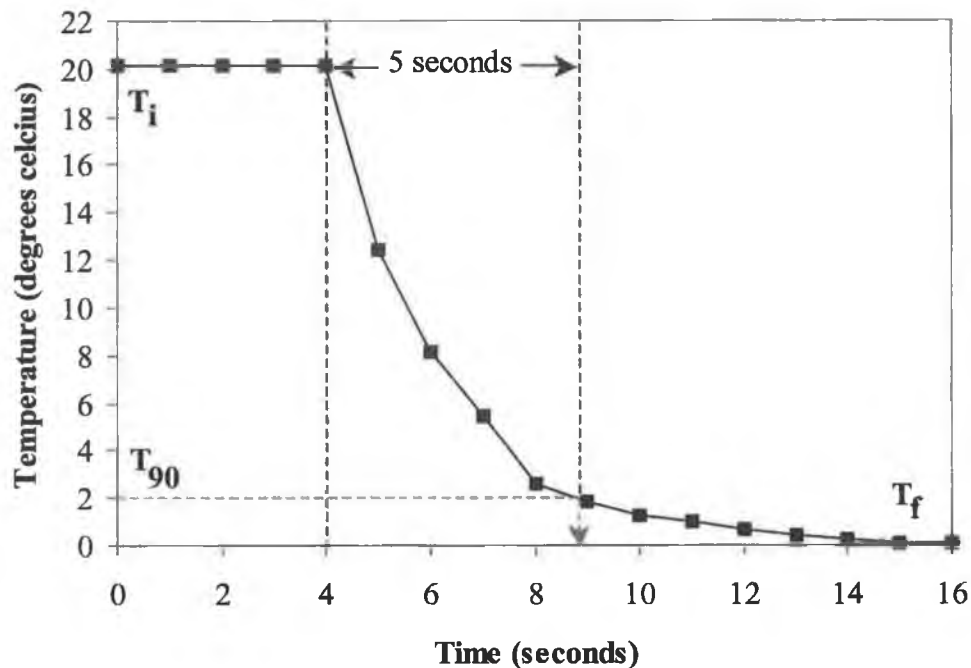


Figure 2-14 Illustrates the temperature response time of the Wireless pH/Temperature Monitoring System. The temperature reached 90% of the step change ( $T_{90}$ ) in 5 seconds.  $T_i = 20.10^\circ\text{C}$ ,  $T_f = 0^\circ\text{C}$  (iced water), therefore  $T_{90} = 2.0^\circ\text{C}$ .

### 2.3.4 Calibration of the Wireless pH/Temperature Monitoring System

The determination of the temperature dependence of buffer pH 7.00 was carried out using the Wireless pH/Temperature Sensing System according to the experimental procedure outlined. The results were then compared to the IUPAC values of the temperature dependence for buffer 7.00 (values are traceable to the IUPAC pH scale; Radiometer). Electrodes cannot be produced with exactly identical characteristics and different manufacturers produce different electrodes. The results from these studies prove that the pH probes of loggers 1 & 2 performed well and with great similarity. The results show that the pH probes perform closely to the IUPAC pH scale. This allows valid comparisons of meat pH and temperature measurements between different carcasses to be made.



### 2.3.4.1 Logger 1 Calibration

Figure 2-15 shows the experimental pH and temperature relationship for a pH 7.00 standard buffer solution over the temperature range 0°C to 50°C. This illustrates the temperature dependence of pH and the possible error associated with it if the data is not corrected to the 'true' IUPAC values.

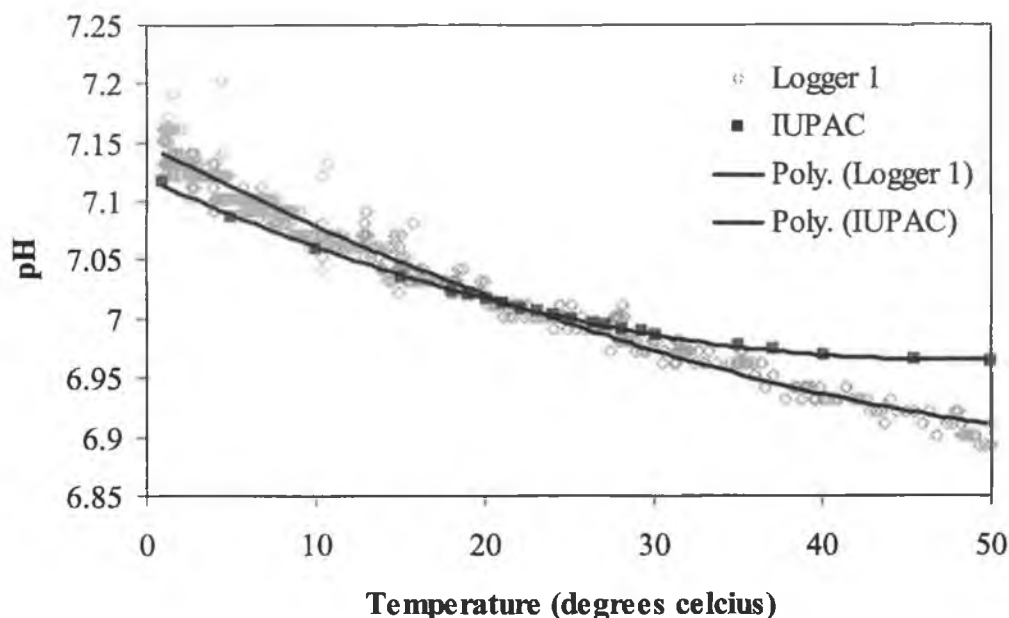


Figure 2-15 The pH and temperature relationship for a pH 7.00 standard buffer solution over the temperature range of 0-50°C demonstrated using the pH and temperature probes of logger 1 – see Appendix 1-6 for experimental data.

A polynomial curve is the best fit for both sets of data. The polynomial equations are as follows:

$$\text{Logger 1: } y = 5 \times 10^{-5} x^2 - 0.0075x + 7.1592 \quad \text{Equation 2-1}$$

$$\text{IUPAC: } y = 7 \times 10^{-5} x^2 - 0.0063x + 7.1167 \quad \text{Equation 2-2}$$

The above polynomial equations relate the pH of the standard buffer pH 7.00 with temperature over the range 0°C to 50°C. By substituting the x values in the above equations with temperature values ranging from 0°C to 50°C (see Appendix 1-6) the curves in Figure 2-16 are obtained.

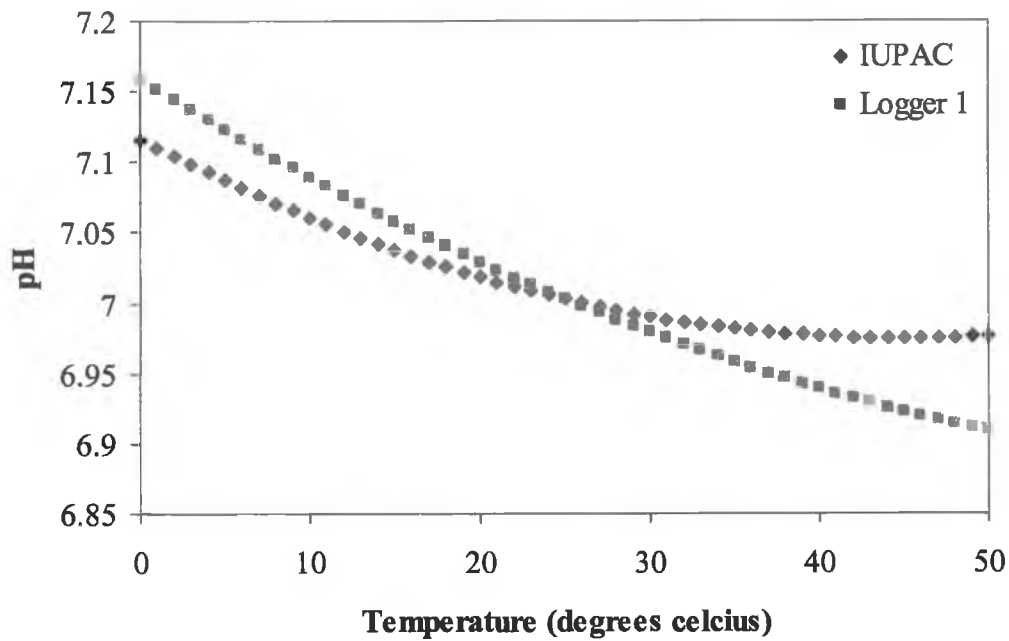


**Figure 2-16 Compares the temperature dependence for pH 7.00 standard buffer using logger 1 with the IUPAC pH scale**

The pH probe of logger 1 was corrected to the IUPAC values (see Appendix 1-6) and the difference was expressed in the form of a simple equation:

$$Y = 2 \times 10^{-5} x^2 + 0.0012x + 0.00425 \quad \text{Equation 2-3}$$

Equation 2-3 thus represents the correction formula applied to the pH and temperature profiles for logger 1. The same procedure was repeated for logger 2.

### 2.3.4.2 Logger 2 Calibration

Figure 2-17 shows the experimental pH and temperature data for pH 7.00 standard buffer as the buffer solution is heated from ~0°C to 50°C. This illustrates the temperature dependence of pH and the possible error associated with it if the data is not corrected to the 'true' IUPAC values.

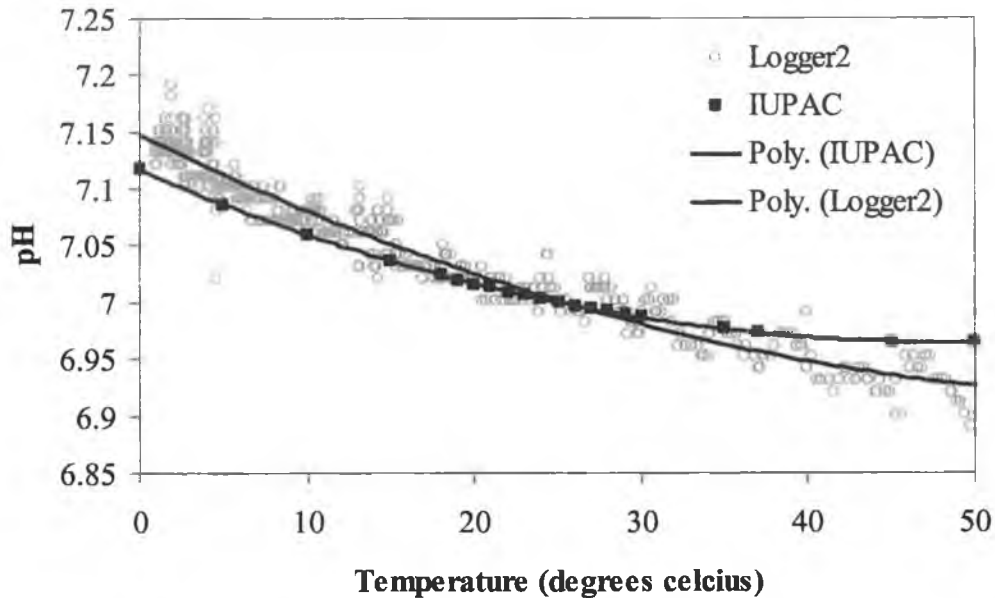


Figure 2-17 The pH and temperature relationship for a pH 7.00 standard buffer solution over the temperature range of 0-50°C demonstrated using the pH and temperature probes of logger 2 – see Appendix 1-7 for experimental data.

A polynomial curve is the best fit for both sets of data. The polynomial equations are as follows:

$$\text{Logger 1: } y = 6 \times 10^{-5} x^2 - 0.0073x + 7.1486 \quad \text{Equation 2-4}$$

$$\text{IUPAC: } y = 7 \times 10^{-5} x^2 - 0.0063x + 7.1167 \quad \text{Equation 2-5}$$

The above polynomial equations relate the pH of the standard buffer pH 7.00 with temperature over the range 0°C to 50°C. By substituting the x values in the above equations with temperature values ranging from 0°C to 50° (see Appendix 1-7) the following curves in Figure 2-18 are obtained.

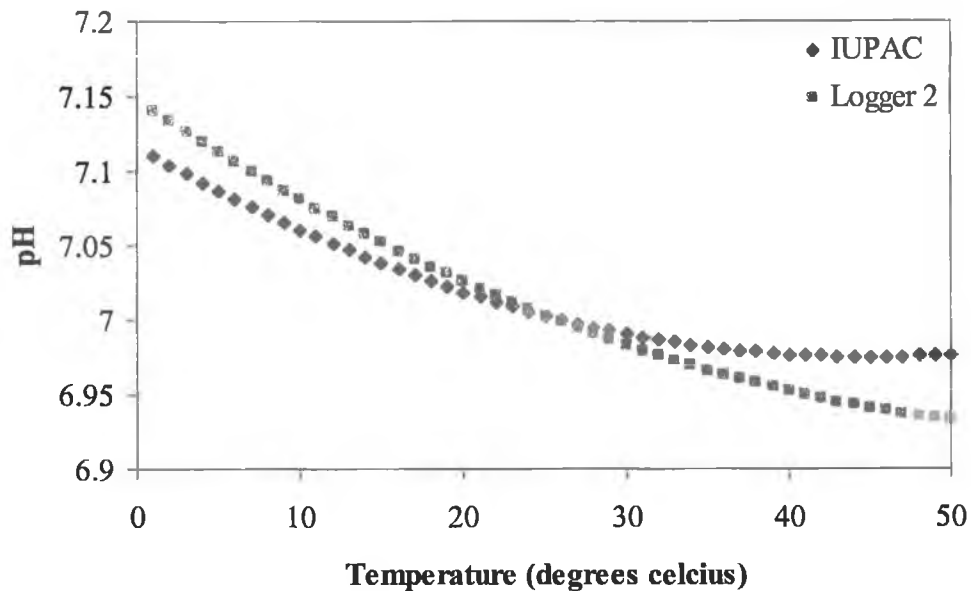


Figure 2-18 Compares the temperature dependence for buffer pH7.00 using logger 1 with the IUPAC pH scale

The pH probe of logger 2 was corrected to the IUPAC values and the difference expressed in the form of a simple equation:

$$Y = 1 \times 10^{-5} x^2 + 0.001x - 0.0312 \quad \text{Equation 2-6}$$

Equation 2-6 is the correction factor applied to the pH and temperature profiles for logger 2.

### 2.3.5 Repeat Calibration Studies

Repeat (n=2) pH-temperature correlation studies were performed 8 months later to evaluate the stability of the pH probes of both loggers, Figure 2-19 and Figure 2-21. The same experimental procedures and data processing techniques were followed as discussed in section 2.2.3. These repeat studies show that both pH probes were very stable considering their repeated use for the pH and temperature monitoring trials carried out at Galtee Meats, Mitchelstown, Co. Cork. The margin of error was very narrow between all three studies for both probes. The standard deviation over the 8-month period was 0.012 pH units for logger 1 and 0.015 pH units for logger 2 over a temperature range of 0°C to 50°C. The measuring temperature range for pig carcasses was approximately between 42°C (initial temperature at ~45 minutes post-mortem) and 3°C (final temperature at ~24 hours post-mortem). The largest standard deviation

between 42°C and 3°C was 0.0069 pH units for logger 1, Figure 2-20, and 0.0096 pH units for logger 2, Figure 2-22. In the meat industry an accuracy of  $\pm 0.05$  pH is often expected (3). As a result of performing the pH and temperature correlation studies and correcting the pH values for temperature effects using easily derived equations, the pH probes were extremely stable during the 8-month period and the error was well below the typical accuracy of 0.05 pH units for meat measurements.

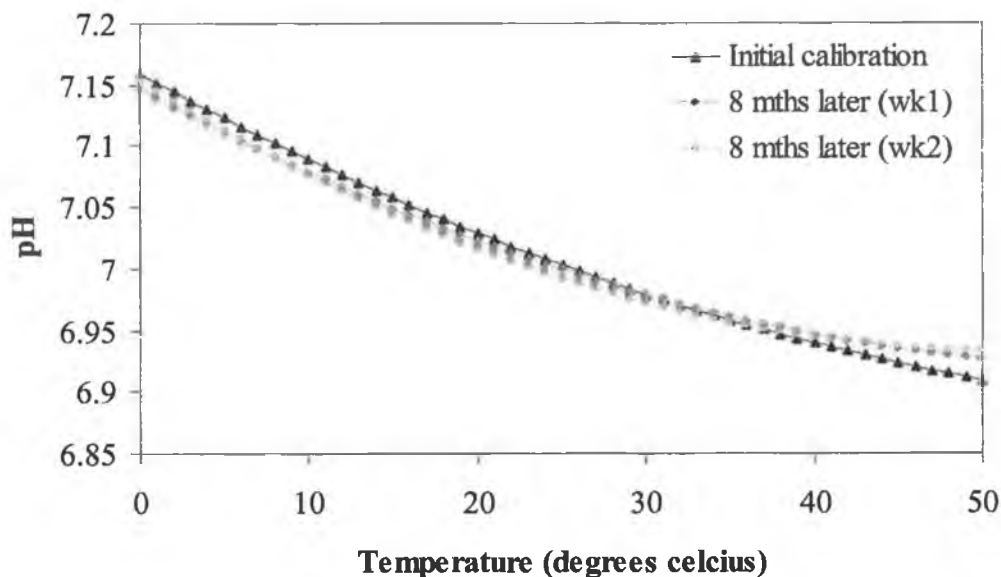


Figure 2-19 Repeat calibrations of logger 1 to illustrate the stability of the pH probe. An initial calibration was performed followed by 2 calibrations 8 months later.

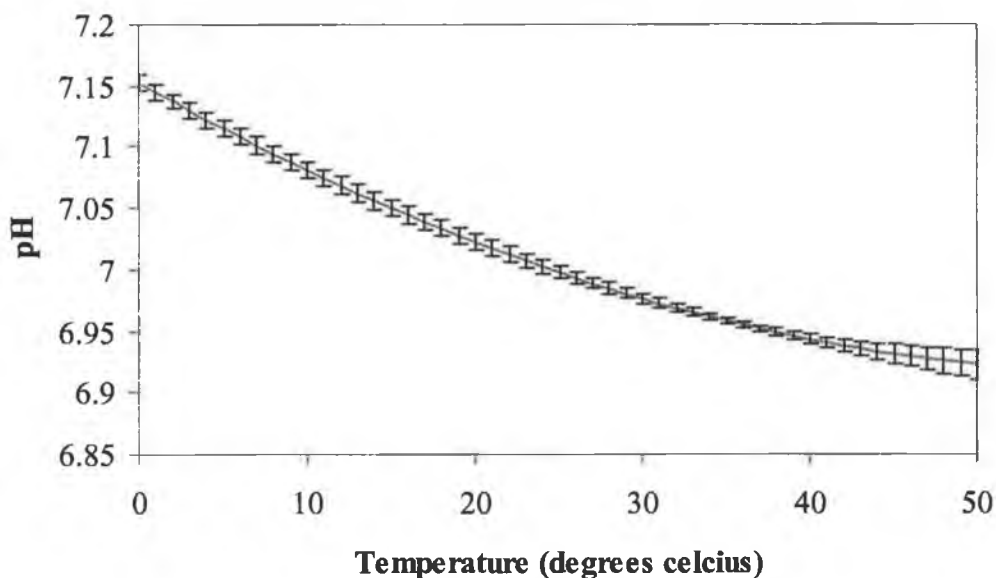
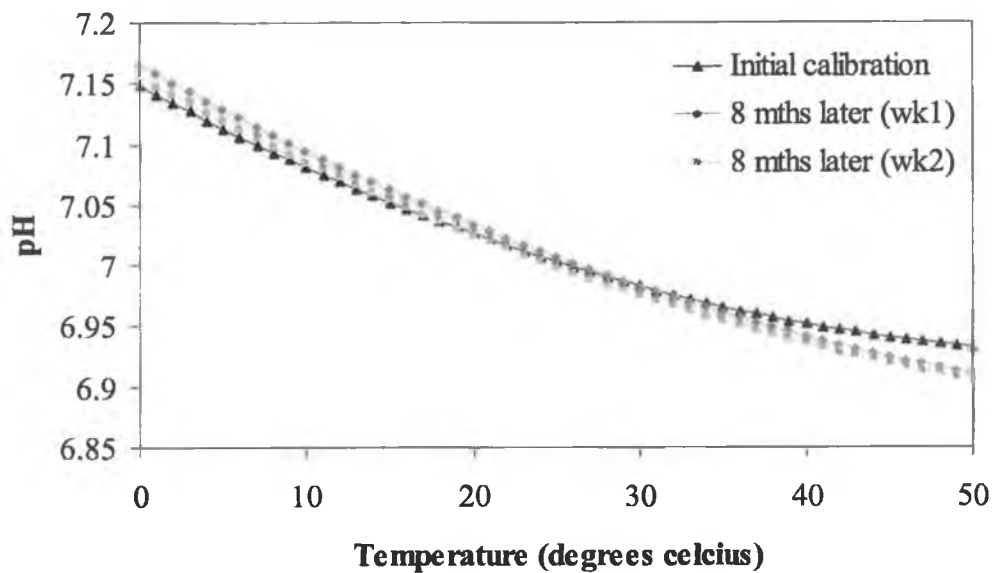
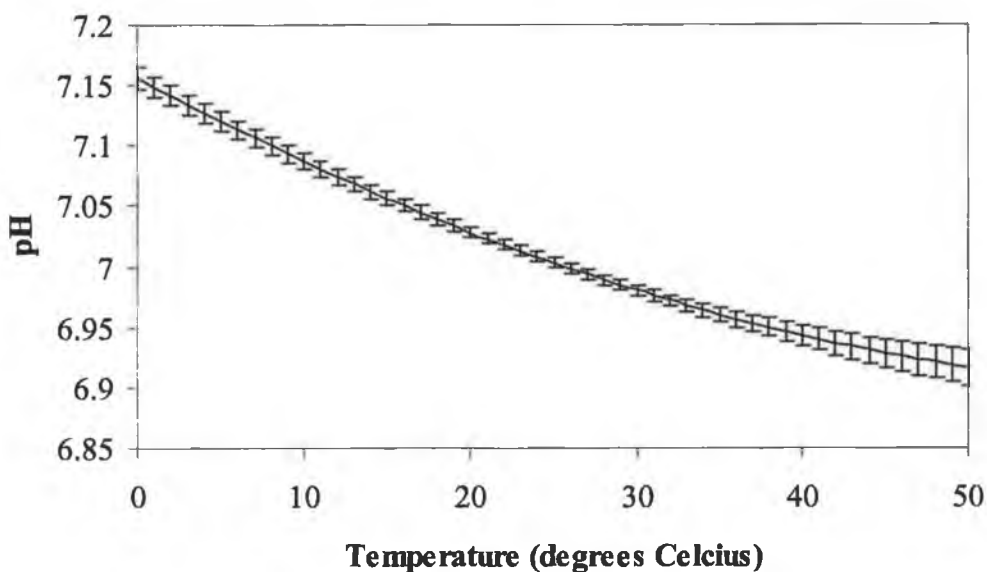


Figure 2-20 Standard deviation curve of all three calibrations for logger 1. As the temperature increases from 0°C to 50°C the pH decreases. The largest deviation occurs at 50°C. STDEV = 0.012 pH, at 50°C pH = 6.92  $\pm$  0.012 (see Appendix 1-8 for STDEV values)



**Figure 2-21 Repeat calibrations of logger 2 to illustrate the stability of the pH probe. An initial calibration was performed followed by 2 calibrations 8 months later.**



**Figure 2-22 Standard deviation curve of all 3 calibrations for logger 2. As the temperature increases from 0°C to 50°C the pH decreases. The largest STDev occurs at 50°C STDEV = 0.015 pH, at 50°C pH = 6.91 ± 0.015 (see Appendix 1-9 for STDEV values)**

### 2.3.6 pH and Temperature Monitoring of Pig Carcasses

As already discussed in Chapter 1, the rate and extent of post-mortem pH decline has a large affect on meat quality. A rapid rate of pH decline in the immediate post-mortem period results in low quality PSE meat. The extent of pH decline at 24 hours post-mortem (pHu) will also affect meat quality. A high ultimate pH (above 6.1) will likely result in meat that is DFD. The results in this section will show how the Wireless pH/Temperature Sensing System helps demonstrate this effect.

Three Large White x Landrace carcasses were chosen based on spot pH measurements taken (at 45 minutes post-mortem) as the carcasses enter the chill room – normal carcasses, PSE suspected carcasses and DFD suspected carcasses. The wireless pH/temperature sensors were attached to the carcass at 45 minutes post-mortem and removed the following day as the carcasses left the chill room. The profiles were taken from carcasses placed in different chill rooms on different days. The carcasses were placed in similar positions in all chill rooms i.e. near the outer wall of the chill room.

Figure 2-23 and Figure 2-24 show pH and temperature profiles, over an approximate 20-hour period, of a normal and suspected PSE carcass respectively. The PSE suspected carcass has a high internal carcass temperature (42°C) and very low pH value (~5.5) at 45 minutes post-mortem. The normal carcass displays a gradual decrease of pH from 6.4 to 5.6 over a 20-hour period. Today, pH is generally measured within one hour of slaughter (initial pH or pH<sub>45</sub>) or at 24 hours (ultimate pH or pH<sub>u</sub>) post-mortem. If the initial pH is below 5.8, the pork may be PSE positive because pH dropped both too low and too quickly. This meat will have an ultimate pH value of ~5.6, as demonstrated by the Wireless pH/Temperature Monitoring System in Figure 2-24. In normal muscles the pH drops to ~5.6 at a moderate rate over a prolonged period, as indicated in Figure 2-23. However, both normal carcasses and PSE carcasses end up with similar pH values. On the other hand, meat with an ultimate pH above 6.1 may be classified as DFD, because pH did not drop to normal levels. The pH profiles displayed in Figure 2-25 follow these trends for the DFD, normal and PSE carcasses.

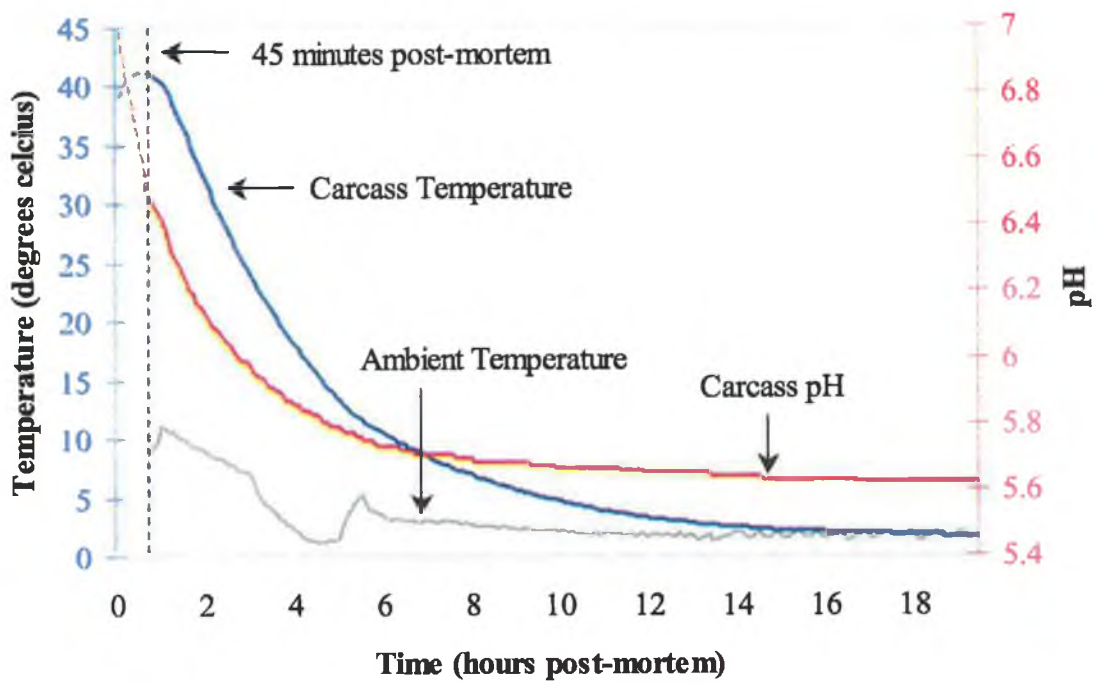


Figure 2-23 Temperature and pH profile of a normal carcass. The pH declines gradually from 6.4 to 5.6 over a 20-hour period.

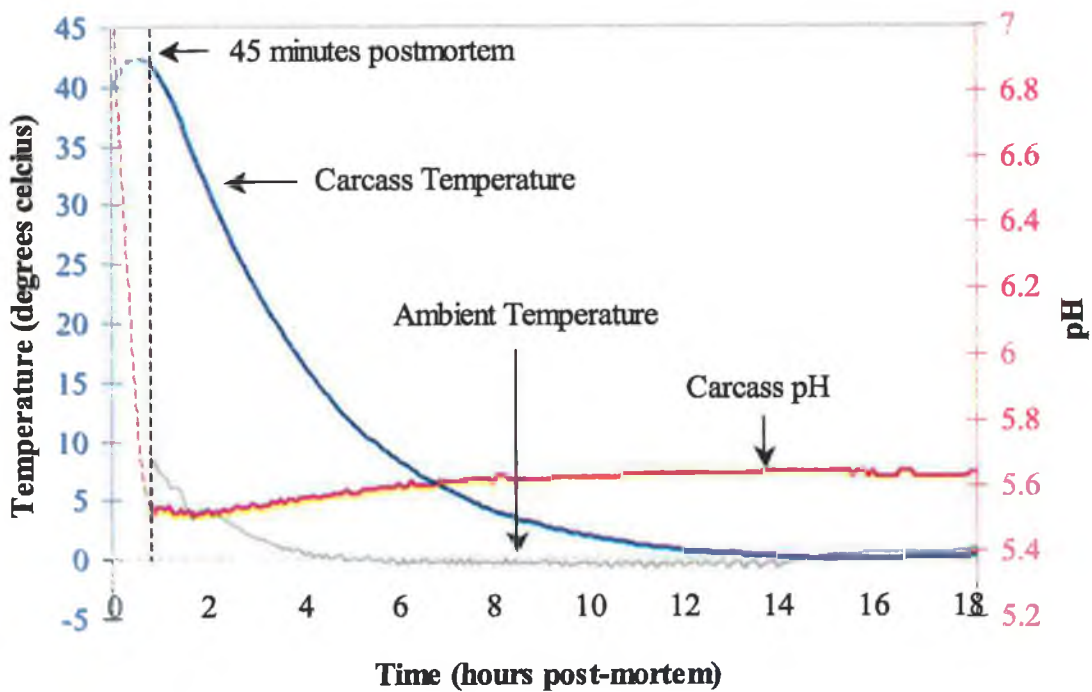
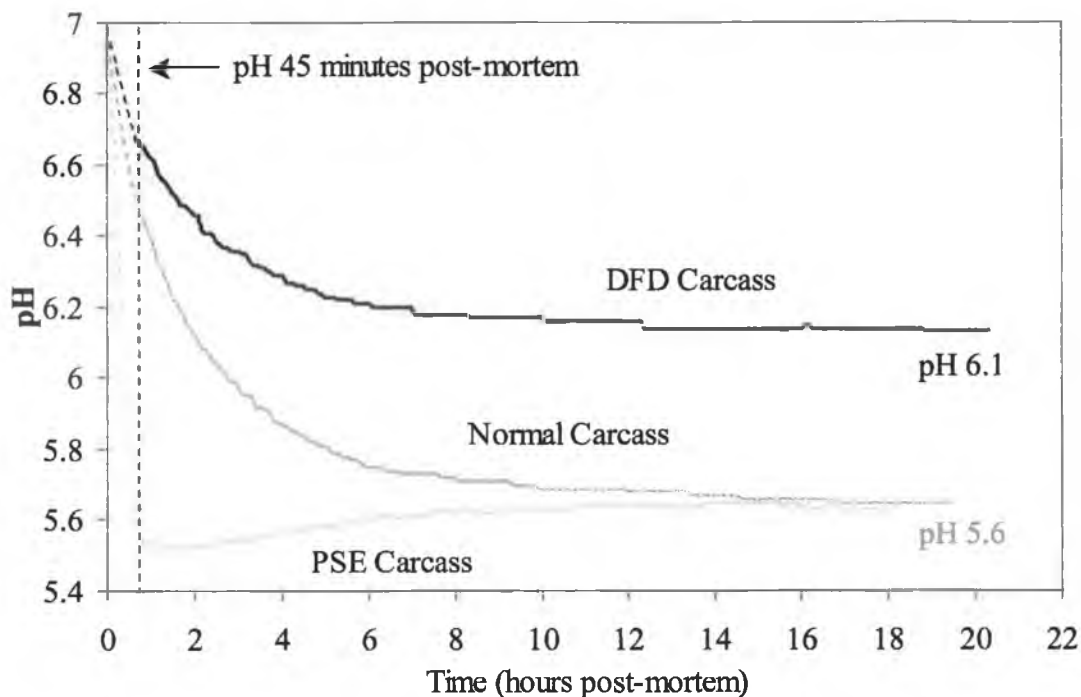


Figure 2-24 Temperature and pH profile of a PSE carcass. The pH is ~5.5 at 45 minutes post-mortem.





**Figure 2-25 pH profiles of PSE, Normal and DFD carcasses. The Normal and PSE carcasses have similar pH<sub>u</sub> values while the DFD carcass has a pH<sub>u</sub> value >6.0.**

From Figure 2-25, at 45 minutes post-mortem, it is possible to distinguish severe PSE carcasses from DFD and normal carcasses. On the other hand, at pH<sub>u</sub> (ultimate pH ~ 20 hours post-mortem) it is possible to distinguish DFD carcasses from PSE and normal carcasses. It would be very difficult to differentiate between normal and PSE carcasses from pH<sub>u</sub> alone as both end up with similar ultimate pH values. In order to discriminate PSE from normal carcasses it would be necessary to know the rate of pH decline for both from 45 minutes post-mortem. Figure 2-25 confirms how misleading a single pH measurement would be either at pH<sub>45</sub> or pH<sub>u</sub>.

There were also a number of shorter pH and temperature profiles of normal and PSE carcasses taken during the first couple of hours after slaughter. The results can be seen in Figure 2-26, Figure 2-27, Figure 2-28 and Figure 2-29. Figure 2-26 represents the pH and temperature profile of a typical PSE carcass. At 45 minutes post-mortem this particular carcass has a high internal muscle temperature (42°C) and a low pH (5.7). Figure 2-27 also represents a typical PSE carcass with a high intramuscular temperature (42°C) and a very low pH (5.5) at 45 minutes post-mortem. From an early stage these carcasses can be described as PSE. Figure 2-28 represents a carcass suspected of being PSE. At 45 minutes post-mortem the internal carcass temperature is slightly lower (41°C) and the pH is 6.0.

Figure 2-27 and Figure 2-28 represent 2 carcasses side by side on the same day. Both graphs show a dashed line in the pH and temperature curves. This represents a time period when the results from both loggers were lost. This can easily be explained. During the trial a staff member accidentally pushed the carcasses out of range of the base station. The carcasses were returned to their original position and loggers 1 & 2 continued to send the pH and temperature readings to the base station.

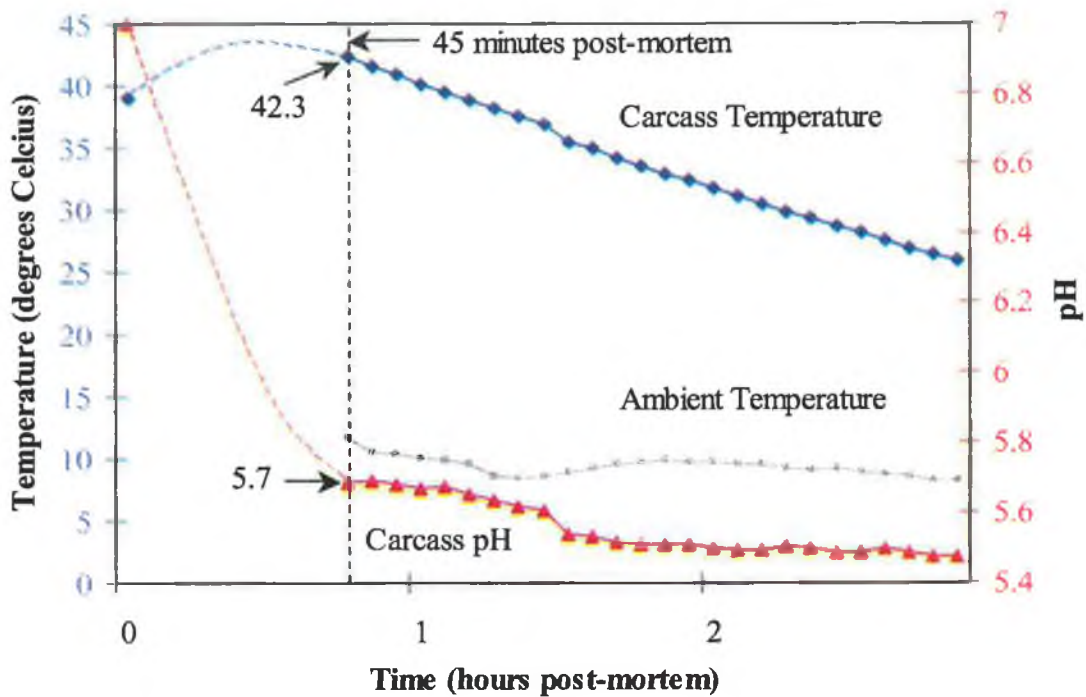


Figure 2-26 Represents a pH & temperature profile of a PSE carcass.

The added advantage of monitoring pH and temperature is that carcasses can be more easily identified from an early stage. Take for example Figure 2-28 – at 45 minutes post-mortem the pH is 6.0. According to the literature this carcass falls into the ‘suspected PSE’ category. If the pH of the muscle falls to 5.8 or lower while the muscle temperature is above 35°C then the carcass is prone to PSE. From the graph we can clearly see that this carcass falls into the PSE category. As already mentioned, recent work at the Danish Meat Research Institute has shown that a few, critical pH and temperature measurements early post-mortem are sufficient to predict the quality of the meat. By focussing on the initial post-mortem period as in Figure 2-29 we can see the varying rates of post-mortem pH decline between PSE and normal carcasses.

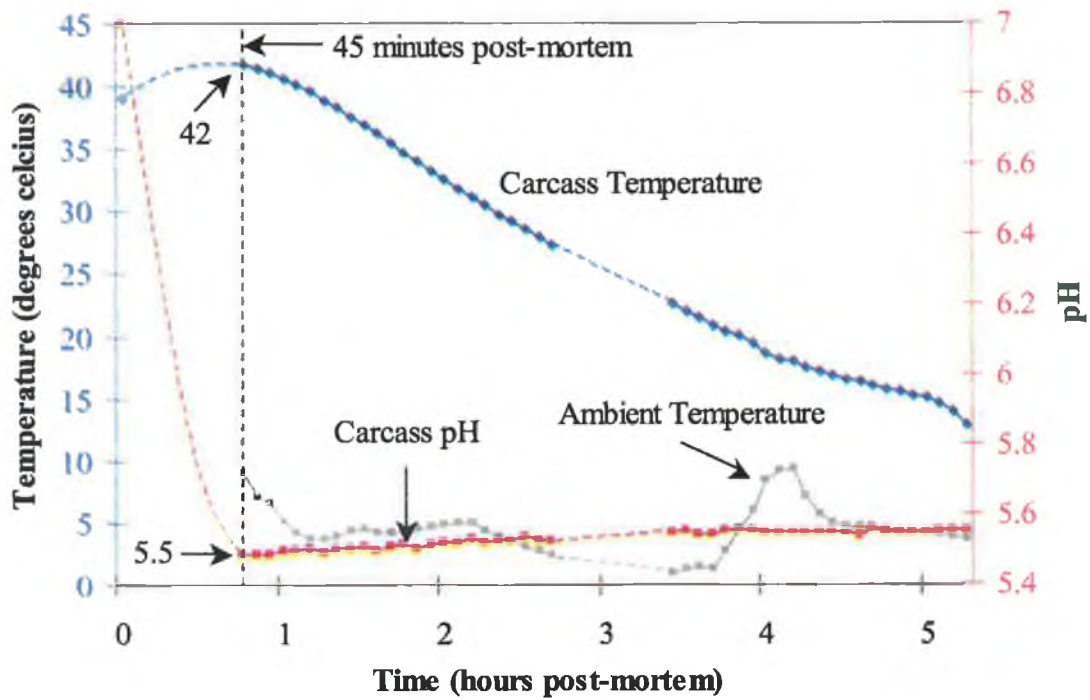


Figure 2-27 Represents the pH & temperature profile of a suspected PSE carcass. A loss of communication between the loggers and the base station due to interference is represented by the gaps in the profiles.

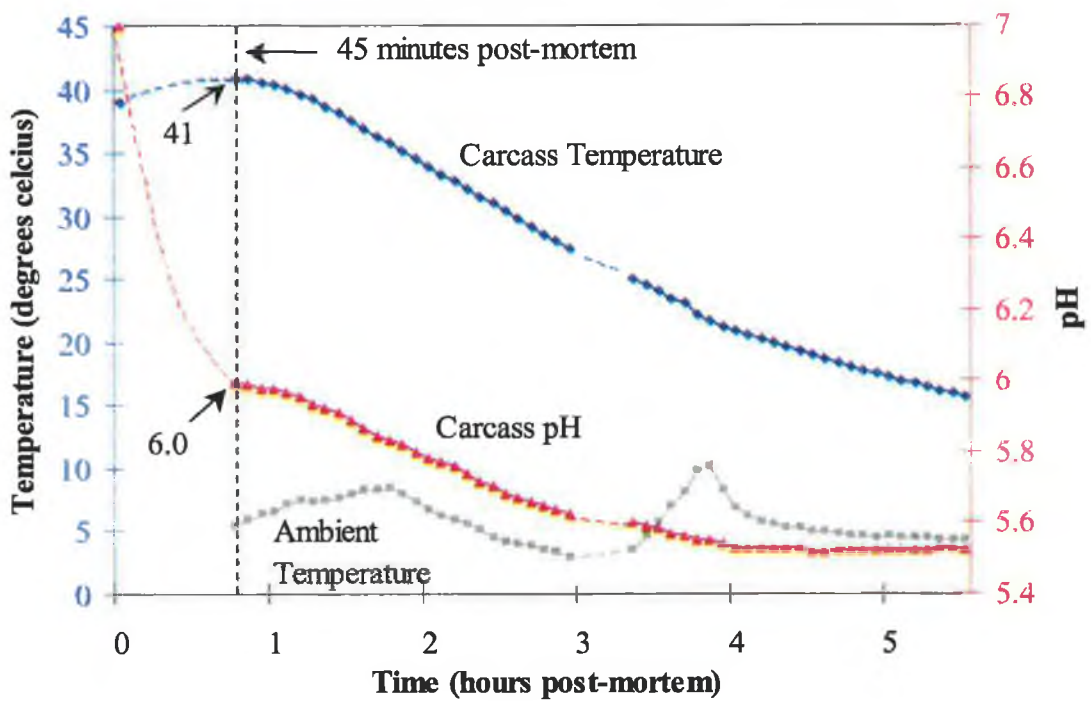


Figure 2-28 Represents a pH & temperature profiles of a suspected PSE carcass

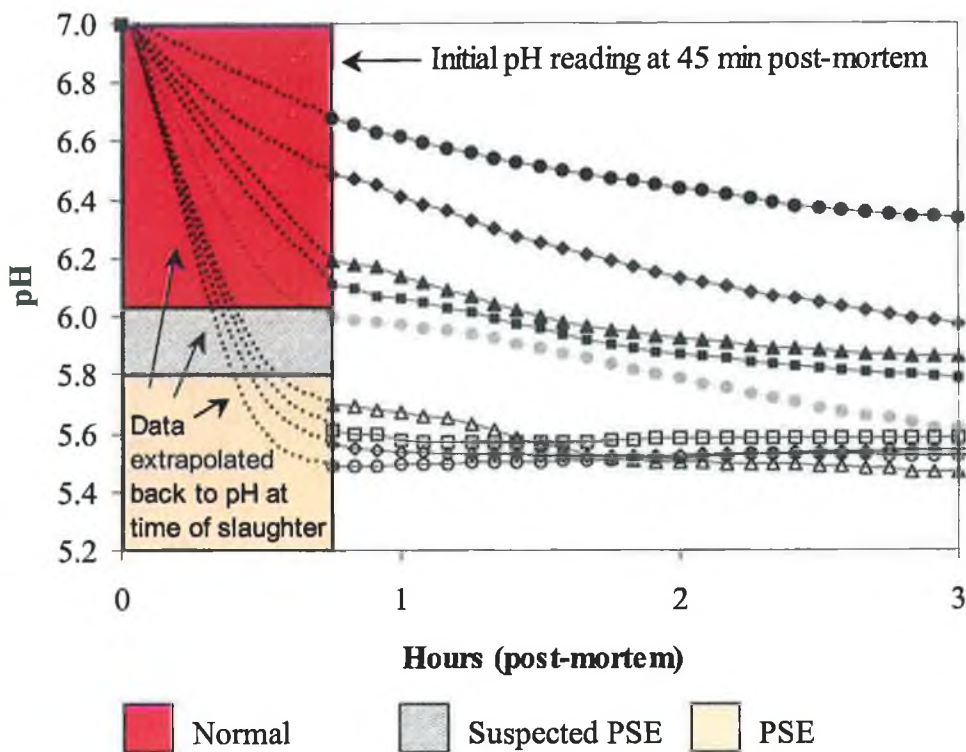


Figure 2-29 Initial pH profiles of 9 carcasses

Figure 2-29 represents the pH profiles of nine individual carcasses, which were sampled using the wireless pH/temperature monitoring system. From an early stage, it is evident that there is a clear distinction between PSE and Normal or DFD carcasses. As can be seen from the graph, one carcass falls into the suspected PSE category and as time progresses the pH profile follows that of a PSE carcass. This observation is strengthened further by the pH and temperature data supplied in Figure 2-28 that suggests that this carcass is a PSE carcass.

Rapid chilling of animal carcasses after slaughter is important for retarding the growth of both pathogenic and spoilage bacteria. Also, immediate post-slaughter chilling can reduce the adverse effects of mild forms of PSE (4) because as temperature decline is accelerated, the rate of pH decline will decrease (5). Monitoring the ambient temperature and internal carcass core temperature is therefore essential to ensure that the muscle temperature is lowered as quickly as possible soon after slaughter without compromising other meat qualities such as tenderness. As a guideline, normal pork muscles need to be at least 35°C or lower within 2.5 hours after slaughter and should reach at least 7°C or lower by 22 hours after slaughter (6). Temperature monitoring is therefore essential to ensure acceptable temperature control within the chill rooms.

The added advantage of monitoring pH and temperature in real time is that carcass quality can be more easily identified from an early stage. For example Figure 2-28 shows that at 45 minutes post-mortem the pH is 6.0. According to the literature this carcass falls into the 'suspected PSE' category. If the pH of the muscle falls to 5.8 or lower while the muscle temperature is above 35°C then the carcass is prone to PSE. The graph clearly indicates that this carcass falls into the PSE category. Without a detailed pH and temperature trace provided by the Wireless pH/Temperature Monitoring System this PSE carcass, unidentified during the early post-mortem period by the single pH45 measurement, is likely to enter the production line and cause great financial loss as a consequence. Treating mild cases of PSE in the early post-mortem period can greatly improve the pig meat quality and overall economic gain (4).

Mild forms of PSE must therefore be identified as soon as possible after slaughter in order for the tissue degradation to be prevented. This can be achieved by monitoring the course of the pH and temperature decline in real-time by the Wireless pH/Temperature Monitoring System. Out of control signals such as high temperatures and moderate to rapid decreases in pH decline may be detected by the pH and temperature sensors and transmitted to a control station, via RF communications, where a developing PSE carcass may be quickly identified allowing corrective actions to take place accordingly i.e. decreasing the ambient temperature of the chill room.

## **2.4 Conclusion**

The 'Wireless pH/Temperature Sensing System' provides valuable information with its ability to monitor three parameters simultaneously, internal carcass pH and temperature as well as ambient temperature. This new prototype, which incorporates the temperature sensor into a stainless steel probe, has an excellent response time. This allows more accurate internal carcass temperatures to be recorded as soon as the temperature probe is inserted into the carcass in contrast to previous designs, which had a sluggish response due to inefficient heat transfer. The stainless steel probe allows the meat to be easily penetrated with minimum sample destruction. The purpose built stainless steel 'knipHe' pH electrode offers maximum protection against glass breakage than conventional glass pH electrodes designed for meat applications. The probe cuts through the meat, forming a slurry that allows pH measurements to be taken easily with fast response times. This provides an easy method of monitoring pH and temperature of individual carcasses on-line as they cool down. The probes remain attached to the carcass until it leaves the chill

room for further processing which allows the pH & temperature probes time to equilibrate, resulting in more accurate readings than spot measurements. This eliminates the need for taking spot pH and temperature measurements at defined intervals i.e. every hour, which can be very time consuming. Sampling errors are also minimised, as the sampling position and sampling times are constant.

The Wireless pH/Temperature Monitoring System is a predictive meat quality indicator. Real time pH and temperature analysis facilitated by wireless communications allows poor quality carcasses to be identified early post-mortem. This real-time analysis capability allows this prototype to act as a preventative system in quality control i.e. initiation of corrective protocols may prevent suspected cases of PSE from becoming seriously PSE. The unique ability to track pH and temperature data from multiple sources over time forms an excellent traceability system allowing data to be accessed further down the process line, and facilitating information input into other traceability systems that integrate specific carcass information such as *'farrow-to-finish'* operations (7).

## References

1. Honikel, K., Reference methods for the physical characteristics of meat, *Meat Science*, 49, 447 (1998).
2. IP Ratings Datasheet <http://www.microscribe.co.uk/files/ip.pdf>.
3. Jansen, M. L., Determination of meat pH – temperature relationship using ISFET and glass electrode instruments, *Meat Science*, 58 (2001).
4. Offer, G., Modelling of the formation of pale, soft and exudative meat: Effects of chilling regime and rate and extent of glycolysis, *Meat Science*, 10, 155 (1984).
5. Rees, M. P., Trout, G. R., and Warner, R. D., The influence of the rate of pH decline on the rate of ageing for pork. II: Interaction with chilling temperature, *Meat Science*, 65, 805 (2003).
6. Huff-Lonergan, E., and Page, J., The Role of Carcass Chilling in the Development of Pork Quality, in *Facts*, National Pork Producers Council (2001).
7. Madec, F., Geers, R., Vesseur, P., Kjeldsen, N., and Blaha, T., Traceability in the pig production chain, *OIE*, 20, 526 (2001).

### **3 Development of a Web-based Wireless Temperature Sensing System for the Fishing Industry**



### **3.1 Introduction**

Maintaining the quality of chilled fish at sea is very important for maximising shelf life and value. One of the major tools at our disposal for ensuring quality is remote temperature monitoring. Coupling temperature sensors with new technologies developed by the communications industry opens the door to temperature sensing systems that are autonomous, low power, and capable of transmitting data to, and receiving instructions from, remote base stations. Autonomous sensing is necessary in order to realise the full potential of temperature profiling at sea as well as maximising quality control and traceability. We have developed a unique temperature monitoring system that incorporates both Radio Frequency (RF) and Global Systems for Mobile (GSM) communications with temperature logging units, enabling temperature data to be easily accessed onshore while the fishing vessel is still at sea (1-3). The temperature data is transmitted to a base station on board the fishing vessel via RF communications. The base station is connected to a GSM modem phone that allows the temperature data to be continuously transferred to an on-line website. The value of temperature profiling of fish catches at sea has been previously demonstrated using commercially available temperature logging devices (4). The following project highlights the benefits of using the newly developed system compared to previous designs, demonstrating the rapid technological developments in the area of autonomous sensing.

### **3.2 Preliminary Temperature Monitoring Field Trials using the RF Temperature Logging System**

The RF Temperature Logging System, described in section 2.1.1, used to record the chilling rates of pig carcasses in cold storage was also used to monitor the temperature of fish catches stored on-board fishing trawlers at sea. Although the bulky design of the temperature logger proved ineffective for recording the internal temperature of pig carcasses the same logger design is more suitable for recording the storage temperature of fish catches, as it is more feasible to submerge a bulky logger into a large container of iced fish than to submerge it into a single carcass. The effectiveness of the logger shape and design depends upon the intended application. A spear type probe is more effective for measuring internal carcass temperature but a bulky design is most effective for monitoring the temperature of a large container of fish i.e. 40kg container. The following preliminary trials are based on recording the temperature of fish catches at sea

using pre-programmed autonomous sensing devices which are submerged inside containers of freshly caught fish and retrieved from the containers as soon as the trawlers return to the shore where the data is downloaded and analysed.

### **3.3 RF-GSM Temperature Monitoring Field Trials**

#### **3.3.1 RF-GSM Temperature Monitoring System**

The prototype Wireless RF-GSM Temperature Monitoring System was built under contract by Whistonbrook Technologies Ltd to a specification provided by the DCU team.

The prototype system consists of:

- 3 RF Temperature Loggers
- RF Base Station
- GSM Base Station (Vodafone 087 network)
- Remote Server Software (Visual Basic 6.0)
- Web Connection (Modem)
- Web Server ([www.remotesensors.dcu.ie](http://www.remotesensors.dcu.ie))

A schematic of the wireless temperature monitoring system can be seen in Figure 3-1. As illustrated, the logger completely submerged in a container of fish records the storage temperature of the fish in real time on-board the fishing vessel. While still at sea the logger communicates the temperature data to the base station via RF communications. The base station is connected to a GSM modem phone that allows the temperature data to be transmitted to a remote server. Here, the data is automatically processed using the specially designed software, Figure 3-3, which uploads the temperature data onto the web site, Figure 3-4. This system allows the temperature data of the fish catch to be accessed from anywhere in the world while the fishing vessel is still at sea.

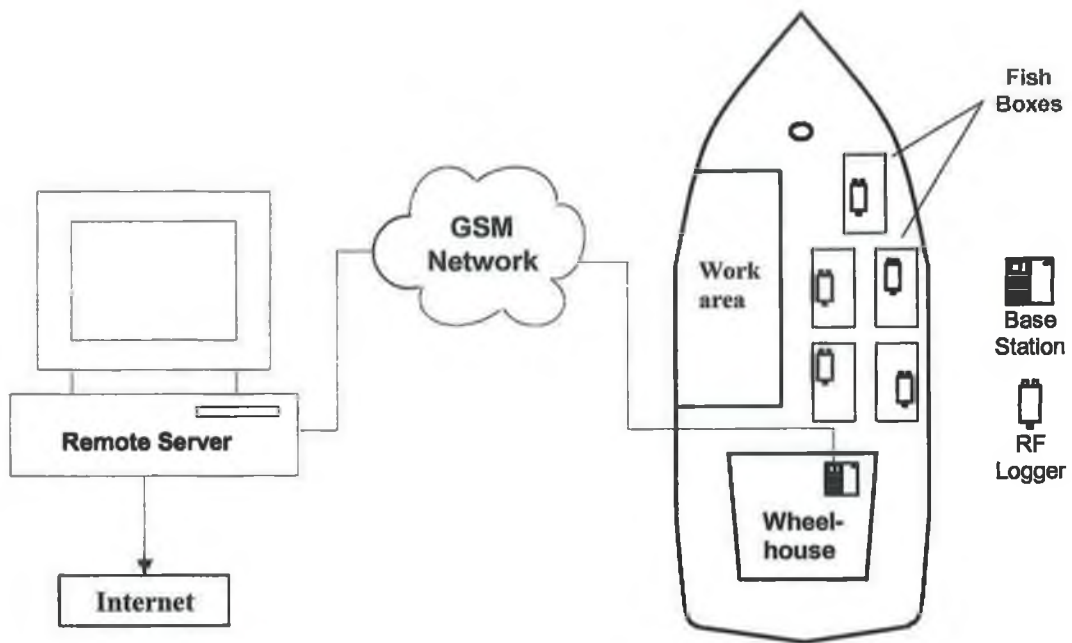


**Figure 3-1 Schematic of the wireless RF-GSM Temperature Monitoring System**

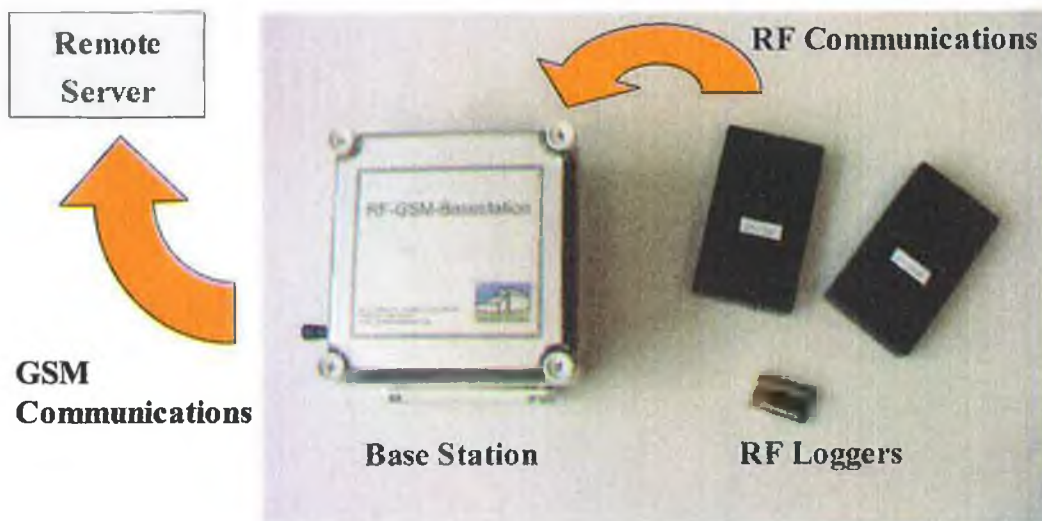


**Figure 3-2 The RF-GSM Temperature Monitoring System Hardware**

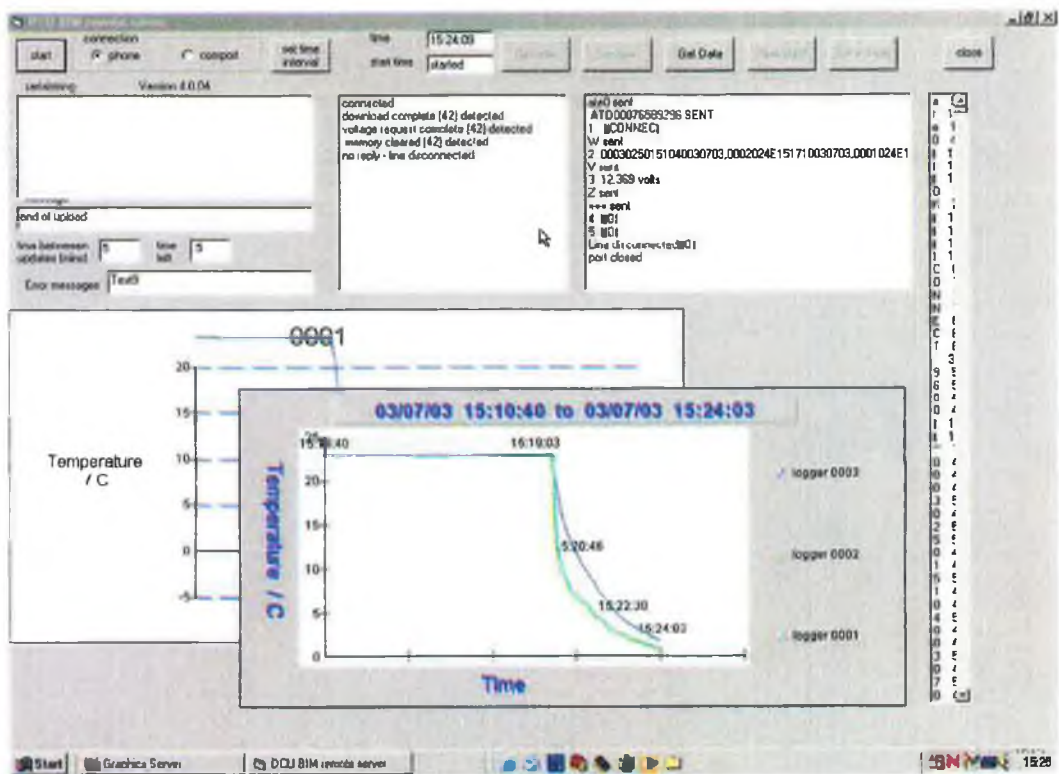


Figure 3-3 The Remote Server Software

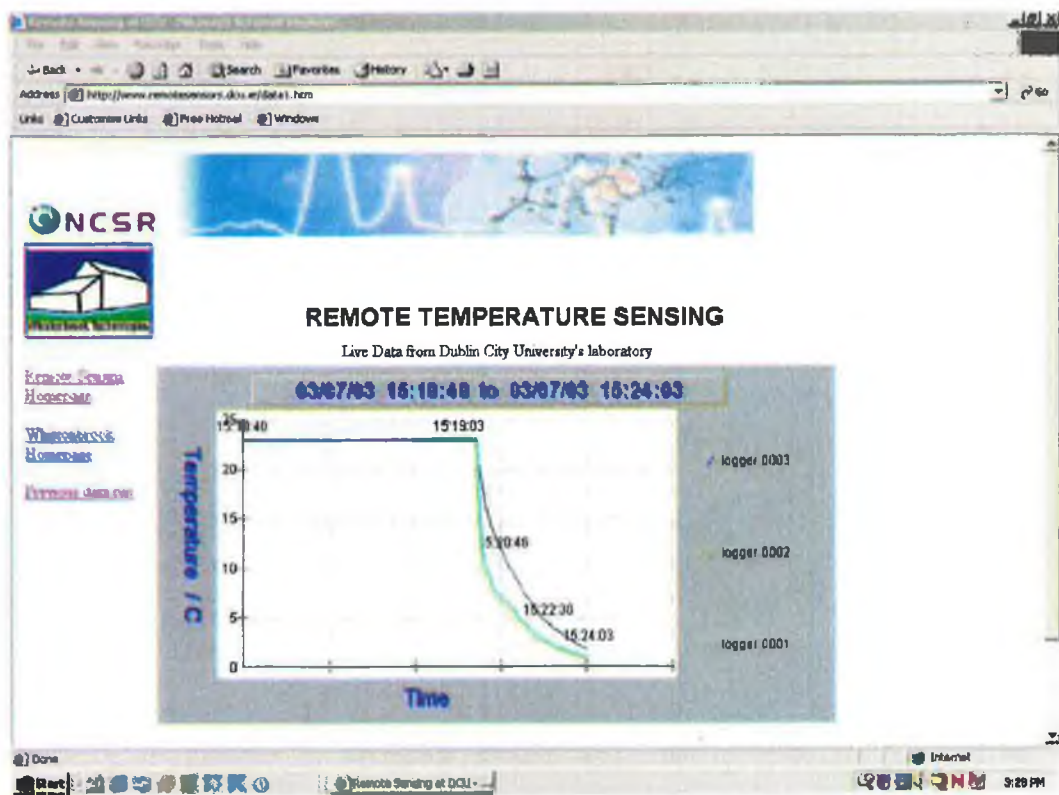


Figure 3-4 Web page displaying the temperature profiles in real-time [www.remotesensors.dcu.ie](http://www.remotesensors.dcu.ie)

### 3.4 RF-GSM Temperature Monitoring Hardware Specification

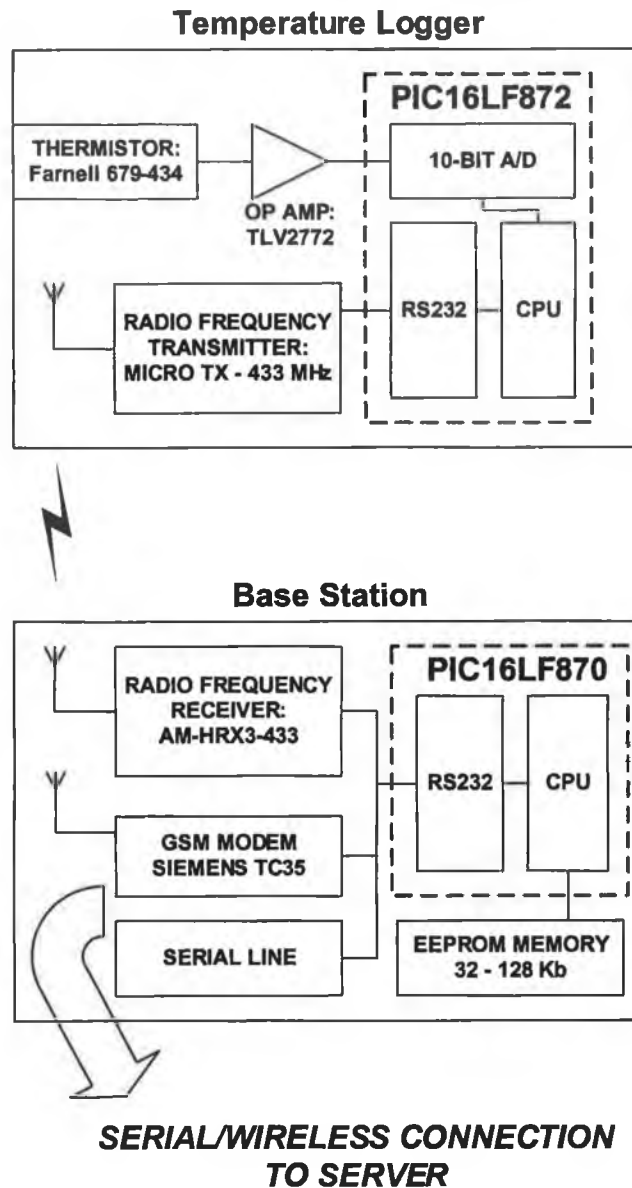
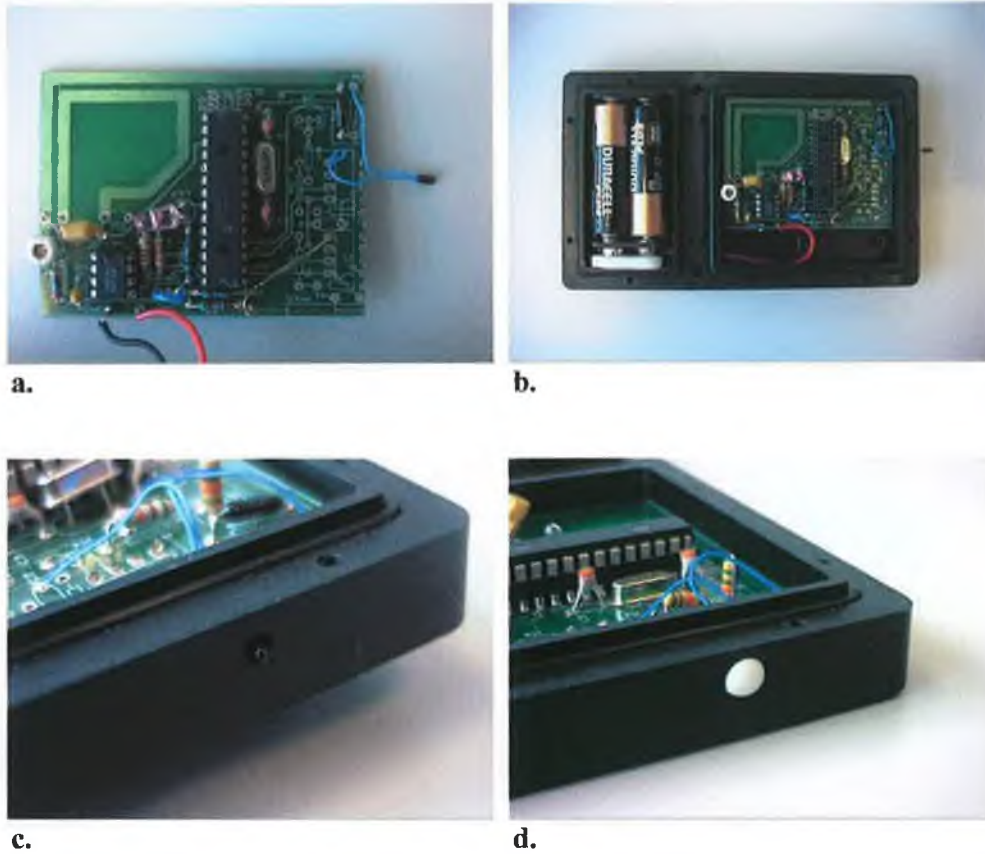


Figure 3-5 Block diagram of the prototype logger and base station system

#### 3.4.1 Logger Description and Operating Method

The temperature is measured by a 5k 679-434 thermistor (Farnell) in a simple potential divider circuit, through a TLV 2772 operational amplifier (Texas Instruments) to a 3V PIC16LF872 microprocessor (Microchip). The data is processed through the on-board

10-bit A/D converter and C programmed CPU. The logger ID and 10-bit string containing the temperature value is generated and transmitted through a Micro TX RF transmitter (433MHz, LPRS Ltd) at 5-minute intervals. Aside from the thermistor, the entire system is enclosed within a rugged and waterproof plastic casing, Figure 3-6a & b. To ensure very rapid responses to changes in temperature, the thermistor is embedded in thermally conductive epoxy in the wall of the casing Figure 3-6c & d.



**Figure 3-6a. Logger circuit board with 5k 679-434 thermistor b. Circuit board fixed into rugged waterproof plastic box (8.4 × 14.2 × 2.5 cm) c. Thermistor embedded in a cavity in the wall of the plastic casing d. The cavity filled with thermally conductive epoxy**

### 3.4.2 Base Station Description and Operating Method

The data string transmitted by the logger is received by the base station via a AM-HRX3-433 RF receiver (433 MHz, LPRS Ltd), where it is processed by the PIC16LF870 microprocessor (5 V, Microchip) and transferred to the EEPROM memory as a 20-bit string containing the 4 bit logger ID, 4 bit temperature value and 12 bit time

and 12 bit time stamp. The base station keeps time through a RTC (real-time-clock) powered by a Lithium-ion battery. The base station simultaneously listens for RF/Server communications. On receiving a request from the central server, the base station transfers the data through the mobile phone network, via the TC35 GSM modem (Siemens), or through a direct serial connection. During field trials, communication between the server and the base station was always executed using the GSM network; the serial connection was only generally used for diagnostic testing. The base station is encased within a water resistant plastic box and is powered by a 12 V lead-acid battery with a lifetime of approximately 1 week with continuous operation.

### **3.5 Experimental**

#### **3.5.1 Preliminary Temperature Monitoring Field Trials using the RF Temperature Logging System**

Although the RF Temperature Monitoring System described in section 2.1.1 is capable of monitoring temperature in real time by transmitting the data via RF communications to a base station connected to a PC/laptop, for the purpose of this experiment the loggers were pre-programmed before commencing each trial to operate remotely and data was retrieved once the trial was terminated. It was not practical to install the base station in the hold of the trawler, as there was no outlet from the trawler hold for the RS323 cable, which linked the base station to the laptop.

Six RF temperature loggers, ID numbers 01020A, 01020C, 01020E, 010215, 010206 & 010202 were programmed as follows:

- Sampling frequency – 1 temperature reading every 10 minutes
- Start delay – 244 minutes (to allow for transportation of the loggers to the fishing port at Castletownbere, Co. Cork, Ireland)
- Mode – Logger in Mode 2 (logging until stopped)

The temperature loggers were programmed at Dublin City University. Once programmed the loggers were transported to the Irish Marine Fisheries, Bord Iascaigh Mhara (BIM) based at Castletownbere, Co. Cork, Ireland. The coastal staff was responsible for placing the loggers in the fish boxes on-board the fishing trawlers. Once

the fishing trawlers returned to the shore the loggers were retrieved and returned to DCU where the temperature data was downloaded. The coastal staff provided a record of events as follows:

- Freshly caught fish were stored in containers packed with ice in the hold of the trawler.
- The loggers were placed in the containers of fish once the fish were caught and removed from the containers when the trawler returned to the harbour.
- Three containers of fish were monitored based on the type of fish, the weight of the container and the position of the container in the hold.
- Two loggers were placed in each container i.e. one in the centre and one at the outer edge (to assess temperature variation within a single container).

### 3.5.2 Measuring the Sensor Response Time of the RF-GSM Temperature Monitoring System

The RF-GSM Temperature Monitoring System was programmed to operate in 'Modem' mode and the sampling frequency was set to 5 seconds. The loggers were allowed to equilibrate at room temperature before they were completely submerged into a polystyrene container of ice and water. The time taken for the temperature to reach 90% of the step change was used to determine the response time.

### 3.5.3 Temperature Monitoring Field Trials using the RF-GSM Temperature Monitoring System

During the salmon season, June and July 2003, field trials using the RF-GSM Temperature Monitoring System were performed with the assistance of BIM, based at Dunmore East Harbour, Co. Waterford, on-board salmon and mackerel fishing boats Figure 3-7a. The salmon fishing boats were suitable for the initial temperature monitoring field trials, as there was already a system in place under the *Wild Salmon Quality Scheme* to promote good temperature monitoring (i.e. insulated bins were distributed for use on-board vessels to store ice and fish Figure 3-7b). Also, as individual salmon were tagged under the quality scheme, this presented a perfect opportunity to provide real-time temperature data for the tagged salmon, maximising the value of the catch.





a.

b.

**Figure 3-7a. Salmon and mackerel fishing boats at Dunmore East Harbour, Co. Waterford b. Insulated bins for ice storage on-board salmon fishing boats**

Five temperature-monitoring trials were carried out during the months of June and July 2003. The field trials were performed on-board salmon and mackerel fishing boats, based at Dunmore East Harbour, Co. Waterford. The details of each of the trials are given in table 3-1 below:

<b>Trial Number</b>	<b>Date of Trial</b>	<b>Vessel Name And Fishing Port</b>	<b>Species of Fish</b>
Trial 1	17/06/03	An Searrach Dunmore East	Salmon
Trial 2	23/06/03	An Searrach Dunmore East	Salmon
Trial 3	24/06/03	An Searrach Dunmore East	Salmon
Trial 4	15/07/03 Morning Trial	Nova Dawn Dunmore East	Mackerel
Trial 5	15/07/03 Evening Trial	Nova Dawn Dunmore East	Mackerel

**Table 3-1 Details of the salmon and mackerel trials**

### 3.5.4 RF-GSM Temperature Monitoring System Set-up on-board the Fishing Vessel

#### 3.5.4.1 Base Station

Before commencing each trial, the RF-GSM base station was switched “On” in “Modem” mode and was secured in place (with the aid of cable ties or a length of rope) at a safe elevated location, i.e. above the wheelhouse, on-board the fishing vessel, Figure 3-8a. & b.

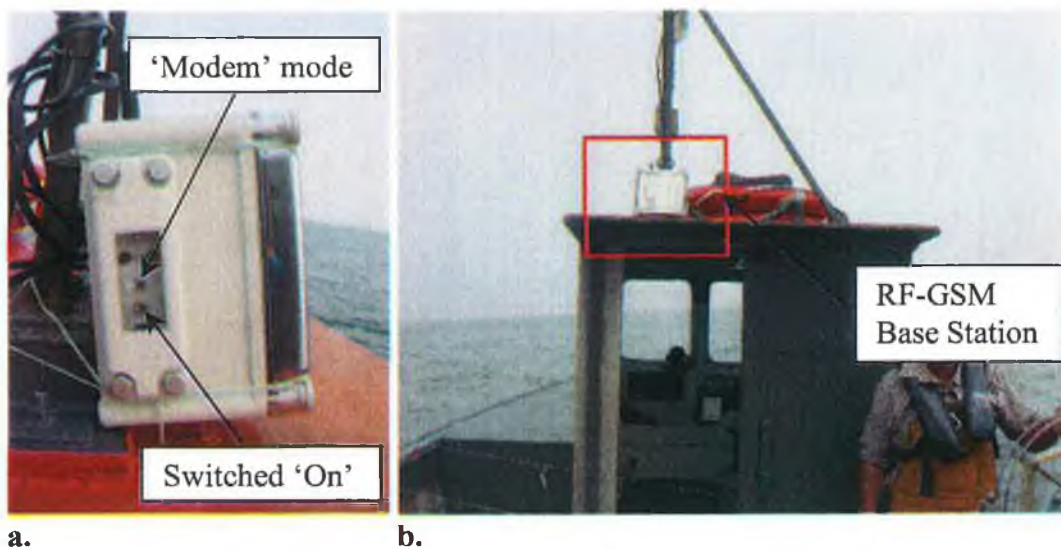


Figure 3-8a. & b. RF-GSM base station secured on top of the wheelhouse

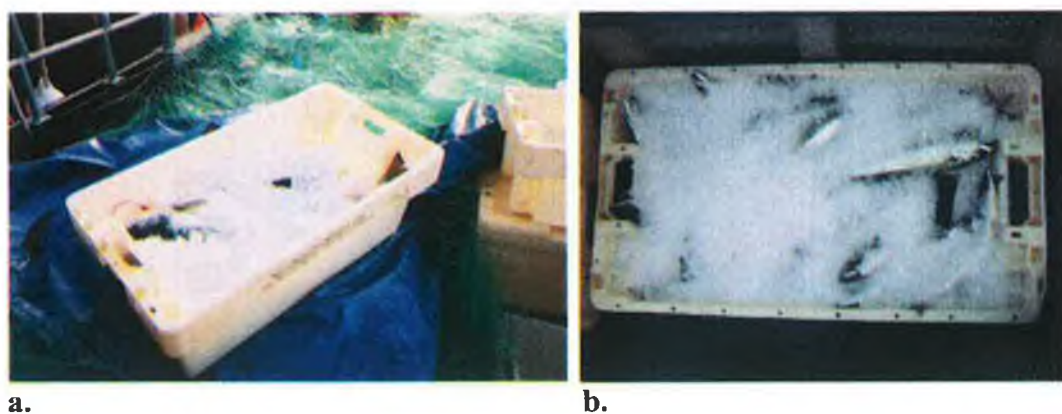


Figure 3-9a. Iced salmon b. Iced mackerel

### 3.5.4.2 Temperature Loggers

As soon as the salmon and mackerel were caught they were placed in containers where they were washed down with seawater for ~10 minutes. The fish were then iced and the containers were allowed to sit on the deck for the remainder of the trial, Figure 3-9a & b. The temperature loggers, immersed in the containers of iced fish, were programmed to transmit a temperature reading to the base station every 5 minutes, where the temperature data was stored. Model DS1921-F1 iButton temperature loggers were attached to each RF temperature logger to allow a direct comparison between the two systems Figure 3-10.

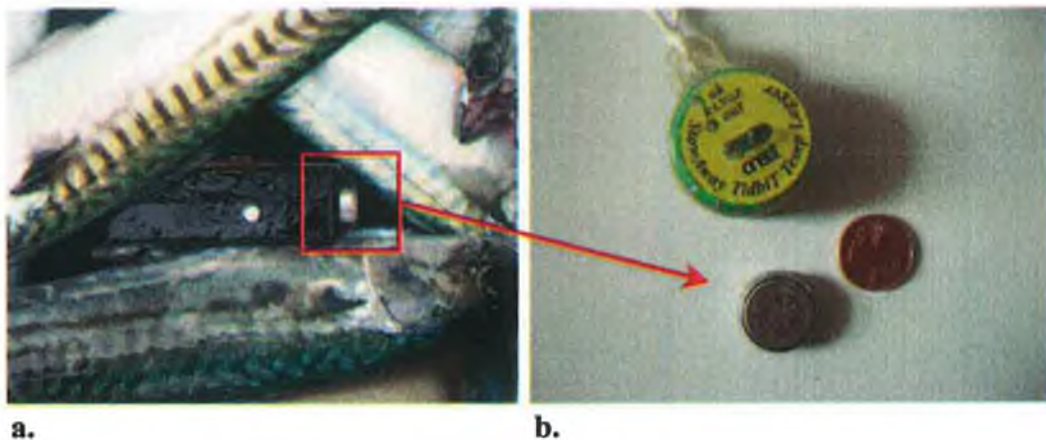


Figure 3-10a. RF temperature logger (iButton attached to the side of the logger) b. iButton and Tidbit temperature data loggers

### 3.5.4.3 Remote Server Software

The Remote Server Software was programmed to allow the server (based at Dublin City University) connect with the base station via GSM communication every 30 minutes. After a successful connection the temperature data was retrieved from the base station and downloaded onto the server database from where the [www.remotesensors.dcu.ie](http://www.remotesensors.dcu.ie) website was automatically updated. The above procedure was repeated every 30 minutes, continuously updating the website. When the fishing vessel returned to the shore the RF temperature loggers were removed and the RF-GSM base station was switched off. The temperature history of the salmon and mackerel from 'ship to shore' was retrieved from the server database and further data processing was performed using MS Excel.

## 3.6 Results and Discussion

### 3.6.1 Preliminary Temperature Monitoring Field Trials using the RF Temperature Logging System

The loggers were programmed to start on the 18<sup>th</sup> February 2002 and were stopped on the 15<sup>th</sup> April 2002. The loggers were recording continuously for 57 days. A total of 8,022 data points were recorded by each of the six loggers. During this time temperature profiles for two fish catches were captured:

- First catch: From the 3/03/02 to 5/03/02
- Second catch: From the 3/04/02 to 6/04/02

Figure 3-11 shows the temperature profiles obtained by loggers 01020A (placed at the outer edge) & 010206 (placed in the centre) of a 40kg container of haddock. The loggers were positioned at midday on the 3<sup>rd</sup> March 2002. Within 30 minutes, the loggers registered a value below 3°C. The temperature remained below 1.5°C for the 2 days while the fish were stored in the hold of the trawler. On the 4<sup>th</sup> March at 9.30pm, the cooling was shut down for ~12 hours. During this time the temperature increased slightly and then fell as the cooling was turned back on the following morning at 9am. The graph indicates that the temperature profiles for the centre (logger 01020A) and outer edge (logger 01020A) of the container were very similar signifying that there was little temperature variation within the container.

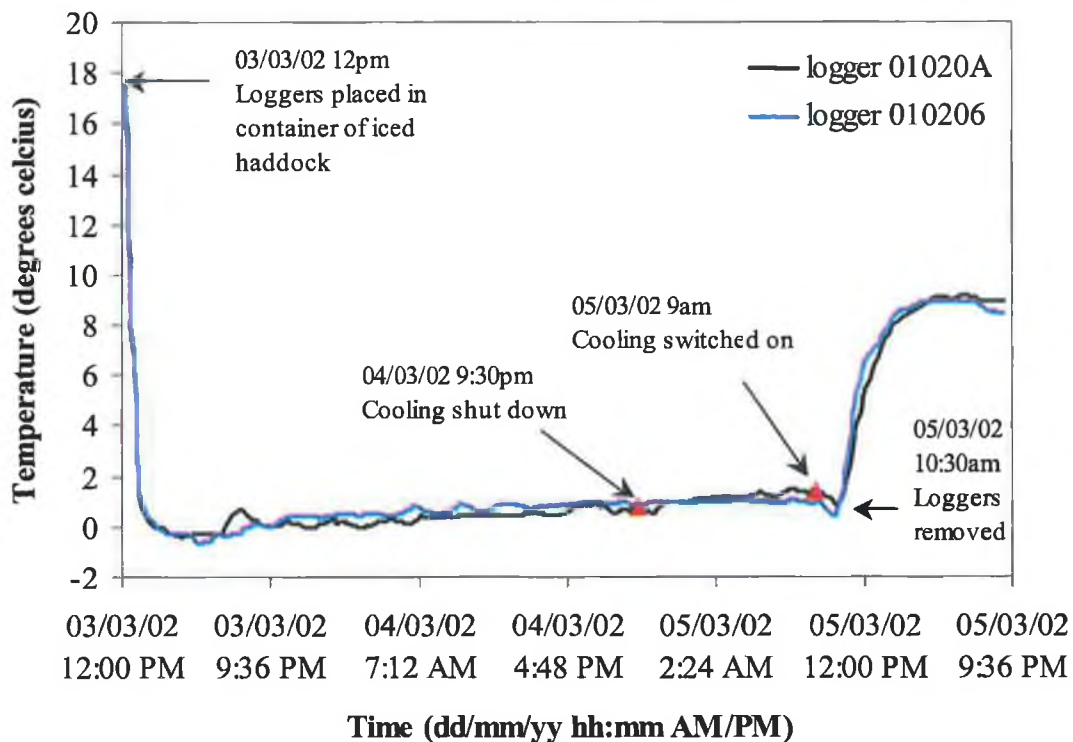


Figure 3-11 Shows the temperature profiles obtained by loggers 01020A (placed at the outer edge) & 010206 (placed in the centre) of a 40kg container of haddock.

Appendix 2-1 represents the temperature profile of a 40kg container of iced haddock in the same hold. The temperature remained below 0°C for the 2 days while the fish were stored in the hold of the trawler. Again, the graph indicates that there was little temperature variation within a container. Appendix 2-2 represents the temperature profile of a 25kg container of iced hake. Once again, the temperature remained below 0°C for the 2 days while the trawler was at sea. Unfortunately, there is no data for the exact position of the three fish containers in the hold but the graphs indicate that the temperature differences between the three containers are negligible. The temperature profiles of a 40kg container of iced hake caught on the 3<sup>rd</sup> April 2002 are presented in Figure 3-12. The recorded storage temperature for the hold was between -1°C & 0°C (data supplied by the Irish Marine Fisheries coastal staff). During the 3-day period at sea no re-icing took place. The centre (logger 010215) and outer edge (logger 01020C) temperature profiles for this container of iced hake were similar and remained below 0°C for the 3-day period. A second 40kg container of iced hake and a 40kg container of iced haddock from the same hold were also monitored over the 3-day period and the temperature data is presented in Appendix 2-3 & Appendix 2-4. All six loggers recorded similar temperature profiles for the three containers of iced fish demonstrating

that there were no significant temperature fluctuations for the catch of fish stored in the trawler hold during this period. The temperature data recorded by the loggers is also in agreement with the trawler hold temperature recorded by the coastal staff.

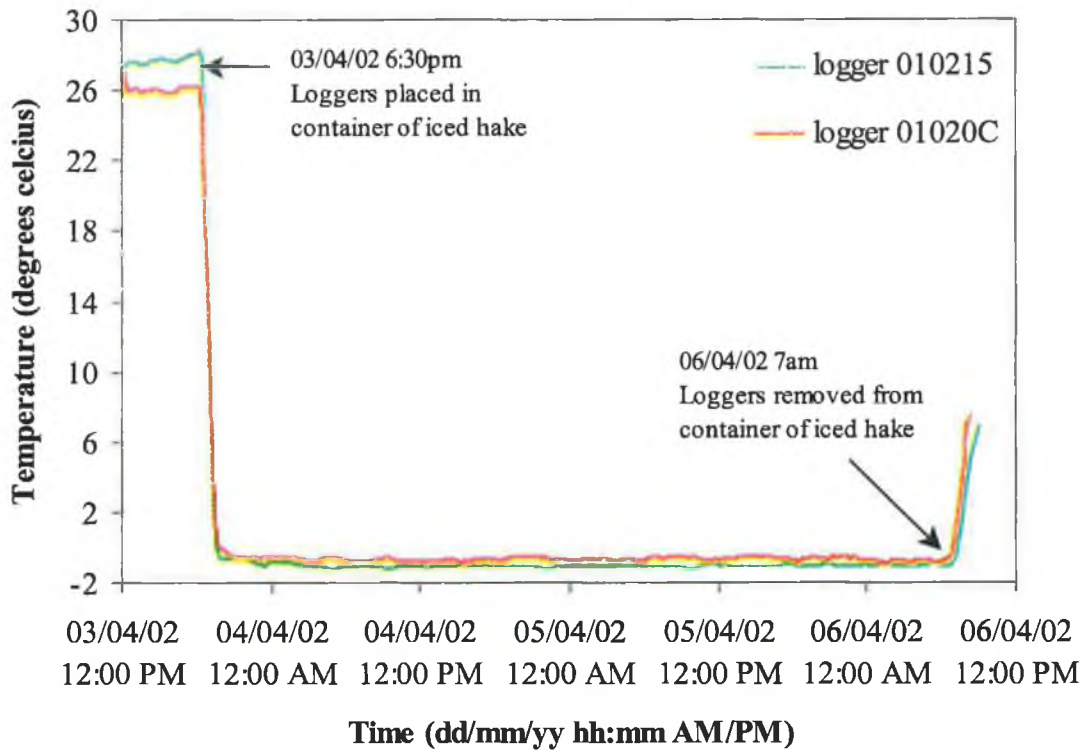
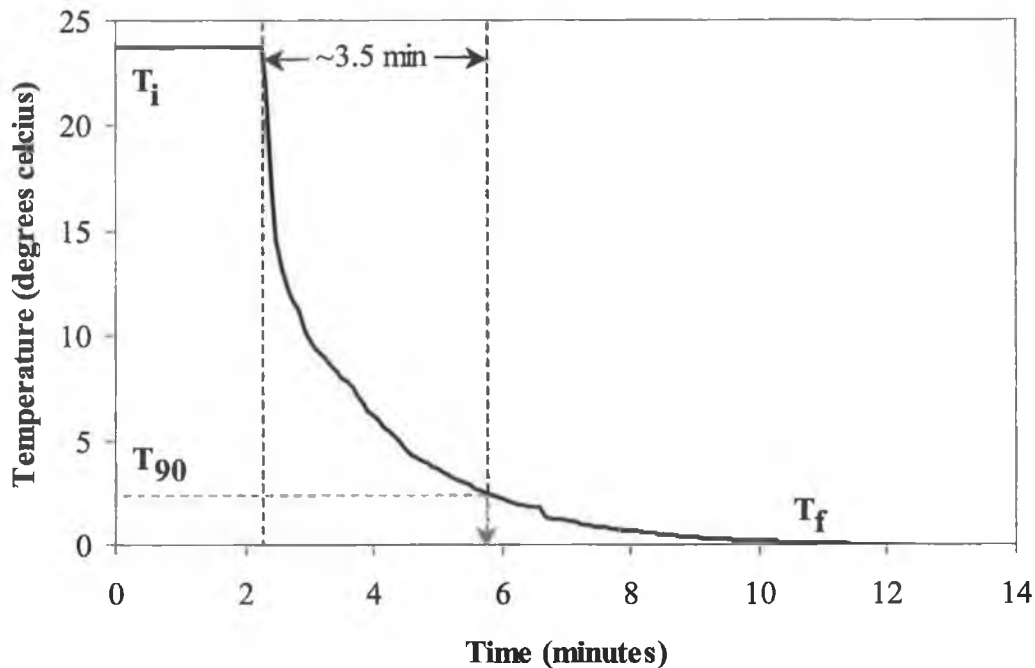


Figure 3-12 Temperature profiles captured by loggers 010215 (placed in the centre) and logger 01020C (placed at the outer edge) of a 40kg container of iced hake caught on the 3<sup>rd</sup> April 2002

### 3.6.2 Measuring the Sensor Response Time of the RF-GSM Temperature Monitoring System

Figure 3-13 indicates that when the 3 temperature loggers were submerged in a polystyrene container of iced water they reached 90% of the step change in ~3.5 minutes. The initial temperature ( $T_i$ ) for the 3 loggers was taken as  $24.0 \pm 0.1^\circ\text{C}$  and the final temperature ( $T_f$ ) was  $0 \pm 0.1^\circ\text{C}$ , the temperature of iced water. Therefore, a step change of 90% ( $T_{90}$ ) is equivalent to  $2.4 \pm 0.1^\circ\text{C}$ . The temperature response time is significantly faster for the RF-GSM Temperature Monitoring System compared to the RF Temperature Logging System, which was experimentally determined to be ~8 minutes (see section 2.3.1).



**Figure 3-13** Illustrates the temperature response time for the RF-GSM Temperature Monitoring System. The temperature reached 90% of the step change ( $T_{90}$ ) in  $\sim 3.5$  minutes.  $T_i = 24.0^\circ\text{C}$ ,  $T_f = 0^\circ\text{C}$  (iced water), therefore  $T_{90} = 2.4^\circ\text{C}$ .

### 3.6.3 Temperature Monitoring Field Trials using the RF-GSM Temperature Monitoring System

#### 3.6.3.1 Trial 1

The fishing boat 'An Searrach' set out to sea at 5.00pm. The 3 RF temperature loggers were left out on the deck recording the ambient temperature. One salmon was caught and tagged (Tag ID No: 02651) at 7:40pm and was washed for 10 minutes before it was placed on ice. The 3 temperature loggers were also placed in the box containing the iced salmon. Unfortunately due to severe weather conditions the RF-GSM base station had to be removed from the deck and the trial was terminated. Although the RF-GSM Temperature Monitoring System was shut down, the iButtons attached to the loggers continued to record the storage temperature. The fishing boat returned to the shore at 8:30pm and the salmon was placed in cold storage overnight at Dunmore East harbour. The loggers were removed the next day and the iButton temperature data was downloaded, see Figure 3-14.

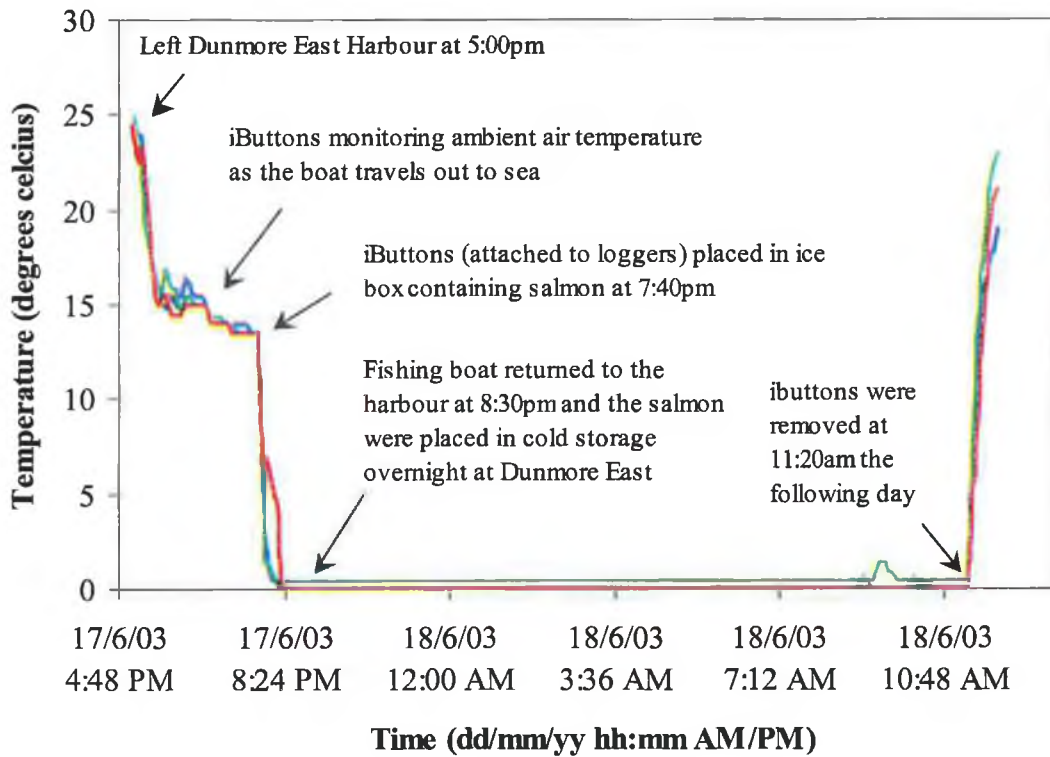


**Figure 3-14** Illustrates the storage temperature of an individual tagged salmon (Tag No: 02651) recorded by 3 iButtons.

### 3.6.3.2 Trial 2

The fishing vessel left the harbour at 7:00 am. The 3 temperature loggers and iButtons were placed in a container of ice at 7:50 am. Four salmon were caught and tagged (Tag ID No's: 02633, 02634, 02635, 02636) at 9:50 am and were washed for 10 minutes before they were placed in the container of ice along with the temperature loggers. Due to a fault in the software and communications early that morning there was a delay in starting the RF-GSM Temperature Monitoring System. As a result the system only began recording temperature data from 11:00 am until the loggers were removed at 2:30pm when the boat returned to the harbour. Only one logger out of the three loggers communicated with the RF-GSM base station, see Figure 3-15.



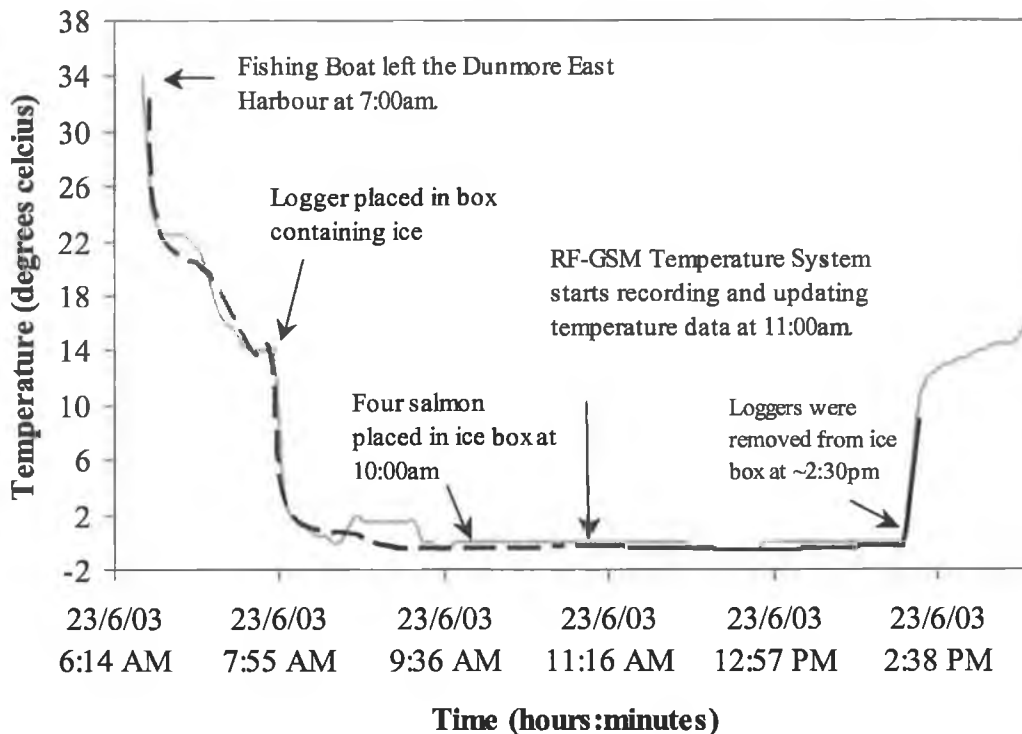


**Figure 3-15** Illustrates the storage temperature of 4 salmon (Tag No's: 02633, 02634, 02635,02636) at sea captured via logger 3 of the RF-GSM Temperature Monitoring System and the iButtons.

### 3.6.3.3 Trial 3

On the 24<sup>th</sup> June 2003 the salmon fishing trial commenced at 8 am. One salmon was caught at 12:30pm and was washed for 10 minutes before it was put on ice. The 3 temperature loggers were also placed in the container along with the iced salmon at 12:40pm. The salmon remained in ice for four hours on-board the boat before reaching the shore. During this time the temperature began to raise gradually but still remained below 5°C, see Figure 3-16. The temperature loggers were removed at 5:00pm as soon as the fishing vessel returned to the harbour. Once again only one logger out of the three loggers communicated with the RF-GSM base station.

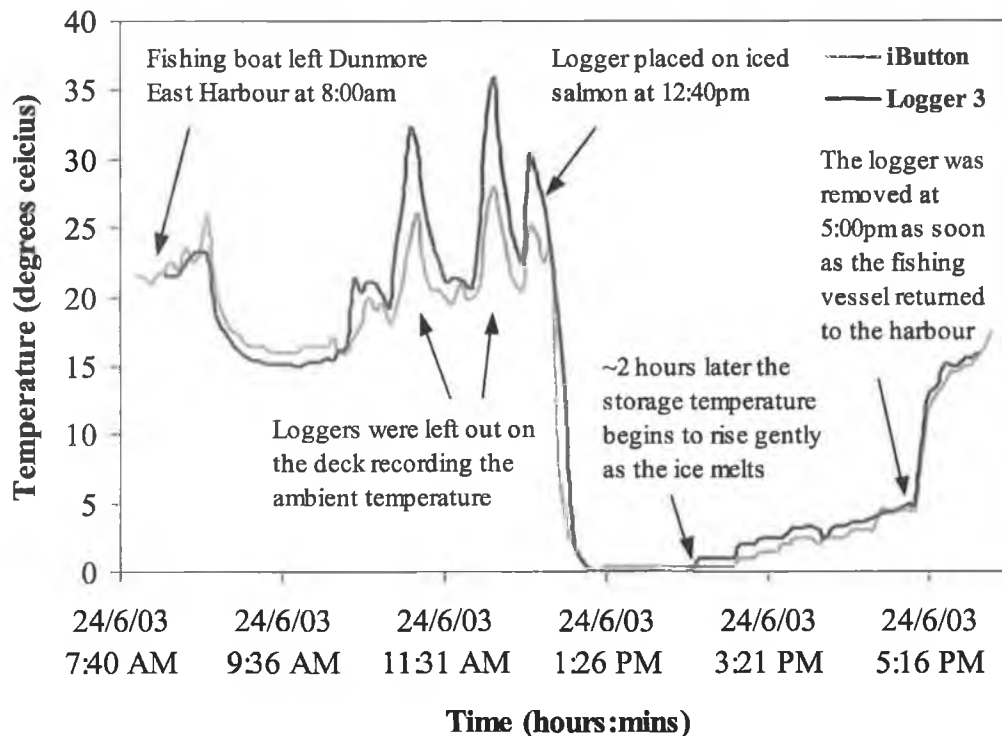


**Figure 3-16** Illustrates the storage temperature of an individual salmon on-board the fishing boat at sea captured via logger 3 of the RF-GSM Temperature Monitoring System and an iButton.

#### 3.6.3.4 Trial 4 & Trial 5

Two field trials were carried out on the 15<sup>th</sup> July 2003. These trials took place on-board mackerel fishing vessels with the help of BIM Coastal Staff. The first trial (Trial 4) commenced at 4:00am. At 6:30am one of the loggers (logger 1) was placed in a box of iced mackerel and was removed at 9:40am when the boat returned to the shore. Unfortunately, the RF-GSM base station was shielded by a large metal mast, which prevented it from receiving any information from the RF loggers. When the vessel returned to the harbour the RF-GSM base station was re-positioned and a second trial (Trial 5) commenced at 3:45pm. Initially, the three loggers monitored ambient temperature and were placed in storage containers as the fish were caught; see Figure 3-20 for temperature profiles. At 6:15pm logger 3 was placed in an upright position in a box of mackerel (no-ice) along with a Tidbit temperature logger (provided by BIM coastal staff), Figure 3-10 and Figure 3-17, see Figure 3-21 for temperature profile. The storage temperature of the fish remained between 16 and 17°C for approximately 3.5 hours while the boat was at sea. At 7:45pm logger 2 was placed in a box of partially iced mackerel, Figure 3-18, see Figure 3-23 for temperature profile. The storage

temperature of the fish quickly fell below 5°C and soon began to rise again. Re-icing at 9:15pm caused the storage temperature to fall rapidly. At 9:10pm logger 1 was placed in another box of mackerel (completely iced), Figure 3-19, see Figure 3-25 for temperature profile. The storage temperature quickly fell below 5°C. At 9:50pm the boat returned to the harbour and the loggers were removed from the fish boxes. The temperature data from all three loggers was successfully transmitted and uploaded onto the web pages, see Figure 3-22, Figure 3-24 & Figure 3-26.



**Figure 3-17 RF Temperature logger 3 placed in a box of mackerel (no-ice)**



**Figure 3-18 RF Temperature logger 2 placed in a box of mackerel (partially iced)**

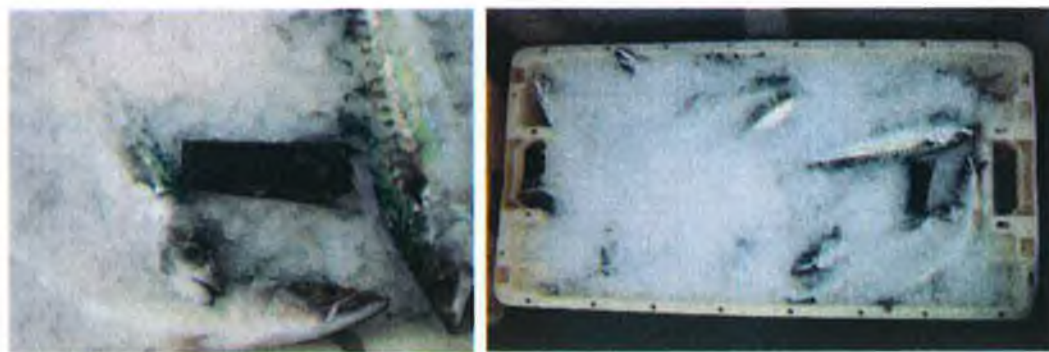


**Figure 3-19 RF Temperature logger placed in a box of mackerel (fully iced)**

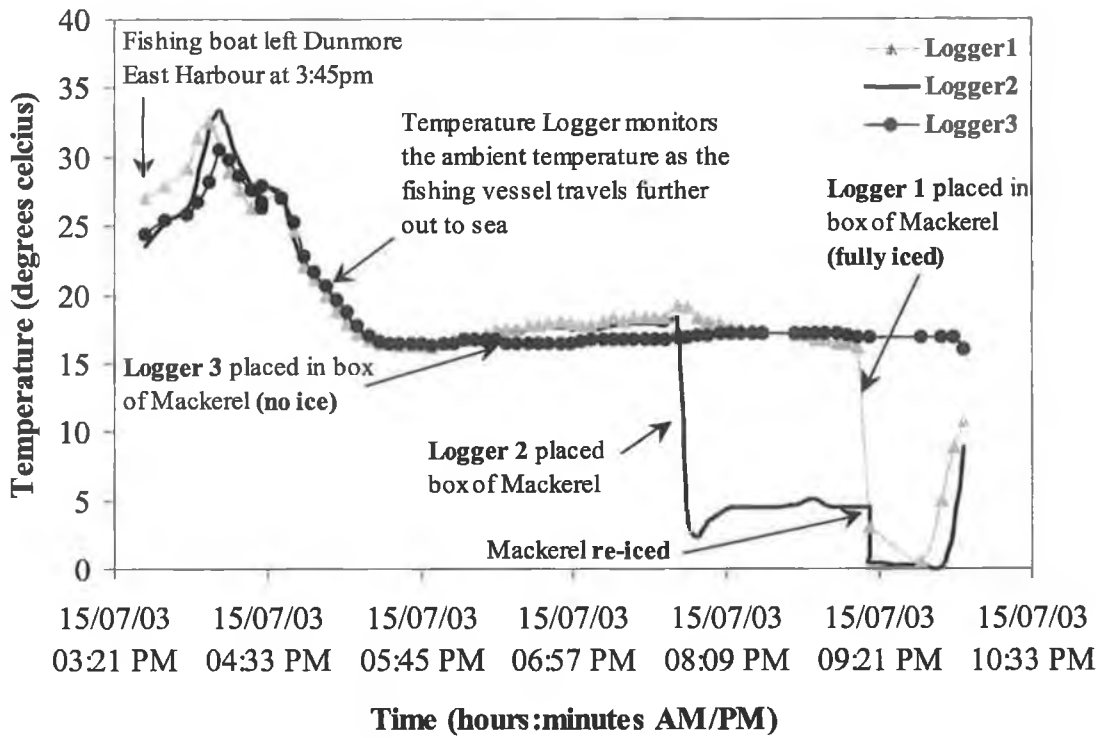


**Figure 3-20** Illustrates the storage temperature of mackerel under different conditions at sea captured via the RF-GSM Temperature Monitoring System.

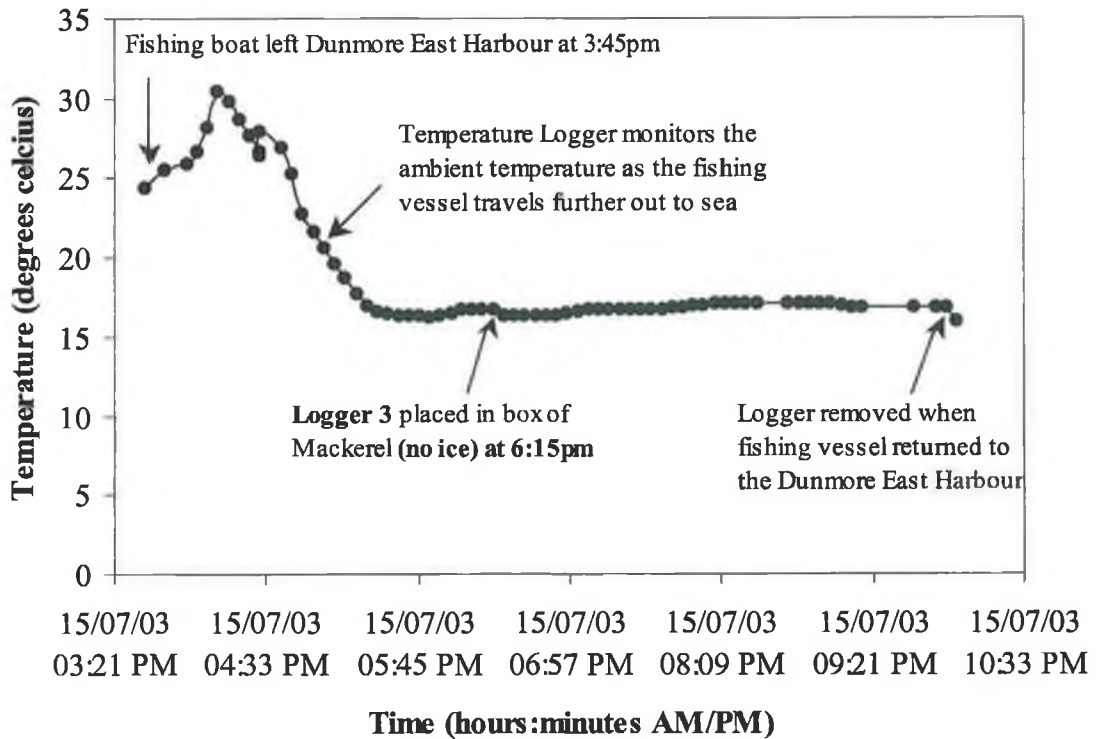


Figure 3-21 Illustrates the storage temperature of a box of mackerel (no-ice) while at sea via logger 3. The logger was placed in the full box of mackerel at 6:15pm and was removed at ~9:50pm when the boat returned to the harbour.

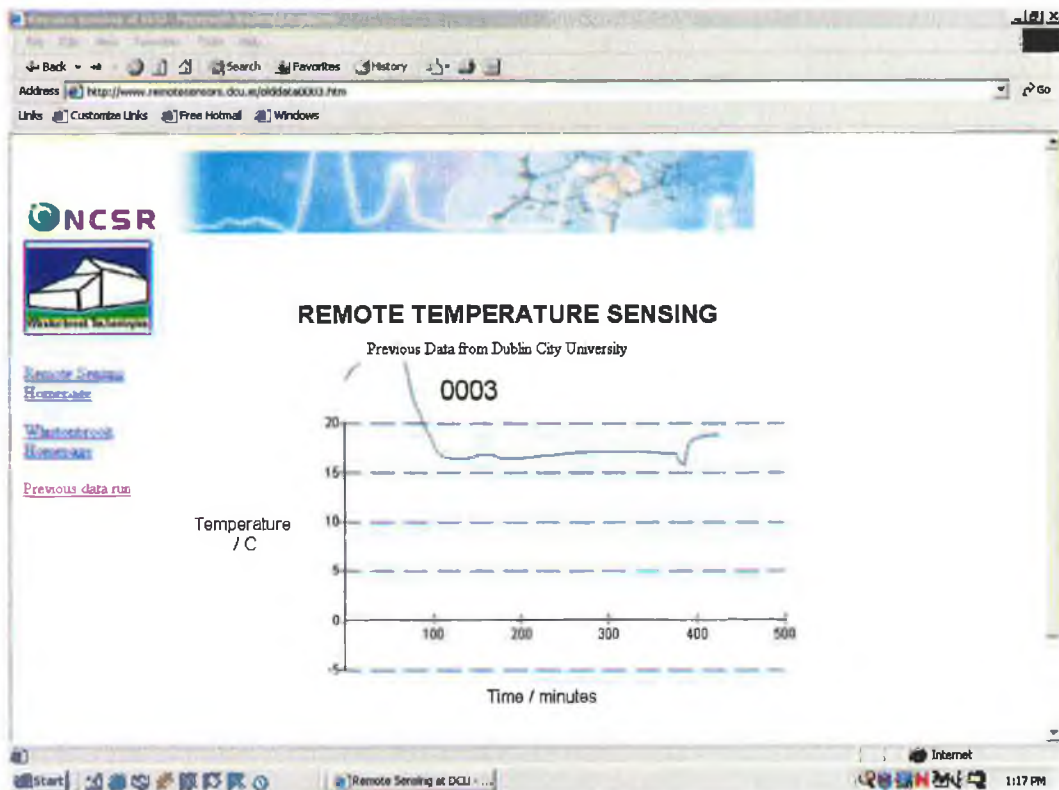


Figure 3-22 The temperature profile for logger 3 displayed on the web page

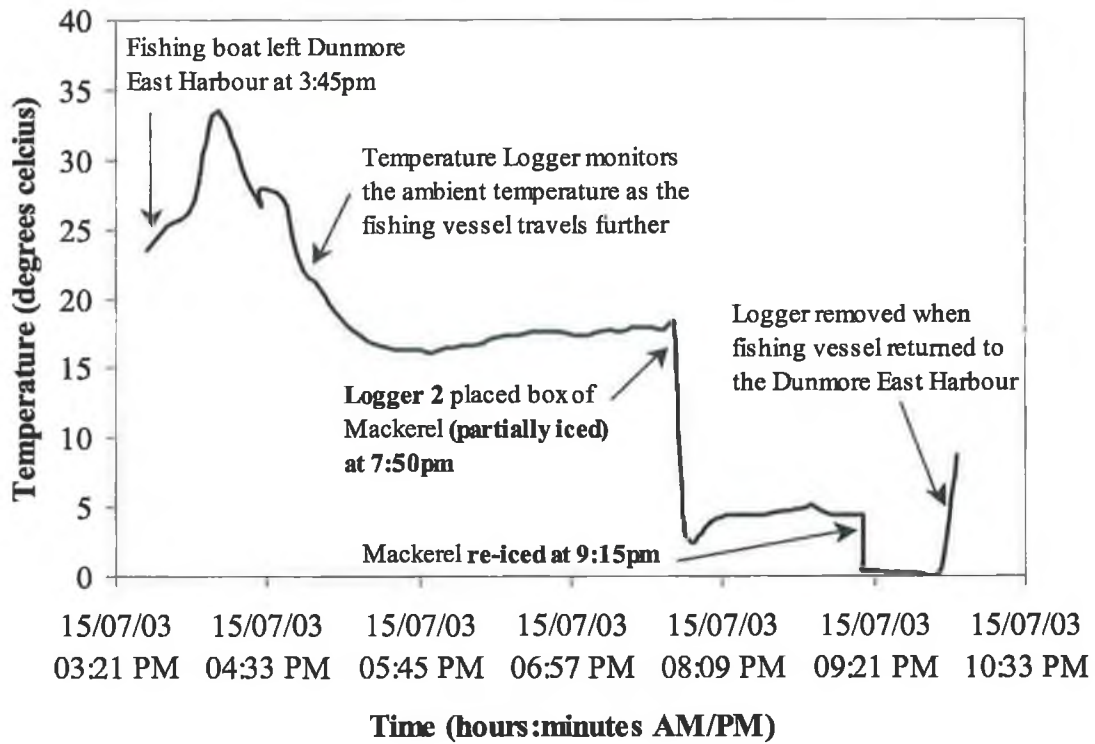


Figure 3-23 The storage temperature of a box of mackerel (partially iced) while at sea captured via logger 2. The logger was placed in the full box of mackerel at 7:50pm and was removed at 9:50pm when the boat returned to the harbour.

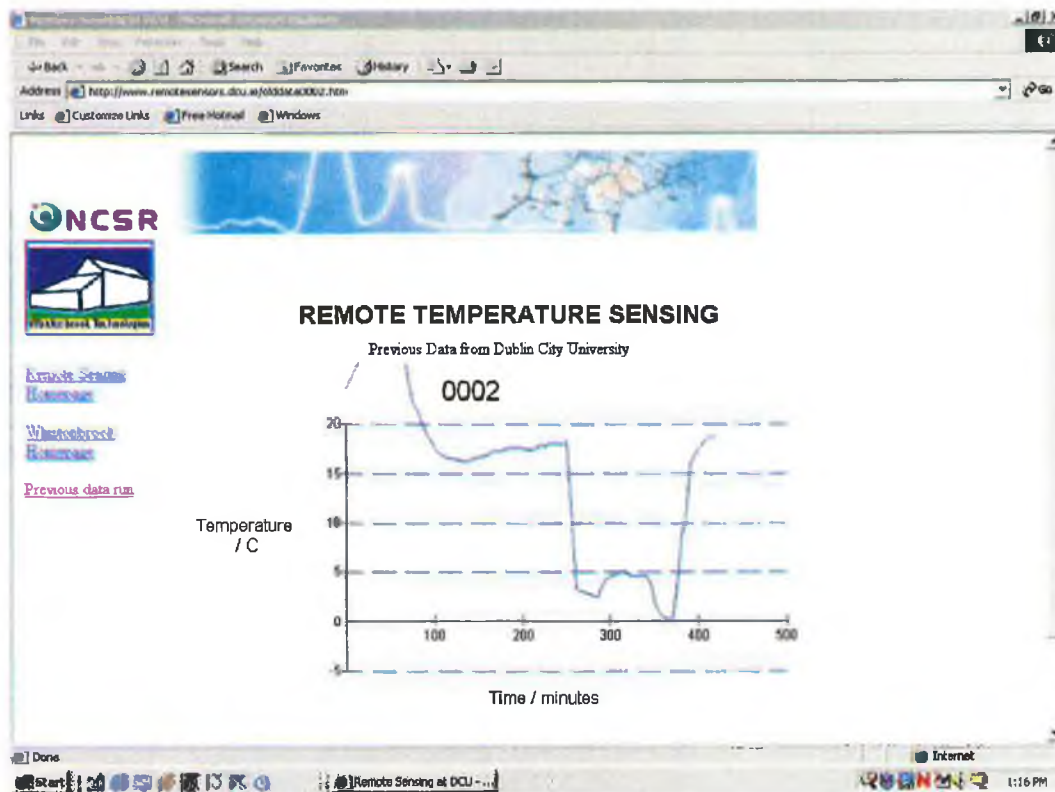


Figure 3-24 Illustrates the updated web page for logger 2

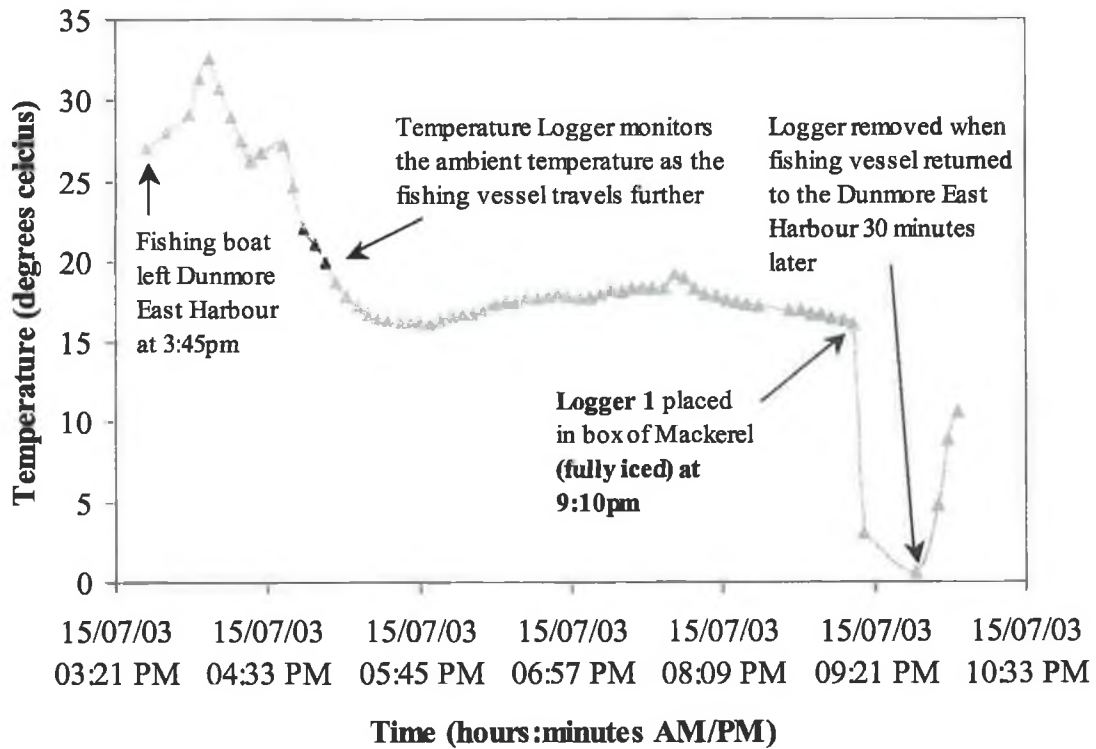


Figure 3-25 The storage temperature of a box of mackerel (fully iced) while at sea captured via logger 1. The logger was placed in the full box of mackerel at 9:10pm and was removed approx. 30 min later when the boat returned.

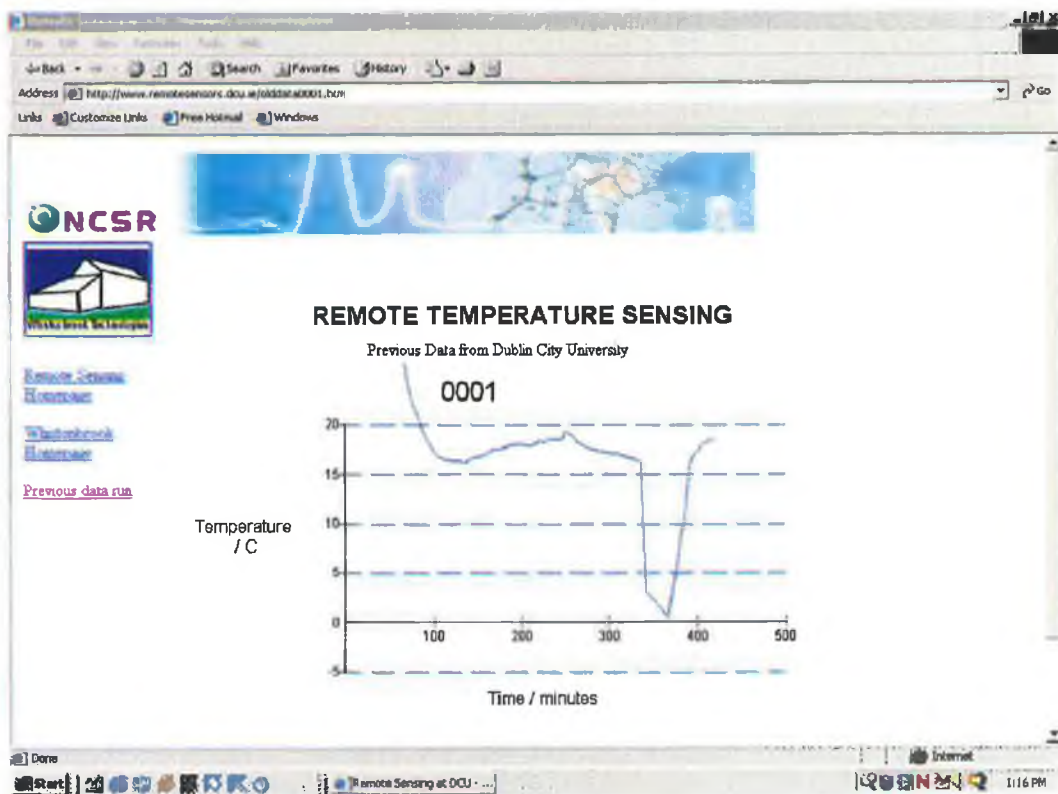


Figure 3-26 Illustrates the updated web page for logger 1

The field trials provided a perfect opportunity to test and improve the prototype RF-GSM Temperature Monitoring System. The system was presented with a number of challenges that were only realised through carrying out real trials at sea. Initially, communication links and software programs were problematic but were soon improved due to the numerous field trials that were carried out. As a result, real time temperature profiles of fish catches at sea were successfully generated on the World Wide Web.

On the 24<sup>th</sup> June 2003, Trial 3, the temperature profile of an individual salmon stored on ice was successfully captured using the RF-GSM Temperature Monitoring System and was continuously updated onto the web while the fishing boat was still at sea. Figure 3-16 compares the temperature data obtained by the RF-GSM Temperature Monitoring system and the iButtons of a salmon stored on ice for four hours on-board the boat before reaching the shore. During this time the temperature began to rise gradually but still remained below 5°C. The iButton temperature logger registered ambient temperatures at sea of ~25° before the logger was placed in the box. The RF Temperature Logger registered ambient temperatures as high as 36°C. The heat radiated by the sun was absorbed by the black surface of the RF Temperature Logger and caused it to register a higher ambient temperature than expected. A more reflective outer surface, i.e. a white surface, would help overcome this problem. The iButton data for each trial was very useful as a reference temperature system.

Before the *Wild Salmon Quality Scheme* was introduced the salmon were stored in boxes on the open deck without ice until the boat reached the shore and then the salmon were placed in cold storage. Storage temperature plays an important role in fish spoilage rates. If the salmon were stored on-board the fishing vessel for several hours without ice, an ambient daytime temperature of 25°C during the salmon season months of June and July would have a dramatic effect on the overall quality and spoilage of the salmon. The mackerel fishing trials also provided very interesting results. The RF-GSM Temperature Monitoring System illustrated how icing fish at sea greatly reduced the storage temperature. In trial 5, the mackerel fishing boat was not at sea long enough to realise the benefits of using larger quantities of ice on the fish as indicated by logger 1, see Figure 3-25.



Field-testing has allowed the system hardware to be evaluated. The main issues arising from the trials to date are as follows:

- RF communications between the loggers and the RF-GSM base station were problematic during the initial trials. The communication was improved by strategic placement of the RF-GSM base station and the RF loggers on-board the fishing vessel ensuring the path between the loggers and the base station was completely free from any metal obstructions and also ensuring that the loggers were placed within the working RF range.
- Data was successfully transmitted from the RF-GSM base station to the DCU central server via the GSM network at the specified time intervals (i.e. every 30 minutes) except on one occasion (Trial 2). The fault in this case was due to a software malfunction that was rectified within a couple of hours of the trial commencing.
- The RF-GSM base station operating controls, i.e. the On/Off switches, were originally covered over with a protective solid casing. This was replaced with a transparent window allowing the user to check if the system was in the correct operating mode i.e. Serial/Modem and On/Off modes, Figure 3-8. The transparent window protecting the operating controls on the RF-GSM base station also allowed the user to have a clear view of the red and green LEDs. The green LED flashed each time it received information from one of the loggers i.e. 3 consecutive flashes every 5 minutes indicated that all 3 loggers were communicating with the base station at 5-minute intervals. A flashing red LED indicated that the central server was communicating with the RF-GSM base station. This simple check confirmed that the RF-GSM Temperature Monitoring system was fully functioning.

The field trials also highlighted a number of issues regarding the capabilities of the software. As a result of developing the wireless data collection system, a significant amount of data was gathered which needs to be stored on the web site in a way that allows users access the information easily. The information gathered via the wireless RF-GSM Temperature Monitoring System includes logger ID, date, time and temperature. Other descriptive information which is not provided by the system includes: name/registration/location of the fishing vessel, name of skipper, fish species type (i.e. mackerel and/or salmon), individual fish registration number if necessary

(individual salmon are tagged), time/date of catch, number of boxes of each species caught, weather conditions (warm summer days may affect temperature profiles i.e. re-icing may be required more often), location of catches, time/date fish reached the shore. In order for this information to be accessible on the web a system is needed that allows the operator to input this information at sea. The Wireless RF-GSM Temperature Monitoring System is controlled via the software on the DCU central server. The start/stop and dial up frequency parameters are all set via this software before any trial begins. An operator at DCU must control these parameters while another operator installs the RF-GSM Temperature Monitoring System on-board a fishing vessel. Before the system operator on-board the fishing vessel sets out to sea, he/she must call the DCU operator (via a mobile phone) to start the remote sensor software with the dial-up settings. Once the software is initiated, the external modem dials the GSM modem phone (RF-GSM base station) at user defined intervals via an analogue phone line and the time-temperature data is retrieved as a simple data/text file. This information is automatically updated onto the web. Currently, the operator on-board the fishing vessel has some control of the system such as changing the RF-GSM base station to the ON/OFF position and switching the logger-sampling mode via a magnetic switch. Ultimately, the system operator on-board the fishing vessel should have more control over the RF-GSM Temperature Monitoring System. Chapter 7 addresses these issues further and highlights the tremendous progress and ongoing research activities in this particular area since the commencement of the project.

### **3.7 Conclusion**

The purpose of the preliminary temperature monitoring trials was to demonstrate that time-temperature profiles for fish stored in the hold of a trawler while at sea could easily be captured using autonomous temperature data loggers. The RF Temperature Logging System used initially was successfully programmed to operate independently on-board the fishing trawlers prior to commencing the trials. The loggers were positioned in the containers of iced fish stored in the trawler hold where they remained recording the storage temperature for the duration of the trial. As soon as the trawler returned to the shore the loggers were removed and the temperature data was successfully downloaded. A more sophisticated approach to monitoring the temperature of fish catches at sea was demonstrated using a newly developed RF-GSM Temperature Monitoring System where real-time temperature profiles were displayed live on the

internet while the fishing vessel was still at sea. The field trials demonstrated the feasibility of the system in real temperature monitoring applications and provided a perfect opportunity to pinpoint areas for further development in the area of autonomous temperature sensing.

## References

1. Frisby, J., Raftery, D., and Diamond, D., Temperature Monitoring with Autonomous Sensing Devices, in *WEFTA 2002 (Western European Fishing Technologists Association)*, Bord Iascaigh Mhara, Galway, Ireland., pp. 22 (2002).
2. Frisby, J., and Diamond, D., Development of Temperature Logging Technology for the Fishing Industry, in *TAFT 2003 (First Joint Trans Atlantic Fisheries Technology Conference)*, The Icelandic Fisheries Laboratories, Reykjavik, Iceland, pp. 236 (2003).
3. Crowley, K., Frisby, J., Murphy, S., Roantree, M., and Diamond, D., Web-based real-time temperature monitoring of shellfish catches using a wireless sensor network, *Sensors and Actuators* (In press).
4. McAteer, K., Raftery, D., and Diamond, D., Temperature Logging of Fish Catches Using Autonomous Sensing Units, *Trends in Food Science & Technology*, 11, 291 (2001).

**4 Fabrication and Characterisation of pH Sensitive Membranes and their Response to Spoilage Volatiles Released by Cooked Shellfish**

## 4.1 Introduction

The following chapter gives a detailed account of the fabrication and characterisation of pH sensitive membranes. A preliminary investigation was performed to demonstrate the sensors response to the spoilage volatiles released by cooked shellfish over time under different storage conditions.

### 4.1.1 Fabrication and Characterisation of pH Sensitive Membranes

Most indicator chemistry is adapted to aqueous solution (for titration in water). Therefore, the molecules are water-soluble and if dissolved in lipophilic polymers, they are rapidly washed out. In order to make dyes, ionophores and ligands soluble in polymers and to avoid leaching of the components, they have to be made lipophilic. Lipophilic molecules can be obtained, for example, by introduction of long alkyl chains, Figure 4-1 & Figure 4-2.

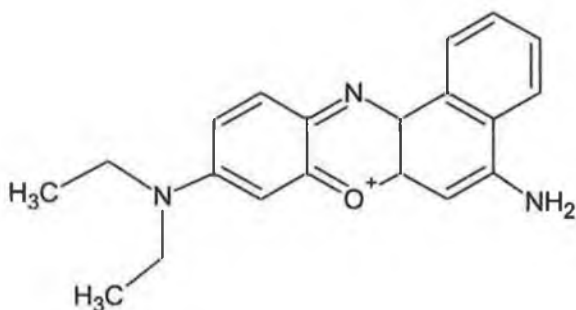


Figure 4-1 Water-soluble pH indicator (Nile Blue  $pK_a \sim 11.6$ )



Figure 4-2 Polymer/plasticiser-soluble pH indicator (Octadecyl Nile Blue)

However, the chemical synthesis involved can be tedious. Therefore, an alternative strategy is to use ion pairing. For example, when the pH indicator dye bromocresol green, Figure 4-3, and the lipophilic compound tetraoctylammonium bromide, Figure 4-4, are together in solution, the positive and negative ions come together to form a solvated unit called an ion-pair, Figure 4-5. The pH indicator is now lipophilic and polymer/plasticiser-soluble.

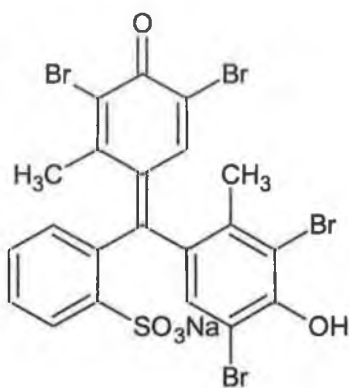


Figure 4-3 Bromocresol Green, Sodium Salt (BCG)

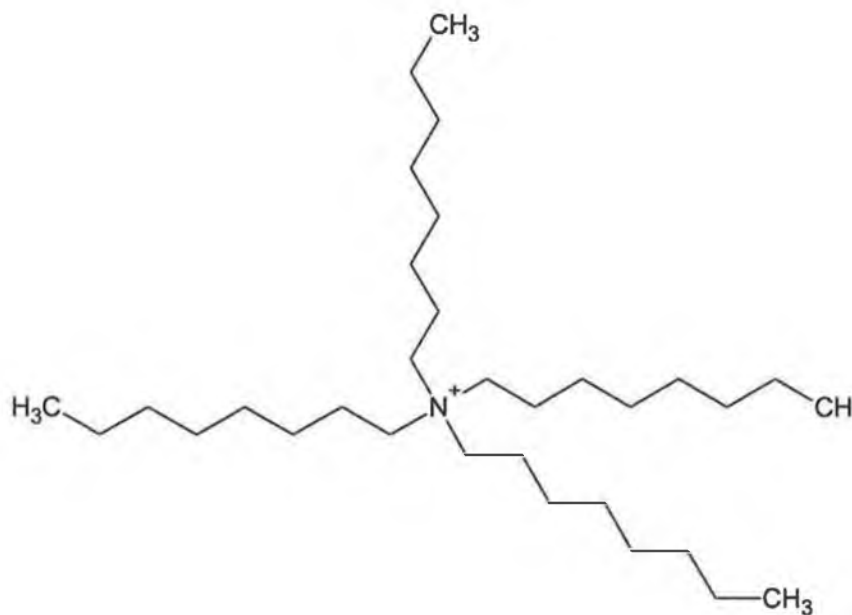
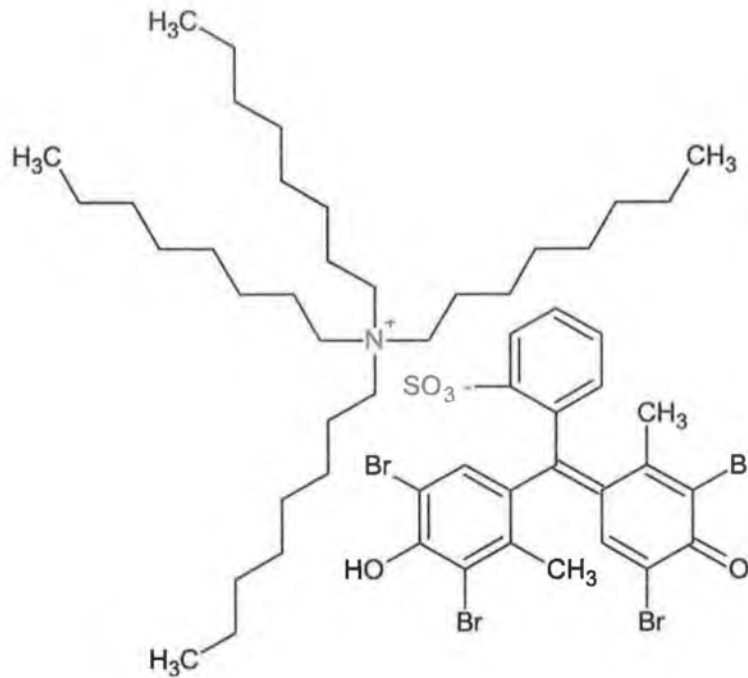


Figure 4-4 Tetraoctylammonium Bromide (TOABr)



**Figure 4-5 BCG and TOABr ion pair**

#### 4.1.1.1 Lipophilic Salt Selection

In order for the lipophilic salt to be effective the salt itself must be soluble and compatible with all the components in the membrane. Three lipophilic salts were chosen and their effectiveness in the polymer membrane was determined by their ease of solubility, their effect on dye leaching and their compatibility with other components i.e. plasticisers. The structures of the 3 salts can be seen in Figure 4-4, Figure 4-6 & Figure 4-7.

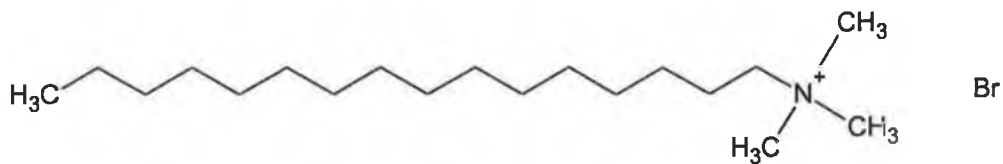


**Figure 4-6 Cetyltrimethylammonium Bromide, CTABr**

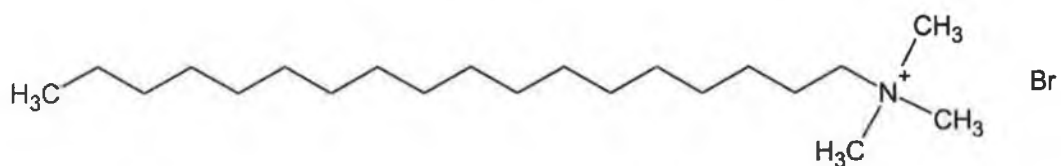


**Figure 4-7 Octadecyltrimethylammonium Bromide, OCTABr**



#### 4.1.2 Monitoring of Headspace Spoilage Volatiles Released from Cooked Whelk in Different Storage Conditions using the pH Sensitive Membranes

Preliminary trials were carried out at DCU to correlate the sensor response to spoilage volatiles released by whelk, a gastropod from the molluscan shellfish family. Molluscan meats contain high levels of nitrogen bases, as do other shellfish. It has been reported that certain types of shellfish i.e. crustaceans, contain over 300mg of nitrogen/100g meat, which is considerably higher than that for fish (1). The presence of high levels of nitrogenous bases makes them more susceptible to rapid attack by the spoilage flora. For this reason, it is important that the sensors are optimised for this particular species. As molluscan shellfish have higher levels of nitrogenous bases compared to fish the sensor formulation must be optimised so that it is not completely saturated by the initial levels of volatile basic nitrogenous compounds present. On the other hand, the sensor must be sensitive enough to detect the onset of spoilage by responding to increasing levels of Total Volatile Basic Nitrogen (TVB-N). Preliminary trials at Dublin City University and field trials at Errigal Fish Co. LTD (see Chapters 5 & 6) were conducted to aid the optimisation of a pH sensitive sensor suitable for detecting whelk spoilage.

## 4.2 Experimental

### 4.2.1 Fabrication and Characterisation of pH Sensitive Membranes

#### 4.2.1.1 Membrane Components

The membrane components; pH sensitive dyes bromocresol green (BCG, sodium salt), bromothymol blue (BTB, sodium salt), and m-cresol purple (m-CP, sodium salt), lipophilic salts cetyltrimethylammonium bromide (CTABr), tetraoctylammonium bromide (TOABr), octadecyltrimethylammonium bromide (OCTABr) and solvent cyclohexanone (99.8%), were obtained from Sigma-Aldrich (Dublin, Ireland). The binder poly(vinyl chloride) (PVC, high molecular weight) and the plasticiser dibutyl sebacate (DBS) were supplied by Fluka Chemicals (Dublin, Ireland). Optically clear poly(ethylene terephthalate) (PET) was obtained from Oxley plc (Cumbria, UK). Polypropylene reinforcement rings and polytetrafluoroethylene (PTFE) gas permeable membrane (Thread Seal Tape: 12m × 12mm × 0.075mm) were supplied by Radionics (Dublin, Ireland).

#### 4.2.1.2 Membrane Formulation

Ten membrane formulations in total were prepared and labelled “A” to “J”, as seen in Table 4-1. Formulations “A” to “D” were initially prepared. Each formulation contains the same quantity of BCG (5mg), PVC (350mg) and CTABr (10mg) but each formulation “A”, “B”, “C” & “D” contains 350mg, 262.5mg, 175mg & 87.5mg DBS, respectively. Formulations “E” and “F” contain a different lipophilic salt TOABr (10mg), compared to formulations “A” to “D”. Each contains the same quantity of BCG (5mg) and PVC (350mg) but different concentrations of DBS, 350mg and 175mg respectively. Formulations “G” and “H” contain a third type of lipophilic salt OCTABr. Once again each have the same quantity of BCG (5mg) and PVC (350mg) but different concentrations of DBS, 350mg and 175mg respectively. Formulations “I” and “J” both have the same quantities of PVC (350mg), DBS (350mg) and TOABr (10mg) but the formulations contain different pH sensitive dyes. Formulation “I” contains BTB (5mg) and formulation “J” contains m-CP (5mg).

Formulation	A	B	C	D	E	F	G	H	I	J
<b>Dye (mg)</b>										
BCG	5	5	5	5	5	5	5	5		
BTB									5	
m-CP										5
<b>Binder (mg)</b>										
PVC	350	350	350	350	350	350	350	350	350	350
<b>Plasticiser (mg)</b>										
DBS	350	262.5	175	87.5	350	175	350	175	350	350
<b>Salt (mg)</b>										
CTABr	10	10	10	10						
TOABr					10	10			10	10
OCTABr							10	10		
<b>Solvent (ml)</b>										
Cyclohexanone	8ml	8ml	8ml	8ml	8ml	8ml	8ml	8ml	8ml	8ml

**Table 4-1 Components of each formulation A to J**

All formulations were prepared following the same procedure. For example, formulation "A" was prepared by accurately weighing 5mg BCG, 10mg CTABr and 350mg DBS into a 20ml disposable polypropylene container. 2ml of cyclohexanone were added and the container was swirled gently to mix the contents. 350mg of PVC were added all at once followed immediately by the remaining cyclohexanone. The container was sealed with a polypropylene cap and shaken vigorously for 10 minutes to prevent the PVC from aggregating. The solution was then sonicated until all the components were fully dissolved. The same procedure was carried out for formulations "B" to "J". Formulation "J" required a couple of drops of reagent grade methanol to aid the solubility of the dye.

#### *4.2.1.3 Sensor Fabrication*

A schematic diagram illustrating each step of the sensor spot fabrication is shown in Figure 4-8. The PET sheets were manually cut into sections (~15cm × 10cm). The strips were washed in distilled water and allowed to air dry. Polypropylene rings were fixed to the PET surface (step 1). This formed a mould and a solid matrix for the polymeric pH sensitive films. 5.5µl aliquots of the sensor spot formulation were dropped into the centre of the polypropylene rings using a Brand® 0.5µl – 10µl transferpipette and the films were allowed to dry in a dark environment (to prevent photo bleaching of the dye) at room temperature for 24 hours (step 2). After solvent evaporation, the pH sensitive films attached to the PET surface were punched out in the shape of circular discs 6mm in diameter (step 3). Polypropylene rings were fixed to the PTFE gas permeable membrane (thread seal tape) and the 6mm circular discs were placed (pH sensitive layer facing down) inside the rings (step 4). An optically clear protective adhesive layer was placed on top to form a solid support for the sensor disc and the PTFE gas permeable membrane (step 5). The PTFE membrane protects the sensor surface from moisture while allowing gaseous compounds to permeate. Finally, a scissors was used to cut around the edges of the polypropylene ring to give a circular shaped sensor spot (step 6). Digital images were taken of steps 2, 3 & 6 during the sensor spot production and can be seen in Figure 4-9.

#### *4.2.1.4 Measurement of Sensor Thickness*

The thickness of 4 sensors was measured using a Dektak V 200-Si Profilometer. The Dektak V 200-Si is an advanced surface texture measuring system, which accurately measures surface texture and film thickness (2). The sensor thickness was also determined using a scanning electron microscope, SEM Hitachi S-3000N.

#### *4.2.1.5 Dye Leaching Studies*

The effectiveness of the lipophilic salts CTABr and TOABr in preventing dye leaching was determined by allowing the sensor membranes to soak in distilled water for a known amount of time and analysing the distilled water using UV-Vis spectroscopy. Dye leaching can easily be recognised by the presence of a peak at the characteristic  $\lambda_{\text{max}}$  for bromocresol green, 617nm, in the distilled water. The effect of plasticiser concentration on dye leaching was also determined.

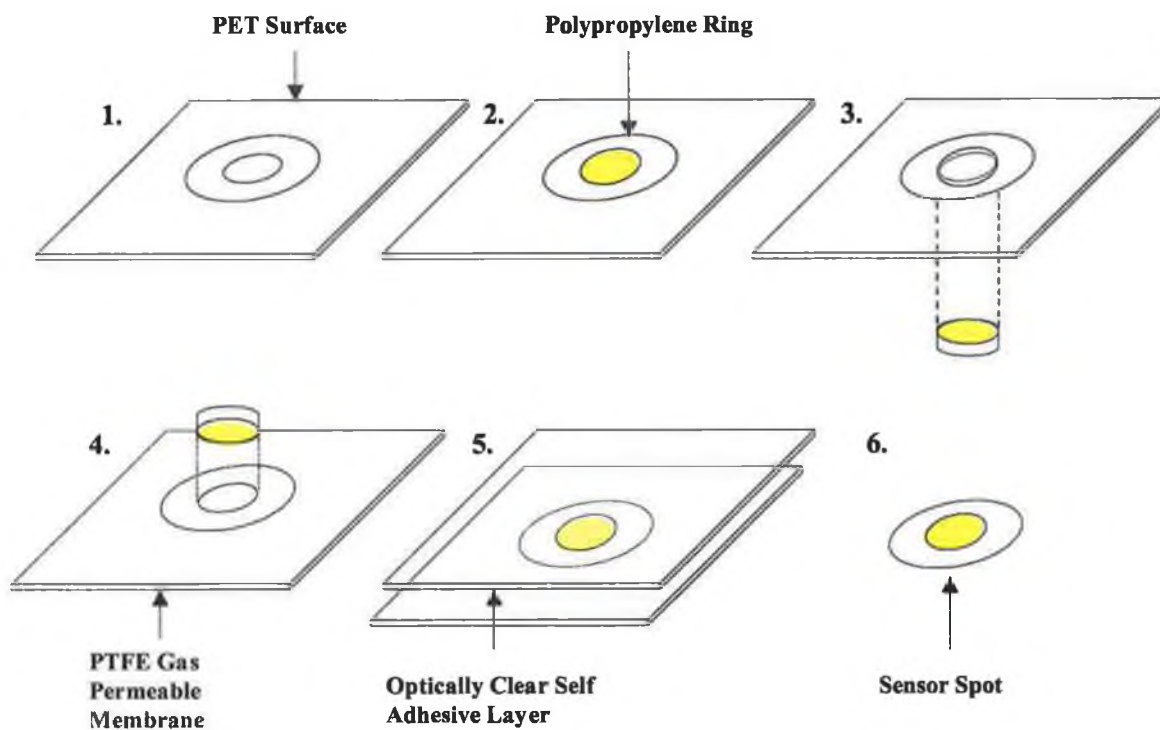


Figure 4-8 Schematic of the sensor fabrication process



Figure 4-9 Digital images of steps 2, 3 & 6 of the sensor spot fabrication process

6 sensor spots prepared from each of the 6 formulations “A” to “F” were placed in 10ml polypropylene containers. 2ml of distilled water was added to each of the 6 containers. The containers were sealed with polypropylene caps and allowed to sit for 3 hours. After 3 hours, 200 $\mu$ l of distilled water from each of the 6 containers were deposited into the wells of a 96-well plate using a pipette. 200 $\mu$ l distilled water acted as a blank. All samples were prepared in triplicate. A UV-Vis spectrum (350nm to 700nm) of each sample was obtained using a plate-well reader (Model  $\mu$ -Quant, supplied by the Medical Supply Company, Dublin, Ireland).

#### 4.2.1.6 Preparation of pH Buffer Solutions

Buffer solutions were prepared from pH  $4.00 \pm 0.02$  and pH  $7.00 \pm 0.02$  buffer tablets obtained from BDH Laboratory Supplies, Dublin, Ireland. For example, 1 pH 4 buffer tablet dissolved in 100ml of distilled water produces a solution of pH  $4.00 \pm 0.02$ . Buffer solutions ranging from pH 4 to pH 7 were prepared from stock pH  $4.00 \pm 0.02$  and pH  $7.00 \pm 0.02$  buffer solutions. To prepare a pH 5.00 buffer solution, 4M NaOH was added dropwise to 50ml of pH  $4.00 \pm 0.02$  buffer solution until the pH reached 5.00 measured using a calibrated pH meter (Metrohm 713 pH Meter; Metrohm pH probe, code no: 0022 0018. The pH meter was calibrated before use according to the instrument guidelines using pH  $4.00 \pm 0.01$  and pH  $7.00 \pm 0.01$  standard buffer solutions obtained from Sigma Aldrich, Dublin, Ireland). Likewise, to prepare a pH 6.00 buffer solution, 0.1M HCl was added drop wise to 50ml of pH  $7.00 \pm 0.02$  buffer solution until the pH reached 6.00 measured using a calibrated pH meter. A range of pH buffers were prepared following this procedure and were used in the  $pK_a$  determinations of the dye in the sensor membrane.

#### 4.2.1.7 $pK_a$ Determination of Dye in the membrane

The  $pK_a$  of the dye in the membrane was determined using a newly developed handheld Colourmeter, which is discussed in detail in section 4.2.1.10, as well as using UV-Vis spectroscopy. For each technique, the  $pK_a$  was determined by plotting the change in absorbance of the dye at  $\lambda_{max}$  (or the change in the Colourmeter response) with changing pH and a best-fit sigmoid curve was fitted to the data using the Solver function in Microsoft Excel. The equation used was:

$$\text{Abs}(\lambda_{max}) = \left[ \frac{a}{(1 + \exp[b(\text{pH} - z)])} \right] e + d \quad \text{Equation 4-1}$$

Abs ( $\lambda_{max}$ )= absorbance of the dye at  $\lambda_{max}$  in a pH buffer solution / au (absorbance units)

a = peak height at  $\lambda_{max}$  / au

b = slope coefficient

z = pH from the beginning of the peak to the inflection of the rise (i.e. the  $pK_a$ )

d = baseline offset / au

e = symmetry parameter for the sigmoid

The formula was entered into Microsoft Excel to model the fit of the data obtained. The residuals, the squared residuals and the sum of the squared residuals (SSR) were all calculated. Solver minimised the SSR values by changing the values a, b, z, d and e. The value of e was set to 1 and a best-fit sigmoid curve was obtained. The parameters of the best-fit curve were used to compute extrapolated values between the data points, i.e. every 0.01 pH units, to produce best-fit curves to the data collected. This facilitated the determination of the  $pK_a$  of the dye.

#### *4.2.1.8 $pK_a$ Determination of the Dye in the Membrane by UV-Vis Spectroscopy*

Sensor spots of the optimised formulation “E” were prepared as described in section 4.2.1.3. The 6mm sensor discs were placed on the base of individual wells in a 96-well plate. 200 $\mu$ l of buffer solution was added to each well. The sensor discs were allowed to sit in the buffer solutions for 1 hour to allow the buffer solutions impregnate the sensor membranes and react with the dye to give a colour change. Absorbance values were obtained using the plate-well reader. Sensors were prepared in triplicate for each buffer solution.

#### *4.2.1.9 The Effect of Temperature on the $pK_a$ of the Dye in the Membrane*

The 6mm sensor discs of formulation “E” were prepared and placed in the base a 96-well plate as described above. The buffer solutions and the plates with the sensor discs were all placed in the fridge (4°C, measured by a thermometer) for 2 hours to allow the temperature of the plates, sensor discs and the buffer solutions to reach equilibrium. 200 $\mu$ l of the cold buffer solutions were then pipetted into the wells containing the sensor discs and the plates were immediately placed into the fridge for 1 hour. A UV-Vis scan for an entire row (12 wells) over a wavelength range of 400-700nm takes approximately 90 seconds to complete. The sensors were prepared in triplicate. If all the sensors were to occupy the 96-well plate they would fill 3 rows therefore a UV-Vis scan would take approximately 4 minutes to complete. This would be sufficient time to raise the temperature of the sensor discs and buffer solutions rendering the experiment futile.

To minimise the temperature effects the sensors were placed in 3 separate trays and were scanned individually, each scan taking approximately 90 seconds.

#### 4.2.1.10 *pK<sub>a</sub> Determination of the Dye in the Sensor Membrane using the Handheld Colourmeter*

##### 4.2.1.10.1 Instrumentation

The handheld Colourmeter comes with four interchangeable heads i.e. red, blue, green and yellow heads, Figure 4-10. The most suitable LED head for this application was selected by comparing the  $\lambda_{\max}$  of the LEDs with the  $\lambda_{\max}$  of the bromocresol green dye in its basic form in the sensor membrane. The LED head is connected to the handheld Colourmeter unit Figure 4-10, which is attached to a PC via an RS323 cable where the specifically designed Colourmeter software allows parameters such as sampling intervals to be programmed. Two control buttons on the front of the handheld Colourmeter unit allows the user to operate the system manually without the need to be connected to a PC. The handheld Colourmeter displayed in Figure 4-10 is the new and improved version of the original prototype, Figure 4-11, designed by Dublin City University and Whistonbrook Technologies Ltd to measure the reflected light intensity of fish spoilage sensor dots (3).

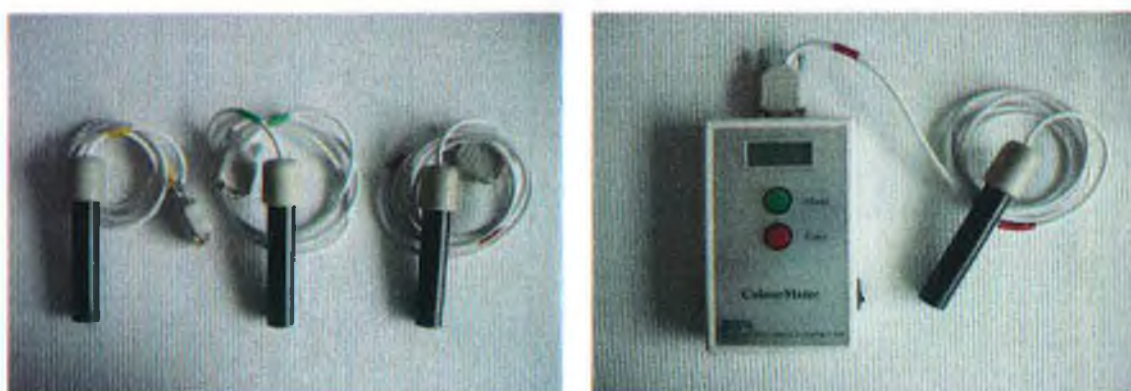


**Figure 4-10** Yellow, green, and red interchangeable heads for the handheld Colourmeter (left). Red LED head attached to the handheld Colourmeter (right).

The original prototype consists of 2 yellow LEDs, with a  $\lambda_{\max}$  of 590nm, positioned at a 45° angle to the sensor surface to minimise reflection effects, and a photodiode detector (positioned at a 90° angle), Figure 4-11. Light emitted from the LEDs illuminate the sensor surface at a 45° angle (A). Light reflected back from a region of interest at 90° falls onto the photodiode detector (B). Light reflected back from the highly reflective



sensor surface is at 45° and is therefore not measured by the photodiode. The LED illumination is pulsed to eliminate interference from ambient light.

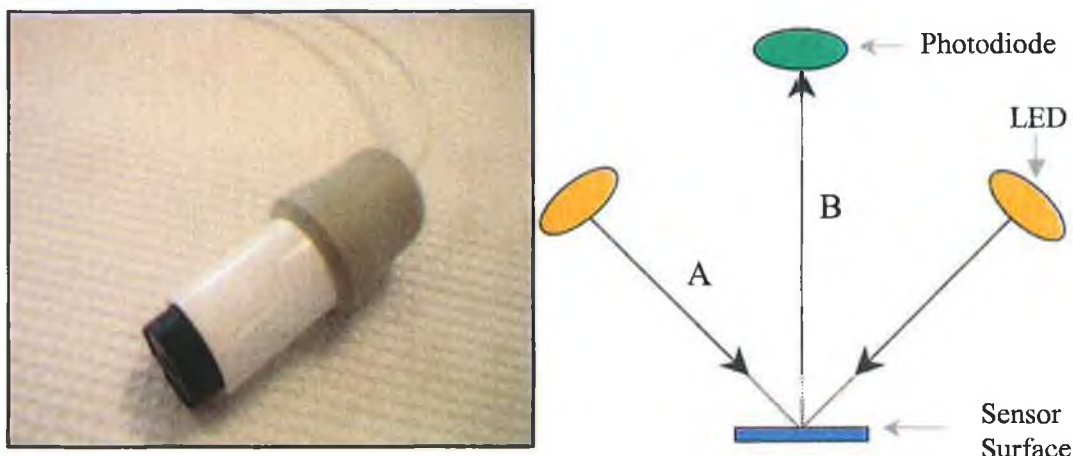


**Figure 4-11** A photograph of the original prototype handheld Colourmeter (left) and a schematic diagram of the internal component configuration (right) (3)

The same principle described here is also used in the new and improved prototype handheld Colourmeter. The major difference between the two systems is that the new system has interchangeable heads with blue, red, yellow and green LEDs allowing more sensitive reflectance measurements to be performed over a wider wavelength range.

#### 4.2.1.10.2 Experimental Set-up

Buffer solutions were prepared as described previously and the apparatus shown in Figure 4-12 was set up. A circular disc of optically clear PET was attached to the Red LED Head. This protected the inner electronics from the pH buffer solutions into which it was immersed. The optical scanner is not designed for liquid immersion but for the purpose of this experiment a slight alteration of the head allowed the scanner to be immersed into liquids. A sensor prepared from formulation "E" was attached to the head using epoxy glue. The glue was allowed to dry overnight. A circular o-ring was attached to the Red LED head also using epoxy glue. This allowed the head to sit at a fixed height in the apparatus. The head is positioned ~2mm from the white reflective surface in the base of the container. This provides enough space for the buffer solution to come in contact with the sensor without affecting reflectance. There is an inlet tube where buffer solution is pumped through using a syringe and a drainage tube at the bottom where the buffer solution can be easily drained.

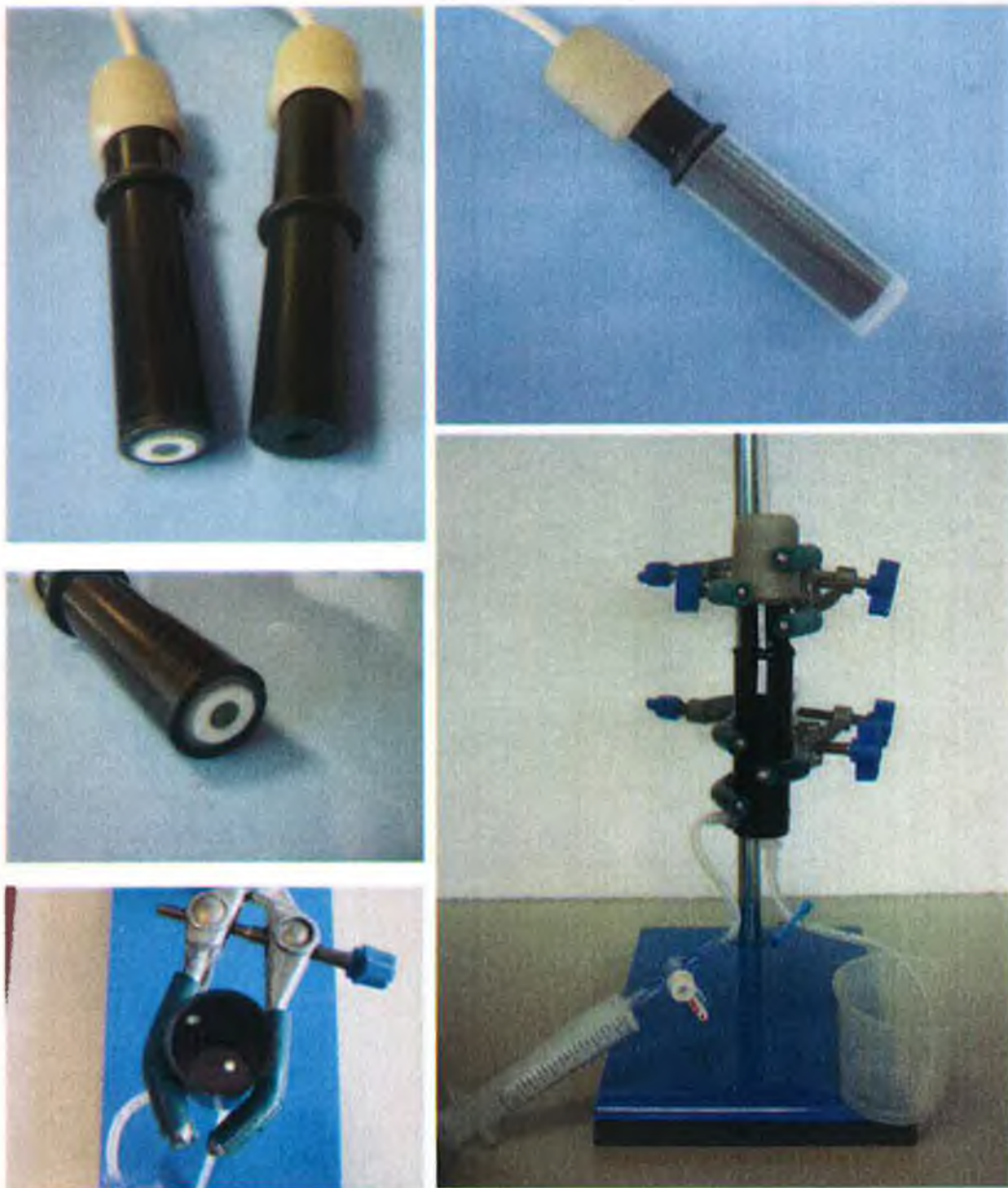


**Figure 4-12 Experimental apparatus for pH buffer calibrations.** A circular disc of optically clear PET was attached to the Red LED Head, which protected the inner electronics from the pH buffer solutions into which it was immersed. A sensor prepared from formulation “E” was attached to the head using epoxy glue (top left). A circular o-ring was attached to the Red LED head, which allowed the head to sit at a fixed height in the apparatus (top right). The head is positioned ~2mm from the white reflective surface in the base of the container (bottom left). This provides enough space for the buffer solution to come in contact with the sensor without affecting reflectance. There is an inlet tube where buffer solution is pumped through using a syringe and a drainage tube at the bottom where the buffer solution can be easily drained (bottom right).

#### 4.2.1.11 *Reproducibility of the Sensor Response in pH Buffer Solutions*

Buffer solutions pH  $4.00 \pm 0.02$  and pH  $7.00 \pm 0.02$  were prepared as described previously. The Red LED was attached to the Colourmeter. A spot prepared from formulation "E" was attached to the Red LED Head. The software was set to take a reading every 5 seconds. The height of the head in the calibration flow cell was adjusted to give the best response (no buffer solution inside). The flow cell was flushed out with buffer pH 4 solution. 2ml of pH 4 buffer solution was injected into the flow cell and the response was allowed to equilibrate. The flow cell was allowed to drain then washed through with buffer pH 7. The drain was closed using a clamp on the outlet tube and 2ml of the buffer pH 7 solution were injected into the flow cell. The response was allowed to equilibrate. The cell was allowed to drain and washed with pH 4 buffer solution and the procedure was repeated several times to investigate the reproducibility of the step change from pH 4 to pH 7.

#### 4.2.1.12 *Ammonia Gas Calibration*

Measurements were performed using the handheld Colourmeter. The experimental set-up for the sensor measurements is shown in Figure 4-13. Mass flow controllers enabled known concentrations of ammonia gas to be delivered to the flow-cell by mixing different proportions of pure nitrogen (maximum flow rate  $100\text{-}900\text{cm}^3 \text{min}^{-1}$ ) and 0.01% ammonia in nitrogen (maximum flow rate  $50\text{cm}^3 \text{min}^{-1}$ ). The pure nitrogen was allowed to flow through a humidifier before it was mixed with 0.01% ammonia in nitrogen. The gas mixture entered the flow cell through the inlet tube where it reacted with the sensor. The sensor was attached to the Red LED head of the Colourmeter using epoxy glue and the Colourmeter head was secured inside the flow cell with the aid of a rubber o-ring seal. The Colourmeter was attached to a PC via an RS232 cable that enabled the LabView software Version 4.501 to record the sensor response to ammonia in real time at user-defined intervals (i.e. every 5 seconds). The data was saved as a DAT file in Microsoft Notepad. Data analysis was performed using Microsoft Excel. For the data analysis, the reported values (arbitrary units, au) are calculated as the average of 60 values of the final 5 minutes of the measurements subtracted from the initial value (i.e. initial value = the average of 120 values (10 minutes) before the measurement starts). This is taken as the baseline which represents 0ppm  $\text{NH}_3$ .

#### 4.2.1.12.1 Experimental Set-up

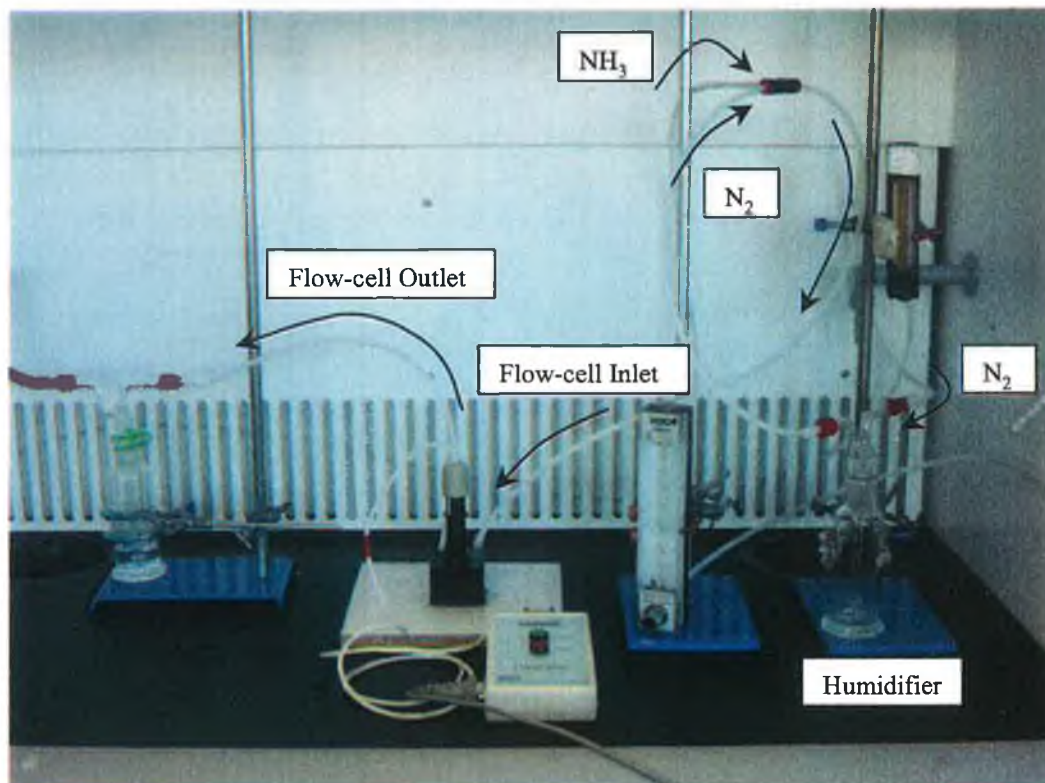


Figure 4-13 Experimental set-up for sensor calibration using ammonia gas. Mass flow controllers enabled known concentrations of ammonia gas to be delivered to the flow-cell by mixing different proportions of pure nitrogen (maximum flow rate  $100\text{-}900\text{cm}^3\text{ min}^{-1}$ ) and 0.01% ammonia in nitrogen (maximum flow rate  $50\text{cm}^3\text{ min}^{-1}$ ). The pure nitrogen was allowed to flow through a humidifier before it was mixed with 0.01% ammonia in nitrogen. The gas mixture entered the flow cell through the inlet tube where it reacted with the sensor.

## 4.2.2 Monitoring of Headspace Spoilage Volatiles Released from Cooked Whelk in Different Storage Conditions using the pH Sensitive Membranes

### 4.2.2.1 Materials

The membrane components, pH sensitive dye bromocresol green (BCG,  $pK_a$  4.7), lipophilic salt tetraoctylammonium bromide and solvent cyclohexanone (99.8%), were obtained from Sigma-Aldrich (Dublin, Ireland). The binder poly(vinyl chloride) (PVC, high molecular weight) and the plasticiser dibutyl sebacate (DBS) were supplied by Fluka Chemicals (Dublin, Ireland). Optically clear poly(ethylene terephthalate) (PET) was obtained from Oxley plc (Cumbria, UK). Polypropylene reinforcement rings and polytetrafluoroethylene (PTFE) gas permeable membrane (Thread Seal Tape: 12m × 12mm × 0.075mm) were supplied by Radionics (Dublin, Ireland). The sensors were fabricated as described previously. Self-adhesive clear covering film (33cm × 1m) and 500ml clear plastic containers were used.

### 4.2.2.2 Equipment

The red LED head ( $\lambda_{max} = 659\text{nm}$ ) of the Handheld Colourmeter was used to monitor the colour change of the pH sensitive membranes in response to spoilage volatiles. The Colourmeter was attached to a PC laptop (Dell, Latitude) via an RS232 cable that enabled the LabView software Version 4.501 to record the colour change. The data was saved as a DAT file in Microsoft Notepad. Data analysis was performed using Microsoft Excel. A digital camera (Sony DS1234 Cyber Shot) was used to capture colour digital images of the sensors as they changed colour. Model DS1921-F51 iButton temperature data logger obtained from Dallas Semiconductor monitored ambient temperature conditions.

### 4.2.2.3 History of whelk Samples

#### 4.2.2.3.1 Preliminary Trial 1

Whelks freshly caught on the day of the trial in Dublin bay were collected from a fishing trawler at Howth Harbour Co. Dublin, Ireland. The whelks were immediately

placed into a polystyrene box containing foam refrigerant blocks and the samples were transported to DCU.

#### 4.2.2.3.2 Preliminary Trial 2

6 whelks were purchased from Wright's of Howth (Howth Harbour, Dublin, Ireland). The whelks were foil packed and placed into an insulated polystyrene container as described above and were immediately transported to DCU.

#### 4.2.2.4 Preparation and Cooking Whelk Samples

On arrival at the DCU laboratory the whelks were placed in boiling water. The water was allowed to boil again and the whelks were boiled continuously for 12 minutes, Figure 4-14. The whelks were then removed from the boiling water and allowed to cool for 5 minutes before they were placed into individual 500ml clear plastic containers.

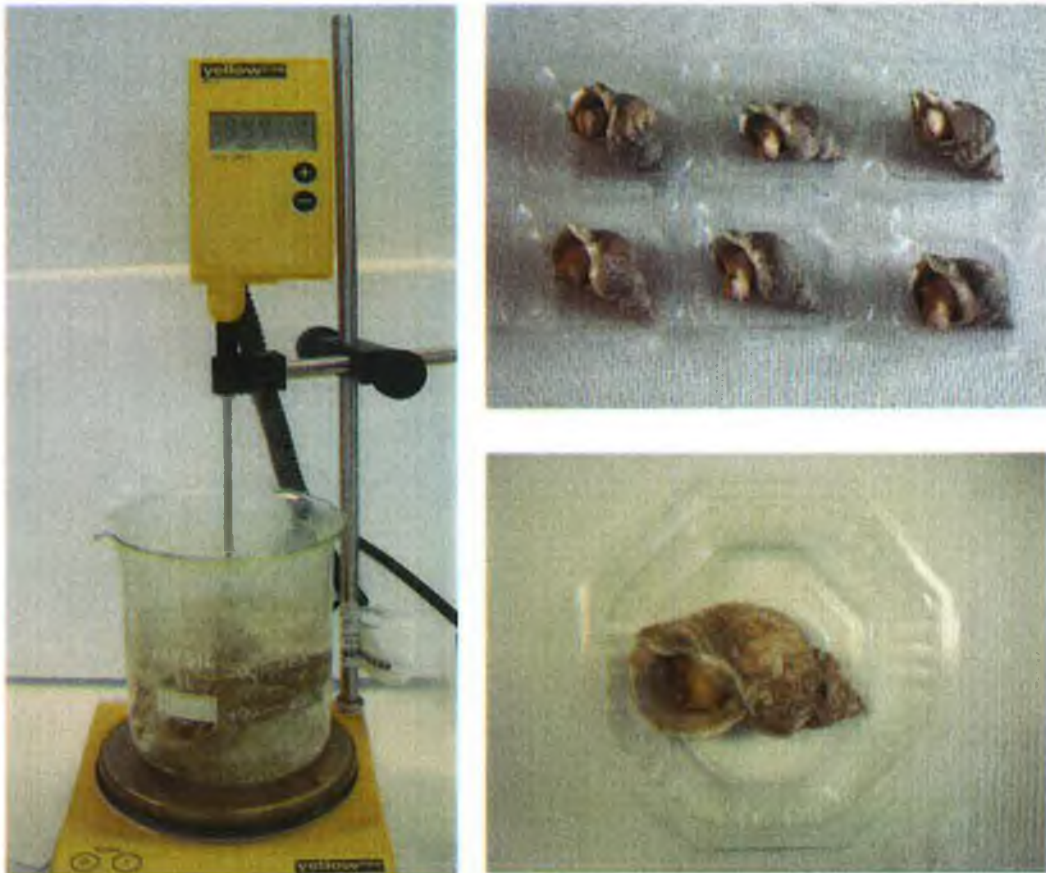


**Figure 4-14** Cooking and preparation of whelk samples

#### 4.2.2.5 Experimental Set-up

##### 4.2.2.5.1 Preliminary Trial 1



**Figure 4-15 Sensor spot before and after spoilage**

One sensor spot was attached to the self-adhesive clear covering film that was placed over the 500ml plastic container to form a tight seal. The Red LED Head of the Colourmeter was placed directly in contact with the sensor spot and secured in position with a retort stand, Figure 4-16. The Colourmeter was connected to a PC Laptop where the Colourmeter software version 4.501 was programmed to take a reading every 10 minutes. A layer of tinfoil was placed over the set-up to eliminate ambient light interference. An iButton was also programmed to take a temperature measurement every 10 minutes. The whelk was allowed to spoil at room temperature over a 72-hour period.

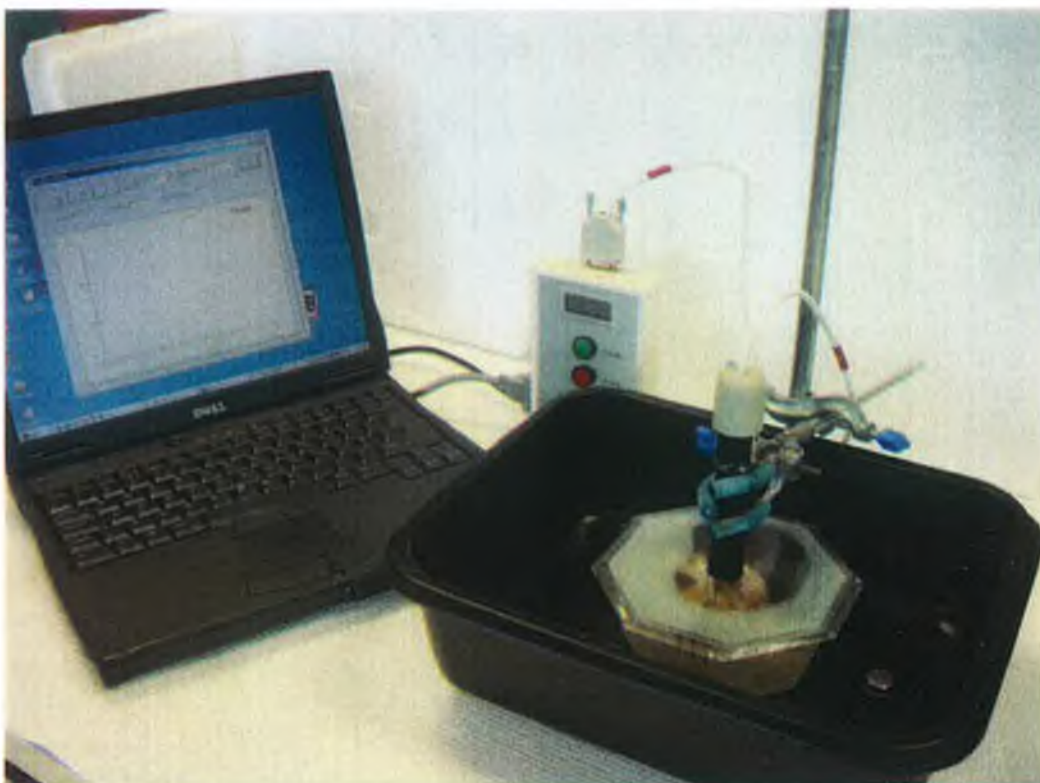


**Figure 4-16 Red LED Head of the Colourmeter monitoring the colour change of the sensor spot over time as the whelk spoils. The software allows a reading to be taken at defined time intervals.**

#### *4.2.2.6 Bertholot's Reaction – A Test for the Presence of Amines*

After 72 hours 1ml of distilled water was syringed into the container. After 5 minutes the water was removed again from the container with the aid of a syringe and was allowed to react with Bertholot's reagent. Bertholot's reaction is used to determine the concentration of ammonia in water samples. The Bertholot Reaction Mechanism consists of three steps. The initial step involves the reaction of ammonia with hypochlorite to form a monochloramine,

Figure 4-17-1, which subsequently reacts with phenol to form the intermediate monochloramine,

Figure 4-17-2. Finally, this intermediate couples with a second phenolic molecule to form the blue indophenol chromophore (4),

Figure 4-17-3.



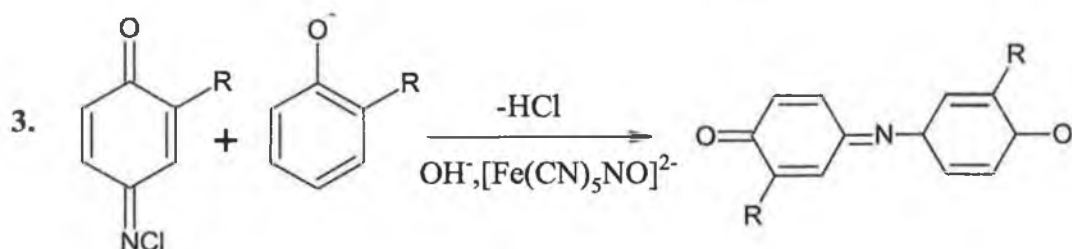
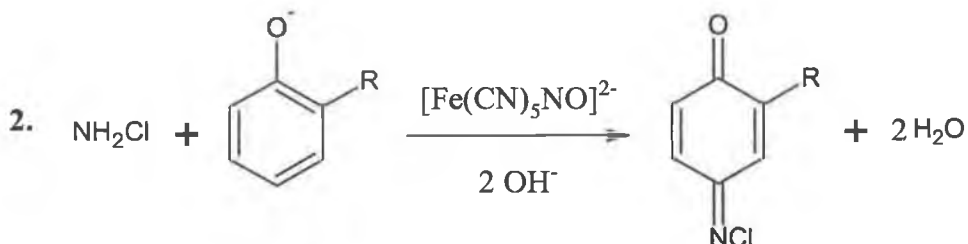


Figure 4-17 Reaction scheme for indophenol formation (4)

#### 4.2.2.7 Preliminary Trial 2

Three sensor spots were attached to each of the 6 self-adhesive clear covering films, which were then placed over the containers to form a tight seal. Two of the wheelks, labelled *RT 1 and 2* (Room Temperature 1 and 2), were stored at room temperature (temperature monitored by iButton code no: AB34C00001E0E221). Two more wheelks, labelled *F to RT 1 and 2* (Fridge to Room Temperature 1 and 2), were placed in the fridge (temperature measured by iButton code no: DA34C00001E2B621) and then removed from the fridge approximately 14 hours later and stored at room temperature. The remaining two wheelks, labelled *F 1 and 2* (Fridge 1 and 2), were placed in the fridge for the initial 24 hours before they were taken out and stored at room temperature for the remainder of the experiment. The handheld Colourmeter was used to record the colour change of the individual sensor membranes at 0, 1, 2.5, 16, 24, 27.5 and 40 hours approximately. The Colourmeter software was set to take a reading every 2 seconds. The red LED head of the handheld Colourmeter was placed directly onto the sensor spot and held in place for approximately 12 seconds during the measurement. The reported

measured value for each individual sensor spot at each of the time intervals is an average of six readings.

### 4.3 Results and Discussion

#### 4.3.1 Fabrication and Characterisation of pH Sensitive Membranes

##### 4.3.1.1 Measurement of Sensor Thickness

The thickness of four sensor spots was determined using a profilometer and the results are given in Table 4-2 below. The average sensor thickness is  $8.78 \pm 1.45 \mu\text{m}$ .

Sensor	Sensor Thickness ( $\mu\text{m}$ )
1	7.19
2	7.91
3	10.09
4	9.94
Average Thickness	$8.78 \pm 1.45$

**Table 4-2 Sensor thickness determined using a Profilometer**

Images of the sensor surface were also captured using SEM Figure 4-18, which gives an indication of the film thickness Figure 4-19. The sensor was sliced in half using a sharp blade to allow the thickness across the diameter to be determined, which is  $\sim 10 \mu\text{m}$ . The image indicates that the thickness varies across the diameter of the sensor, which may also be due to the cutting process. The thickness measurements obtained by both techniques are very similar.

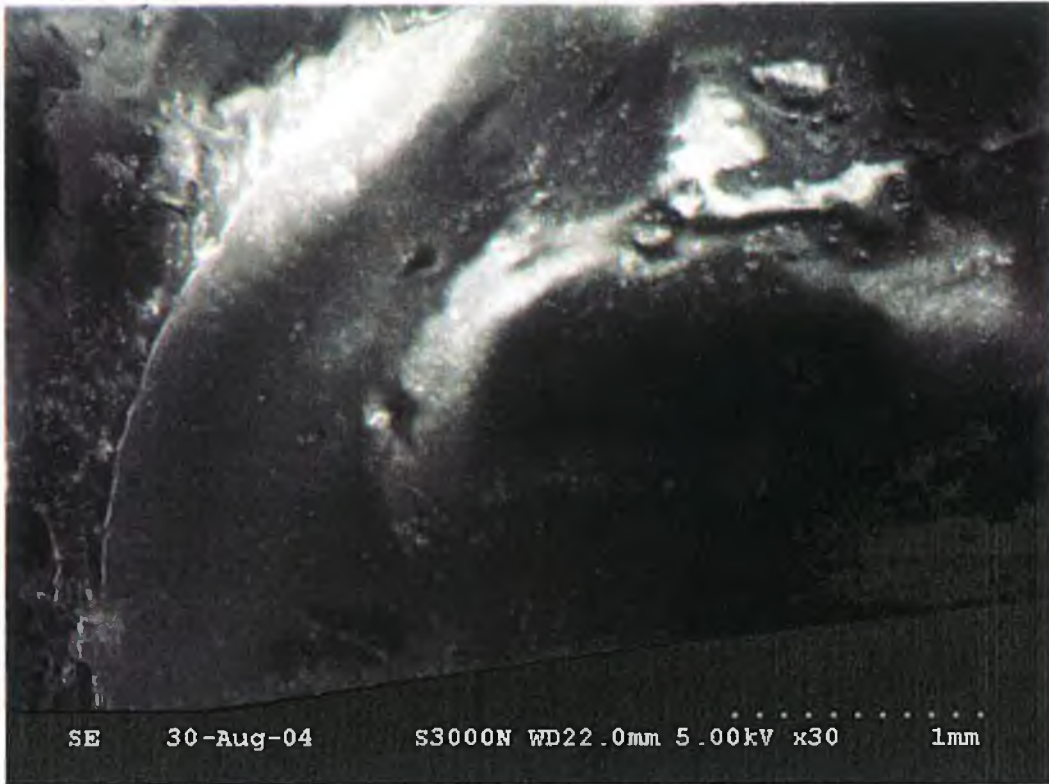


Figure 4-18 SEM image of the sensor surface. The circular outer edge of the sensor can be seen towards the left hand side of the image. The straight edge at the bottom of the image indicates where the sensor was cut in half.

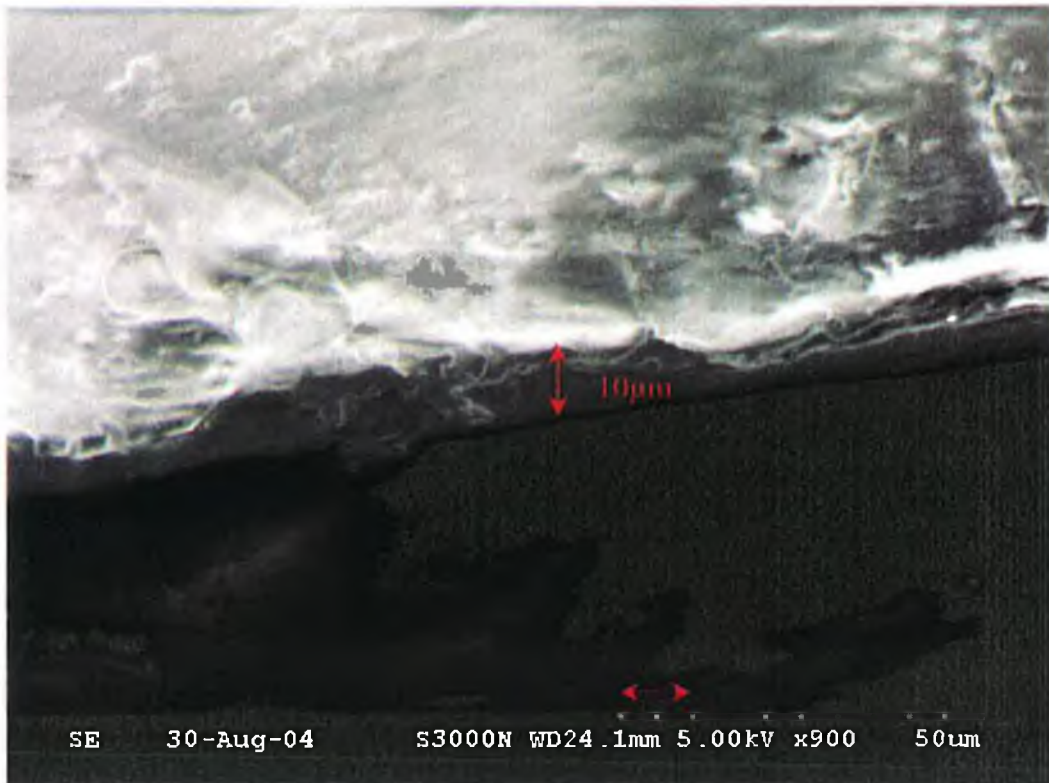


Figure 4-19 An SEM image showing the thickness of the sensor ~10µm

#### 4.3.1.2 Solubility of the Salt

Formulations “A” to “J” all contain the same concentration of lipophilic salt. The concentration of the salt relative to the dye is 2:1 for each formulation. Formulations “A” to “D” were prepared using CTABr. Formulations “E, F, I & J” contained TOABr while formulations “G & H” were prepared using OCTABr. The cetyltrimethylammonium bromide salt in formulations “A” to “D” eventually dissolved after ~3 hours in the sonicator, followed by 1 hour sonication at a higher temperature  $35^{\circ}\text{C} \pm 2^{\circ}\text{C}$  (measured using a mercury thermometer). The solutions were allowed to cool to room temperature before the sensor spots were prepared. Two days later, solid particles were visible in each of the formulation solutions “A” to “D”. The lipophilic salt appeared to have crystallised out. This may explain the presence of “leaf-like” crystalline structures on the surface of these spots, Figure 4-20.



**Figure 4-20** Images of the sensor surface with “leaf-like” structures. Magnification  $\times 2$  (left) and magnification  $\times 10$  (right).

All the components of formulations “E” and “F” including the lipophilic salt TOABr were completely dissolved after just 20 minutes in the sonicator while the lipophilic salt OCTABr in formulations “G” and “H” proved difficult to dissolve. For this reason, formulations “G” and “H” were eliminated.

#### 4.3.1.3 Dye Leaching Studies

Leaching studies were carried out on the sensor spots prepared from formulations “A” to “D” in duplicate while leaching studies were carried out on formulations “E” and “F” in triplicate. The presence of a peak at  $\sim 620\text{nm}$  indicates the presence of bromocresol green in the sample. If an absorbance band is seen at  $\sim 620\text{nm}$ , then this proves that dye is leaching from the sensor membrane into the distilled water. Formulations “A” to “D”

all contain CTABr but have decreasing concentrations of DBS. From Figure 4-21 it is clear that within 3 hours in some cases dye leaching has occurred and that the degree of leaching decreases with decreasing concentrations of DBS for formulations "A" to "D". Formulations "E" and "F" contain the lipophilic salt TOABr and different DBS concentrations, 350mg and 175mg respectively. It is clear from the graph that, after 3 hours, dye leaching is not evident in formulations "E" and "F" and plasticiser concentration does not appear to have any influence on the dye leaching. For this reason, formulations "A" to "D" were eliminated from the study due to their dye leaching, their difficulty in dissolving the lipophilic salt CTABr and finally the presence of crystalline structures on the surface of the sensor spots compared to the clear surface membranes of sensor spots prepared from formulations "E" and "F". This leaves 2 sensor spot formulations that could be used. Formulation "E" was chosen as from the literature, the greater the plasticiser concentration the faster the migration of gas molecules through the sensor membrane and the faster the response of the sensor. Formulation "E" is the optimised formulation.  $pK_a$  determination of the dye in the sensor membrane was performed using UV-Vis spectroscopy to determine the effect of membrane components on the  $pK_a$  of the dye. The  $pK_a$  of the dye was also determined in pH buffer solutions using the handheld Colourmeter. The optimised sensor spots were calibrated with ammonia gas.

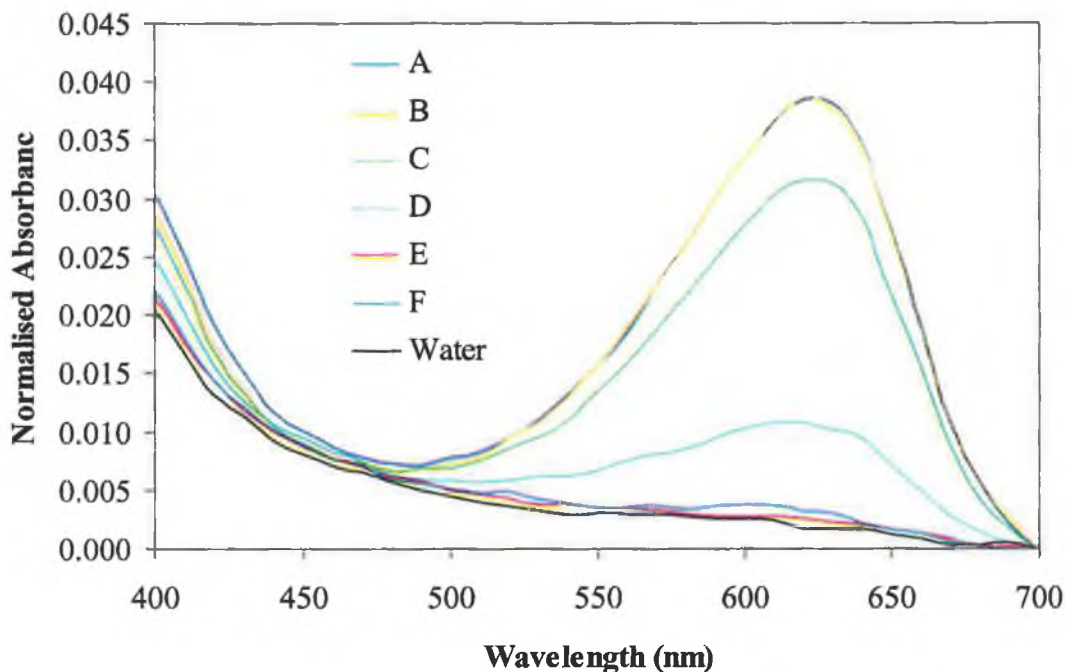


Figure 4-21 The presence of a peak at ~617nm in water samples indicates dye leaching after 3 hours from membranes made using formulations "A" to "F" (Table 4-1), and water as a reference.

#### 4.3.1.4 $pK_a$ Determination of the Dye in the Membrane by UV-Vis Spectroscopy

A UV-Vis scan indicated that the  $\lambda_{max}$  of the dye shifted slightly from 620nm in free solution to 630nm in the polymer membrane "E", Figure 4-22. A best-fit sigmoid function was modelled to the absorbance data at 630nm to allow the  $pK_a$  of the entrapped dye to be estimated, Figure 4-23. The value of the  $pK_a$  was calculated to be  $5.56 \pm 0.01$  (0.10% RSD,  $n=3$ ).

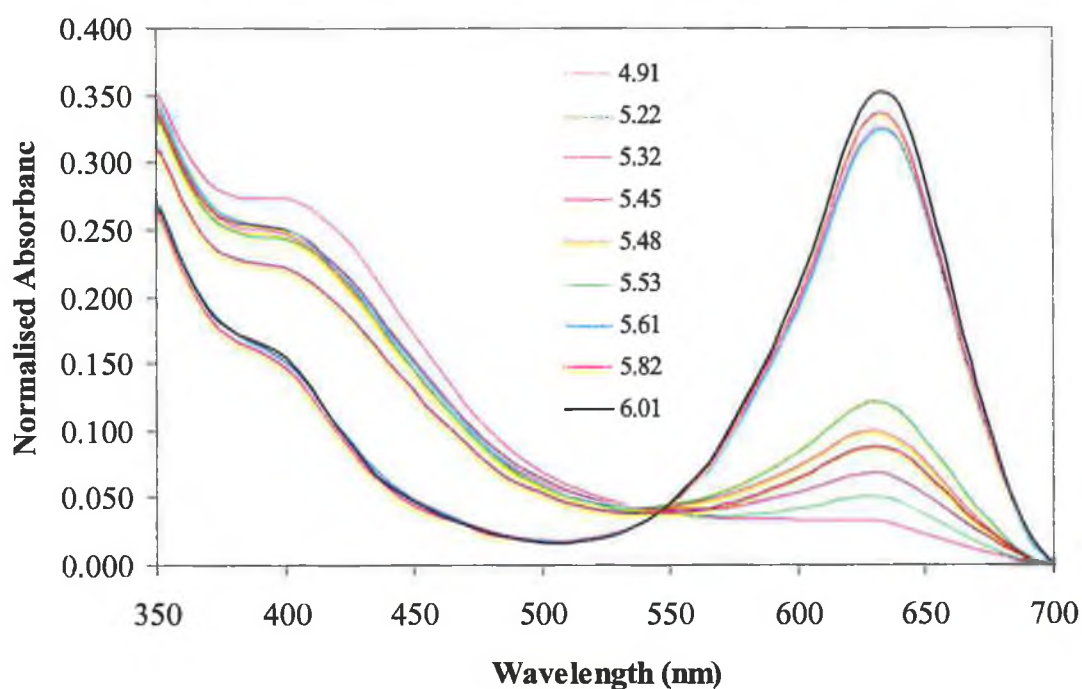


Figure 4-22 A UV-Vis scan of the dye in the polymer membrane in buffer solutions ranging from pH 4.91 to pH 6.01

#### 4.3.1.5 Effect of Temperature on the $pK_a$ Dye in the Membrane

The  $pK_a$  of the dye in the membrane at 4°C, Figure 4-24, was determined to be  $5.56 \pm 0.01$  (0.10% RSD,  $n=3$ ) which is identical to the  $pK_a$  of the dye in the membrane determined at room temperature, Figure 4-23. Therefore, temperature has minimal effect on the  $pK_a$  of the dye in the polymer membrane.

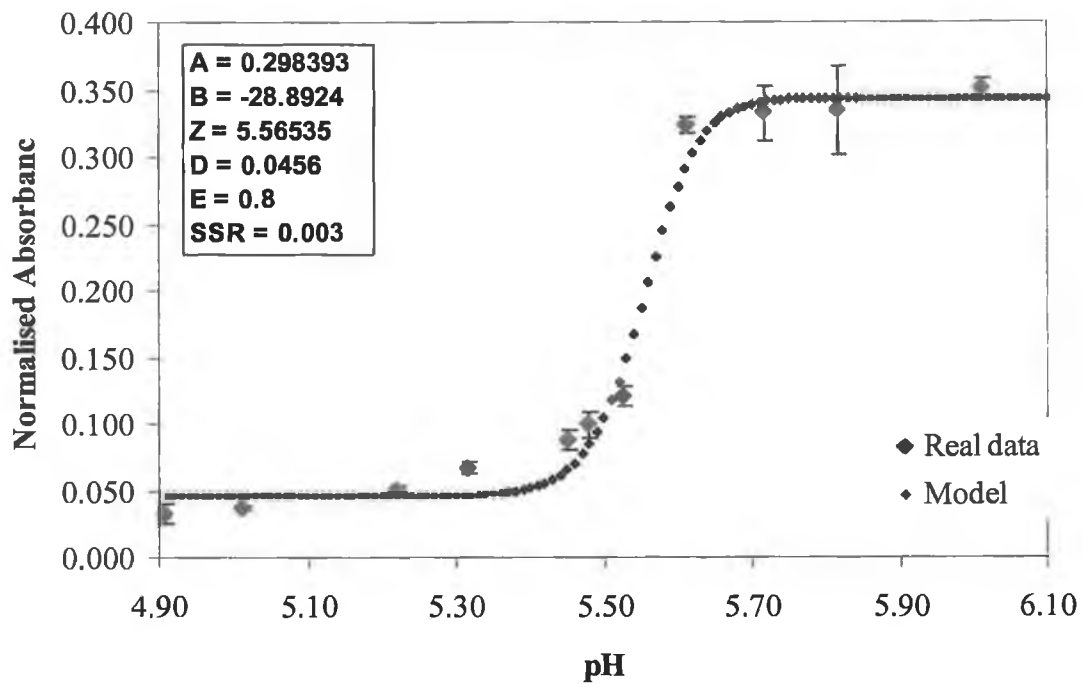


Figure 4-23 A best-fit sigmoid function modelling the absorbance data at 630nm. The  $pK_a$  of the dye in the membrane at  $T = 20^\circ\text{C}$  was calculated to be  $5.56 \pm 0.01$ , 0.10 % RSD,  $n=3$ .

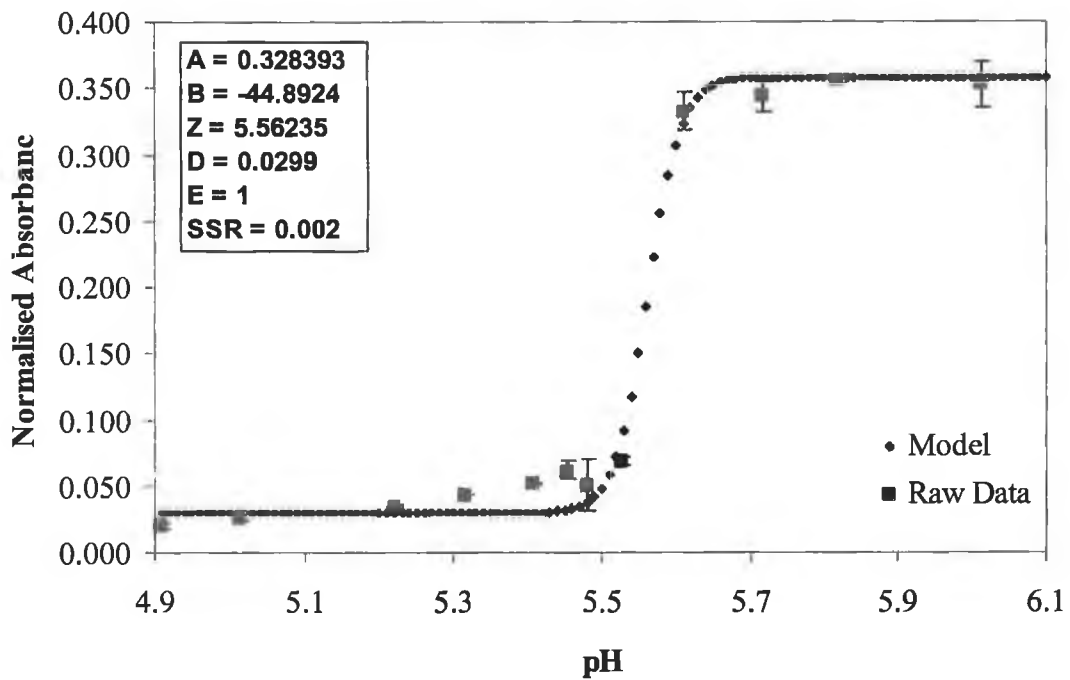
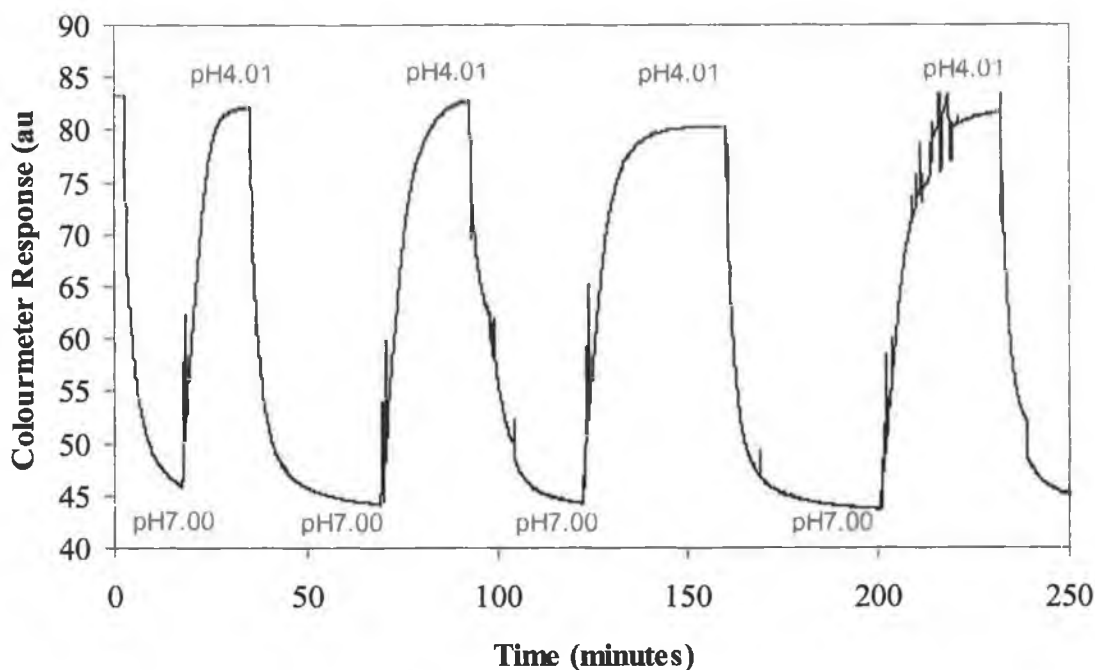


Figure 4-24 A best-fit sigmoid function modelling the absorbance data at 630nm for the dye in the polymer membrane at  $4^\circ\text{C}$ .  $pK_a = 5.56 \pm 0.01$ , 0.10 % RSD,  $n=3$ .

#### 4.3.1.6 Reproducibility of the Sensor Response in pH Buffer Solution

Figure 4-25 illustrates the reproducibility of the sensor response in pH 4.01 and pH 7.00 buffer solutions. The noise at the top of peak number 4 is noise caused by the presence of a bubble in the flow cell. The average Colourmeter response for the sensor in buffer pH 4.01 is  $81.98 \pm 1.14$  where  $n = 5$ , and in buffer pH 7.00 is  $44.66 \pm 0.88$  where  $n = 5$ .



**Figure 4-25** This graph illustrates the reproducibility of the sensor response in pH buffer solutions. The average Colourmeter response for the sensor in buffer pH 4.01 is  $81.98 \pm 1.14$  where  $n = 5$ , and in buffer pH 7.00 is  $44.66 \pm 0.88$  where  $n = 5$ .

#### 4.3.1.7 pKa Determination of the Dye in the Sensor Membrane using the Handheld Colourmeter

The most suitable LED head was chosen by comparing the spectral emission of the yellow and red LEDs with the spectral absorbance of the bromocresol green sensors in their basic form Figure 4-26. Both the red ( $\lambda_{\max}$  659nm) or yellow ( $\lambda_{\max}$  596nm) LED heads would be suitable as their emission spectra is close to the absorbance spectra for the bromocresol green sensors ( $\lambda_{\max}$  630nm) but for the purpose of these trials only one LED was used, the red LED head.



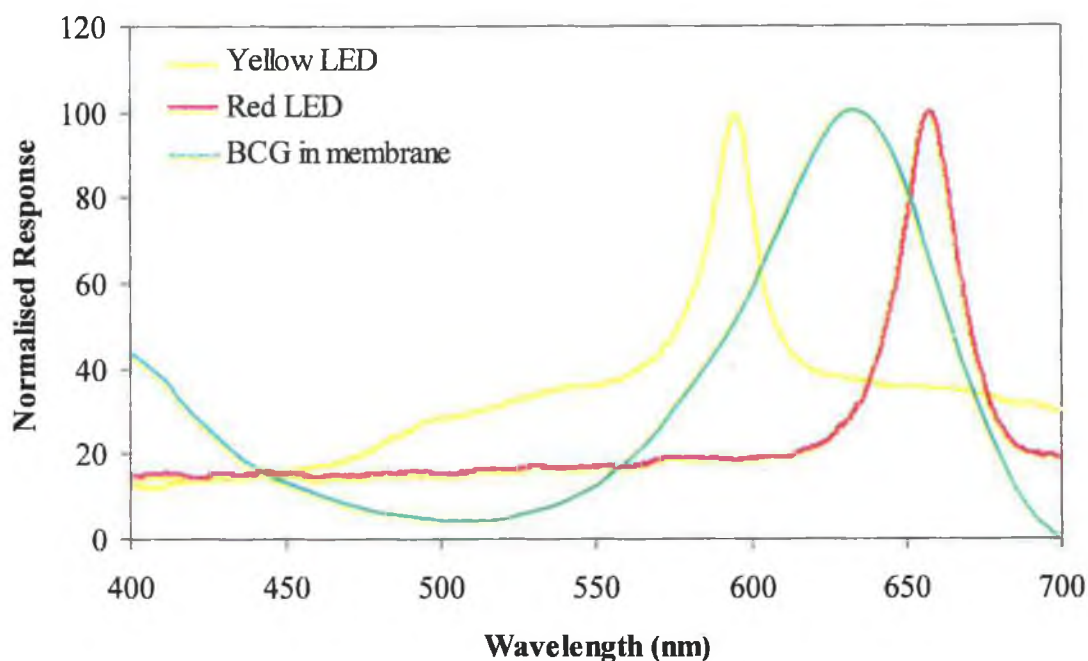


**Figure 4-26** Comparison of the emission spectra of the red ( $\lambda_{\max}$  659nm) and yellow ( $\lambda_{\max}$  596nm) LEDs with the absorbance spectra for bromocresol green in the sensor membrane ( $\lambda_{\max}$  630nm).

The experimental set-up with the red LED head as shown in Figure 4-12 was used for the  $pK_a$  determination of the dye in the sensor membrane. A number of buffer solutions ranging from pH 4.01 to pH 7.00 were prepared as described previously. Starting with buffer solution pH 4.01, each buffer solution was injected into the flow cell and the response was allowed to equilibrate. This procedure was repeated once and the results are plotted in Figure 4-27 and Figure 4-28. The calibration curves are displayed in Figure 4-29 and Figure 4-30. A best-fit sigmoid plot models the average response to increasing pH for the sensor, Figure 4-31. The  $pK_a$  of the dye in the membrane was calculated to be  $5.43 \pm 0.02$  (% RSD = 0.39,  $n = 2$ ). Comparing this  $pK_a$  value to the  $pK_a$  value determined using the plate-well reader,  $5.56 \pm 0.01$  (% RSD = 0.10,  $n=3$ ), it is clear that there is very little difference between the two techniques.

This is an important factor as it demonstrates the reliability and accuracy of the handheld Colourmeter for measuring the sensor response. Compared to the plate-well reader the handheld Colourmeter has the added advantage of being portable and can be used at point-of-need giving an immediate quantitative result.

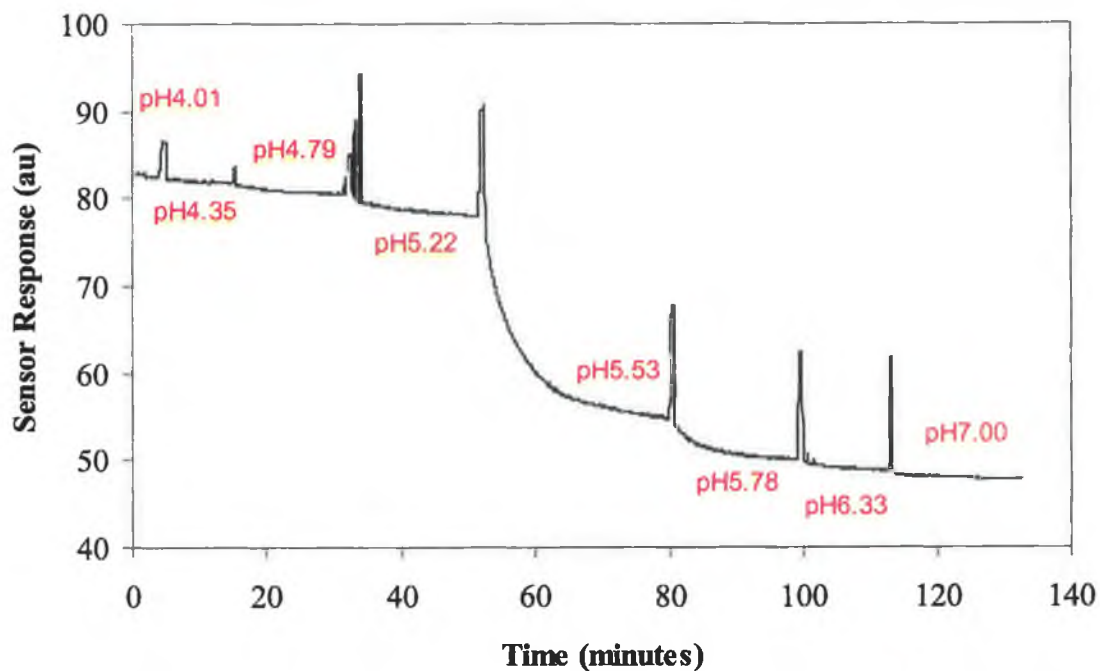


Figure 4-27 Sensor response to increasing pH – 1<sup>st</sup> Calibration. The flow cell was allowed to drain before injecting a new buffer solution. This explains the presence of a ‘spike’ before each injection.

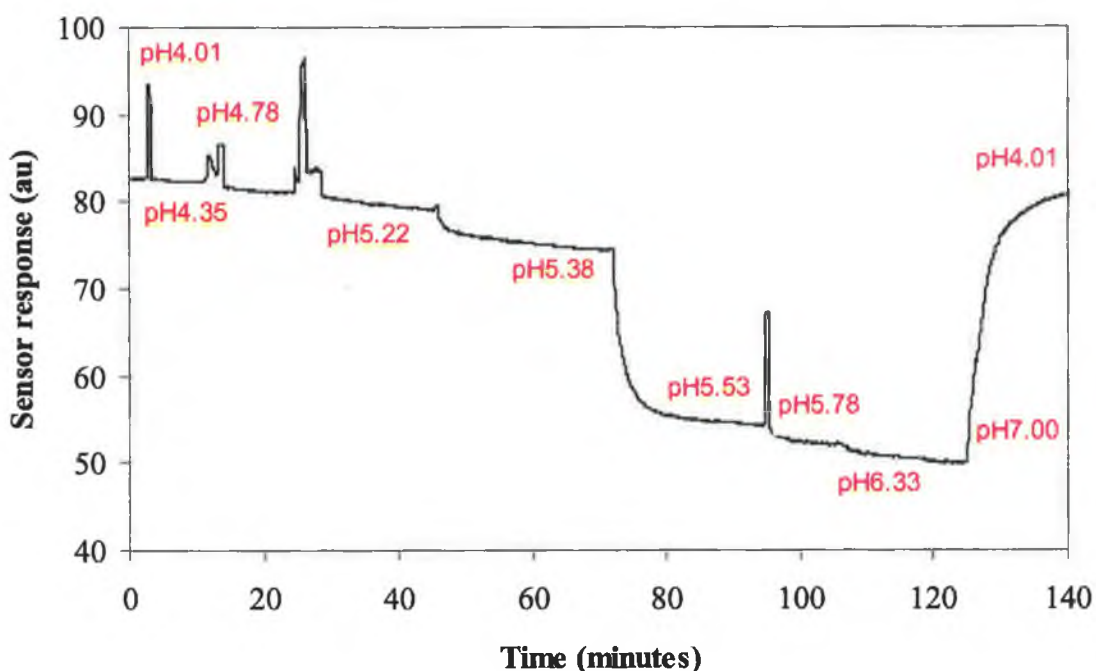


Figure 4-28 Sensor response to increasing pH – Repeat Calibration. The flow cell was allowed to drain before injecting a new buffer solution. This explains the presence of a ‘spike’ before each injection.

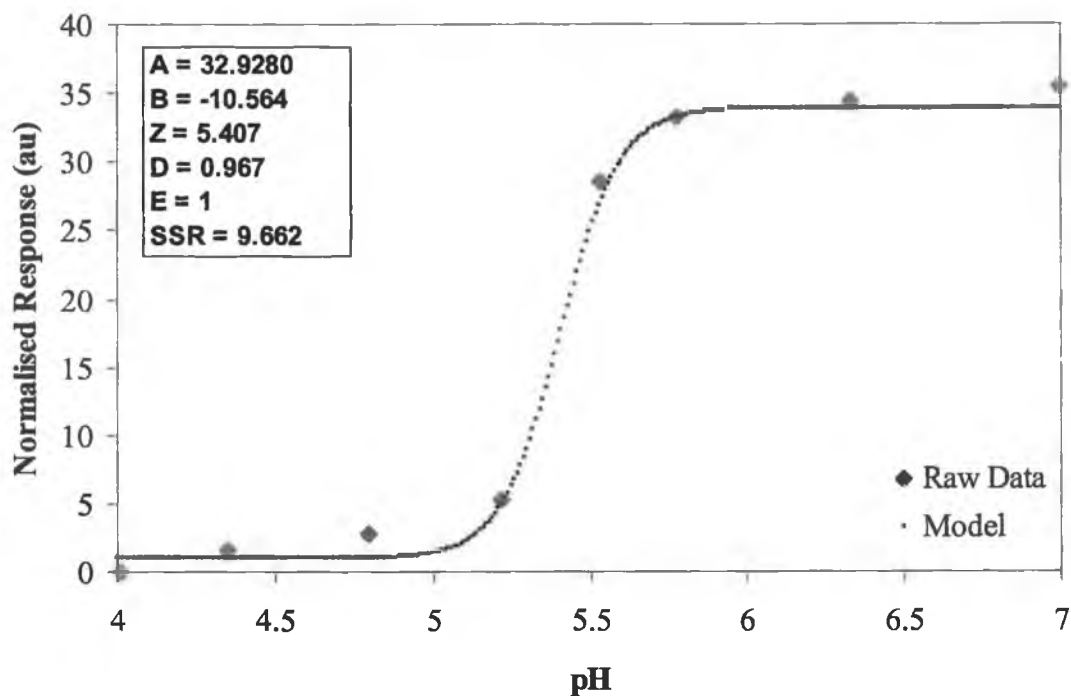


Figure 4-29 A best-fit sigmoid curve modelling the sensor response to increasing pH to determine the  $pK_a$  (5.41) of the dye in the polymer membrane – 1<sup>st</sup> Calibration.

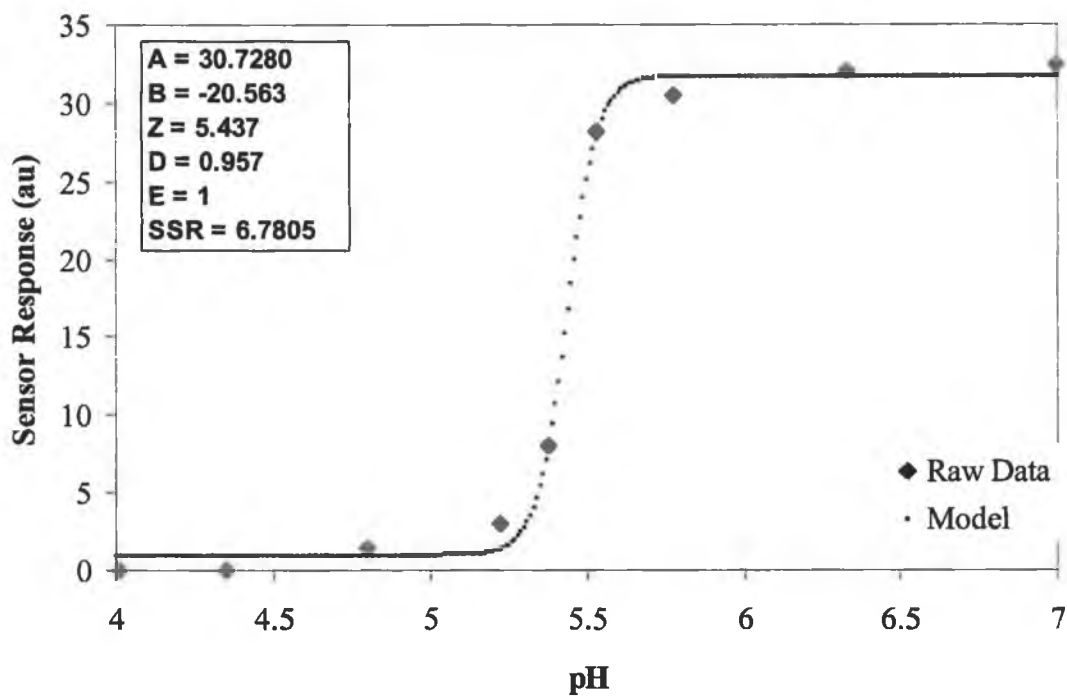


Figure 4-30 A best-fit sigmoid curve modelling the sensor response to increasing pH to determine the  $pK_a$  (5.44) of the dye in the polymer membrane – Repeat Calibration.

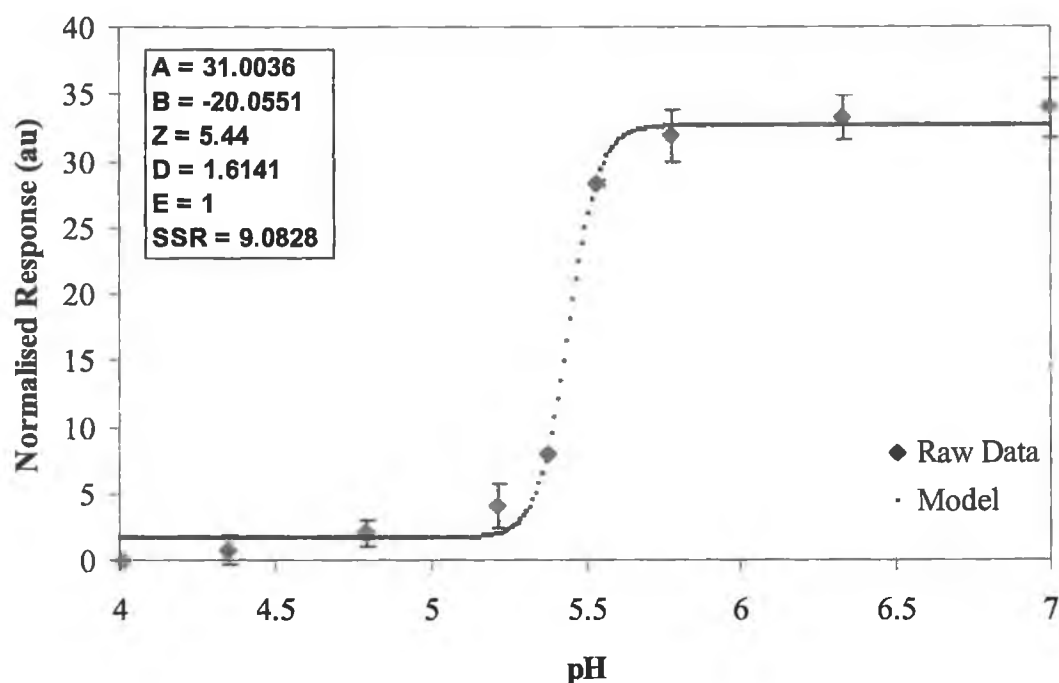


Figure 4-31 A best-fit sigmoid curve modelling the average sensor response to increasing pH to determine the  $pK_a$  of the dye in the polymer membrane. The  $pK_a$  of the dye in the membrane was calculated to be  $5.43 \pm 0.02$ , % RSD = 0.39, where  $n = 2$ .

#### 4.3.1.8 Ammonia Gas Calibrations

Calibration experiments ( $n=3$ ) of the sensor using the Colourmeter in the range between 0 and 33ppm ammonia are displayed in Figure 4-32, Figure 4-33 and Figure 4-34 (see also Appendix 3-1 to Appendix 3-3). The sensor was exposed to increasing ammonia concentrations by adjusting the mass flow controller connected to the ammonia supply. The nitrogen flow was fixed to  $100\text{ml min}^{-1}$ . The ammonia concentration was calculated from the equation below:

$$C_{NH_3} = \left( \frac{V_{NH_3}}{V_{NH_3} + V_{N_2}} \right) \times 100 \quad \text{Equation 4-2}$$

$C_{NH_3}$  = concentration of ammonia in ppm

$V_{NH_3}$  = volume of ammonia gas ( $\text{ml min}^{-1}$ )

$V_{N_2}$  = volume of nitrogen gas ( $\text{ml min}^{-1}$ )

The concentration of the stock NH<sub>3</sub> was 100 ppm therefore the values were multiplied by 100. The ammonia concentrations from 10, 20, 30 40 and 50 ml min<sup>-1</sup> 1% ammonia in 100ml min<sup>-1</sup> N<sub>2</sub> were calculated to be 9, 17, 23, 29 and 33 ppm respectively. The repeatability of the measurements was evaluated by calculating the coefficient of variability (*CV*) when measuring each concentration in triplicate where:

$$CV = \frac{S}{\bar{x}} \times 100 \quad \text{Equation 4-3}$$

Where *S* = standard deviation,  $\bar{x}$  = mean

$$LOD = 3 \times S \text{ (background response)}$$

The limit of detection (*LOD*), defined as three times the standard deviation of the background response i.e. 0ppm NH<sub>3</sub>, for 3 calibrations was calculated to be 0.23 ± 0.07 ppm. The 0ppm NH<sub>3</sub> baseline value for each calibration was taken as the average of 120 values of the initial and final baseline measurements. Figure 4-35 shows the calibration curve obtained from this experiment.

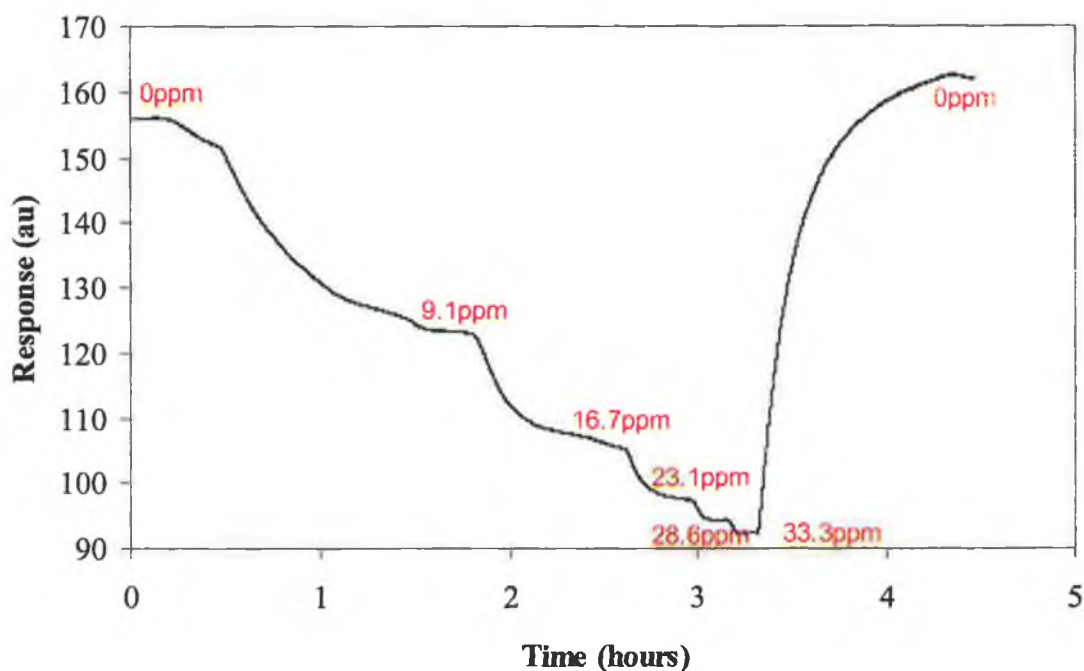


Figure 4-32 Sensor response to increasing ammonia concentration (1<sup>st</sup> calibration – See Appendix 3-1 for experimental data)

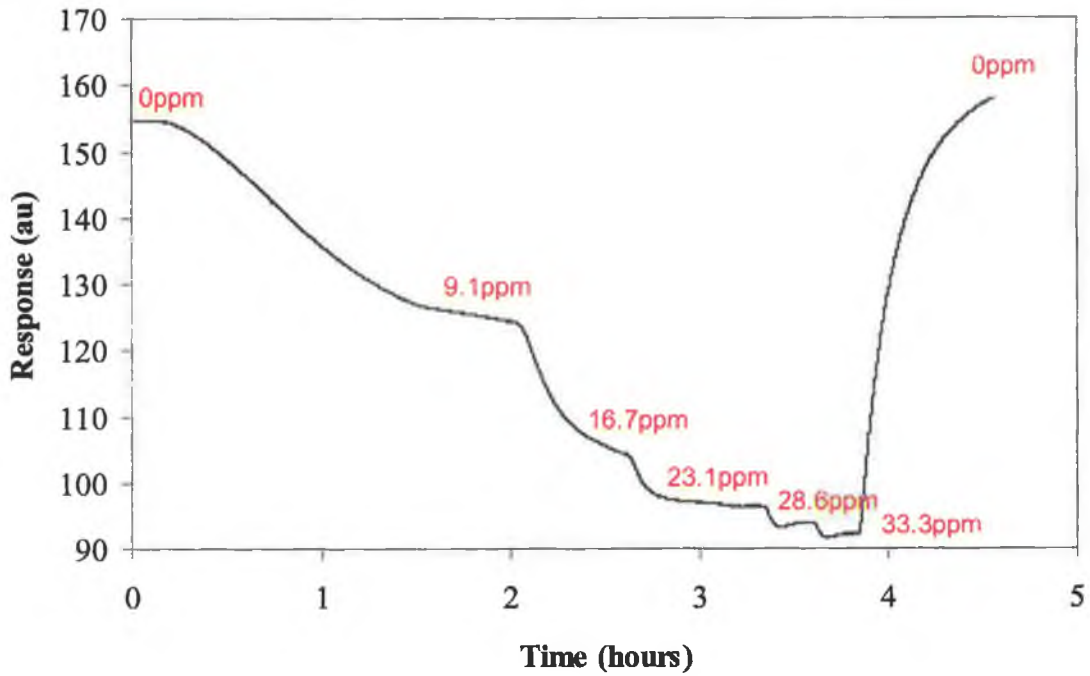


Figure 4-33 Sensor response to increasing ammonia concentration (2<sup>nd</sup> Calibration – See Appendix 3-1 for experimental data)

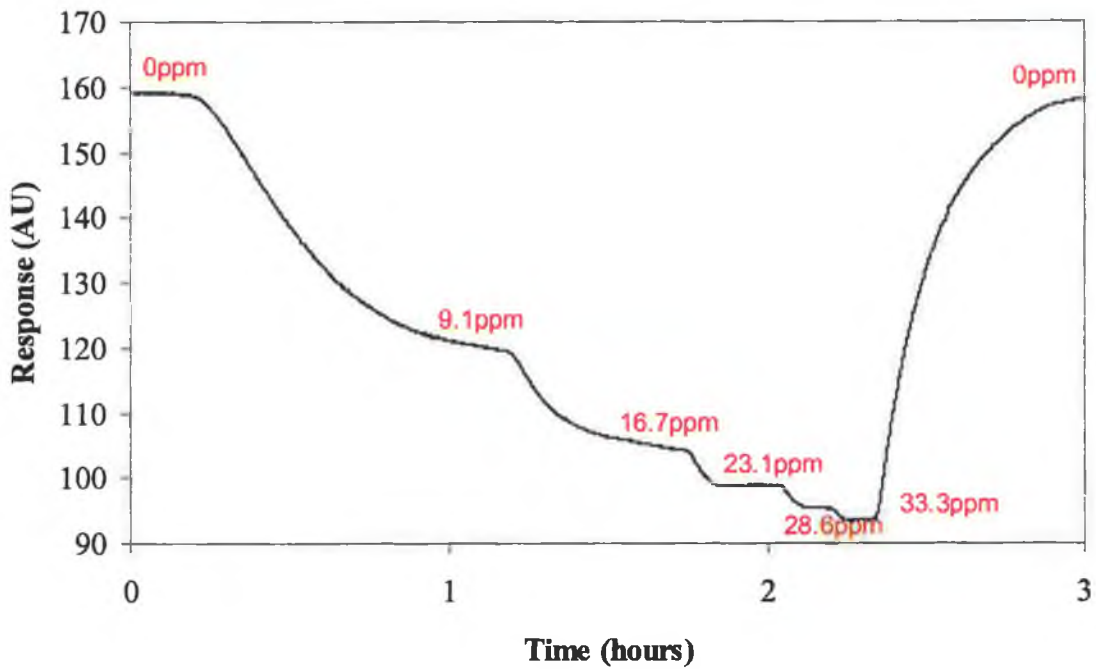
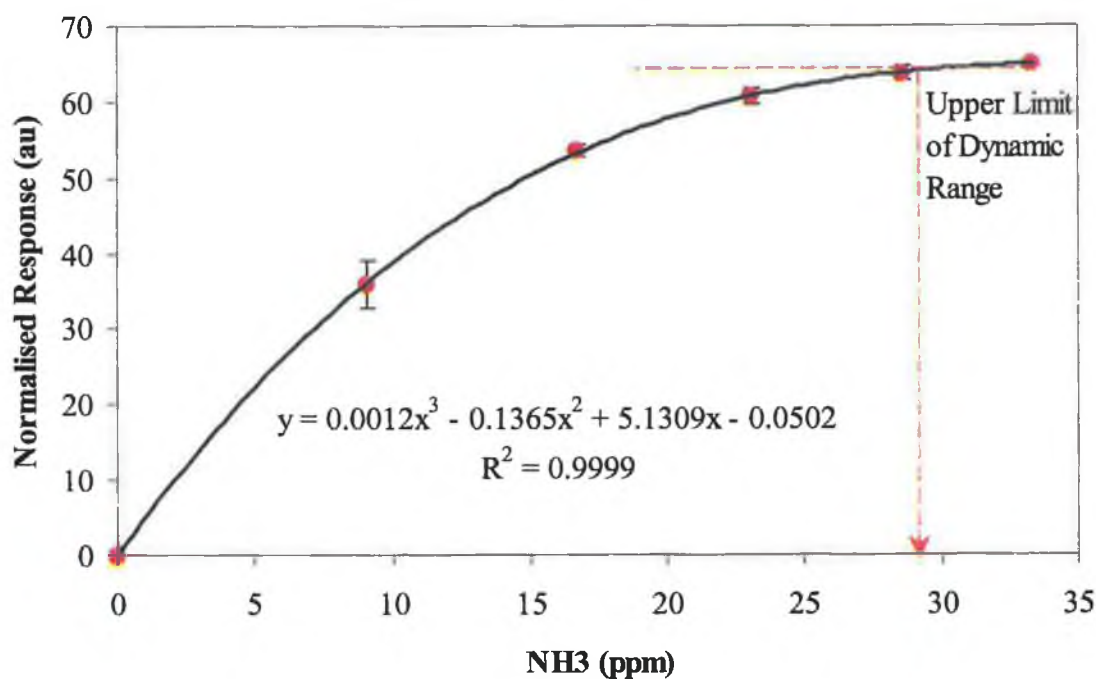


Figure 4-34 Sensor response to increasing ammonia concentration (3<sup>rd</sup> calibration – See Appendix 3-1 for experimental data)



**Figure 4-35** A calibration curve of the sensors response to increasing ammonia concentration (n=3)  
– See Appendix 3-3

Figure 4-35 shows how the sensor responds to the change in ammonia concentration. It is clear that the sensor does not respond linearly between 0 and 33 ppm. The increase in the amplitude of the signal is smaller at higher concentrations of ammonia, that is, the sensitivity of the sensor is higher at lower ammonia concentrations. The upper limit of the dynamic range is ~29ppm. From Figure 4-32, Figure 4-33 and Figure 4-34, it is evident that the sensor response time is concentration dependent i.e. it is very slow at low concentrations. This is very common in bulk optical sensors. The rate of diffusion of the gas molecules through the polymer membrane is dependent on the concentration, the concentration difference, and also on the sensor thickness. Additional calibration experiments were also performed in the linear region at lower ammonia concentrations. To obtain lower ammonia concentrations the flow rate of the N<sub>2</sub> supply was increased to 400ml min<sup>-1</sup>, therefore 10, 20, 30, 40 and 50 ml min<sup>-1</sup> of ammonia in 400 ml min<sup>-1</sup> N<sub>2</sub> gave 2, 5, 7, 9 & 11 ppm NH<sub>3</sub> respectively. This experiment was carried out in duplicate and a calibration curve can be seen in Figure 4-36. Once again Figure 4-36 illustrates that the sensor response is not linear with ammonia concentration. Increasing the flow rate of the N<sub>2</sub> supply to 900 ml min<sup>-1</sup> further reduced the ammonia concentration. Therefore, 10, 20, 30 and 40 ml min<sup>-1</sup> NH<sub>3</sub> in 900 ml min<sup>-1</sup> N<sub>2</sub> gave 1, 2, 3 & 4 ppm NH<sub>3</sub> respectively. The experiment was carried out in triplicate at 900ml min<sup>-1</sup> N<sub>2</sub>. A linear

sensor response to increasing ammonia concentration was obtained, as shown in Figure 4-37.

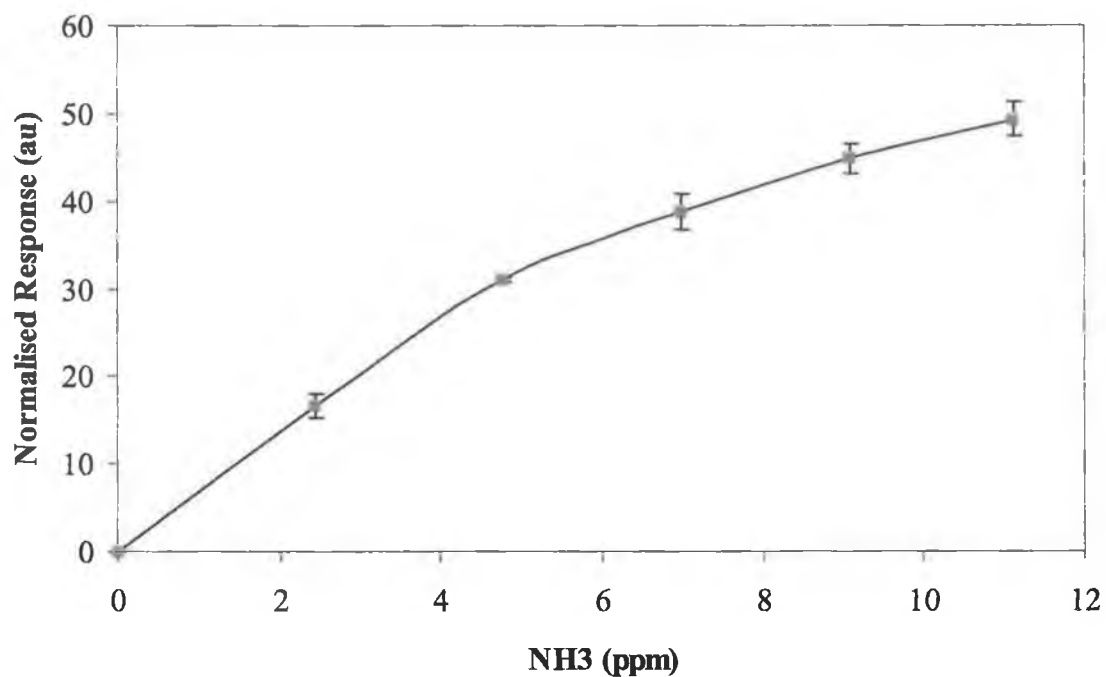


Figure 4-36 A calibration curve of the sensors response to increasing ammonia concentration (n=2)

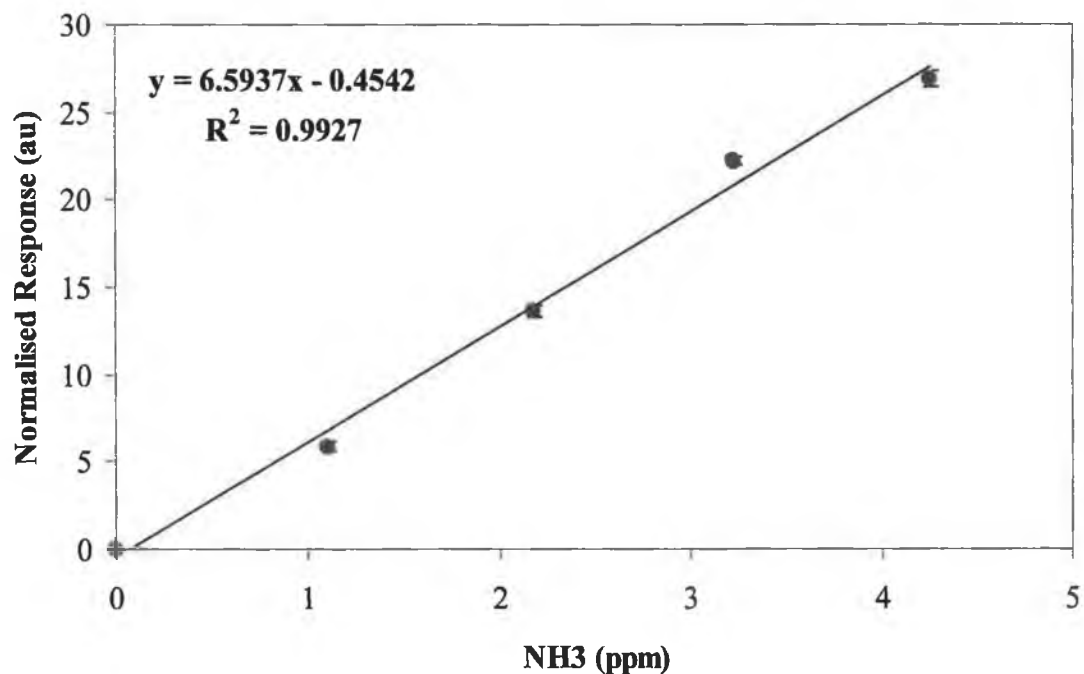
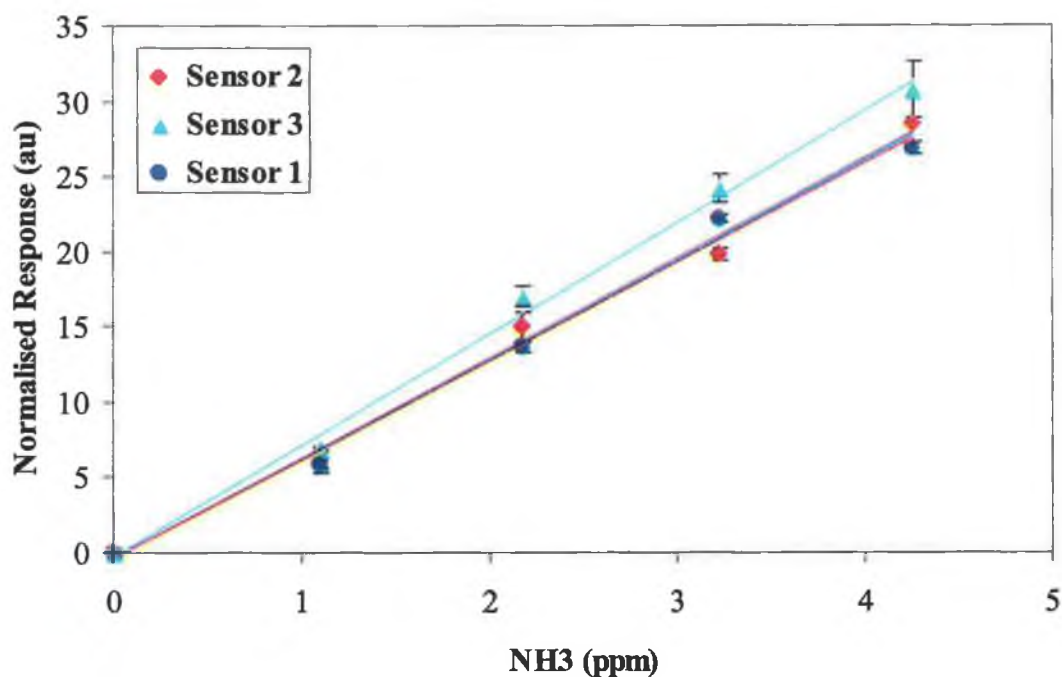


Figure 4-37 Linear sensor response to increasing ammonia concentration. The  $N_2$  flow-rate was increased to  $900\text{ml min}^{-1}$  to achieve a concentration range between 0 and 4.3ppm (n=3) – See Appendix 3-6 to Appendix 3-8.



The same experiment was carried out on 2 more sensors in duplicate. The 2 sensors were exposed to 1, 2, 3 and 4 ppm NH<sub>3</sub>. The response for all 3 sensors to increasing ammonia concentration can be seen in Figure 4-38. An average response of the 3 sensors to increasing ammonia concentration is plotted in Figure 4-39. The % RSD of the 3 sensors for each concentration is below 12%.



**Figure 4-38 Response for 3 sensors to increasing ammonia concentration. Calibrations were carried out in triplicate for sensor 1 and in duplicate for sensors 2 and 3 – See Appendix 3-8, 3-11 & 3-14.**

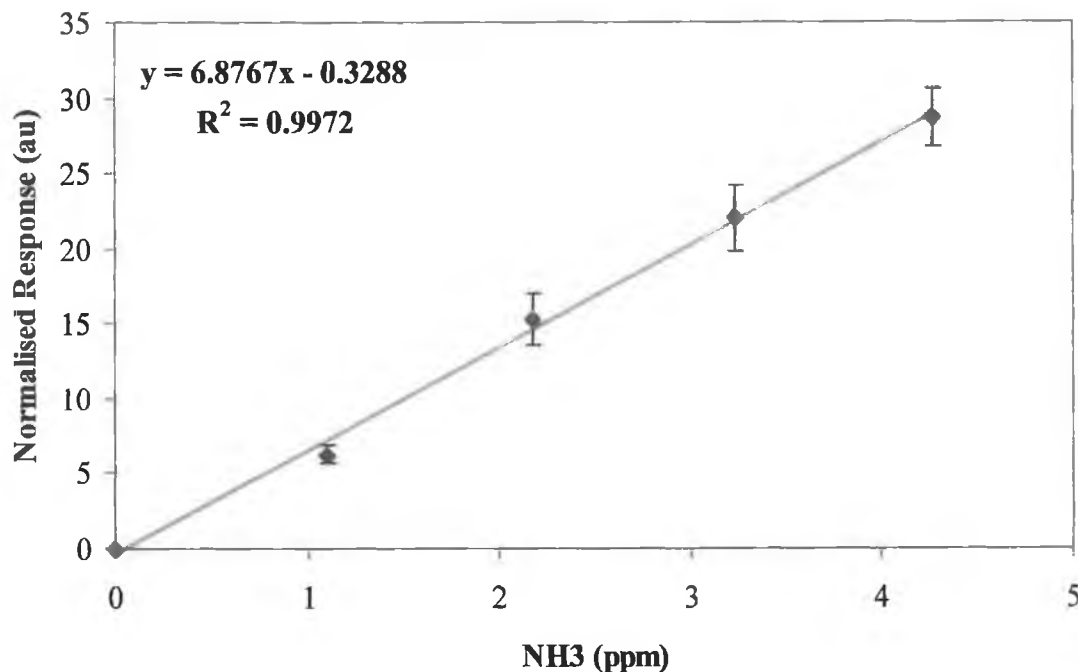


**Figure 4-39 Average response to increasing ammonia concentration for 3 sensors. The %RSD for at each concentration is below 12%. This demonstrates the inter-sensor reproducibility – See Appendix 3-5 for experimental data.**

#### 4.3.1.9 Precision – Repeatability and Reproducibility

The precision of the sensor was determined by measuring the repeatability and the reproducibility. Repeatability was measured by repeating the same experiments on the same sensor, while reproducibility was measured by repeating the same experiments on different sensors. 3 sensors in total were used for the repeatability and reproducibility studies. The repeatability of the measurements was evaluated by calculating the coefficient of variability *CV* when measuring the concentration of four standards in triplicate (in duplicate in some cases). The reproducibility was evaluated by calculating the %*CV* between the responses of the 3 sensors at four NH<sub>3</sub> concentrations. Sensors 1, 2 and 3 showed excellent repeatability with a %*CV* < 5% for Sensors 1 and 2 and a %*CV* < 6.2% for Sensor 3. The reproducibility between the sensors was excellent with an overall %*CV* < 12% for all 3 sensors – See Appendix 3-5. The %*CV* for individual sensors is given in the Appendix 3-4.

Although the inter-sensor reproducibility is excellent there is still a degree of variation between the sensors that must be addressed if the sensors are to be deployed on a large scale. Currently, the sensors are prepared manually which definitely impacts the reproducibility. An automated process whereby the formulation is screen-printed or spin

coated uniformly onto a rigid substrate would certainly minimise the variation between the sensors. The sensor response is relatively slow at low concentrations but this should not be an issue for the intended application where the sensors are expected to respond to high levels of volatile compounds released into a confined headspace over time.

### 4.3.2 Monitoring of Headspace Spoilage Volatiles Released from Cooked Whelk in Different Storage Conditions using the pH Sensitive Membranes

#### 4.3.2.1 Preliminary Trial 1

After 72 hours the sensor spot was visually assessed and a colour image of the sensor spot was captured using a Sony digital camera. The sensor spot changed from yellow to blue over the 72-hour period, Figure 4-15. The sensor response over time was measured via the Colourmeter and the data was processed in Microsoft Excel, Figure 4-40. The response curve indicates that the sensor began to change from the moment the container was sealed and continued to change over the 72-hour period. Microbial counts and TVB-N data are necessary to confirm that the sensor response is due to whelk meat spoilage.

From the graph there appears to be a regular wave pattern particularly noticeable in the latter part of the curve. As the experimental set-up was covered over by tin foil to eliminate ambient light effects the only other interfering factor that appears to correlate with the response is the ambient temperature recorded by the iButton, Figure 4-41. This interfering temperature effect needs to be addressed for future deployment of the system in a variable temperature environment. Integrating a temperature compensation factor into the software or applying a best-fit curve to the data may help achieve this. A best-fit curve was manually applied to the data to give an indication of how the sensor would respond if the temperature effects were eliminated, Figure 4-42.

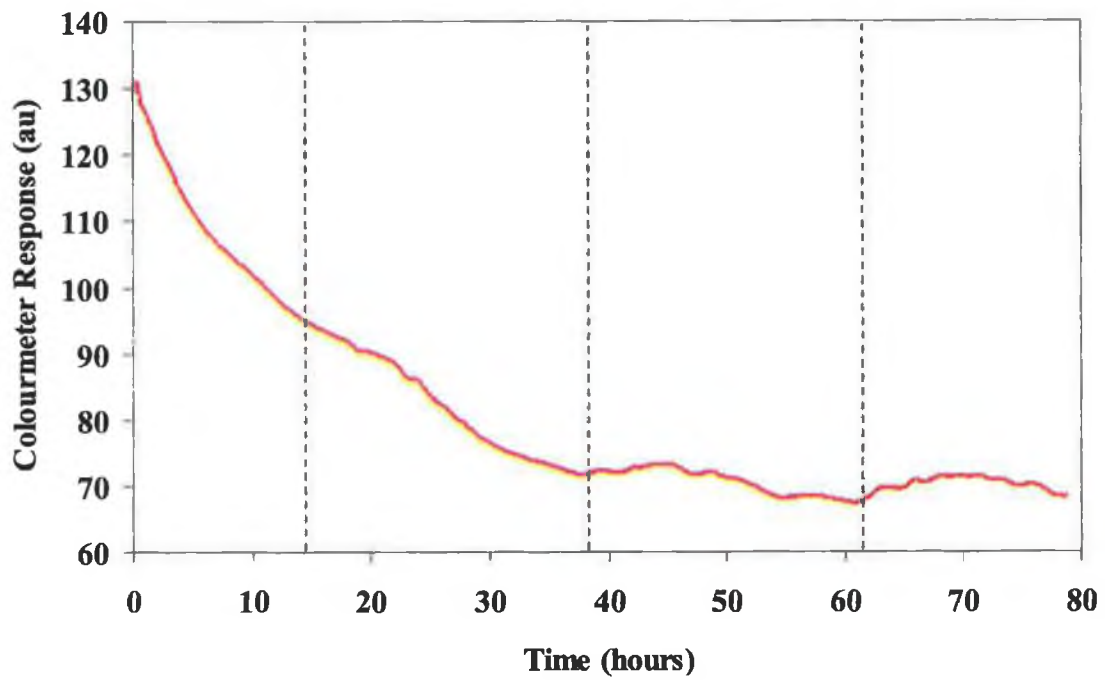


Figure 4-40 Sensor response to the spoilage volatiles released by the cooked whelk at room temperature over time. This graph also illustrates the periodic wave pattern occurring in the sensor response.

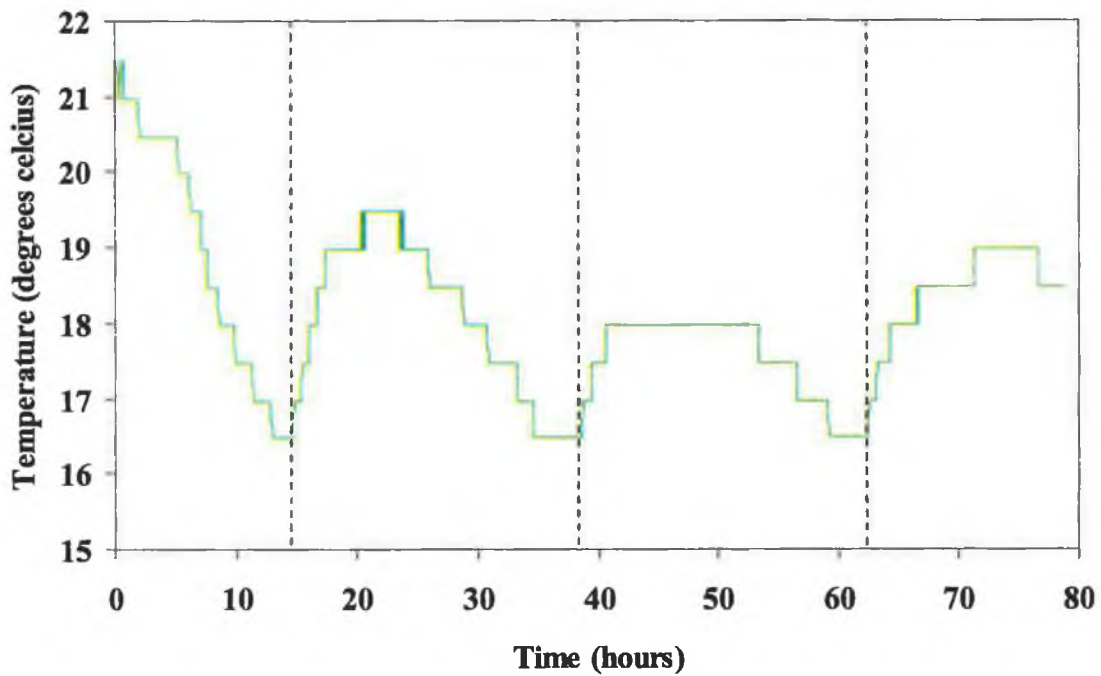
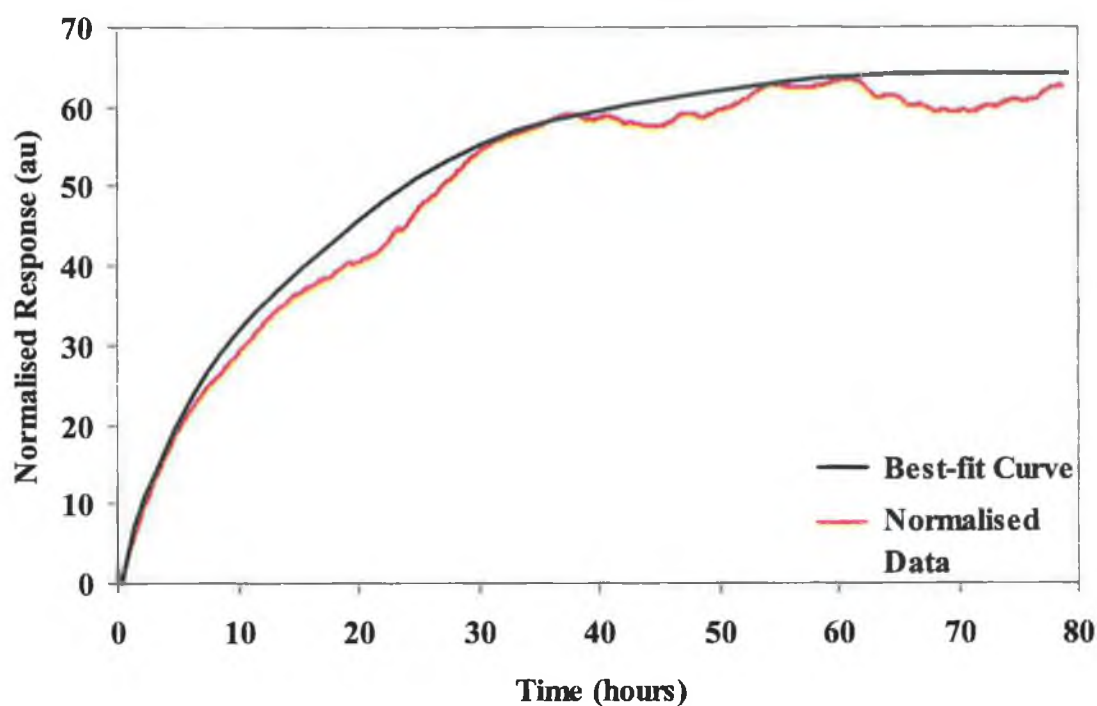


Figure 4-41 This graph illustrates the periodic temperature gradients of the laboratory during the experiment.



**Figure 4-42** Normalised sensor response to the spoilage volatiles released by the cooked whelk stored at room temperature over time. A best-fit curve was manually applied to the data.

#### 4.3.2.2 Bertholot's Reaction

This quick test was performed to ensure that amines were the spoilage compounds released from the cooked whelk sample. Approximately 1ml of distilled water was syringed into the headspace of the container and allowed to absorb the volatile amines for approximately 5 minutes. Using the same syringe, the water lodged at the bottom of the container was retrieved and allowed to react with a few drops of Bertholot's reagent. In less than 2 minutes the solution turned from yellow to blue, Figure 4-43. This test signified the presence of ammonia/amines in the headspace of the container, and therefore supports the view that the volatile basic nitrogenous compounds released by the whelk meat were responsible for the sensor response in Figure 4-42.

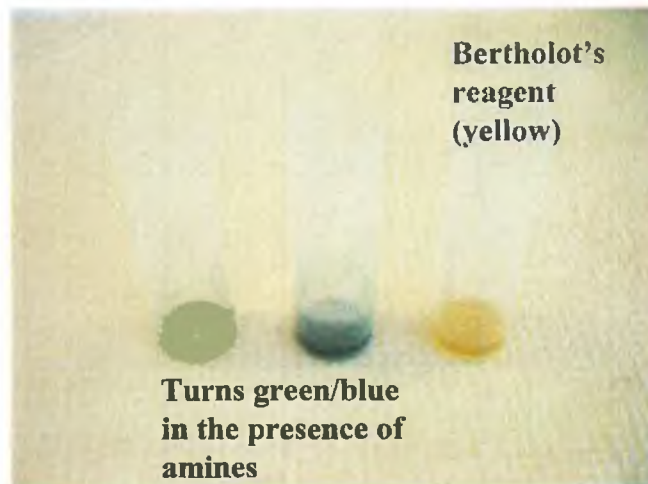


**Figure 4-43** Bertholot's reagent (yellow) turns green when reacted with a sample of water containing the spoilage volatiles released from the spoiled whelk. The colour change indicates the presence of amines.

#### *4.3.2.3 Preliminary Trial 2*

Soon after the individual containers were sealed, the first sensor (left hand side) on each container turned greenish-blue. The photographs in Figure 4-45 clearly illustrate this. Looking at Figure 4-44, the whelks were placed in the exact same position in all containers with the opening of the shell also to the left hand side.



**Figure 4-44** Cooked whelk arranged in the same position with the opening of the shell to the left hand side of each container.

Fresh Molluscan shellfish contain high levels of nitrogenous compounds that can be extracted from the whelk meat by steam distillation. Similarly, during the cooking process some volatile ammonia and amines were released with the steam from the whelk meat into the atmosphere. This may explain the observations of this preliminary trial that some sensors changed to the blue form prematurely. The cooked whelks were packed while they were still warm as they were allowed to cool for only 5 minutes. There were still considerable amounts of steam being released from the sample, which can be clearly seen in Figure 4-45. In all the trays, a layer of condensation was visible around the 1<sup>st</sup> sensor, which in each case was situated above the opening of the shell directly exposed to the whelk meat. As ammonia is highly soluble in water, the layer of condensation on the permeable membrane adjacent to the sensor absorbed and pre-concentrated any ammonia liberated from the cooked whelk. Therefore, the ammonia concentration in the layer of condensation is higher compared to the ammonia in the surrounding headspace. The volatile ammonia diffused from the layer of condensation through the gas permeable membrane of the sensor and induced a colour change before the whelk spoiled.

Another probability was that the heat generated from the steam changed the characteristics of the diffusion control membrane separating the sensor from the headspace to allow excess water vapour to get through to, and eventually condense on the surface of the sensor. This would allow deprotonation of the dye to occur with or without the presence of basic ammonia/amine species. These arguments were supported by the fact that no/insignificant colour change was observed from all other sensors (sensor spots 2 & 3) on which no obvious condensation was observed. These sensors subsequently responded to the increase in concentration of the headspace spoilage volatiles released by the whelk meat over a time period as expected. As the 1<sup>st</sup> sensor spot on each container was completely saturated within the first 10 minutes, the results from this trial are taken from sensor spots 2 and 3 in each container.

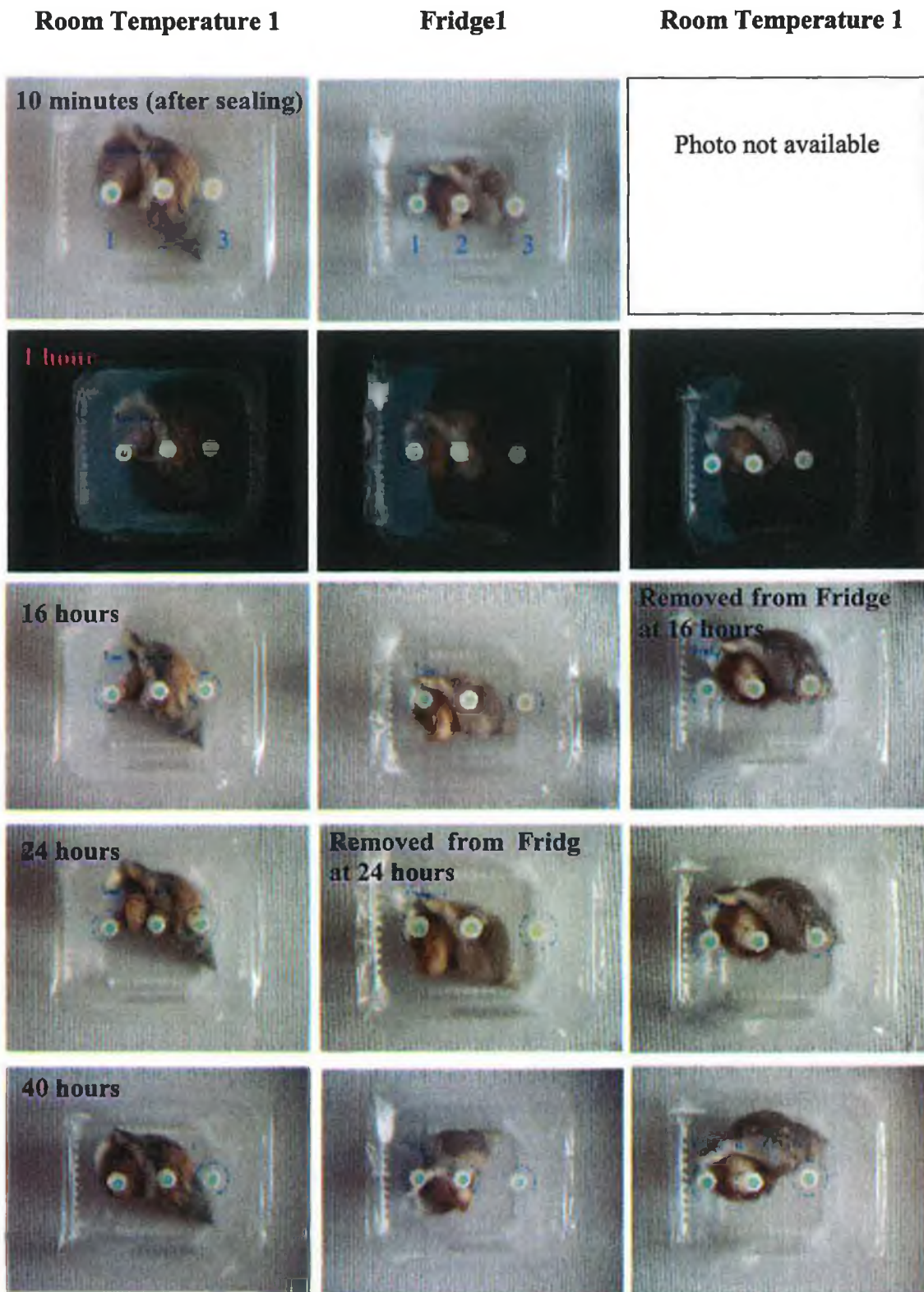


Figure 4-45 Digital images illustrate the colour change of the sensor spots over time as the cooked whelk are allowed to spoil at different temperatures. The images at 1 hour were taken with a black background to highlight the layer of condensation surrounding the first sensor in each container.



The graph below illustrates the sensors response over time, measured via the handheld Colourmeter, to spoiling whelk stored at different temperature conditions. Two whelk samples were monitored at each temperature so each line on the graph represents 4 sensors (n=4, sensors 2 and 3 from each container). Sensor 1 on each tray was eliminated from the results as it was saturated initially.

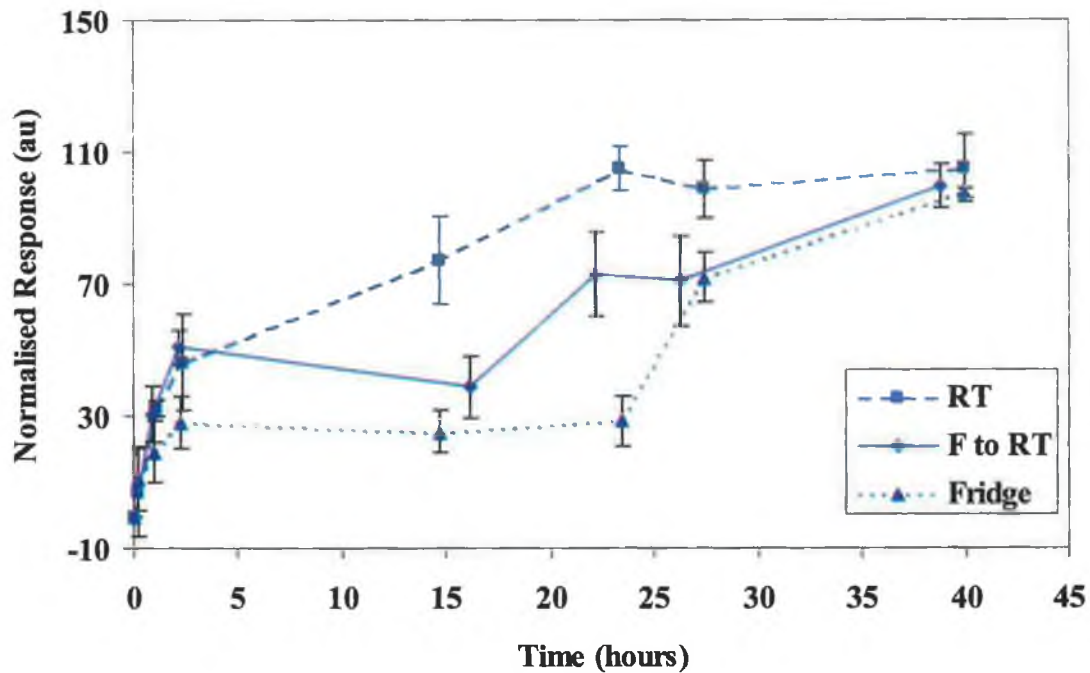


Figure 4-46 Sensor responses (n=4) to the spoilage volatiles released by the cooked whelk stored at different temperature conditions. The *RT* samples were stored at room temperature for the entire trial. The *F to RT* and *F* samples were stored in the fridge until they were removed at 16 and 24 hours respectively.

The *RT* samples were allowed to spoil at room temperature for the entire trial. The *F to RT* and *F* samples were stored in the fridge for 16 and 24 hours respectively, before they were removed from the fridge and stored at room temperature. While the samples were stored in the fridge they were removed momentarily (i.e. up to 1 minute) at various time points to facilitate Colourmeter measurements. The graph illustrates how the sensors representing the *RT* samples responded a lot faster than those sensors representing the samples which were chilled for a period of time before they were exposed to room temperature. Chilling significantly slows down the growth of spoilage bacteria, therefore slows down the production of spoilage volatiles. The sensor response for the samples stored in the fridge increased initially for the first 2 hours and then remained relatively constant until they were removed from the fridge at approximately 16 and 24 hours (*F to RT* and *F* samples respectively). Once the samples were exposed to higher

temperatures there was a visible increase in the sensor response from the time they were removed. This increase in the sensor response represents the increase in the TVB-N concentration in the headspace. The temperature increase boosted bacterial growth and TVB-N production. The accompanying digital images in Figure 4-45 compliment the Colourmeter response to the sensors. Focusing only on sensors 2 and 3 in each container there is a visible difference in the sensor spots over time, changing from yellow to blue. Take for example the sensors representing the *RT* samples. At 10 minutes the sensor spots 2 and 3 are yellow. By 14 hours the same sensor spots are blue while the sensors representing the *F to RT* and *F* samples are a greenish-yellow. The sensors remain this colour until the samples are removed from the fridge. For example the sensors representing the *F to RT* changed from a greenish-yellow to blue after being stored at room temperature for ~6 hours. Likewise, the sensors on the *F* samples changed from a greenish-yellow to blue after being exposed to room temperature for ~4 hours. By ~40 hours all of the sensors on all of the samples were the same colour illustrated by both the sensor response measured via the Colourmeter and the colour digital images captured with the digital camera. The results from this preliminary trial also demonstrate that the colour images of the sensors correlate well with the Colourmeter response.

#### 4.4 Conclusion

Ten different membrane formulations were initially prepared. The optimised formulation was chosen based on a number of factors such as the solubility of the membrane components in the solvent to produce an optically clear membrane and the absence of dye leaching when the membranes were submerged in water. The  $pK_a$  of bromocresol green in the membrane was determined using two different instruments, a plate-well reader and a newly developed handheld Colourmeter, which gave a  $pK_a$  of  $5.56 \pm 0.01$  (0.10% RSD, where  $n = 3$ ), and  $5.43 \pm 0.02$  (0.39% RSD, where  $n=2$ ), respectively. There is very little variation between the two techniques, which validates the reliability of the handheld Colourmeter for measuring the sensor response. Temperature was shown to have minimal effect on the  $pK_a$  of the dye in the membrane. The sensors were calibrated in  $NH_3$  and the limit of detection was calculated to be  $0.23 \pm 0.07$ ppm. The sensors showed excellent reproducibility with an overall %CV < 12% ( $n=3$ ). Preliminary trials were performed where the sensors were exposed to the spoilage volatiles released by cooked whelk stored at different temperatures. The sensor

response was measured via the handheld Colourmeter. The trials demonstrated that sensors representing cooked whelk samples stored at room temperature responded a lot faster than sensors representing samples that were chilled for a period of time. The results obtained during the preliminary trials provided a basis for further optimisation and improvement in the sensor design.

## References

1. Adams, M. R., and Moss, M. O., *Food Microbiology*, The Royal Society of Chemistry (1995).
2. Dektak V 200-Si Installation, Operation and Maintenance Manual, Metrology Group, pp. 7.
3. Byrne, L., Development of colorimetric pH sensors and optical-based detection for monitoring spoilage volatiles from packaged seafood, in *The School of Chemical Sciences*, Dublin City University, Dublin (2003).
4. Lau, K. T., Edwards, S., and Diamond, D., Solid-state ammonia sensor based on Berthelot's reaction, *Sensors and Actuators B: Chemical*, 98, 12 (2004).

## **5 Transfer of the Sensor Technology to the Seafood Processing Industry**

## 5.1 Introduction

With the current whelk package preparation protocol employed by the seafood producer, i.e. Errigal Fish, it is a major challenge to incorporate this sensor technology into sealed containers to monitor the spoilage of freshly cooked whelk. For example, some of the whelk meat products from Errigal Fish must undergo a pasteurisation process once they have been packed. The whelk trays are maintained at 90°C for 20 minutes and then they are maintained at 95°C for 105 minutes followed by cooling. There are three major concerns arising from the pasteurisation process. Firstly, the sensors have to be incorporated into the packaging before the pasteurisation process after which the sealed tray must not be tampered with. Secondly, sealed trays of cooked whelk meat subjected to high temperatures for long periods of time force the volatile nitrogenous compounds present in the whelk meat into the headspace saturating the sensor. Thirdly, the properties of the PTFE gas permeable membrane will be changed under such high temperature and pressure conditions allowing water vapours to be forced through the membrane and deprotonate the pH sensitive dye in the sensor.

The following chapters discuss how the sensor technology can be optimised to overcome these challenges to produce a robust sensor that operates reliably in a real industrial application.

### 5.1.1 Correlation of the Sensor Response to Microbial Spoilage of Cooked Whelk Stored at Different Temperatures

As seen in the previous chapter, the volatile basic nitrogenous compounds released from the whelk meat as a result of the cooking process, saturated the sensors before the onset of spoilage. In a real situation, if the quality of the whelk meat depended solely on the sensor response then a 'false positive' outcome would result in huge losses for the whelk meat processors. The main components of the volatile basic nitrogen compounds i.e. TMA, ammonia and DMA, each have  $pK_a$ s of 9.8, 9.25 and 10.70 respectively. Bromocresol green has a  $pK_a$  of 4.7 (the  $pK_a$  of bromocresol green in the polymer membrane is 5.4 determined in Chapter 8), which is readily deprotonated by the TVB-N released during cooking. In order for the sensor to respond at the critical threshold of interest, where the levels of TVB-N released are relatively high, a dye with a  $pK_a$  of around 2 pH units less than the  $pK_a$ s of the principal amine components of TVB-N must be selected. Two dyes were chosen: bromothymol blue ( $pK_a$  7.0) and m-cresol purple

( $pK_a$  8.3). Sensors were prepared containing the above dyes and their response to spoilage volatiles released by cooked whelk was assessed in a trial carried out at Errigal Fish, Carrick, Co. Donegal. The results of this trial are presented in the following chapter.

## 5.2 Experimental

### 5.2.1 Materials

The membrane components; pH sensitive dyes bromothymol blue (BTB, sodium salt), and m-cresol purple (m-CP, sodium salt), lipophilic salt tetraoctylammonium bromide (TOABr), and solvent cyclohexanone (99.8%), were obtained from Sigma-Aldrich (Dublin, Ireland). The binder poly(vinyl chloride) (PVC, high molecular weight) and the plasticiser dibutyl sebacate (DBS) were supplied by Fluka Chemicals (Dublin, Ireland). Optically clear poly(ethylene terephthalate) (PET) was obtained from Oxley plc (Cumbria, UK). Polypropylene reinforcement rings and polytetrafluoroethylene (PTFE) gas permeable membrane (Thread Seal Tape: 12m × 12mm × 0.075mm) were supplied by Radionics (Dublin, Ireland).

### 5.2.2 Preparation of Sensors

The same procedure as described in Chapter 4 was followed except m-cresol purple and bromothymol blue were used instead of bromocresol green.

### 5.2.3 Equipment

The handheld Colourmeter, a Sony Digital Camera and a Dell Latitude Laptop were used to monitor the sensor response and process the data.

### 5.2.4 History of the Whelk Samples

#### 5.2.4.1 Cooked Whelk-On-Shell

The cooked whelks were obtained from the production line at Errigal Fish. 454g ± 25g of cooked whelk-on-shell were weighed into individual plastic containers also supplied by Errigal Fish.

#### 5.2.4.2 *Cooked Whelk-No-Shell*

The cooked whelk meats without shells were also obtained from the production line at Errigal Fish. They were placed into a plastic container also supplied by Errigal Fish.

### 5.2.5 Experimental Set-up

#### 5.2.5.1 *Cooked Whelk-On-Shell*

The whelk samples were exposed to 4 different conditions as follows:

- Unpasteurised cooked whelk-on-shell at Room Temperature ~ 25°C
- Unpasteurised cooked whelk-on-shell at 0 to 4°C
- Pasteurised cooked whelk-on-shell at Room Temperature ~ 25°C
- Pasteurised cooked whelk-on-shell at 0 to 4°C

The sensors ability to respond to each condition over time was monitored using both subjective (visual assessment) and objective (digital images and Colourmeter measurements) techniques. Microbial tests (TVCs) were also carried out on the samples at regular time intervals.

10 packs of whelk were prepared for each condition i.e. 40 packs of cooked whelk in total. Packs from each of the above sampling conditions were removed at defined time intervals for microbial analysis. The time interval between each microbial analysis depended upon the conditions under which the samples were held. For example, microbial analysis were carried out more frequently on unpasteurised whelk stored at room temperature (every few hours) than pasteurised whelk (once a week) stored at 0 to 4°C. Pasteurised whelk stored at 0 to 4°C have a shelf life of 5 weeks with an extra 3 week period for safety.



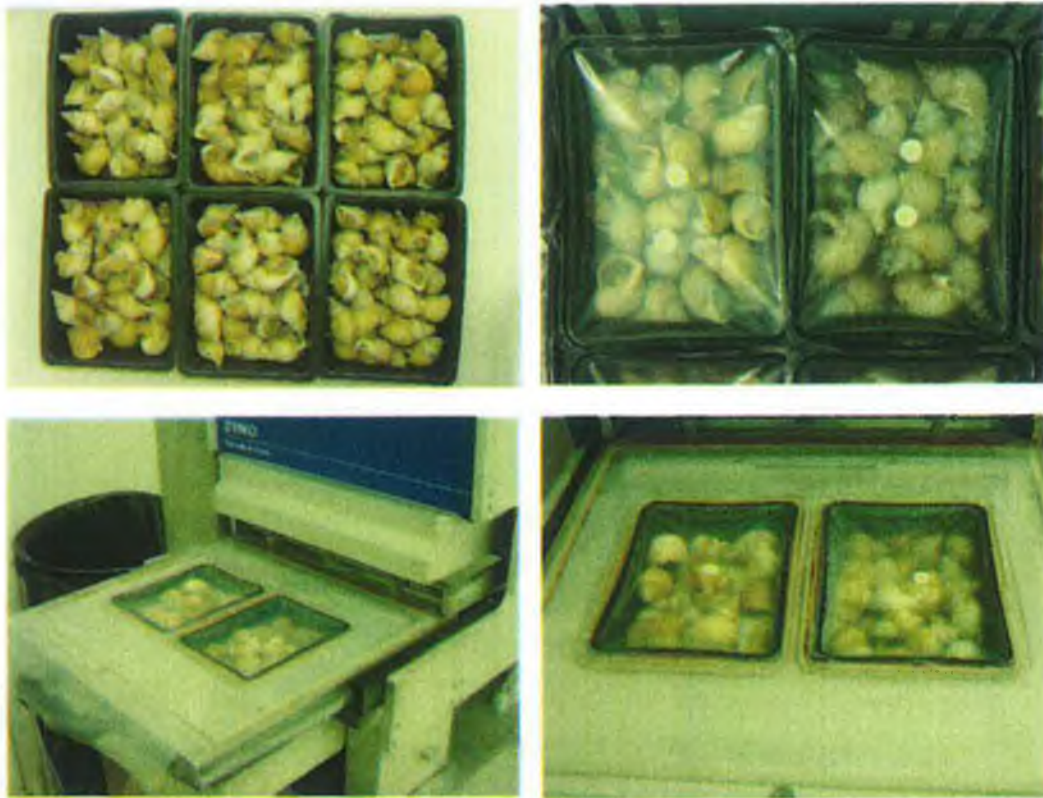


**Figure 5-1 The Bromothymol Blue and m-Cresol Purple Sensors were attached inside the plastic covering before the packs were sealed.**

One bromothymol blue and one m-cresol purple sensor were attached to 40 (weighing  $454\text{g} \pm 25\text{g}$ ) packs of cooked whelk-on-shell. The packaging equipment was manually operated so the sensors were attached inside the plastic covering, via double-sided sellotape, before the packs were sealed. All 40 packs were placed in cold storage until the following morning. The cold temperature inhibits or dramatically slows down bacterial growth allowing the experiment to be delayed until the next day. 20 of the packs were placed in the laboratory fridge (these were not pasteurised) and 20 more packs were placed in cold storage on the production line for pasteurisation the following morning. 15 hours after the whelks were packaged the 20 packs of whelk were removed from the laboratory fridge and randomly divided into 2 groups of 10. 10 of the packs were placed on the bench and initial readings using the Colourmeter were taken. These remained on the bench exposed to ambient temperatures for the remainder of the experiment. The trays of whelk were labelled: *Unpasteurised Bench 1 to 10*. The other 10 trays of whelk were put back into the fridge and were labelled: *Unpasteurised Fridge 1 to 10*. Trays 9 and 10 had only one spot (a bromothymol blue spot as some of the m-cresol spots were mislaid during the packing stage). The other 20 trays of whelk were pasteurised on the production line and were returned to the laboratory once the

pasteurisation process was complete. Once again 10 packs were placed in the fridge, labelled *Pasteurised Fridge 1 to 10*, and the remaining 10 were placed on the bench, labelled *Pasteurised Bench 1 to 10*.

#### 5.2.5.2 Cooked Whelk-No-Shell

5 bromothymol blue and 3 m-cresol purple sensors were attached inside a shallow plastic container of shelled cooked whelk meats. The container was sealed and the tray was stored at room temperature for the duration of the experiment. The sensor response was monitored using the handheld Colourmeter and the digital camera.

### 5.2.6 Pasteurisation Process

The whelk trays were maintained at 90°C for 20 minutes and then they were maintained at 95°C for 105 minutes followed by cooling.

### 5.2.7 Microbial Testing

#### 5.2.7.1 Total Viable Counts (TVC)

TVCs were chosen as the microbial test to be used in this trial for detecting whelk spoilage over time.

##### 5.2.7.1.1 Materials and Equipment

(IMS) Industrial Methylated Spirits, Bunsen burner, chopping board, knife, MRD (Maximum Recovery Diluent), stomacher bags, Petri dishes and plate count agar.

##### 5.2.7.1.2 Method

The sampling area was sanitised with IMS including the chopping board, balance and the outer surface of the whelk tray. The knife was dipped in IMS and flamed over the Bunsen burner. Using the knife 25g ± 0.5g of whelk meat (excluding the guts and nail) was chopped up and weighed into a stomacher bag. 225ml of MRD was poured into the stomacher bag and mashed for ~1 min. The contents were poured into a sterile container and the whelk meat was allowed to settle to the bottom. This represented the 10<sup>-1</sup> dilution. Using aseptic techniques 1ml of this solution was transferred into 9ml of

MRD. This represented the  $10^{-2}$  dilution. This procedure was continued until the required dilution was achieved. 1ml of each dilution was pipetted into a Petri dish ( $\times 2$ ). A small amount of plate count agar was poured into the Petri dish and was gently swirled to evenly cover the bottom of the plate. The plates were allowed to set for approximately ten minutes. The plates were inverted and placed into the incubator at  $30^{\circ}\text{C}$  for 48 hours. At 48 hours the plates were removed and the colonies were counted.

## 5.2.8 Total Volatile Base Nitrogen (TVB-N)

In Errigal Fish Co. Ltd, TVB-N is used as an indicator for whelk freshness.

### 5.2.8.1.1 Materials and Equipment

Kjeldahl flask, condenser, delivery adaptor, splash head, conical flask, heating mantle, 10 grams of chopped whelk meat, 2ml of silicone anti-foaming agent (BDH: Product Code: 33151), 2g magnesium oxide heavy GPR (BDH: Product Code: 291104W), 300ml of distilled water, 2% boric acid, 0.1M HCL

### 5.2.8.1.2 Method

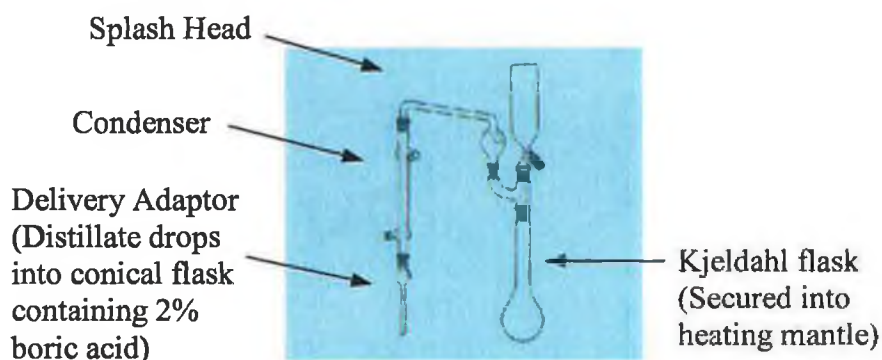


**Figure 5-2 (Kjeldahl, macro determination unit for distillation from Lennox Laboratories Supplies online catalogue: Cat. No. 244/1620/00)**

The above distillation apparatus was assembled for the TVB-N determination. 10g of chopped whelk meat were accurately weighed into the Kjeldahl flask. 2ml of silicone anti-foaming agent and 2g magnesium oxide and 300ml of distilled water were transferred to the flask. The flask was heated over a heating mantle. The mixture was boiled for 25 minutes from boiling point. The blue boric acid solution was titrated

against 0.1M HCL until the blue colour disappeared. The titrate result was used in the following calculation to determine the TVB-N present in the whelk meat:

#### 5.2.8.1.3 Expression of Results

The equation below is the simplified method of calculating the % Nitrogen in a whelk meat sample given in the Errigal Fish Laboratory Sampling and Test Procedures Manual, Section No: EL – 3 –0, for the Determination of Total Volatile Bases.

$$\frac{M_{N_2}}{M_{flesh}} = T_R \times 14 \quad \text{Equation 5-1}$$

$M_{N_2}$  = mg nitrogen

$M_{flesh}$  = 100 mg flesh

$T_R$  = Titrate result

The following guidelines set out in Table 5-1 are used by Errigal Fish Co. Ltd to relate this value to whelk meat freshness:

mg nitrogen /100g flesh	Freshness Description
0-15	Good
15-20	Going off
>20	Gone off

**Table 5-1 TVB-N guidelines relating to whelk meat freshness used by Errigal Fish Co. Ltd.**

## 5.3 Results and Discussion

### 5.3.1 Cooked Whelk-On-Shell

The 40 trays of whelk were placed in cold storage to delay spoilage. 20 packs were placed in the laboratory fridge and 20 packs were placed in cold storage on the production line. 15 hours later the 20 packs of whelk in the fridge were examined and

the bromothymol blue spots on the majority of the packs had changed from yellow to green/blue, Figure 5-3.

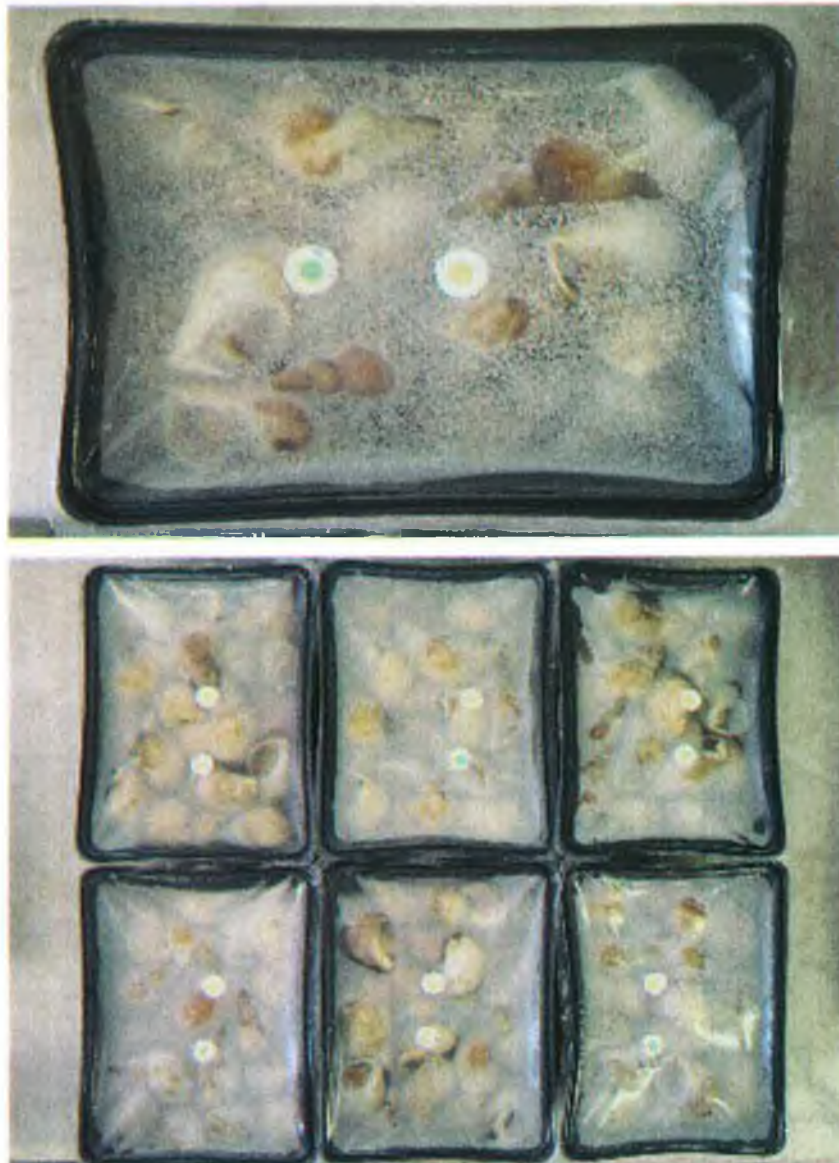


**Figure 5-3 The Bromothymol Blue sensors on the majority of the packs (11 out of 20) had changed from yellow to blue after 15 hours in cold storage.**

Tray No.	1	2	3	4	5	6	7	8	9	10
Bench	B	Y	B	Y	B	Y	Y	Y	B	Y
Fridge	B	Y	B	B	B	B	B	B	Y	Y

**Table 5-2 Colour description of the Bromothymol Blue sensor on the Unpasteurised Bench and Fridge Trays (B = Blue, Y = Yellow)**

The bromothymol blue sensors on the trays labelled *Unpasteurised Bench 2, 4, 6, 7, 8 & 10* remained unchanged. For the *Unpasteurised Fridge* samples the bromothymol blue sensors on trays 2, 9 & 10 also remained unchanged.

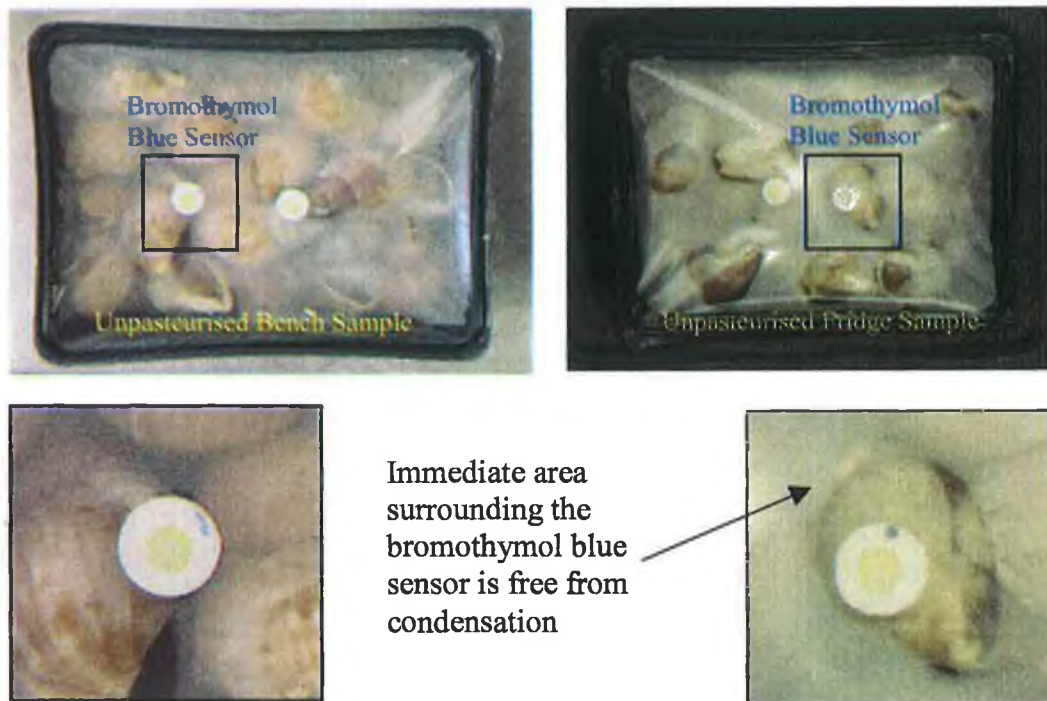


**Figure 5-4** Trays 2 from the *Unpasteurised Bench* and *Fridge* samples. The bromothymol blue sensor remained unchanged after 15 hours in cold storage.

The bromothymol blue spots in each of the above trays, *Unpasteurised Bench Tray 2* and *Unpasteurised Fridge Tray 2*, remained unchanged. Looking closely at the bromothymol blue sensors in each photo the immediate area surrounding each sensor appears free from condensation. This relates back to the preliminary trial carried out previously. Where there was condensation present the sensors had changed colour. This once again supports the fact that the condensation or layer of water surrounding the sensor absorbed and pre-concentrated the ammonia/amines released from the whelk into the headspace allowing the volatile compounds to easily diffuse through the PTFE gas permeable membrane and saturated it before the onset of spoilage.

Therefore, trays 2 from the *Unpasteurised Bench & Fridge* samples were used for colour measurements as the bromothymol blue sensors remained unaffected by the condensation and that any colour change over time may only be due to a response to increasing spoilage volatiles in the headspace. The spots on the remaining trays were also monitored but these trays were primarily used for TVC analysis over time. By 18

hours there was no visual change in the any of the sensors from trays 2 of the *Unpasteurised Bench & Fridge* samples, Figure 5-5.

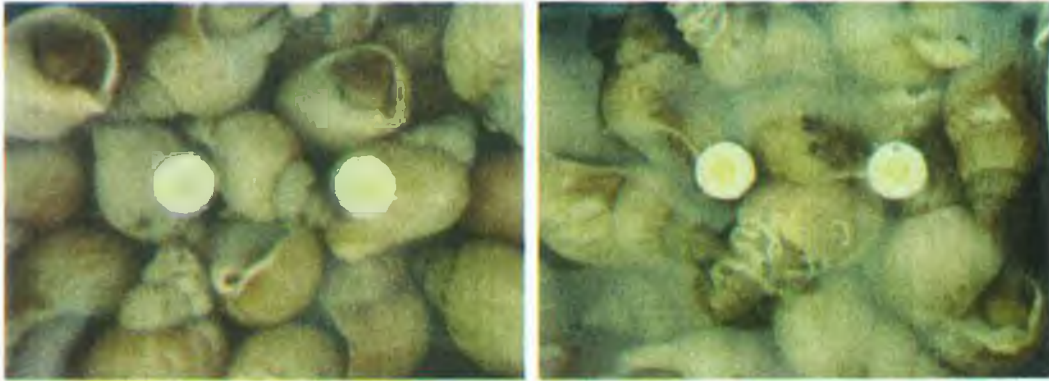


**Figure 5-5** By 18 hours there was still no visual change in any of the sensors for the unpasteurised bench samples (left) unpasteurised fridge samples (right).

When the other 20 trays of whelk returned from pasteurisation the spots were assessed for colour change and physical damage due to the extreme pasteurisation conditions. The photographs in Figure 5-6 clearly describe their appearance following pasteurisation. The bromothymol blue sensors once again changed colour and in some circumstances the sensor was completely destroyed. Clearly, the sensors were not able to withstand the harsh conditions of the pasteurisation process. At 22 hours a very interesting colour change in the bromothymol blue sensors in contact with the *Unpasteurised Bench* samples was observed. All the bromothymol blue sensors had reversed from blue to yellow. There was also no trace of condensation on the packs. The digital images in Figure 5-8 are of trays 2, 4, 5, 6, 7, 8, 9, & 10. Tray 3 was used for microbial analysis previously. The results from the Handheld Colourmeter verify this observation in the graph below, Figure 5-7.

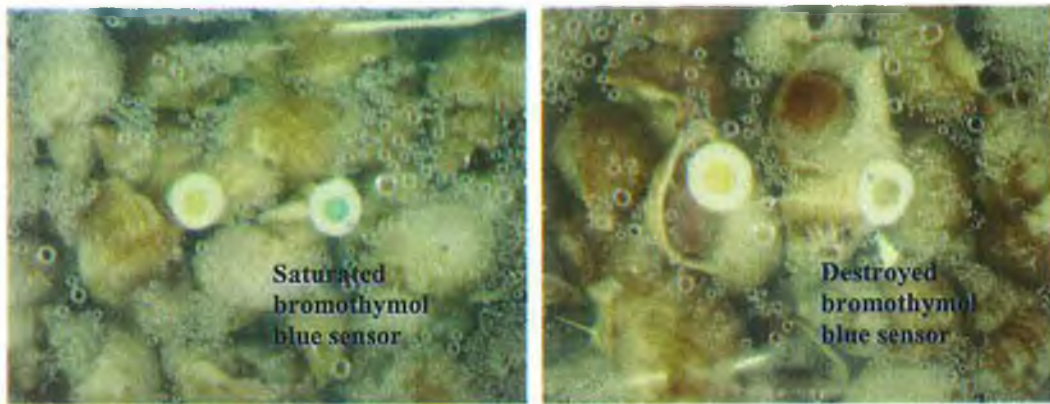


Figure 5-6 The Bromothymol Blue sensor was completed saturated (left) or completed destroyed (right) following pasteurisation.

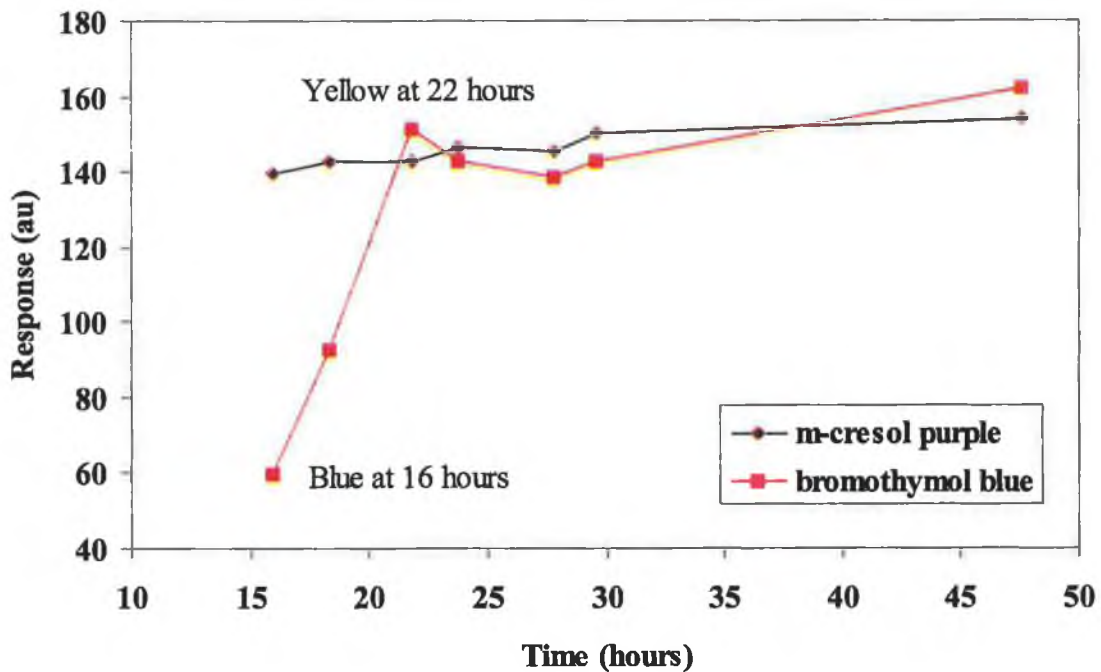
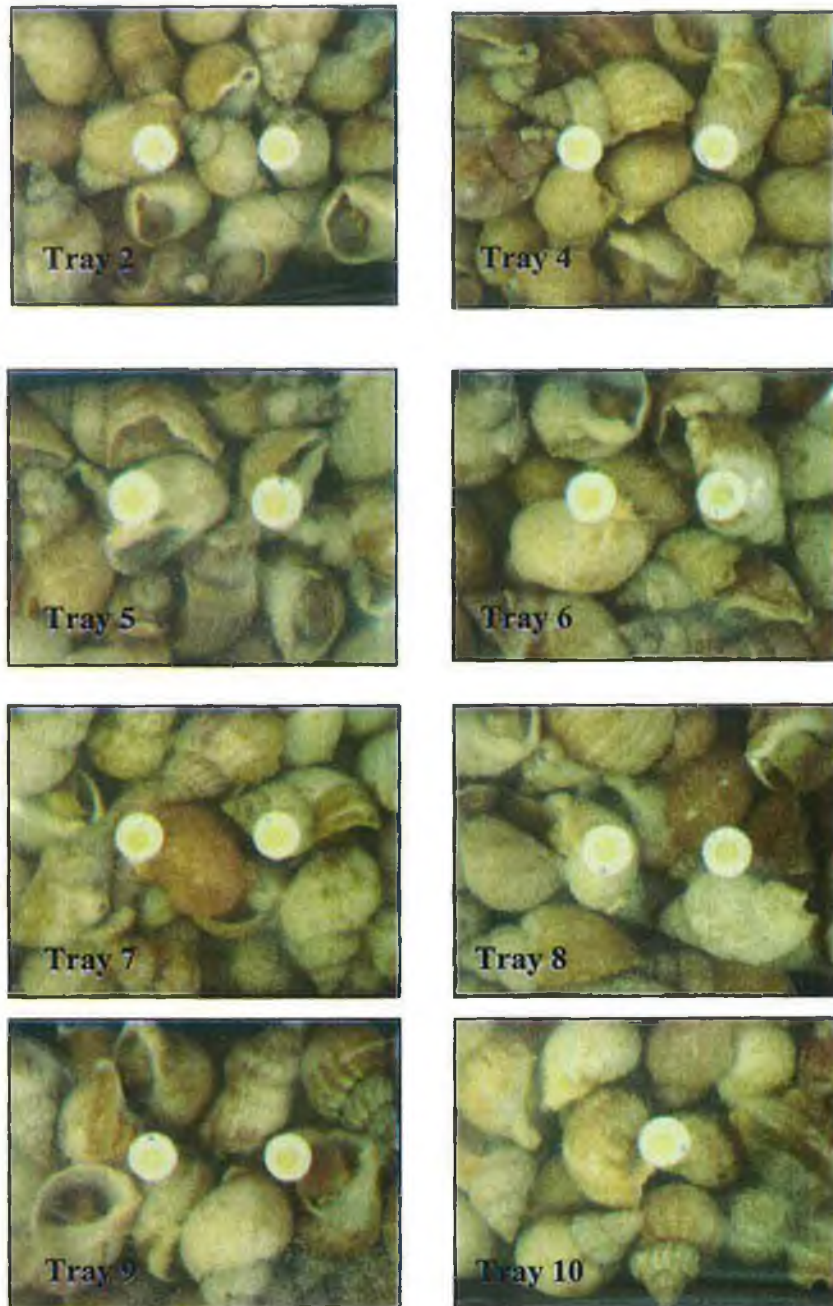


Figure 5-7 The Colourmeter response to the sensor describes how the bromothymol blue sensor reverted back to its original colour by 22 hours. At  $T_0$  both the bromothymol blue and m-cresol purple sensors were yellow. The first Colourmeter reading was taken at 15 hours (all samples were placed in cold storage for ~15 hours to delay the experiment).

This graph clearly illustrates the colour changes experienced by the bromothymol blue sensors for the *Unpasteurised Bench* samples. The m-cresol purple sensor did not change colour during the course of the experiment.





**Figure 5-8 Digital images of the bromothymol blue and m-cresol purple sensors on the Unpasteurised Bench samples taken at 22 hours**

At 44 hours a TVB-N analysis was carried out on the cooked whelk meat stored in one of the trays held at room temperature. The result of the test indicated that the whelk meat contained 28mg nitrogen/100g, which according to the guidelines set down by Errigal Fish indicated that the sample was spoiled.

By 48 hours there was still no visual colour change in the m-cresol purple sensors. The Colourmeter results verify this observation, Figure 5-7. It was obvious at this stage that the sensors were not responding to the spoilage volatiles released by the whelk meat. The experiment was therefore terminated.

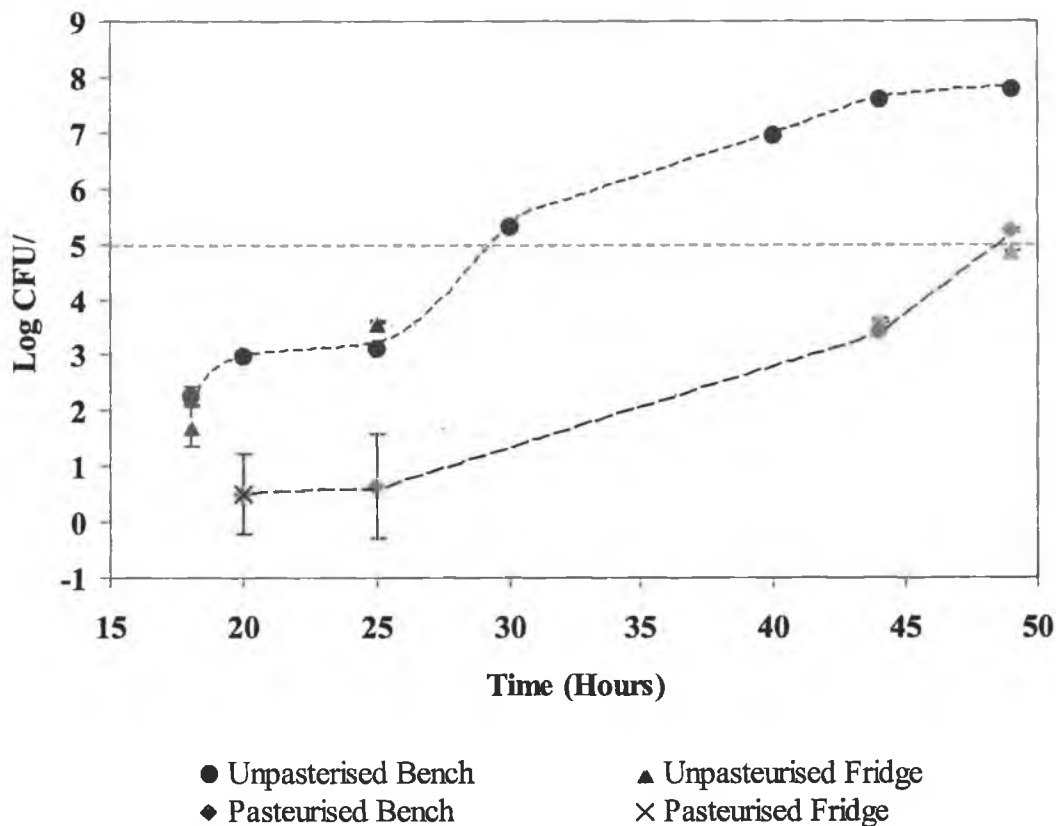


Figure 5-9 Total Viable Counts (n=2, the error bars are hidden behind the marker for some of the data points) for the cooked whelk samples exposed to different conditions i.e. Unpasteurised samples stored in the fridge and at room temperature (all the samples were placed in cold storage for ~15 hours prior to commencing the trial to delay spoilage) and pasteurised samples stored in the fridge and at room temperature (all samples were placed in cold storage for ~17 hours prior to the pasteurisation process which took ~2 hours – the 1<sup>st</sup> TVC analysis was performed at 20 hours). Only 1 TVC test was performed on the pasteurised fridge samples, as the TVC was not expected to change within the given time frame – See Appendix 4-1 for experimental results.

The Total Viable Counts of the whelk samples exposed to different conditions are given in Appendix 4-1. The logarithmic values of the Total Viable Counts are represented in Figure 5-9. As expected the TVCs for the unpasteurised samples stored at room temperature increased at a much faster rate over the 48-hour period compared to the unpasteurised samples stored in the fridge and the pasteurised samples stored at room

temperature. The TVC values are typically lower initially for the pasteurised samples compared with the unpasteurised samples. The cut-off threshold for accepting unpasteurised products at Errigal Fish is 100,000 CFU/g (the logarithmic value is 5). TVCs greater than 100,000 are regarded unfit for human consumption or spoiled. The cut-off threshold for pasteurised products is 10,000 CFU/g (the logarithmic value is 4). Using these guidelines, the unpasteurised samples stored at room temperature reached the critical cut-off point of 100,000 CFU/g at ~30 hours<sup>\*</sup>. Storing the samples in the fridge slowed down microbial growth considerably with the unpasteurised samples reaching their critical threshold limit at ~48 hours. Although the pasteurisation process kills any pathogenic and spoilage bacteria, if the products are not maintained at 0-4°C then microbial growth soon begins to accelerate. According to Figure 5-9, the pasteurised samples stored at room temperature reached their critical threshold limit of 10,000 CFU/g at ~45 hours<sup>\*\*</sup>.

### 5.3.2 Cooked Whelk-No-Shell

At T<sub>0</sub> all the bromothymol blue and m-cresol purple sensors were yellow, Figure 5-10. By 18 hours the bromothymol blue sensors had changed to a greenish colour while the m-cresol purple sensors remained unchanged, Figure 5-10. The Colourmeter results in Figure 5-11 clearly illustrate this colour change in the bromothymol blue sensors. By 48 hours the whelk meats were clearly spoiled as the container had expanded to accommodate for the increased production of gaseous compounds released into the headspace, Figure 5-12. The bromothymol blue sensors reversed back to their original yellow colour while the m-cresol purple sensors showed no sign of colour change.

---

\* The samples were held in cold storage for ~15 hours prior to commencing the trial. For the remaining 15 hours the samples were exposed to room temperature.

\*\* The samples were held in cold storage for ~17 hours prior to pasteurisation. The pasteurisation process took ~2 hours. The samples were then returned to the laboratory where they were exposed to room temperature for the remainder of the trial. Therefore, the time taken for the samples to reach the cut-off threshold when exposed to room temperature was ~25 hours.

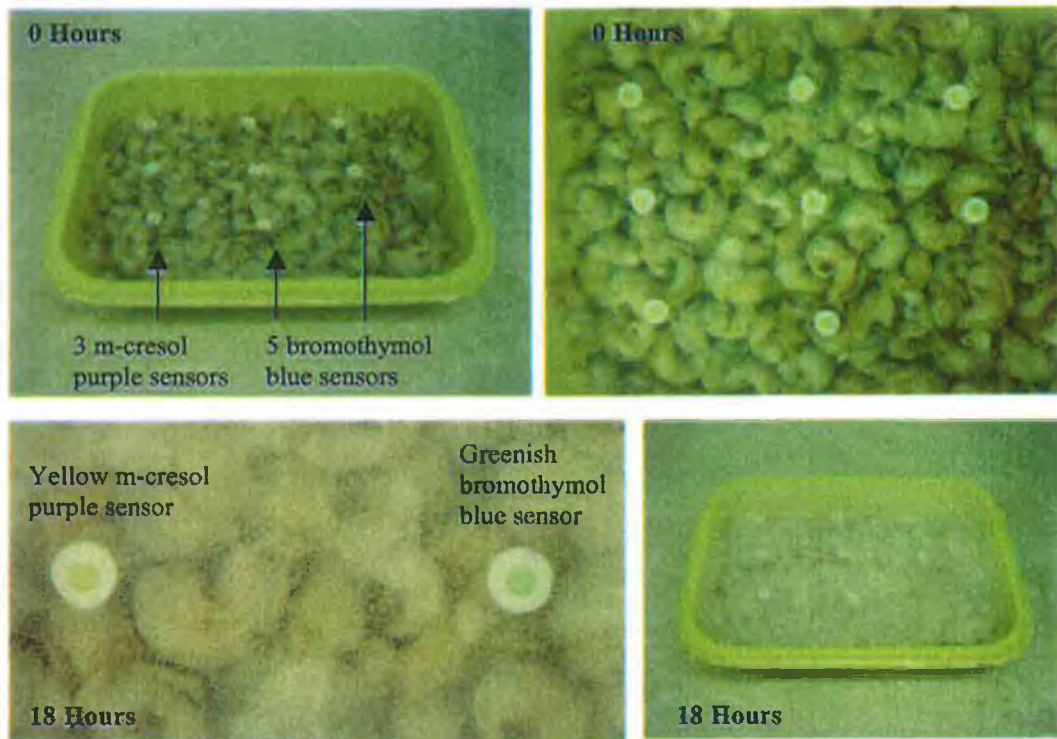


Figure 5-10 m-cresol purple and bromothymol blue sensors monitoring the spoilage of cooked whelk meats

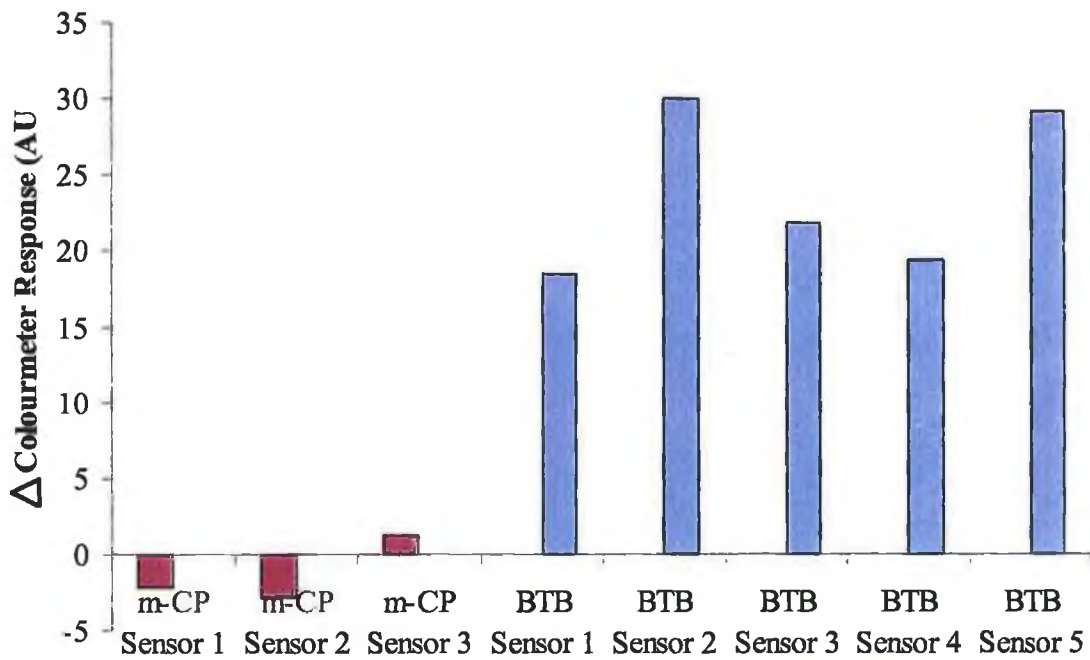
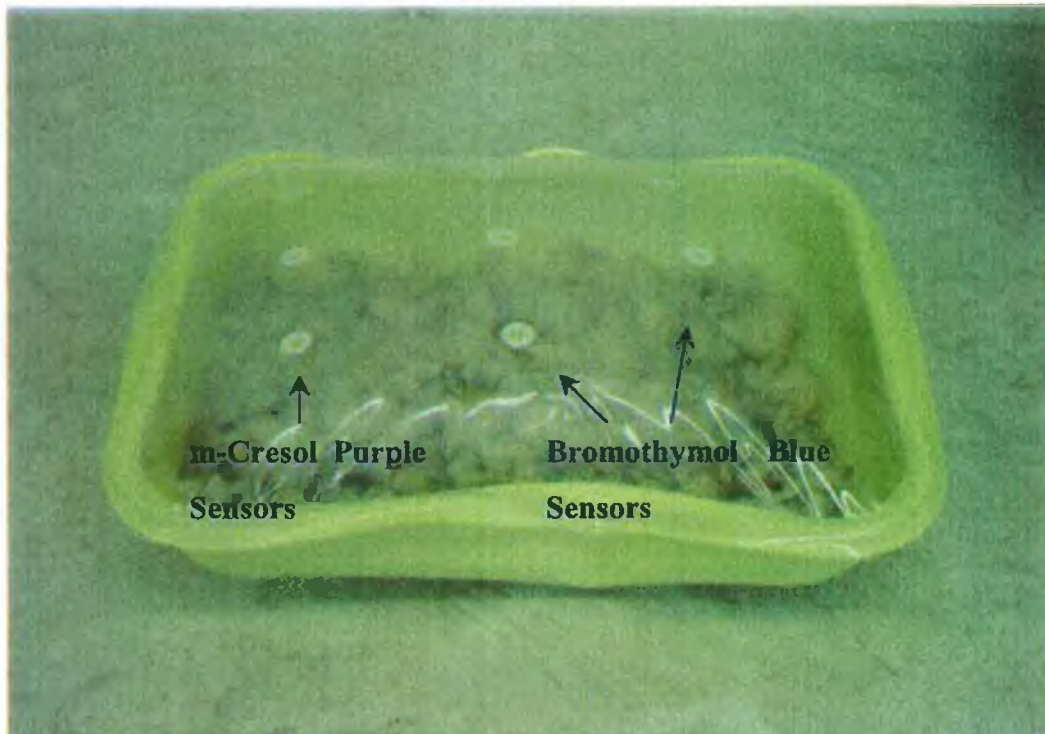


Figure 5-11 Colourmeter response of Bromothymol Blue (BTB) and m-Cresol Purple (m-CP) sensors after 18 hours exposed to room temperature.



**Figure 5-12 Digital image indicates the cooked whelks were well spoiled after 48 hours exposure to room temperatures. The container expanded to accommodate for the increased production of gaseous compounds released into the headspace. The Bromothymol Blue sensors reversed back to their original yellow colour while the m-cresol purple sensors showed no sign of colour change.**

For these trials the bromothymol blue and m-cresol purple sensors did not respond to the microbial growth of the cooked whelk meat samples. This is surprising, as it has been reported in the past that pH sensitive membranes containing the pH sensitive dye cresol red,  $pK_a$  of 8.1, responded very well to the onset of spoilage of a number of different fish species. The sensors containing the pH sensitive dyes bromothymol blue and m-cresol purple have  $pK_{as}$  (7.0 and 8.3 respectively) close to that of cresol red and would be expected to behave in a similar fashion. With some shellfish i.e. crustaceans, the muscle has been reported to contain over 300mg of nitrogen/100g of meat, which is considerably higher than that for fish and initial spoilage of crustacean meats is accompanied by the production of large amounts of volatile base nitrogen, much as in the case with fish.

There is very little information in the literature describing the spoilage patterns of the whelk species. We can only look at the spoilage patterns of other species from the same molluscan shellfish family i.e. oysters, clams, squid and scallops and use this

information as a guide to whelk meat spoilage. Molluscan shellfish differ in their chemical composition from both fish and crustacean shellfish in having a significant content of carbohydrate material and a lower total quantity of nitrogen in their flesh, Table 5-3.

	% Water	% Carbohydrates	% Proteins
<i>Fish</i>			
Bluefish	74.6	0	20.5
Cod	82.6	0	16.5
Haddock	80.7	0	18.2
Halibut	75.4	0	18.6
Herring (Atlantic)	67.2	0	18.3
Mackerel (Atlantic)	68.1	0	18.7
Salmon (Pacific)	63.4	0	17.4
Swordfish	75.8	0	19.2
<i>Crustaceans</i>			
Crab	80.0	0.6	16.1
Lobster	79.2	0.5	16.2
<i>Mollusks</i>			
Clams, meat	80.3	3.4	12.8
Oysters	80.5	5.6	9.8
Scallops	80.3	3.4	14.8

**Table 5-3 Approximate % Chemical Composition of Fish and Shellfish**

The carbohydrate is largely in the form of glycogen, and with levels of the type that exist in molluscan meats, fermentative activities may be expected to occur as part of the microbial spoilage. The higher content of carbohydrate materials in molluscan shellfish is responsible for the different spoilage pattern of these foods over other seafood. The microbial flora of molluscan shellfish may be expected to vary considerably, depending on the quality of the water from which these shellfish were taken and the quality of the wash water and other factors. As spoilage sets in and progresses, *Pseudomonas* and *Acinetobacter-Moraxella* species predominate, with enterococci, lactobacilli, and yeasts dominating the late stages of spoilage. Due to the relatively high level of glycogen, the spoilage of molluscan shellfish is basically fermentative but for squid meat, volatile

base nitrogen increases as spoilage occurs much in the same manner as for crustacean shellfish. As already mentioned, for molluscan shellfish volatile basic nitrogenous compounds are released during the initial stages of spoilage but the final stages of spoilage are predominantly due to fermentative activities. Therefore, the total volatile compounds released during molluscan shellfish spoilage not only consist of total volatile bases (TVB) but also consist of total volatile acids (TVA). TVA includes acetic, lactic and other organic acids produced by lactic acid bacteria during the breakdown of carbohydrates in the fermentation process. While TVB production predominates initially, the overall headspace pH will be lowered by the production of volatile acids such as acetic and lactic acid at the later stages of spoilage. As the two antagonist processes ultimately lower the pH of the headspace this may explain why the bromothymol blue and m-cresol purple sensors did not respond as the whelk meat deteriorated. The concentration of basic compounds present in the headspace may not have been high enough to deprotonate the dye and cause a colour change due to the production of volatile acids.

These two antagonist spoilage processes present an interesting challenge for the pH sensor technology in detecting the spoilage volatiles and may also explain the colour changes observed by the bromothymol blue sensor while monitoring the spoilage of the shelled cooked whelk meats. Initially the bromothymol blue sensors were yellow. After 18 hours of being exposed to room temperatures these sensors changed from yellow to pale green. By 48 hours the bromothymol blue sensors had reversed back to their original colour. The different spoilage patterns experienced by molluscan shellfish may explain these observations. The green colour at 18 hours may represent the initial stages of spoilage where TVB volatiles were predominantly produced. By 48 hours the bulging container clearly indicated that the cooked whelks were in the later stages of spoilage where fermentation activities produced large amounts of volatile organic acids such as lactic acid and acetic acid. The presence of large amounts of volatile acids in the headspace may have protonated the bromothymol blue sensors causing them to return to their original state.

The above phenomenon describes what would happen if the cooked whelk samples were allowed to deteriorate to such extremes that the packaging becomes distorted due to the presence of colossal amounts of spoilage volatiles. In reality, the appearance of the bulging container alone would be enough evidence to indicate that the product is well past its sell-by date!

The initial stage of spoilage is primarily what needs to be addressed where there is an abundance of volatile bases present in the headspace. While it has been proven in the

past by researchers studying the spoilage patterns of fish samples that the indicator dye needs to be approximately 1-2 pH units less than the  $pK_a$ s of the compounds to be detected so that the sensors are not easily deprotonated by the headspace before the onset of spoilage, then the contrary may well be true in this case. A dye with a lower  $pK_a$  i.e. bromocresol green ( $pK_a$  4.7), may be necessary to detect the spoilage volatiles without being reversed back to their acid form by acidic volatiles released in the later stages of spoilage.

## **5.4 Conclusion**

The results from this trial indicate that the m-cresol purple sensors and the bromothymol blue sensors did not respond well to the microbial growth of cooked whelk meat samples. The trials also demonstrated that sensors were not robust enough to withstand the extreme conditions of the pasteurisation process. Developing a sensor to detect cooked whelk meat spoilage proves to be a challenging task. The obstacles described here must be taken into consideration for future optimisation of the pH sensor technology.



## **6 Optimisation of the Sensor Design and Correlation of the Sensor Response to Microbial Spoilage of Cooked Whelk**

## 6.1 Introduction

The results from the last chapter clearly indicate that the sensors prepared from the two dyes bromothymol blue ( $pK_a$  7.0) and m-cresol purple ( $pK_a$  8.3) were not sensitive enough to detect the onset of spoilage using this experimental design, as there was no change in the sensor response when it was obvious that the samples were well spoiled according to the microbial data. Digital images of the sensors following pasteurisation clearly illustrated how the high temperatures and pressures affected their physical structure. The sensors are not yet robust enough to withstand the pasteurisation process and require further development before they can be incorporated into packaging materials destined for such processes. For this reason, subsequent trials were primarily focused on the spoilage patterns of unpasteurised cooked whelk products. From the preliminary trials, the bromocresol green sensors had their drawbacks. A combination of factors caused them to change colour prematurely. The reason behind this premature colour change has been discussed in detail in previous chapters. In the preliminary trials, the cooked whelks were packed while they were still warm. At Errigal Fish the time interval between cooking and packing can vary but in general it is long enough to allow the whelks sufficient time to cool down to ambient temperatures before they are packed. The volatile nitrogenous compounds released during cooking are allowed to escape into the atmosphere so by the time they are packed and sealed into the containers the amounts of amines being released initially into the container headspace are minimal compared to the amounts being released when they are packed straight after cooking. Allowing the whelks sufficient time to cool down to ambient temperature before packing and sealing eliminates the main factors that cause the sensors to change colour prematurely and allows the sensors to respond only to increased TVB-N concentration in the headspace as a result of spoilage. Focusing on unpasteurised products and cooked whelks that are allowed sufficient time to cool down before they are packed and sealed into containers provides a more practical environment for the sensors to perform reliably as they are designed to do.

### 6.1.1 Modification of the Sensor Design

Under high temperatures and pressures the components of the sensor would not be expected to behave as they would under standard temperature and pressure conditions. For example, the function of the hydrophobic PTFE gas permeable membrane is to

allow gaseous compounds through to the sensor while still protecting the sensor surface from water that can cause a colour change with or without the presence of basic gaseous compounds thus saturating the sensor before the onset of spoilage. The high temperature and pressures created during pasteurisation will force the water vapour through the PTFE membrane and saturate the sensor.

An alternative method of reducing the water vapour effects is to significantly reduce the amount of water vapour permeating through the hydrophobic gas permeable membrane. Mechanically modifying the physical morphology of the gas permeable membrane through stretching operations can provide a more tortuous route for the water molecules to travel and ultimately retards the migration through the membrane. A number of sensors were prepared with modified gas permeable membranes and their response to water vapours was measured with the aid of the handheld Colourmeter.

The aim of this experiment at Errigal Fish is to correlate the sensor response of the newly modified sensors to microbial growth as the whelk meat deteriorates at different storage temperatures and to accurately assess the sensor's sensitivity to the spoilage volatiles.

## **6.2 Experimental**

### **6.2.1 Materials**

The membrane components, pH sensitive dye bromocresol green (pKa 4.7, lipophilic salt tetraoctylammonium bromide and solvent cyclohexanone (99.8%), were obtained from Sigma-Aldrich (Dublin, Ireland). The binder poly(vinyl chloride) (PVC, high molecular weight) and the plasticiser dibutyl sebacate (DBS) were supplied by Fluka Chemicals (Dublin, Ireland). Optically clear poly(ethylene terephthalate) (PET) was obtained from Oxley plc (Cumbria, UK). Polypropylene reinforcement rings and polytetrafluoroethylene (PTFE) gas permeable membrane (Thread Seal Tape: 12m × 12mm × 0.075mm) were supplied by Radionics (Dublin, Ireland). Fast Drying Super Glue and fast cure epoxy glue, Araldite, were also used.

## 6.2.2 Sensor Fabrication

3 types of sensors were prepared for this experiment. All of the sensors shared the exact same chemical formulation and were fabricated identically as discussed in Chapter 4 but each type was prepared with a different gas permeable membrane structure as follows:

1. Sensor *Type 1* had one layer of gas permeable membrane
2. Sensor *Type 2* had two layers of gas permeable membrane but the first layer was stretched (see following section) before it was attached to the sensor followed by another layer of the membrane in its original form.
3. Sensor *Type 3* had two layers of gas permeable membrane in its original form.

## 6.2.3 Mechanical Transformation of the PTFE Gas Permeable Membrane Using Stretching Operations

Stretching the PTFE gas permeable membrane was carried out in two stages:

- **Stage 1:** A schematic of the stretching operations is shown in Figure 6-1. 8 cm of the PTFE membrane was laid out on a flat surface. Two lengths of adhesive tape (2.5cm in height) were secured to both sides of the membrane, which allowed the membrane to be pulled in opposite directions. The membrane was gently stretched to ~5 cm.
- **Stage 2:** Two more lengths of adhesive tape were secured to the top and bottom of the stretched membrane, which allowed the membrane to be stretched again in the opposite direction. The original 8 cm × 1.2 cm PTFE tape was reduced to the approximate dimensions 5 cm × 5 cm.

## 6.2.4 Observation

The morphology of the stretched membrane was observed using a scanning electron microscope (SEM Hitachi S-3000N).

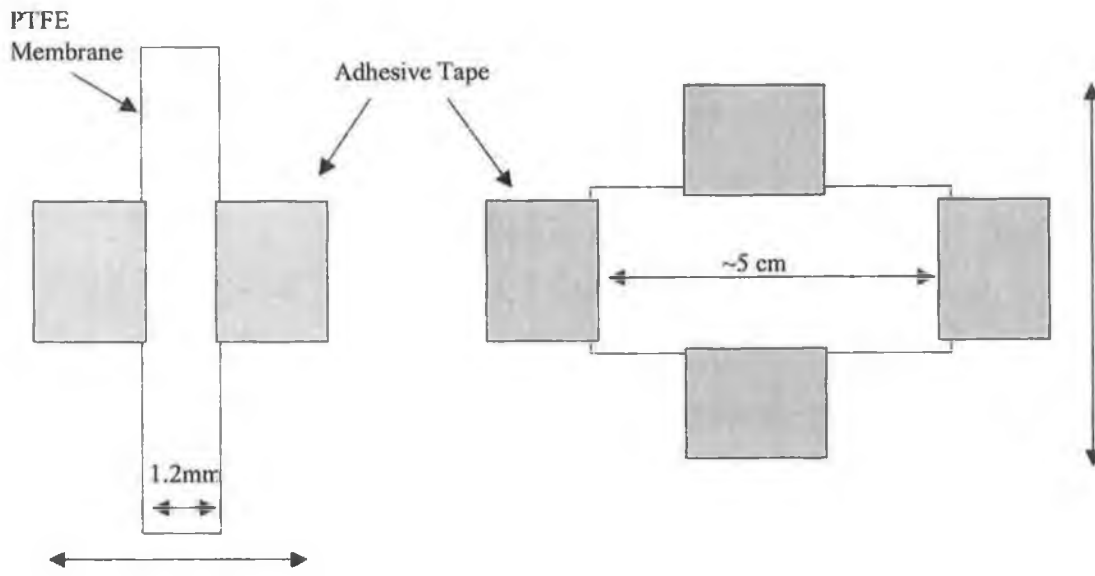
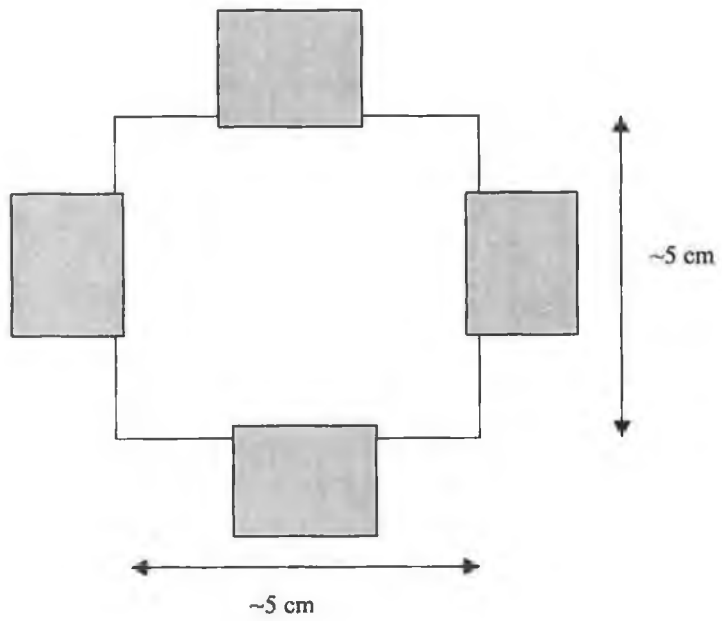


**Figure1 (a) PTFE Membrane**

**(b) Stage 1 Stretching**



**(c) Stage 2 Stretching**

**Figure 6-1 Schematic of the stretching operations**

## 6.2.5 Sensor Response to Water Vapour

### 6.2.5.1 Materials and Equipment

2 sensors from each of the membrane types (*Type 1*, *Type 2* and *Type 3*) prepared as described previously were used for this experiment. Epoxy glue, distilled water, the Handheld Colourmeter, a PC laptop (Dell, Latitude), Colourmeter Software Version 4.501, a retort stand, a heating mantle and a 100ml beaker were also required.

### 6.2.5.2 Monitoring the Sensor Response to Water Vapour

The *Type 1* sensor spot was attached to the red LED head of the Colourmeter with the aid of epoxy glue. The glue was allowed to air dry for 30 minutes. The red LED head was clamped into place using a retort stand over a 100ml beaker containing 50ml of distilled water. The beaker was positioned on top of a heating mantle. The distilled water was allowed to come to boiling point. As soon as the water reached a steady boil the red LED head was positioned at a fixed height directly above the mouth of the beaker allowing the water vapours to permeate through the membrane and react with the sensor. The LabView software Version 4.501 was programmed to record the colour change of the sensor every 2 seconds. The data was saved as a DAT file in Microsoft Notepad. Post-run data analysis was performed using Microsoft Excel. The above procedure was repeated for the *Type 2 and 3* sensors. The response of each type of sensor to water vapour was compared.

## 6.2.6 Sensor Response to Microbial Spoilage of Cooked Whelk

### 6.2.6.1 Materials and Equipment

40 Bromocresol green *Type 2* sensors were prepared and fabricated as discussed in chapter 10. The Handheld Colourmeter, Colourmeter software, laptop (Dell, Latitude) and a Sony digital camera.

### 6.2.6.2 Experimental Set-up

From the previous trial it is clear that the sensors are not durable enough to withstand the extreme pasteurisation conditions. For this reason pasteurised samples were not included. Only 2 sampling conditions were examined:

- Unpasteurised whelk-on-shell stored at room temperature ( $25.9^{\circ}\text{C} \pm 1.0$ )
- Unpasteurised whelk-on-shell stored in the fridge ( $6.9^{\circ}\text{C} \pm 1.1$ )

4 of the newly designed bromocresol green sensors were attached inside shallow yellow pack trays ( $\times 6$ ) containing cooked whelk-on-shell (weighing  $\sim 1\text{kg}$  each). 3 trays were placed in the fridge at 0 to  $4^{\circ}\text{C}$  (labelled *Fridge 1, 2, & 3*) and the remaining 3 trays were left on the bench at room temperature for the entire experiment (labelled *Bench 1, 2 & 3*). 32 stomacher bags were filled with approximately 500g of cooked whelk-on-shell from the same batch and were divided into 2 sets of 16 bags. The bags were sealed and 1 set was placed in the fridge along with the 3 yellow pack samples and the other 16 bags were placed on the bench exposed to the same conditions as the 3 bench samples. TVC and TVB-N tests were performed on these samples at regular intervals using the same methodology as outlined in sections 5.2.7.1 and 5.2.8. The Colourmeter and digital images were used to track the sensor response.

## 6.2.7 Microbial Testing

### 6.2.7.1 TVC

Same methodology as outlined in section 5.2.7.1.

### 6.2.8 TVB-N

Same methodology as outlined in section 5.2.8

## 6.3 Results and Discussion

### 6.3.1 Mechanical Transformation of the PTFE Gas Permeable Membrane Using Stretching Operations

The SEM images show the structure of the PTFE porous membrane produced by the stretching operation. The original membrane comprises of a uniform lattice structure with well-defined pores, Figure 6-3 & Figure 6-5. It would appear from Figure 6-4 that the stretching operation produced larger pores in the lattice structure but increasing the magnification, Figure 6-6, exposes an important feature of the stretched membrane. The stretching operation appears to have formed a convoluted mesh consisting of tiny fibrils.

### 6.3.2 Sensor Response to Water Vapour

Two sensors of *Type 1, 2 and 3* were subjected to extreme conditions by placing them directly into the steam produced from boiling distilled water while continuously monitoring the sensor colour with the Colourmeter. The results from this experiment are graphically displayed in Figure 6-2. Sensor *Type 1* with 1 layer of gas permeable membrane reached 90% saturation within 2.5 minutes. The experiment was terminated before the sensors *Type 2 and 3* reached saturation as prolonged exposure to steam may have permanently damaged the Handheld Colourmeter. It is evident from Figure 6-2 that the *Type 2* sensors with 1 stretched layer together with 1 layer of PTFE gas permeable membrane in its original form was most effective in reducing the amount of water vapours reaching the sensor membrane. This approach may not be the ultimate solution for protecting the sensor surface from water vapours but the results indicate that the situation can be improved and with further research into this area the sensor technology will eventually be incorporated into packaging that must undergo pasteurisation techniques that involve maintaining the product at high temperatures and pressures for extended periods of time without affecting the physical and chemical characteristics of the sensor.

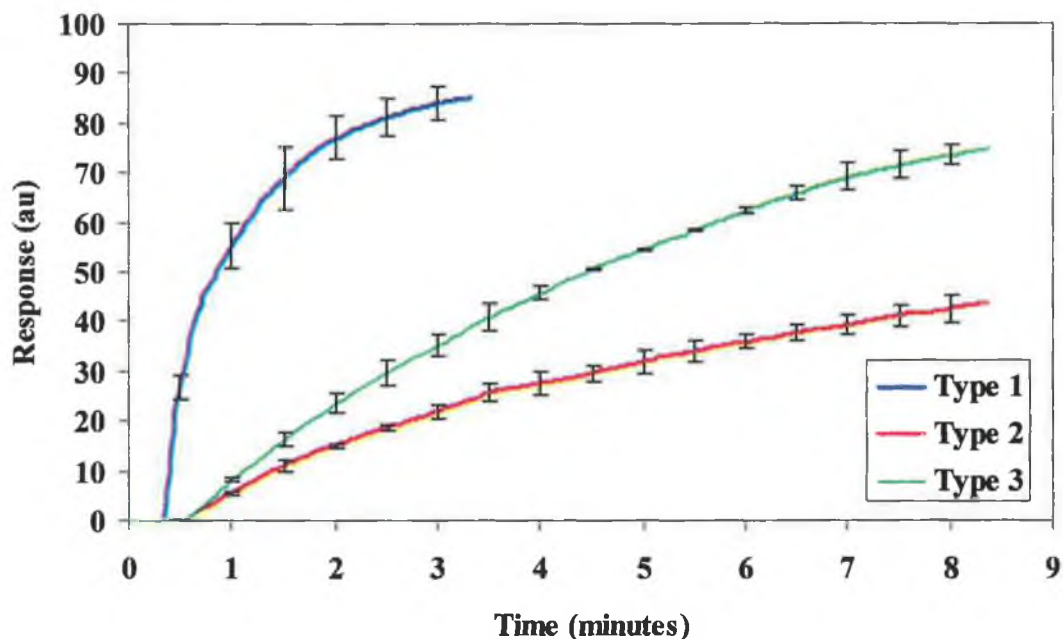
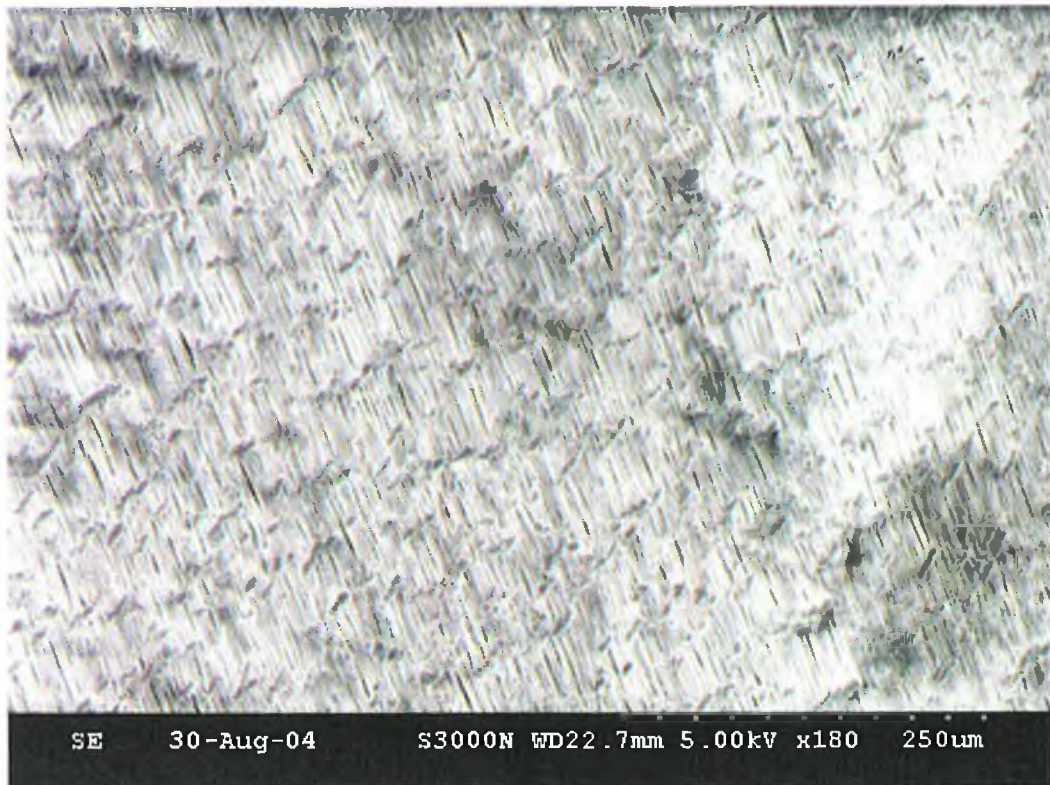
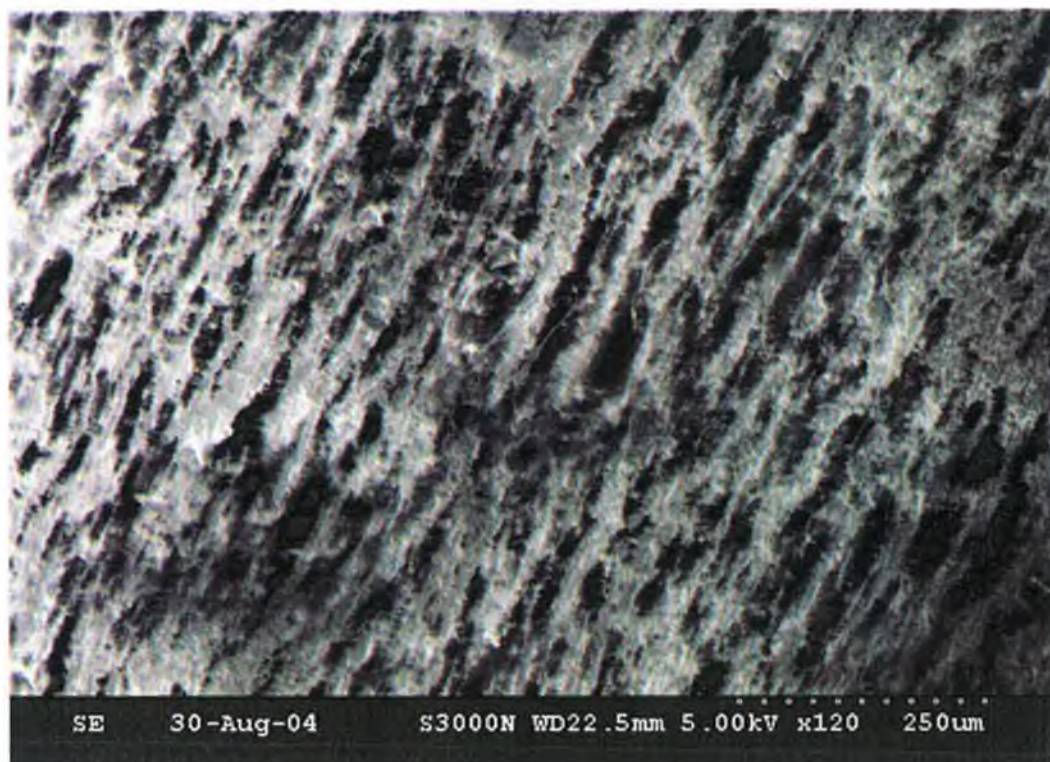


Figure 6-2 Sensor Type 1, 2 & 3 response to water vapour





**Figure 6-3 PTFE membrane (Magnification  $\times 180$ ) in its original form**



**Figure 6-4 Stretched PTFE membrane (Magnification  $\times 120$ )**



Figure 6-5 PTFE membrane in its original form (Magnification  $\times 900$ )

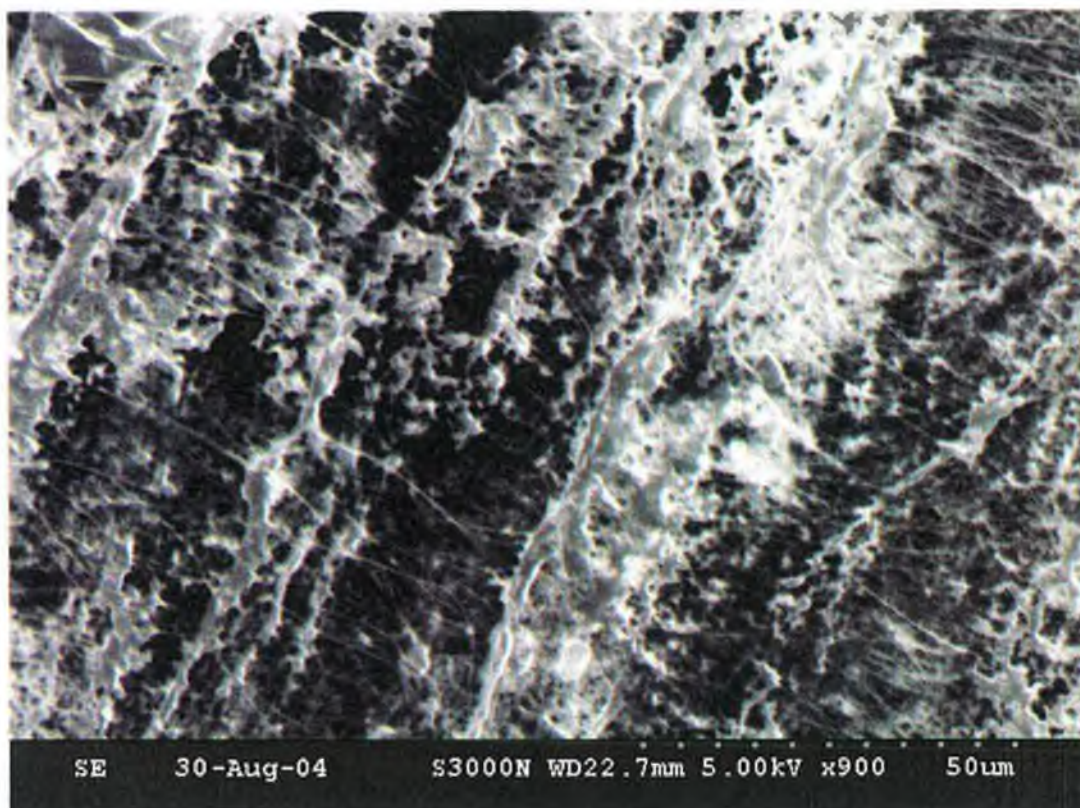


Figure 6-6 Stretched PTFE membrane (Magnification  $\times 900$ )

### 6.3.3 Sensor Response to Microbial Spoilage of Cooked Whelk

There were 4 bromocresol green *Type 2* sensors in total on each of the 6 trays of whelk. 3 trays were stored at room temperature ( $25.9^{\circ}\text{C} \pm 1.0$ ) and 3 trays were stored in the fridge ( $6.9^{\circ}\text{C} \pm 1.1$ ) for the entire duration of the experiment. 12 sensors in total were used to detect the spoilage volatiles released over time for both sampling conditions. The average sensor response ( $n=12$ ) to spoilage volatiles at both temperatures is shown in Figure 6-8 and Figure 6-9 – see also Appendix 5-4 and Appendix 5-8. A best-fit model using the Solver function in Microsoft Excel was fitted to the average sensor response at the 2 sampling temperatures.

The TVB-N and TVC results obtained for the cooked whelk samples stored at room temperature and in the fridge are displayed in Figure 6-10 and Figure 6-11 - see also Appendix 5-9 and Appendix 5-10. Each TVC result is an average of 2 counts from the same sample whereas each TVB-N value was obtained from a single analysis at each time point. Statistically the TVC results in this trial are more reliable due to the very low standard deviation and % RSD. Under normal practices in Errigal Fish, TVB-N analyses are carried out on 6 samples simultaneously i.e.  $6 \times 10\text{g}$  samples. This would definitely improve the correlation. In some cases, a 10g sample could be taken from 1 individual whelk, which is not representative of the entire batch. The procedure for determining TVCs is statistically more favourable because a larger sample is taken from a larger number of whelks i.e. 25g in total is necessary for each analysis.

Log TVC values versus time for the samples stored at room temperature and in the fridge are displayed in Figure 6-10. From guidelines set by Errigal Fish, Total Viable Counts  $< 100,000$  CFU/g are acceptable for unpasteurised cooked whelk. TVCs above 100,000 CFU/g are deemed unacceptable or unfit for human consumption. From the graph,  $S_{RT (TVC)}$  and  $S_F (TVC)$  denote the approximate times at which the TVCs reach 100,000 CFU/g for the room temperature and fridge samples, i.e.  $\sim 9$  hours and  $\sim 29$  hours, respectively.

The TVB-N content for samples stored under both conditions is presented in Figure 6-11. The guidelines followed by Errigal Fish regarding TVB-N levels are summarised in Table 5-1. Cooked whelk products containing  $< 15\text{mg}$  nitrogen/100g are 'OK' to consume, samples containing 15-20mg nitrogen/100g indicate that the samples are 'going off' but are still safe to consume and samples containing  $> 20\text{mg}$  nitrogen/100g are considered 'gone off' or unfit for human consumption. From the graph,  $S_{RT (TVB-N)}$  and  $S_F (TVB-N)$  denote the times at which the TVB-N levels for the room temperature and

fridge samples reach the 'gone off' threshold, i.e. ~11 hours and ~25 hours, respectively.

By integrating both sets of results, i.e. the TVB-N and TVC data, approximate spoilage thresholds were deduced. According to the TVC results the time taken for the room temperature samples to spoil is ~ 9 hours while according to the TVB-N data the samples spoiled after ~11 hours. An average of both gives an approximate spoilage time frame of 10 hours  $\pm$  1 hour. For the purposes of this experiment, the lower limit i.e. 9 hours, was selected as the spoilage threshold,  $S_{RT}$ , for the room temperature samples. The same applies to the fridge samples where a spoilage time frame of 27 hours  $\pm$  3 hours was obtained. Once again the lower limit i.e. 24 hours was selected as the spoilage threshold,  $S_F$ , for the fridge samples. Therefore,  $S_F$  and  $S_{RT}$  denote the estimated times at which the fridge and room temperature samples spoil, respectively, Figure 6-12.  $R_S$  is the sensor response at  $S_F$  and  $S_{RT}$  measured by the Colourmeter.  $R_S$  is equivalent at the critical spoilage threshold for the samples stored under different conditions.

Storing the cooked whelk in the fridge clearly slows down microbial growth as expected. According to the TVC results, the microbial growth for the fridge samples was always slower than that of the samples stored at room temperature and never reached the same levels of microbial growth for the duration of the trial, which is reflected in the sensor response.



**Figure 6-7 Digital images of sensors representing cooked whelk samples stored at room temperature (bottom) and in the fridge (top) taken at 14 hours. The sensors representing the room temperature samples are green (bottom) whereas the sensors representing the fridge samples are greenish-yellow (top). According to the microbial data and TVB-N values, at 14 hours the room temperature samples are ‘gone off’ while the fridge samples are ‘going off’. The colour of the sensors can be used as a crude indication of the on-set of spoilage.**

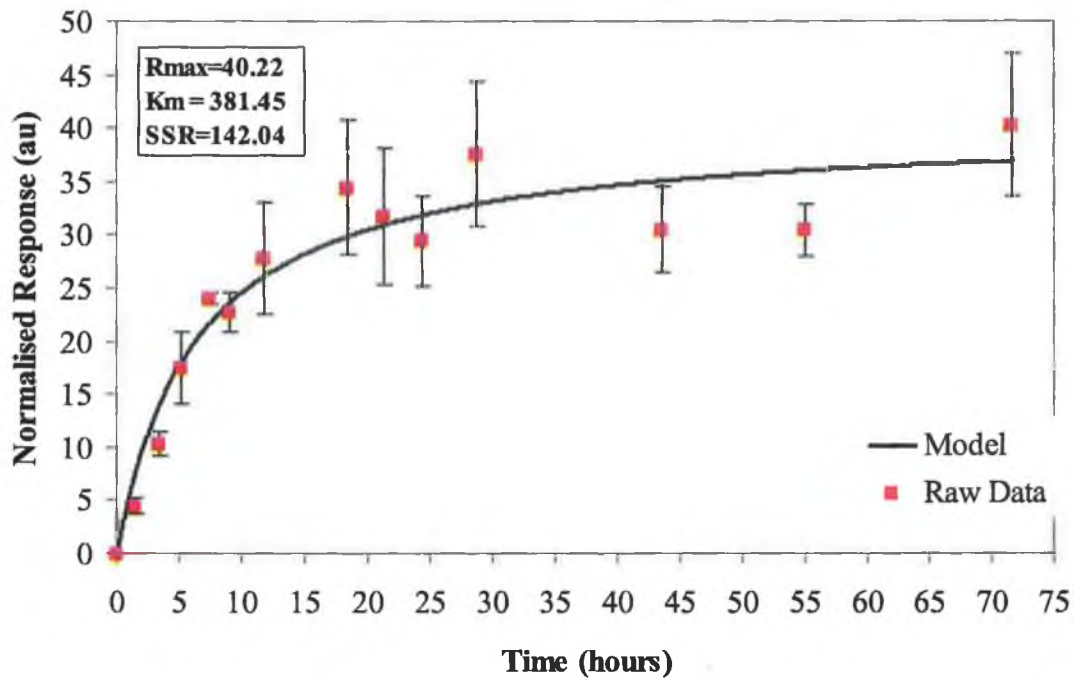


Figure 6-8 Average response of all sensors on all 3 trays stored at room temperature (n=12) – See Appendix 5-4 for experimental data.

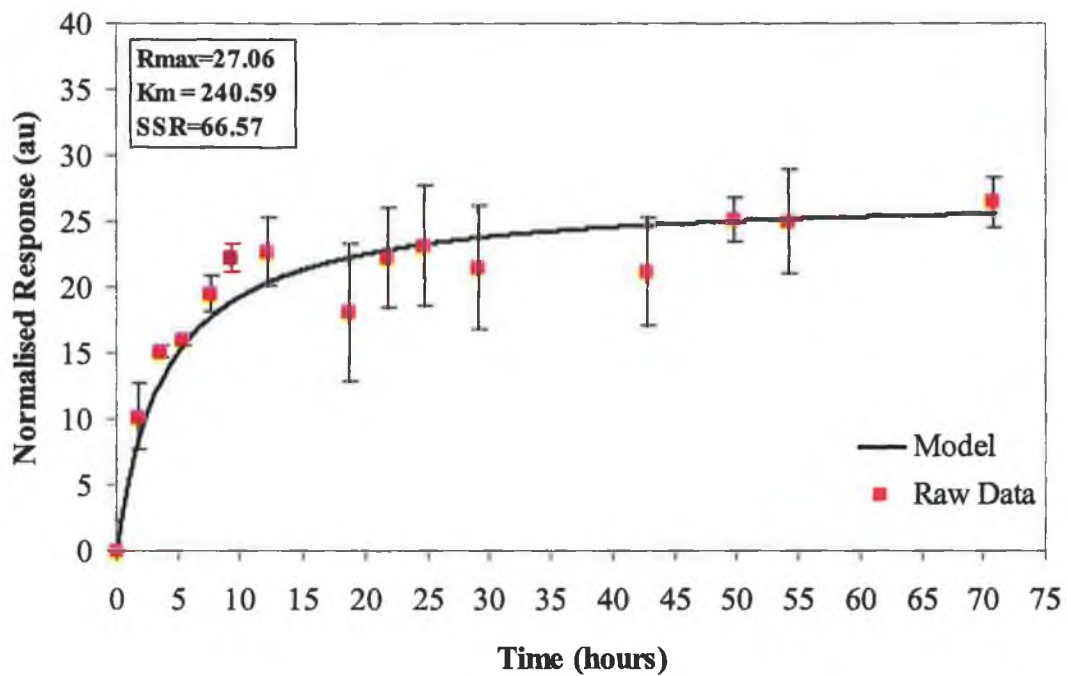


Figure 6-9 Average response of all sensors on all trays stored in the fridge (n=12) – See Appendix 5-8 for experimental data.

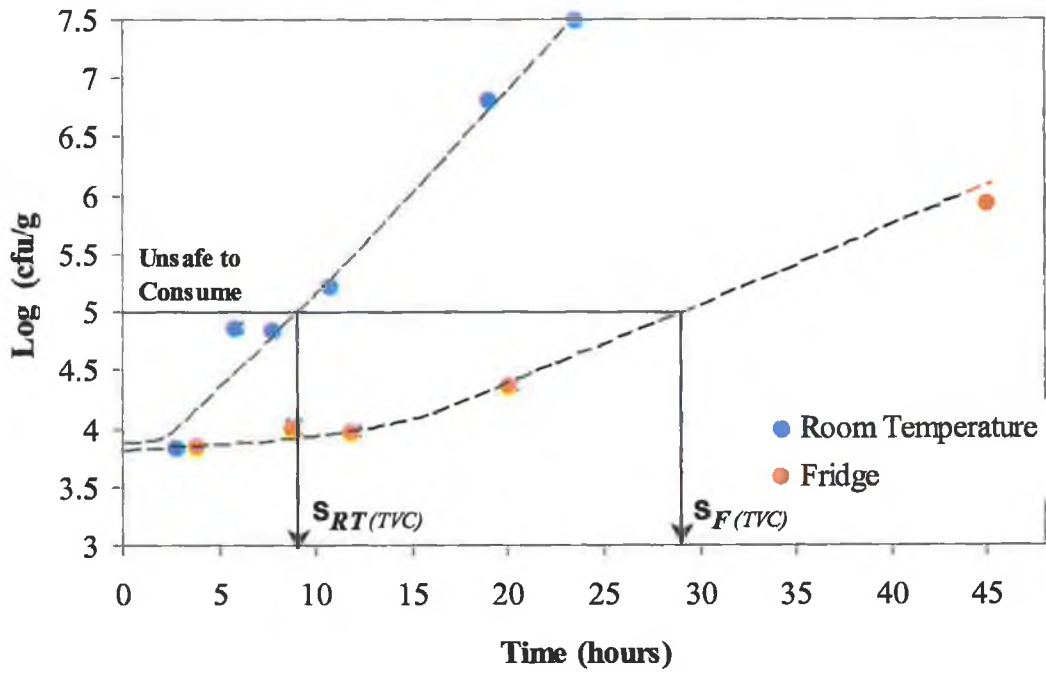


Figure 6-10 Comparison of Total Viable Counts for the cooked whelk meat samples stored at room temperature and in the fridge

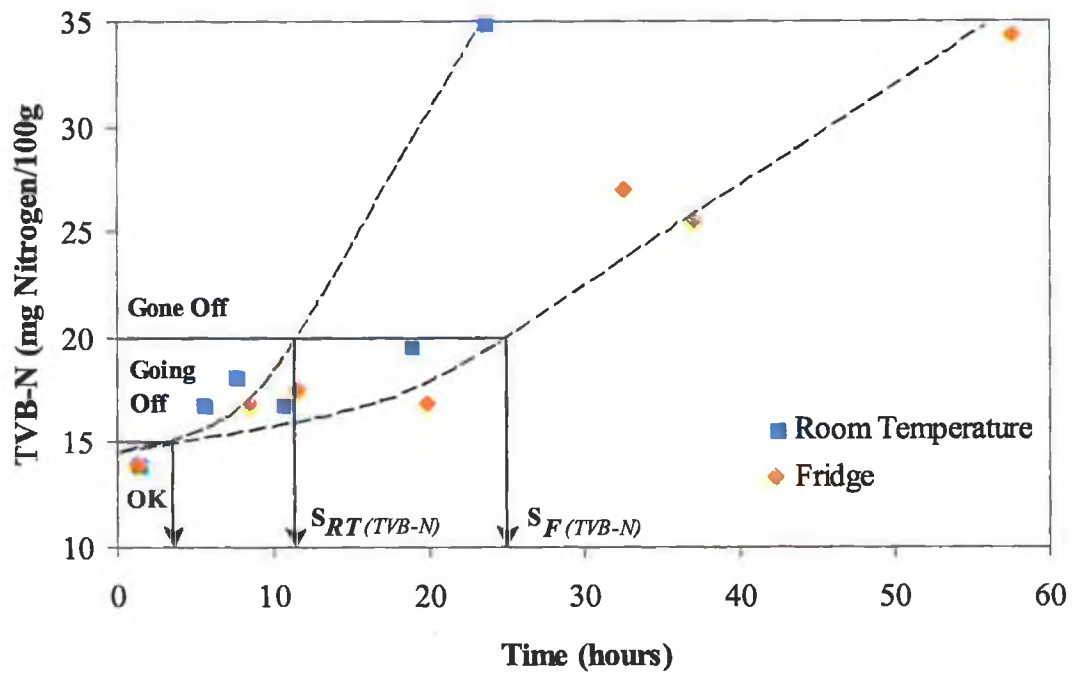


Figure 6-11 Comparison of Total Volatile Basic Nitrogen for the cooked whelk meat samples stored at room temperature and in the fridge

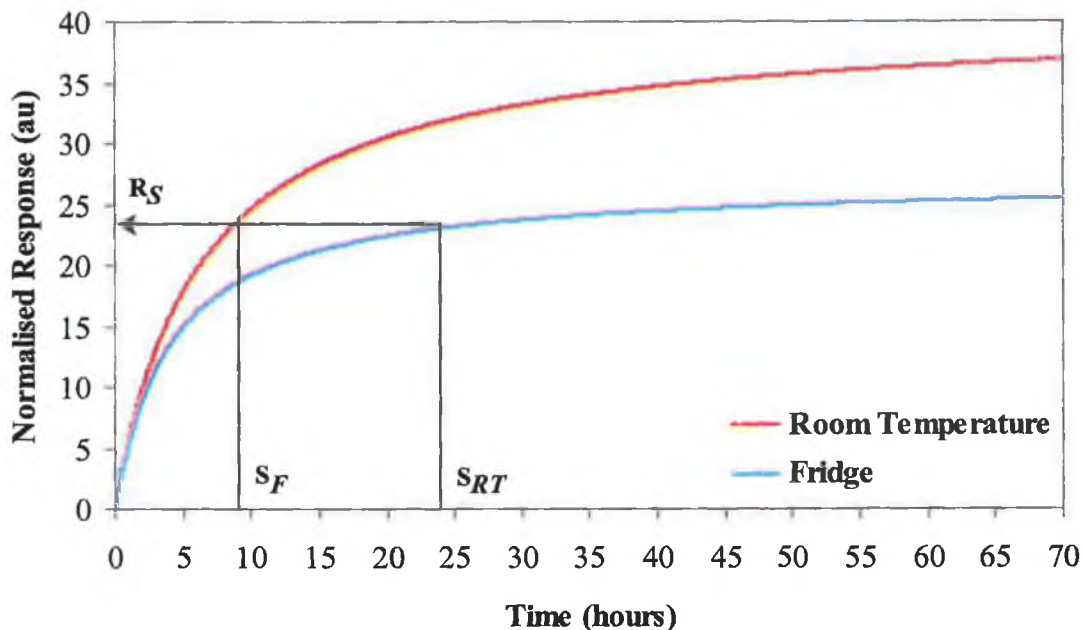


Figure 6-12 Comparison of the models for the average sensor response to the spoilage volatiles released by cooked whelk stored in the fridge and at room temperature.

Figure 6-13 and Figure 6-14 combine the TVB-N, TVC and sensor response data for the cooked whelk samples stored under different conditions, at room temperature and refrigerated temperature, respectively. The graphs illustrate the effect of temperature on microbial growth and TVB-N production. This effect is also reflected in the sensor response, which is evidently faster for those samples stored at room temperature than those stored in the fridge. The TVB-N and TVC tests for the room temperature samples were ceased after 24 hours as at this stage the samples were clearly spoiled and the sensor response had almost reached a plateau. Focusing on the sensor response to whelk spoilage at each storage condition it is quite clear that the sensors begin to change as soon as they are placed inside the containers. Molluscan shellfish naturally contain high levels of nitrogenous bases and the initial sensor response may be due to the residual amines present following the cooking process. The sensor response continues to change overtime and the relationship between the TVB-N, TVC and sensor response data displayed in Figure 6-13 and Figure 6-14 indicates that this change is due to microbial spoilage. This high degree of correlation between the microbial spoilage and the sensor response demonstrates that these pH sensitive polymer membranes can potentially be used as spoilage indicators for cooked whelk meat products stored in sealed containers.



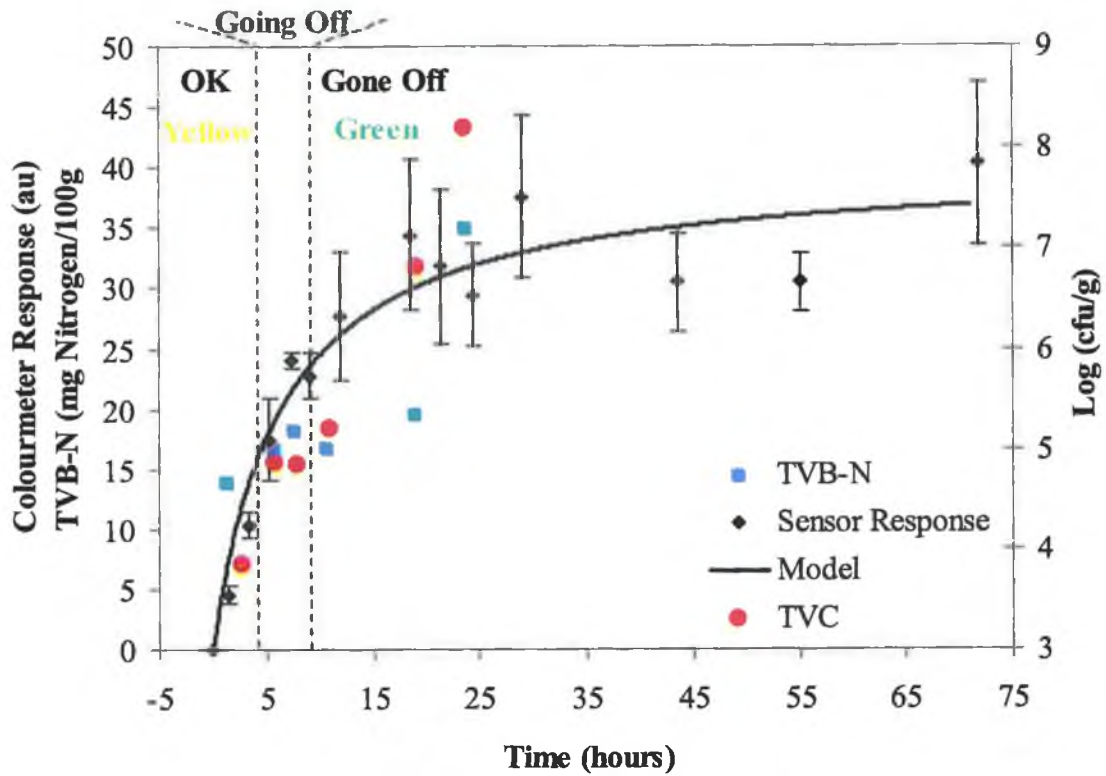


Figure 6-13 Correlation of the sensor response with the TVB-N and TVC values obtained for the cooked whelk samples stored at room temperature.

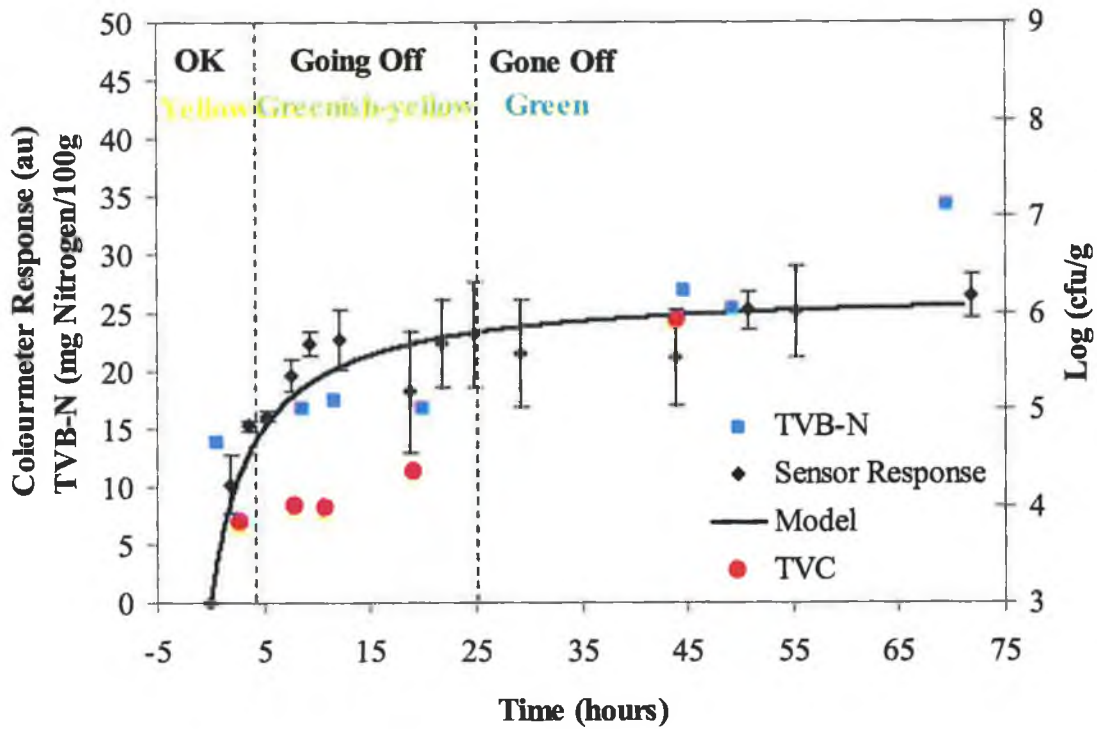


Figure 6-14 Correlation of the sensor response with the TVB-N and TVC values obtained for the cooked whelk samples stored in the fridge.

The colour of the sensors can be used as a crude indication of the on-set of spoilage. The sensors are yellow when they are first placed inside the containers and remain this colour for a period of time indicating that the samples are 'OK' to consume. As the microbial populations and TVB-N levels increase over time the sensors change to a greenish-yellow colour warning the user that the samples are 'going off' but are still safe to consume. Once the samples are 'gone off', i.e. ~9 hours for samples stored at room temperature or ~25 hours for samples stored in the fridge, the sensors turn green and this colour intensifies to the point of saturation as the sample continues to deteriorate.

## **6.4 Conclusion**

Sensors prepared from the pH indicator dye, bromocresol green, entrapped in a polymer matrix were placed inside a sealed container of cooked whelk. The volatile amines released during spoilage permeated through the PTFE gas permeable membrane and deprotonated the dye to produce a visible colour change that was successfully measured via a specially designed handheld Colourmeter. A high degree of correlation between the sensor response and the TVC and TVB-N data for samples held at different storage conditions indicates how the pH sensitive sensors can be used as spoilage indicators for packaged whelk meat products. These studies also indicate that the Colourmeter can be used to generate a 'value' that can be stored like a bar-code value for future objective analysis of the sensor spots.

## **7 Overview, Ongoing Activities and Future Work**

Projects 1 and 2 give a detailed account of the development of wireless sensor technology designed for two specific food quality applications. The first application, Project 1 (Chapters 2), describes an autonomous pH and temperature sensing system for monitoring pig meat quality. A comprehensive review of the project background is provided in Chapter 1 - Section 1.1 where the importance of monitoring intramuscular pH and temperature as the carcass cools following slaughter is emphasised. Chapter 2 describes a wireless temperature sensing system that was used initially to monitor the temperature of cooling carcasses but this particular system had a number of drawbacks that were soon identified during field trials carried out at Galtee Meats, Mitchelstown, Co. Cork. Consequently, a unique Wireless pH/Temperature Sensing System was designed to monitor post-slaughter pH and temperature. Field trials were performed to demonstrate the effectiveness of the system in distinguishing between different classes of pig meat quality i.e. DFD, RFN and PSE carcasses. The results from this project were published in the international journal Meat Science (1).

A number of issues arose during the trials that need to be addressed for future development of the Wireless pH/Temperature Sensing System. Firstly, the pH and temperature data is transmitted in real-time from the loggers (attached to the carcasses) via RF communications to the base station (attached to the chill room wall). On one occasion the RF link between the loggers and the base station was interrupted as the carcasses were accidentally moved out of the RF operating range to another location in the chill room. Fortunately, the carcasses were repositioned and the trial resumed. Secondly, an RS232 cable (~1m) which connects the base station to a PC allows the user view the information in real-time but for obvious reasons the PC was not set up in the chill room. The safest location was too far away (~50m) so the RS232 cable could not be used. For this reason the base station, holding all the pH and temperature data, was retrieved once the trial was complete and the data was then downloaded onto the PC. For the purpose of these field trials this approach was perfectly acceptable but for future large-scale deployment of these sensors a more user-friendly approach is needed. Finally, initial studies show measurements from 45 minutes post-mortem as processing conditions limit at what point measurements are made and the technologies that can be used. The logger needs to be attached immediately following slaughter to realise the benefits of a real-time pH and temperature monitoring system.

In response to the above issues a number of recommendations are highlighted below to improve the existing Wireless pH/Temperature Sensing System:

- Incorporating GSM communications into the base station design would eliminate the need for an RS232 cable connection. This approach has already proved effective in the real-time temperature monitoring of fish catches on-board fishing trawlers at sea as demonstrated in Chapter 3.
- GSM enabled systems would also allow warning messages to be displayed on a PC or sent to a mobile phone as a text message indicating if a logger is out of the RF operating range. This would allow the operator to reposition the carcass.
- Miniaturisation of the pH and temperature logger would allow the sensor to be embedded into the carcass immediately following slaughter but most importantly small low-power, low-cost sensors are necessary for large-scale deployment to be economically effective.

The second food quality application, Project 2 (Chapter 3), involves the development of temperature logging technology for the fishing industry. Chapter 1 – Section 1.2 emphasises the need for real-time temperature monitoring of fish catches stored on-board fishing vessels at sea and provides an overview of the temperature monitoring systems commercially available on the market today. Chapter 3 demonstrates the use of the autonomous sensing system described in Chapter 2 for monitoring the temperature of fish catches at sea. Once again, the limitations of the system were identified as the user could only access the temperature profiles once the fishing vessel returned to the shore. Consequently, a new RF-GSM Temperature Monitoring System was specifically designed to allow temperature profiles of fish catches to be conveniently accessed via the Internet while the fishing vessel was still at sea. Chapter 3 gives a detailed description of the new system and highlights the benefits of using such a system over existing temperature monitoring systems.

A number of software issues were highlighted in Chapter 3 and as a result of the extensive field-testing and ongoing research activities in this area researchers from the Adaptive Sensors Group and the Interoperable Systems Groups based at DCU have made excellent progress in improving the RF-GSM Temperature Monitoring System. Consequently, a web-based prototype with an XML database is now fully operational (2). The controlling software and database are completely web-based and can be

accessed using a web browser on any Internet capable device (e.g. PC, laptop or PDA) through a password-protected connection. Field trials on-board larger inshore fishing trawlers have since been executed where the RF-GSM Temperature Monitoring System is controlled and monitored using a GPRS enabled XDA II Pocket PC. Through the web interface, the software allows the following procedures to be performed:

- Initiation/cessation of a trial
- In-trial verification of data acquisition and querying of previously recorded data
- Access to a user-defined rule mechanism that allows triggers for particular events to be set, e.g. reporting problems such as temperatures outside of upper/lower control levels, loss of communication etc.
- Data storage in a database with tabular or graphic output and query functionality

The field-testing has been extended to include temperature monitoring from the fishing port to the processing plant i.e. transportation of whelk catches from Howth Harbour, Dublin to Errigal Fish, Carrick, Co. Donegal.

Tremendous progress has been made in this project, which describes the development of a temperature monitoring system that first existed as an autonomous temperature-measuring device with limited capabilities to a fully operational web-based system remotely controlled through the Internet allowing the temperature of fish catches to be monitored in real time from the moment of catch to the shore and finally to the processing plant. This real time temperature monitoring system provides excellent traceability with added value as all the details of the catch are entered into a web based password-protected database to accompany the temperature data. The rapid technological and wireless communication developments in this project alone highlight the speed at which the communications and IT industry are growing. The demand for traceable systems and temperature control within the fishing industry is driven by both the consumer and the regulatory bodies and with the cost and size of electronic components continuously decreasing and data transfer becoming more and more feasible large-scale deployment of such Internet-based temperature sensing systems on-board fishing trawlers will be possible in the near future.

Chapters 4-6 of the thesis focus on the development of on-package colorimetric pH sensors to detect shellfish spoilage (Project 3). The theory and background behind this

project is provided in Chapter 1 – Section 1.3, which includes a comprehensive review of the current methods to evaluate the freshness and quality of fish as well as the fundamentals of UV-Vis spectroscopy and pH indicator chemistry.

Chapter 4 describes the fabrication and characterisation of pH sensitive polymer membranes. A number of different formulations were tested which involved varying the ratio of binder to plasticiser, the type of lipophilic salt used and the concentration of the lipophilic salt. An optimised formulation was developed that contained 5mg BCG, 350mg PVC, 350mg DBS, 10mg TOABr and 8mls of cyclohexanone. UV-Vis spectroscopic techniques indicated that the  $\lambda_{\text{max}}$  of the dye shifted slightly from 620nm in free solution to 630nm in the polymer membrane. Studies also confirmed that temperature had minimal effect on the  $\text{pK}_a$  of the dye in the polymer membrane. The sensors were calibrated in  $\text{NH}_3$  and the limit of detection was calculated to be  $0.23 \pm 0.07\text{ppm}$ . The sensors showed excellent reproducibility with an overall  $\%CV < 12\%$  ( $n=3$ ). An account of the preliminary trials conducted to aid the optimisation of a pH sensitive sensor suitable for detecting whelk spoilage is also given in Chapter 4. The trials demonstrated that sensors representing cooked whelk samples stored at room temperature responded a lot faster than sensors representing samples that were chilled for a period of time. The sensor response was measured via the handheld Colourmeter and digital images of the sensors captured at selected time intervals provided a useful visual aid. An important issue arose during the preliminary trials regarding the sensors response to water vapours and nitrogenous compounds, released as a result of the cooking process, which caused the sensors to change colour prematurely. Chapters 5 & 6 discuss how the sensor technology can be optimised to overcome this obstacle to produce a robust sensor that operates reliably in real industrial applications.

Chapter 5 discusses an approach whereby the dye is replaced with a similar dye with a higher  $\text{pK}_a$  that is not readily deprotonated by water vapours or the nitrogenous compounds released during the cooking process. Two dyes were investigated, bromothymol blue ( $\text{pK}_a$  7.0) and m-cresol purple ( $\text{pK}_a$  8.3). Unfortunately, sensors prepared from the bromothymol blue and m-cresol purple dyes did not respond to the spoiled whelk meat samples.

Chapter 6 describes a method of optimising the bromocresol green sensors by mechanically modifying the physical morphology of the gas permeable membrane

through a number of strategic stretching operations. The sensors were used to monitor the spoilage rates of cooked whelk meat samples at two different conditions i.e. at room temperature and at refrigerated temperatures. Excellent correlation was obtained between the sensor response and whelk meat spoilage determined by TVC's and TVB-N values for the samples stored at the two different conditions. Overall, the sensors performed remarkably well considering the complexity of the application and the harsh environments to which the sensors were exposed.

A number of areas that need to be targeted for the future development of pH sensitive membranes that detect fish and shellfish spoilage are listed below:

- The pH sensitive membranes described in this project were all prepared manually. An automated fabrication process would certainly improve the reproducibility of the sensor response as well as the correlation between the response and microbial spoilage.
- Some fish and shellfish products undergo a pasteurisation process once they have been packed inside sealed containers. Presently, the sensors are not robust enough to withstand the harsh conditions posed by the pasteurisation process so it is important to decide at what stage during the process the sensors can be incorporated into the packaging.
- The working range of the sensor needs to be extended to allow the onset of spoilage to be accurately detected. Molluscan shellfish naturally contain high levels of nitrogenous compounds that are released into the atmosphere during the cooking process. These residual amines deprotonate the sensor causing a premature colour change before spoilage begins. By adding a compound that neutralises the residual amines present initially (i.e. a weak acid), the sensors will only respond to the volatiles amines released as a result of spoilage.

Researchers at Dublin City University have since made excellent progress in developing the pH sensors and a number of key issues have been addressed as follows

- The sensor matrix now comprises FDA approved binders i.e. ethyl cellulose.
- The 'brightness' of the sensors has been dramatically improved by the addition of titanium dioxide, which is used in paint technology.
- The sensors are now fabricated using a simple screen-printing technique.



- Discussions with packaging companies regarding the integration of the sensors into food packaging in the form of 'chemical barcodes' are underway.
- Finally, a new improved Colourmeter prototype is currently being used to measure the sensor response.

The 3 projects described in this thesis focus on the different sensing techniques developed for monitoring food quality and freshness. As seen from the research performed, monitoring the intramuscular pH of a pig carcass and monitoring the headspace pH of a sealed container of fish are two separate applications and require different sensing techniques. The Wireless pH/Temperature Monitoring System for detecting pig meat quality delivers data in real-time to a local PC allowing the user easy access to the information. The optical pH sensitive sensor for detecting fish spoilage provides a visual response in real-time at a glance. Integrating sensor technology with information technology and mobile communications paves the way for Internet scale sensing where the development of a Wireless RF-GSM Temperature Monitoring system allows temperature data of fish catches to be conveniently accessed via the Internet in real-time facilitating traceability and electronic auctions. Ongoing research activities at DCU have provided traceable temperature profiles of whelk caught in Dublin Bay all the way to the processing plant. Section B of the thesis has demonstrated how pH sensitive membranes incorporated into sealed containers of cooked whelk at the processing plant respond to whelk meat spoilage to give a visual colour change which can be easily detected by the customer. Combining the above sensing techniques, Internet enabled sensor technology for on-line traceable temperature monitoring and optical sensor technology for on-line detection of fish spoilage, and applying such techniques to different fish and shellfish species will facilitate future monitoring of the quality and freshness of fish products during every stage from "*harvest-to-home*".

## References

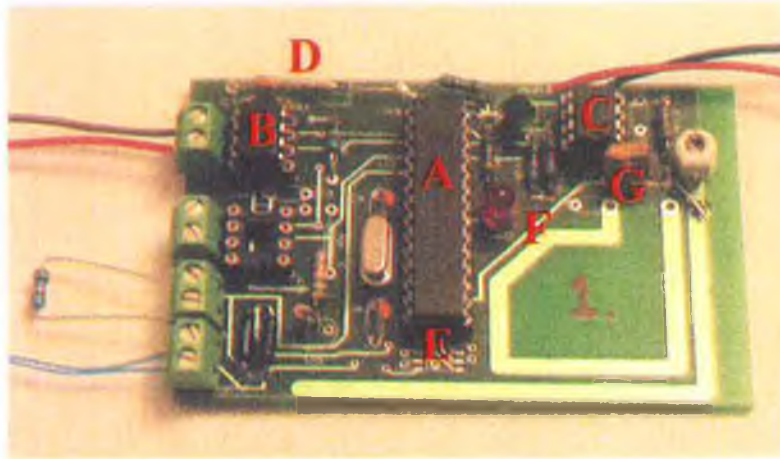
1. Frisby, J., Raftery, D., Kerry, J. P., and Diamond, D., Development of an autonomous, wireless pH and temperature sensing system for monitoring pig meat quality, *Meat Science*, 70, 329 (2005).
2. Crowley, K., Frisby, J., Murphy, S., Roantree, M., and Diamond, D., Web-based real-time temperature monitoring of shellfish catches using a wireless sensor network, *Sensors and Actuators* (In press).

## **Appendix**

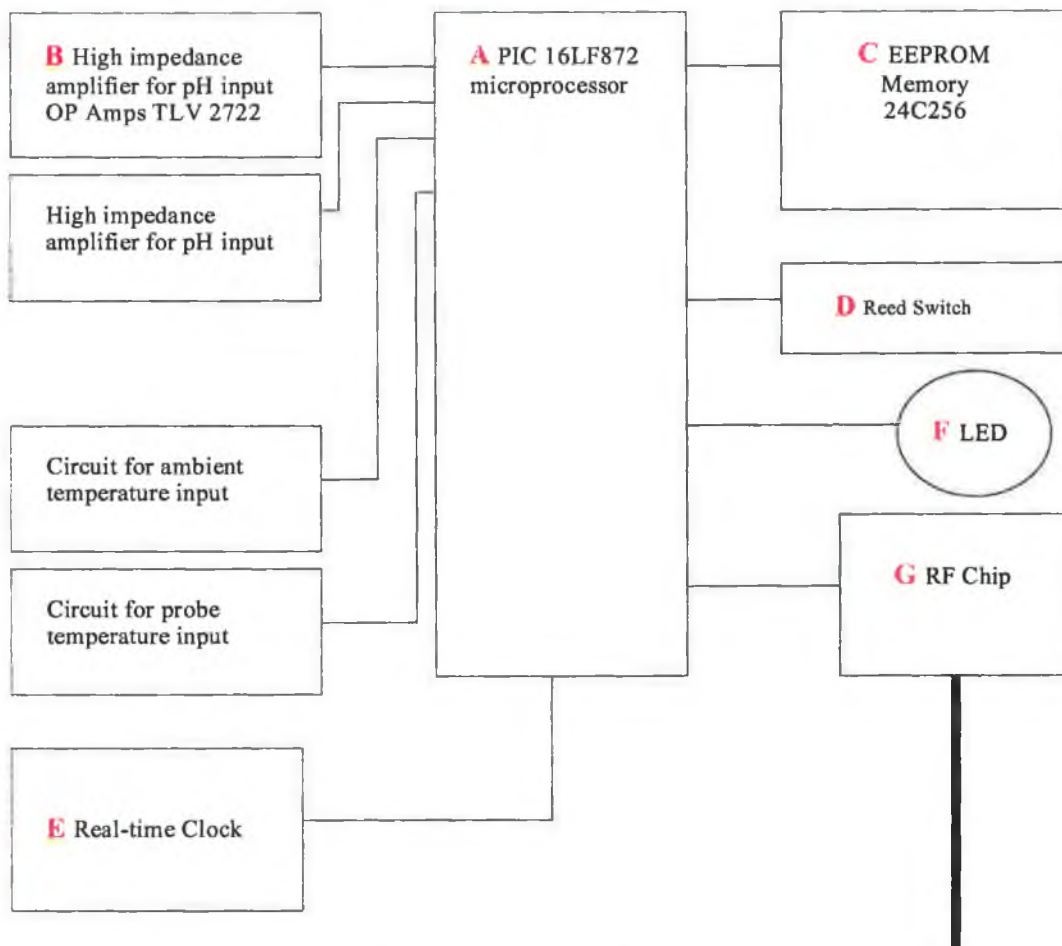
## Appendix 1

### 1.1 Wireless pH/Temperature Monitoring System Specification

#### 1.1.1 Logger Unit

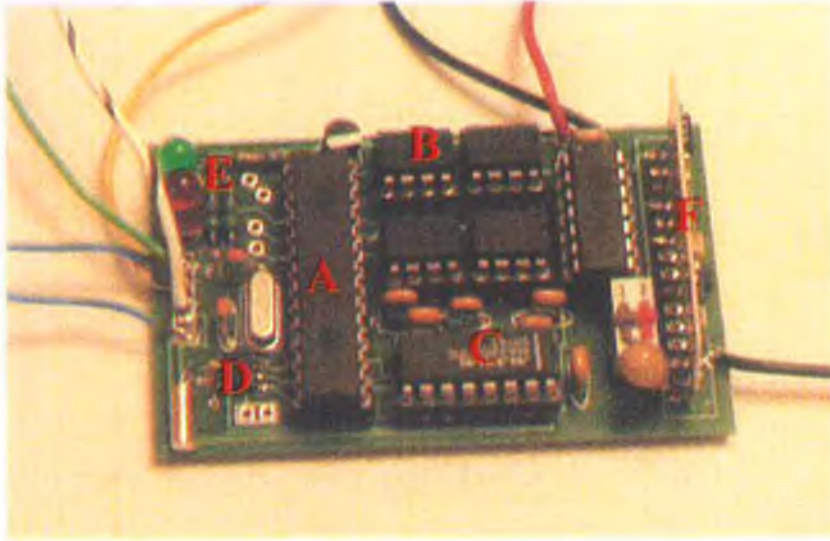


Appendix 1-1 Photograph of Logger circuit board

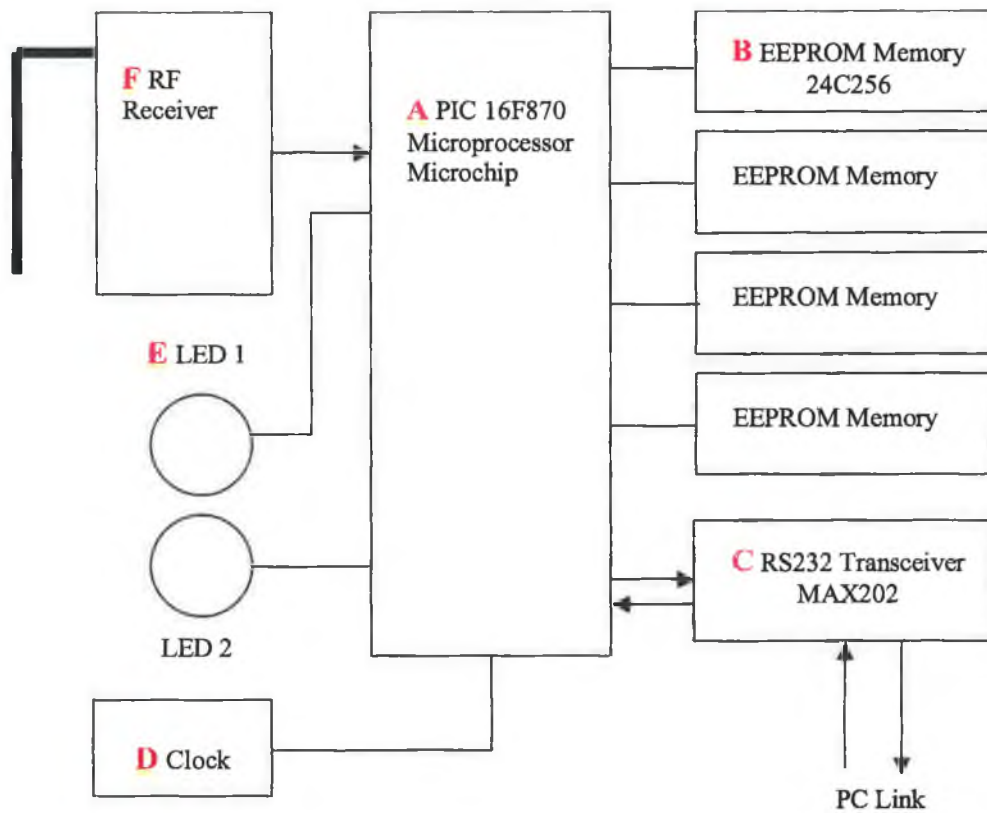


Appendix 1-2 Block diagram of temperature logger circuitry

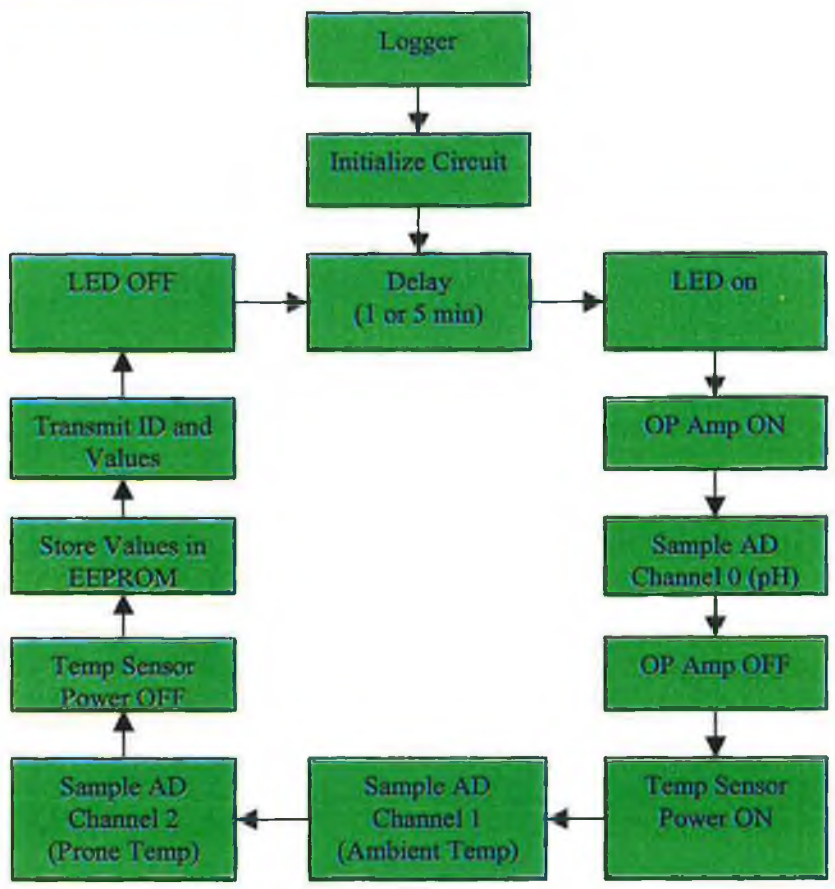
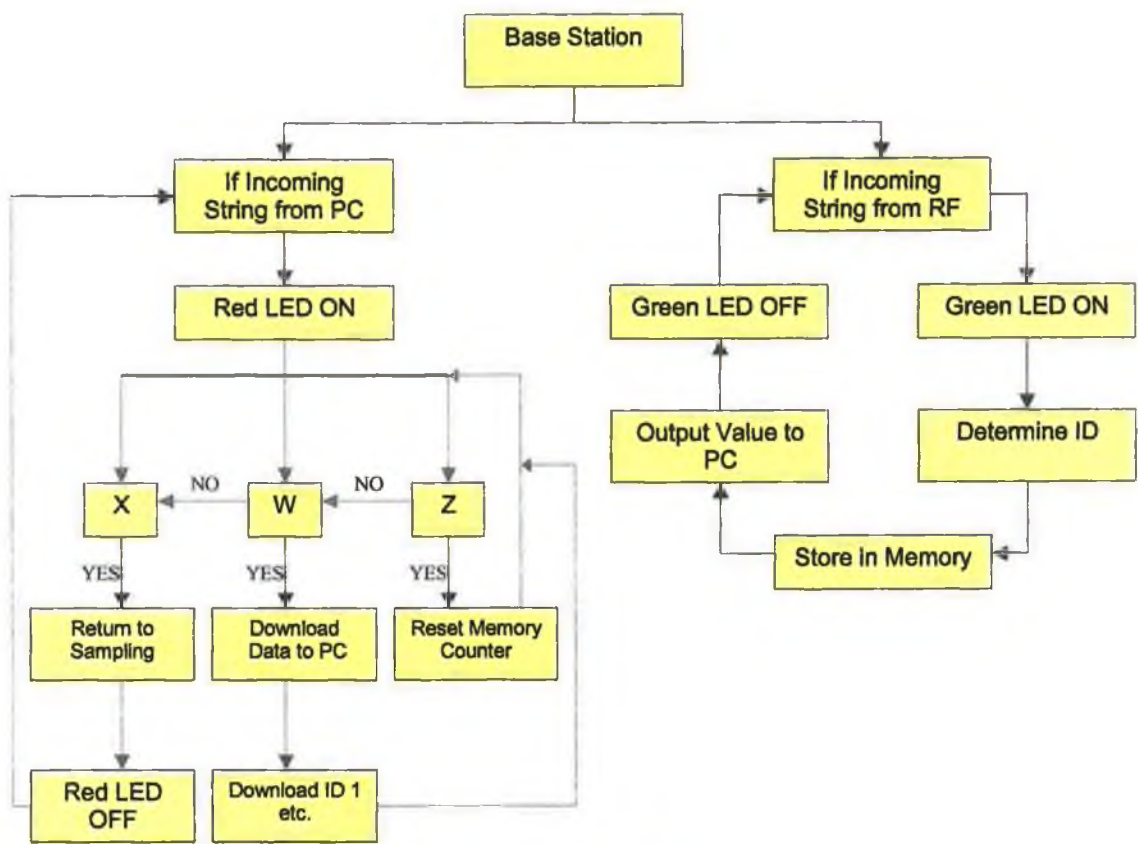
### 1.1.2 Base Station



Appendix 1-3 Photograph of base Station circuit board design



Appendix 1-4 Block diagram of base station circuitry



Appendix 1-5 Software flow diagrams for the base station (top) and the logger unit (bottom)

**Temp °C IUPAC Logger 1 Difference**

0	7.1167	7.1592	-0.0425
1	7.11047	7.15175	-0.04128
2	7.10438	7.1444	-0.04002
3	7.09843	7.13715	-0.03872
4	7.09262	7.13	-0.03738
5	7.08695	7.12295	-0.036
6	7.08142	7.116	-0.03458
7	7.07603	7.10915	-0.03312
8	7.07078	7.1024	-0.03162
9	7.06567	7.09575	-0.03008
10	7.0607	7.0892	-0.0285
11	7.05587	7.08275	-0.02688
12	7.05118	7.0764	-0.02522
13	7.04663	7.07015	-0.02352
14	7.04222	7.064	-0.02178
15	7.03795	7.05795	-0.02
16	7.03382	7.052	-0.01818
17	7.02983	7.04615	-0.01632
18	7.02598	7.0404	-0.01442
19	7.02227	7.03475	-0.01248
20	7.0187	7.0292	-0.0105
21	7.01527	7.02375	-0.00848
22	7.01198	7.0184	-0.00642
23	7.00883	7.01315	-0.00432
24	7.00582	7.008	-0.00218
25	7.00295	7.00295	0
26	7.00022	6.998	0.00222
27	6.99763	6.99315	0.00448
28	6.99518	6.9884	0.00678
29	6.99287	6.98375	0.00912
30	6.9907	6.9792	0.0115
31	6.98867	6.97475	0.01392
32	6.98678	6.9704	0.01638
33	6.98503	6.96615	0.01888
34	6.98342	6.962	0.02142
35	6.98195	6.95795	0.024
36	6.98062	6.954	0.02662
37	6.97943	6.95015	0.02928
38	6.97838	6.9464	0.03198
39	6.97747	6.94275	0.03472
40	6.9767	6.9392	0.0375
41	6.97607	6.93575	0.04032
42	6.97558	6.9324	0.04318
43	6.97523	6.92915	0.04608
44	6.97502	6.926	0.04902
45	6.97495	6.92295	0.052
46	6.97502	6.92	0.05502
47	6.97523	6.91715	0.05808
48	6.97558	6.9144	0.06118
49	6.97607	6.91175	0.06432
50	6.9767	6.9092	0.0675

**Logger 1:  $y = 5E-05x^2 - 0.0075x + 7.1592$**

**IUPAC:  $y = 7E - 05x^2 - 0.0063x + 7.1167$**

The above 2 equations were obtained by applying a polynomial curve to the experimental data (Chapter 2, Figure 2-15). By substituting the x-values in the above equations with the temperature values ranging from 0°C to 50°C the results in the following table are obtained.

The pH probe of logger 1 was corrected to the IUPAC values by calculating the difference.

The difference is then expressed by a simple equation:

$$Y = 2E-05x^2 + 0.0012x - 0.0425$$

This equation was then applied to all the pH profiles obtained using logger 1.

Temp °C	IUPAC	Logger 2	Difference
0	7.1168	7.14805	-0.03125
1	7.11057	7.14081	-0.03024
2	7.10448	7.13369	-0.02921
3	7.09853	7.12669	-0.02816
4	7.09272	7.11981	-0.02709
5	7.08705	7.11305	-0.026
6	7.08152	7.10641	-0.02489
7	7.07613	7.09989	-0.02376
8	7.07088	7.09349	-0.02261
9	7.06577	7.08721	-0.02144
10	7.0608	7.08105	-0.02025
11	7.05597	7.07501	-0.01904
12	7.05128	7.06909	-0.01781
13	7.04673	7.06329	-0.01656
14	7.04232	7.05761	-0.01529
15	7.03805	7.05205	-0.014
16	7.03392	7.04661	-0.01269
17	7.02993	7.04129	-0.01136
18	7.02608	7.03609	-0.01001
19	7.02237	7.03101	-0.00864
20	7.0188	7.02605	-0.00725
21	7.01537	7.02121	-0.00584
22	7.01208	7.01649	-0.00441
23	7.00893	7.01189	-0.00296
24	7.00592	7.00741	-0.00149
25	7.00305	7.00305	0
26	7.00032	6.99881	0.00151
27	6.99773	6.99469	0.00304
28	6.99528	6.99069	0.00459
29	6.99297	6.98681	0.00616
30	6.9908	6.98305	0.00775
31	6.98877	6.97941	0.00936
32	6.98688	6.97589	0.01099
33	6.98513	6.97249	0.01264
34	6.98352	6.96921	0.01431
35	6.98205	6.96605	0.016
36	6.98072	6.96301	0.01771
37	6.97953	6.96009	0.01944
38	6.97848	6.95729	0.02119
39	6.97757	6.95461	0.02296
40	6.9768	6.95205	0.02475
41	6.97617	6.94961	0.02656
42	6.97568	6.94729	0.02839
43	6.97533	6.94509	0.03024
44	6.97512	6.94301	0.03211
45	6.97505	6.94105	0.034
46	6.97512	6.93921	0.03591
47	6.97533	6.93749	0.03784
48	6.97568	6.93589	0.03979
49	6.97617	6.93441	0.04176
50	6.9768	6.93305	0.04375

**Logger 2:**  $y = 6E-05x^2 - 0.0073x + 7.1486$

**IUPAC:**  $y = 7E - 05x^2 - 0.0063x + 7.1167$

The above 2 equations were obtained by applying a polynomial curve to the experimental data (Chapter 2, Figure 2-17). By substituting the x-values in the above equations with the temperature values ranging from 0°C to 50°C the results in the following table are obtained.

The pH probe of logger 2 was corrected to the IUPAC values by calculating the difference.

The difference is then expressed by a simple equation:

$$Y = 1E-05x^2 + 0.001x - 0.0312$$

This equation was then applied to all the pH profiles obtained using logger 2.



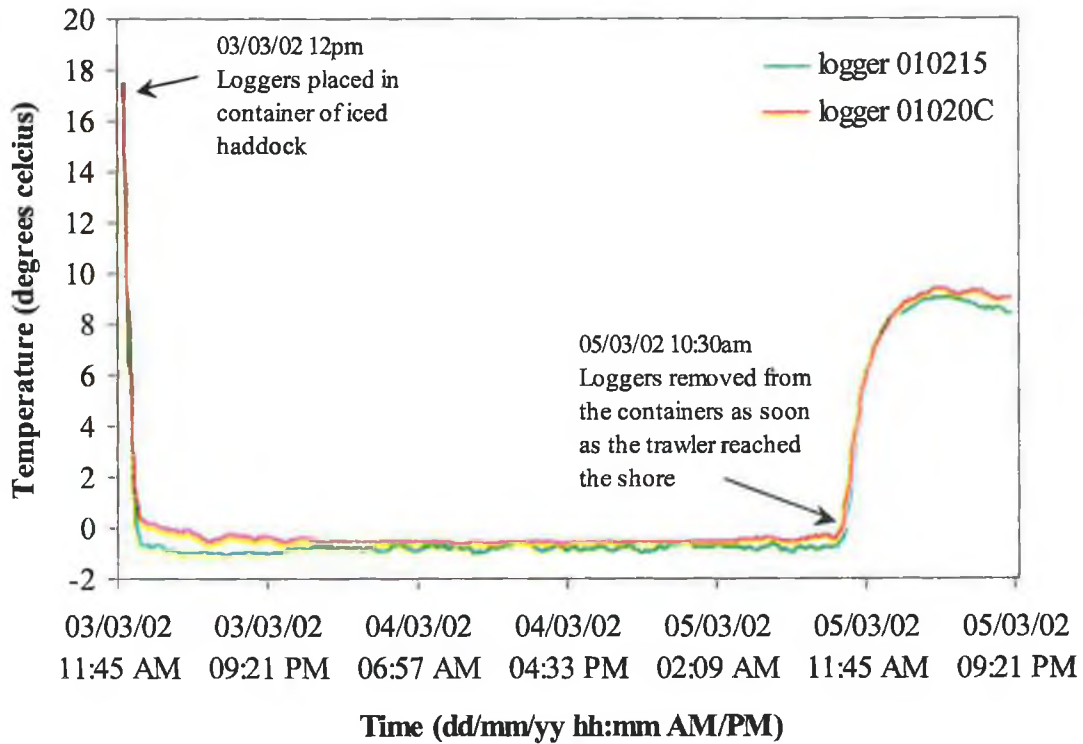
Temp °C	Average	STDEV
0	7.152667	0.006358
1	7.144963	0.006352
2	7.137387	0.006376
3	7.129937	0.006422
4	7.122613	0.006484
5	7.115417	0.006556
6	7.108347	0.006633
7	7.101403	0.00671
8	7.094587	0.006782
9	7.087897	0.006847
10	7.081333	0.006901
11	7.074897	0.006942
12	7.068587	0.006967
13	7.062403	0.006975
14	7.056347	0.006965
15	7.050417	0.006934
16	7.044613	0.006883
17	7.038937	0.006809
18	7.033387	0.006713
19	7.027963	0.006594
20	7.022667	0.006452
21	7.017497	0.006285
22	7.012453	0.006095
23	7.007537	0.005881
24	7.002747	0.005644
25	6.998083	0.005384
26	6.993547	0.005102
27	6.989137	0.0048
28	6.984853	0.004479
29	6.980697	0.004143
30	6.976667	0.003798
31	6.972763	0.00345
32	6.968987	0.003111
33	6.965337	0.0028
34	6.961813	0.002545
35	6.958417	0.002384
36	6.955147	0.002359
37	6.952003	0.002495
38	6.948987	0.002788
39	6.946097	0.003214
40	6.943333	0.003745
41	6.940697	0.004356
42	6.938187	0.005032
43	6.935803	0.005763
44	6.933547	0.006541
45	6.931417	0.007361
46	6.929413	0.008221
47	6.927537	0.009118
48	6.925787	0.01005
49	6.924163	0.011017
50	6.922667	0.012018

**Appendix 1-8 The average and standard deviations for all three calibration studies performed using logger 1. The largest standard deviation occurs at 50°C. The measuring range for this application is between 3°C and 42°C. The largest standard deviation within this range is 0.0069.**

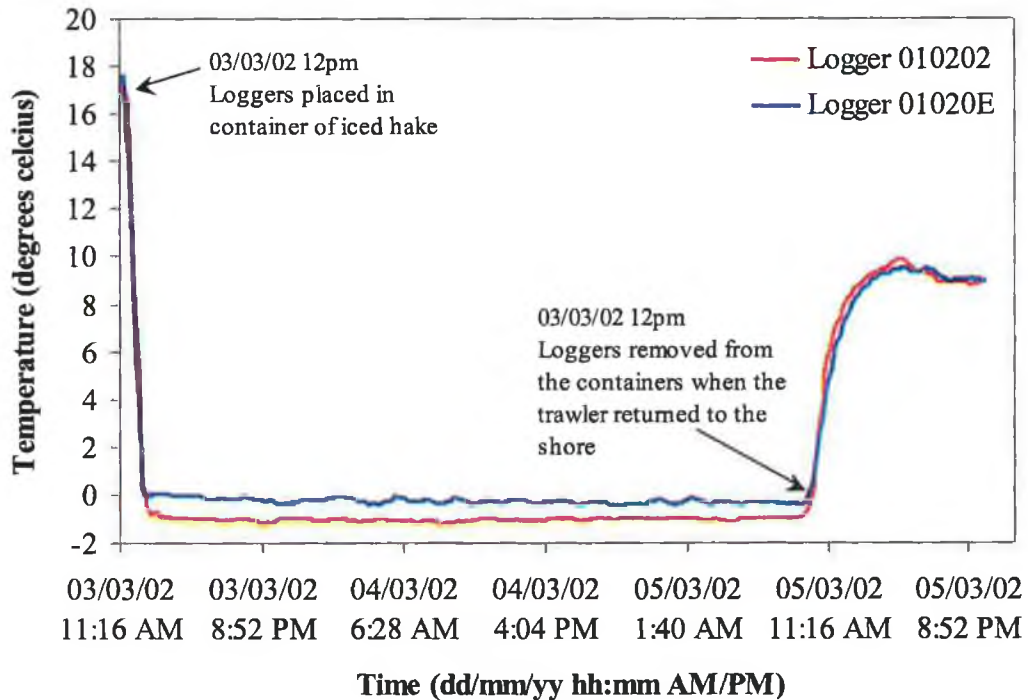
Temp °C	Average	STDEV
0	7.15625	0.008772
1	7.148837	0.008622
2	7.14153	0.008462
3	7.13433	0.008293
4	7.127237	0.008116
5	7.12025	0.00793
6	7.11337	0.007737
7	7.106597	0.007535
8	7.09993	0.007326
9	7.09337	0.00711
10	7.086917	0.006887
11	7.08057	0.006659
12	7.07433	0.006426
13	7.068197	0.006189
14	7.06217	0.00595
15	7.05625	0.005709
16	7.050437	0.005469
17	7.04473	0.005231
18	7.03913	0.004999
19	7.033637	0.004776
20	7.02825	0.004566
21	7.02297	0.004374
22	7.017797	0.004205
23	7.01273	0.004066
24	7.00777	0.003962
25	7.002917	0.003902
26	6.99817	0.00389
27	6.99353	0.003931
28	6.988997	0.004027
29	6.98457	0.004178
30	6.98025	0.004382
31	6.976037	0.004636
32	6.97193	0.004936
33	6.96793	0.005277
34	6.964037	0.005655
35	6.96025	0.006065
36	6.95657	0.006506
37	6.952997	0.006973
38	6.94953	0.007465
39	6.94617	0.007979
40	6.942917	0.008514
41	6.93977	0.009068
42	6.93673	0.00964
43	6.933797	0.01023
44	6.93097	0.010836
45	6.92825	0.011458
46	6.925637	0.012095
47	6.92313	0.012747
48	6.92073	0.013414
49	6.918437	0.014094
50	6.91625	0.014789

**Appendix 1-9** The average and standard deviations for all three calibrations performed using logger 2. The largest standard deviation occurs at 50°C. The measuring range for this application is between 3°C and 42°C. The largest standard deviation within this range is 0.0096.

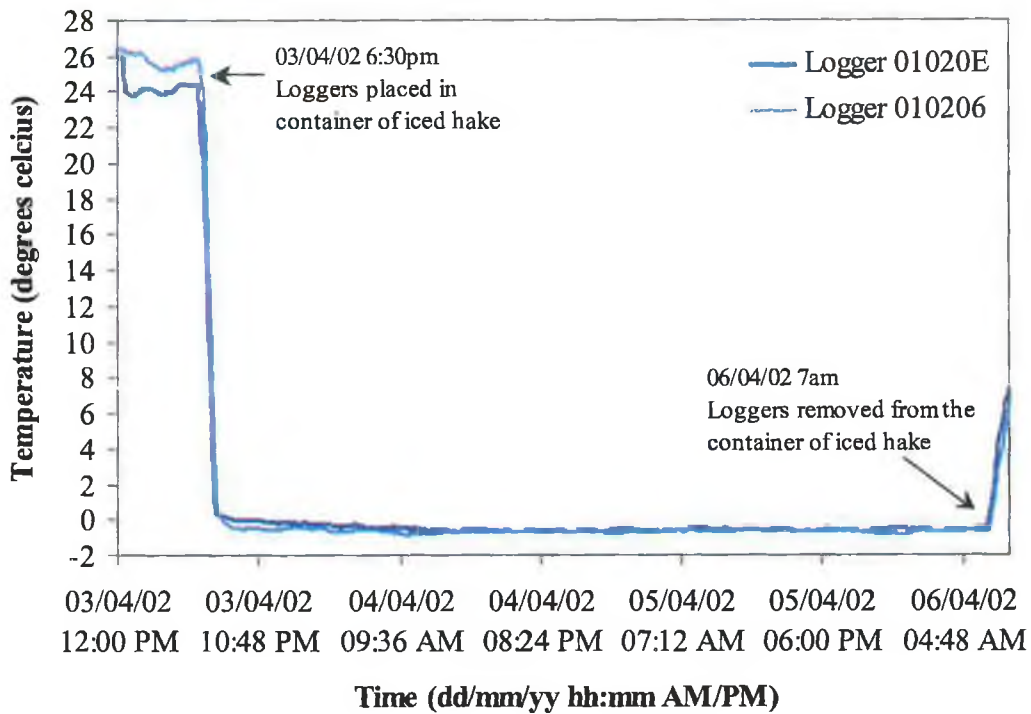
## Appendix 2



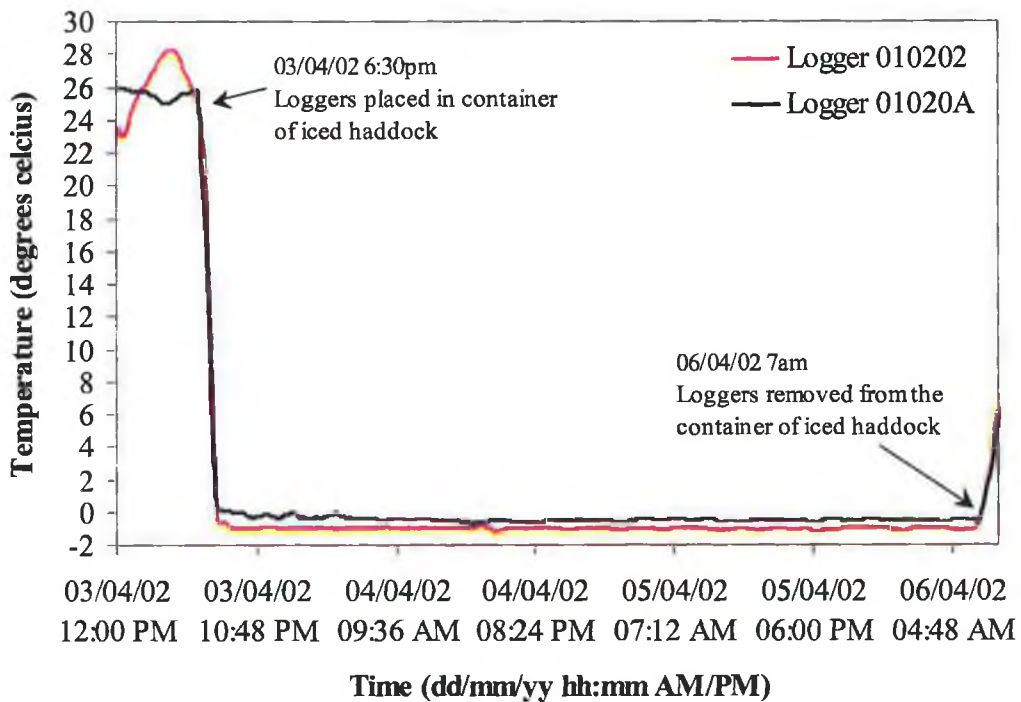
**Appendix 2-1** Temperature profiles of a 40kg container of iced haddock. The temperature remained below 0°C for the 2 days while the fish were stored in the hold of the trawler. The graph indicates that there is little temperature variation within a container.



**Appendix 2-2** Temperature profiles of a 25kg container of iced hake. The temperature remained below 0°C for the 2 days while the trawler was at sea.



**Appendix 2-3 Temperature profiles of a 40kg container of iced hake. The loggers were placed in the containers at 6:30pm on the 3<sup>rd</sup> April and were removed at 7:00am on the 6<sup>th</sup> April. The temperature remained constant over the 3-day period.**



**Appendix 2-4 Temperature profiles of a 40kg container of iced haddock. The loggers were placed in the containers at 6:30pm on the 3<sup>rd</sup> April and were removed at 7:00am on the 6<sup>th</sup> April. The temperature remained constant over the 3-day period.**

### Appendix 3

Calibration	1% ammonia in	Nitrogen	Ammonia	Colourmeter	Sensor
Sensor 1	nitrogen (ml.min <sup>-1</sup> )	(ml.min <sup>-1</sup> )	Conc. (ppm)	Values (AU)	Response (AU)
1	0	100	0	157.08	0
	10	100	9.09	124.27	32.81
	20	100	16.67	104.46	52.62
	30	100	23.08	96.45	60.63
	40	100	28.57	93.95	63.13
	50	100	33.33	92.27	64.81
2	0	100	0	159.14	0
	10	100	9.09	123.05	36.08
	20	100	16.67	105.26	53.88
	30	100	23.08	97.41	61.73
	40	100	28.57	94.35	64.78
	50	100	33.33	93.75	65.38
3	0	100	0	158.63	0
	10	100	9.09	119.50	39.13
	20	100	16.67	104.29	54.33
	30	100	23.08	98.85	59.77
	40	100	28.57	95.28	63.34
	50	100	33.33	93.59	65.03

#### Appendix 3-1 Results for the ammonia calibration (n=3) performed using Sensor 1 (0 to 33ppm)

Ammonia Concentration (ppm)	Average Colourmeter Values (AU)	SD	CV%	n
0	158.28	1.07	0.68	3
9.09	122.27	2.48	2.03	3
16.67	104.67	0.52	0.50	3
23.08	97.57	1.21	1.24	3
28.57	94.53	0.68	0.72	3
33.33	93.21	0.81	0.87	3

#### Appendix 3-2 Average Colourmeter values (n=3) for each ammonia concentration (Sensor 1)

Ammonia Concentration (ppm)	Average Sensor Response (AU)	SD	CV%	n
0	0	0	0	3
9.09	36.01	3.16	8.77	3
16.67	53.61	0.89	1.65	3
23.08	60.71	0.98	1.62	3
28.57	63.75	0.9	1.41	3
33.33	65.07	0.29	0.45	3

#### Appendix 3-3 Average sensor response (n=3) for each ammonia concentration (Sensor 1)

Sensor	Concentration (ppm)	Average Sensor Response (AU)	SD	CV%	n
1	1.10	5.88	0.29	4.96	3
	2.17	13.64	0.34	2.52	3
	3.23	22.23	0.24	1.09	3
	4.26	26.89	0.44	1.63	3
2	1.10	6.08	0.28	4.61	2
	2.17	15.03	0.71	4.72	2
	3.23	19.82	0.99	4.99	2
	4.26	28.53	0.37	1.30	2
3	1.10	6.93	0.12	1.73	2
	2.17	17.07	0.64	3.75	2
	3.23	24.20	0.98	4.05	2
	4.26	30.75	1.88	6.11	2

**Appendix 3-4 Average results (n=3 for Sensor 1; n=2 for Sensors 2 & 3) for the calibration experiments using ammonia gas (0 to 4ppm)**

Concentration (ppm)	Average Sensor Response (AU)	SD	CV%	n
1.10	6.30	0.56	8.88	3
2.17	15.25	1.72	11.30	3
3.23	22.08	2.20	9.94	3
4.26	28.72	1.94	6.74	3

**Appendix 3-5 Average sensor response (n=3) to ammonia gas (0 to 4ppm)**

Calibration Sensor 1	1% ammonia in nitrogen (ml.min <sup>-1</sup> )	Nitrogen (ml.min <sup>-1</sup> )	Ammonia Concentration (ppm)	Colourmeter Values (AU)	Sensor Response (AU)
1	0	900	0	157.20	0
	10	900	1.10	151.52	5.68
	20	900	2.17	143.20	14.00
	30	900	3.23	135.25	21.95
	40	900	4.26	130.52	26.68
2	0	900	0	157.22	0
	10	900	1.10	151.47	5.74
	20	900	2.17	143.89	13.32
	30	900	3.23	134.84	22.38
	40	900	4.26	129.82	27.40
3	0	900	0	157.20	0
	10	900	1.10	150.99	6.21
	20	900	2.17	143.60	13.60
	30	900	3.23	134.84	22.35
	40	900	4.26	130.60	26.60

**Appendix 3-6 Results of the calibration experiments (n=3) performed using Sensor 1 (0 to 4ppm)**

Ammonia Concentration (ppm)	Average Colourmeter Values (AU)	SD	CV%	n
0	157.20	0.01	0.11	3
1.10	151.33	0.30	0.03	3
2.17	143.56	0.35	0.62	3
3.23	134.98	0.24	0.93	3
4.26	130.31	0.43	1.75	3

**Appendix 3-7 Average Colourmeter values (n=3) for each ammonia concentration (Sensor 1)**

Ammonia Concentration (ppm)	Average Sensor Response (AU)	SD	CV%	n
0	0	0	0	3
1.10	5.88	0.29	4.96	3
2.17	13.64	0.34	2.52	3
3.23	22.23	0.24	1.09	3
4.26	26.89	0.44	1.63	3

**Appendix 3-8 Average sensor response (n=3) for each ammonia concentration (Sensor 1)**

Calibration Sensor 2	1% ammonia in nitrogen (ml.min <sup>-1</sup> )	Nitrogen (ml.min <sup>-1</sup> )	Ammonia Concentration (ppm)	Colourmeter Values (AU)	Sensor Response (AU)
1	0	900	0	150.46	0
	10	900	1.10	144.58	5.88
	20	900	2.17	135.93	14.54
	30	900	3.23	129.95	20.51
	40	900	4.26	122.20	28.27
2	0	900	0	149.67	0
	10	900	1.10	143.39	6.28
	20	900	2.17	134.13	15.53
	30	900	3.23	130.55	19.12
	40	900	4.26	120.88	28.79

**Appendix 3-9 Results of the calibration experiments (n=2) performed using Sensor 2 (0 to 4ppm)**

Ammonia Concentration (ppm)	Average Colourmeter Values (AU)	SD	CV%	n
0	150.06	0.56	0.38	2
1.10	143.99	0.85	0.59	2
2.17	135.03	1.27	0.94	2
3.23	130.25	0.42	0.32	2
4.26	121.54	0.93	0.77	2

**Appendix 3-10 Average Colourmeter values (n=2) for each ammonia concentration (Sensor 2)**

Ammonia Concentration (ppm)	Average Sensor Response (AU)	SD	CV%	n
0	0	0	0	2
1.10	6.08	0.28	4.61	2
2.17	15.03	0.71	4.72	2
3.23	19.82	0.99	4.99	2
4.26	28.53	0.37	1.30	2

**Appendix 3-11 Average sensor response (n=2) for each ammonia concentration (Sensor 2)**



Calibration Sensor 3	1% ammonia in nitrogen (ml.min <sup>-1</sup> )	Nitrogen (ml.min <sup>-1</sup> )	Ammonia Concentration (ppm)	Colourmeter Values (AU)	Sensor Response (AU)
1	0	900	0	147.42	0
	10	900	1.10	140.58	6.84
	20	900	2.17	129.90	17.52
	30	900	3.23	122.52	24.90
	40	900	4.26	115.34	32.08
2	0	900	0	147.66	0
	10	900	1.10	140.64	7.02
	20	900	2.17	131.05	16.61
	30	900	3.23	124.15	23.51
	40	900	4.26	118.24	29.42

**Appendix 3-12 Results of the calibration experiments (n=2) performed using Sensor 3 (0 to 4ppm)**

Ammonia Concentration (ppm)	Average Colourmeter Values (AU)	SD	CV%	n
0	147.54	0.17	0.11	2
1.10	140.61	0.04	0.03	2
2.17	130.47	0.81	0.62	2
3.23	123.34	1.15	0.93	2
4.26	116.79	2.05	1.75	2

**Appendix 3-13 Average Colourmeter values (n=2) for each ammonia concentration (Sensor 3)**

Ammonia Concentration (ppm)	Average Sensor Response (AU)	SD	CV%	n
0	0	0	0	2
1.10	6.93	0.12	1.73	2
2.17	17.07	0.64	3.75	2
3.23	24.20	0.98	4.05	2
4.26	30.75	1.88	6.11	2

**Appendix 3-14 Average sensor response (n=2) for each ammonia concentration (Sensor 3)**

## Appendix 4

TVC (CFU/g)								
Time (h)	Unpasteurised Bench		Unpasteurised Fridge		Pasteurised Bench		Pasteurised Fridge	
	Sample 1	Sample 2	Sample 1	Sample 2	Sample 1	Sample 2	Sample 1	Sample 2
18	24 x 10 <sup>1</sup>	14 x 10 <sup>1</sup>	3 x 10 <sup>1</sup>	10 x 10 <sup>1</sup>	-	-	-	-
20	99 x 10 <sup>1</sup>	96 x 10 <sup>1</sup>	-	-	0 x 10 <sup>1</sup>	1 x 10 <sup>1</sup>	0 x 10 <sup>1</sup>	1 x 10 <sup>1</sup>
25	129 x 10 <sup>1</sup>	131 x 10 <sup>1</sup>	38 x 10 <sup>2</sup>	41 x 10 <sup>2</sup>	2 x 10 <sup>1</sup>	0 x 10 <sup>1</sup>	-	-
30	212 x 10 <sup>3</sup>	206 x 10 <sup>3</sup>	-	-	-	-	-	-
40	84 x 10 <sup>5</sup>	92 x 10 <sup>5</sup>	-	-	-	-	-	-
44	402 x 10 <sup>5</sup>	412 x 10 <sup>5</sup>	40 x 10 <sup>2</sup>	46 x 10 <sup>2</sup>	25 x 10 <sup>2</sup>	26 x 10 <sup>2</sup>	-	-
49	608 x 10 <sup>5</sup>	-	76 x 10 <sup>3</sup>	-	168 x 10 <sup>3</sup>	188 x 10 <sup>3</sup>	-	-

**Appendix 4-1 TVC results for cooked whelk-on-shell trial**

## Appendix 5

Sensor Response to Cooked Whelk-On-Shell - Sample Tray 1							
Time	Sensor 1	Sensor 2	Sensor 3	Sensor 4	Ave Response	STDev	%CV
(Hours)	(au)	(au)	(au)	(au)	(au)		
0.0	0.0	0.0	0.0	0.0	0.0	0.0	0.0
1.4	6.6	3.2	3.2	5.5	4.6	1.7	37.1
3.3	14.1	8.8	8.8	12.2	11.0	2.6	23.8
5.1	22.4	17.0	13.7	24.9	19.5	5.1	25.9
7.4	30.0	19.9	17.3	26.7	23.5	5.9	25.1
9.0	23.2	19.1	17.4	24.2	21.0	3.2	15.4
11.8	23.2	21.5	18.7	23.7	21.8	2.3	10.4
18.4	34.0	24.2	25.0	26.0	27.3	4.5	16.6
21.3	28.2	23.1	23.2	23.7	24.6	2.4	9.8
24.4	27.9	19.5	25.2	25.8	24.6	3.6	14.7
28.9	37.6	27.5	27.8	28.4	30.3	4.9	16.0
31.5	32.2	25.3	25.8	22.8	26.5	4.0	15.1
43.0	33.7	22.1	27.9	26.9	27.6	4.7	17.1
59.6	46.6	44.7	49.0	43.8	46.0	2.3	5.0

### Appendix 5-1 Sensor response for tray 1 (cooked whelk-on-shell samples stored at RT)

Sensor Response to Cooked Whelk-On-Shell - Sample Tray 2							
Time	Sensor 1				Ave Response	STDev	%CV
(Hours)	(au)	Sensor 2 (au)	Sensor 3 (au)	Sensor 4 (au)	(au)		
0.0	0.0	0.0	0.0	0.0	0.0	0.0	0.0
1.4	3.5	5.7	6.9	4.7	5.2	1.5	28.4
3.3	11.4	12.3	11.1	9.3	11.0	1.2	11.2
5.1	28.2	22.5	18.0	8.8	19.4	8.2	42.2
7.4	30.6	28.0	21.2	16.4	24.1	6.4	26.7
9.0	30.9	27.0	23.1	18.1	24.8	5.5	22.1
11.8	33.8	31.8	28.5	25.3	29.9	3.7	12.5
18.4	40.0	39.4	35.9	32.8	37.0	3.3	9.0
21.3	37.3	37.0	28.8	34.2	34.3	4.0	11.5
24.4	34.9	33.2	29.2	28.3	31.4	3.1	10.0
28.9	48.5	47.4	38.2	40.0	43.5	5.2	11.8
31.5	32.8	39.4	36.0	30.4	34.6	3.9	11.2
43.0	37.1	32.3	31.1	27.2	31.9	4.1	12.8
59.6	40.4	46.2	37.8	43.2	41.9	3.6	8.6

### Appendix 5-2 Sensor response for tray 2 (cooked whelk-on-shell samples stored at RT)



**Sensor Response to Cooked Whelk-On-Shell - Sample Tray 3**

Time (Hours)	Sensor 1				Ave Response		
	(au)	Sensor 2 (au)	Sensor 3 (au)	Sensor 4 (au)	(au)	STDev	%CV
0.0	0.0	0.0	0.0	0.0	0.0	0.0	0.0
1.4	5.0	3.0	1.7	5.0	3.7	1.6	43.7
3.3	13.3	9.0	3.8	10.2	9.1	4.0	43.6
5.1	17.0	12.1	10.3	14.9	13.6	3.0	21.9
7.4	32.4	21.8	18.6	26.0	24.7	6.0	24.2
9.0	28.9	18.4	19.9	22.9	22.5	4.6	20.5
11.8	37.3	26.4	30.0	33.5	31.8	4.7	14.8
18.4	39.3	34.2	38.3	44.2	39.0	4.1	10.6
21.3	36.2	37.8	35.6	36.9	36.6	1.0	2.7
24.4	30.7	35.1	30.3	33.4	32.4	2.3	7.1
28.9	43.7	36.3	36.7	38.8	38.9	3.4	8.7
31.5	28.5	27.6	30.8	34.5	30.3	3.1	10.2
43.0	33.6	36.0	27.5	30.6	31.9	3.7	11.6
59.6	37.9	33.9	30.7	29.3	33.0	3.8	11.6

**Appendix 5-3 Sensor response for tray 3 (cooked whelk-on-shell samples stored at RT)**

**Sensor Response to Cooked Whelk-On-Shell – Average of 3 Sample Trays**

Time (Hours)	Tray 1	Tray 2	Tray3	Ave Response			n
	(au)	(au)	(au)	(au)	STDev	%CV	
0.0	0.0	0.0	0.0	0.0	0.0	0.0	3
1.4	4.6	5.2	3.7	4.5	0.7	16.6	3
3.3	11.0	11.0	9.1	10.4	1.1	10.7	3
5.1	19.5	19.4	13.6	17.5	3.4	19.4	3
7.4	23.5	24.1	24.7	24.1	0.6	2.5	3
9.0	21.0	24.8	22.5	22.8	1.9	8.3	3
11.8	21.8	29.9	31.8	27.8	5.3	19.1	3
18.4	27.3	37.0	39.0	34.4	6.3	18.2	3
21.3	24.6	34.3	36.6	31.8	6.4	20.1	3
24.4	24.6	31.4	32.4	29.5	4.2	14.4	3
28.9	30.3	43.5	38.9	37.6	6.7	17.8	3
31.5	26.5	34.6	30.3	30.5	4.1	13.4	3
43.0	27.6	31.9	31.9	30.5	2.5	8.1	3
59.6	46.0	41.9	33.0	40.3	6.7	16.6	3

**Appendix 5-4 Average sensor response for the 3 trays (cooked whelk-on-shell stored at RT)**

**Sensor Response to Cooked Whelk-On-Shell - Sample Tray 1**

<b>Time (Hours)</b>	<b>Sensor 1 (au)</b>	<b>Sensor 2 (au)</b>	<b>Sensor 3 (au)</b>	<b>Sensor 4 (au)</b>	<b>Ave Response (au)</b>	<b>STDev</b>	<b>%CV</b>
0.0	0.0	0.0	0.0	0.0	0.0	0.0	0.0
1.8	11.5	12.2	17.3	7.7	12.2	3.9	32.3
3.6	9.9	7.9	19.1	22.1	14.8	6.9	46.7
5.4	13.7	12.1	19.2	19.5	16.1	3.8	23.4
7.6	15.7	13.6	21.0	26.2	19.1	5.7	29.6
9.3	18.2	15.5	27.1	30.8	22.9	7.2	31.6
12.1	18.8	20.1	23.8	33.6	24.1	6.7	27.8
18.7	19.5	16.6	23.2	34.1	23.3	7.7	32.9
21.7	20.1	25.9	22.6	36.8	26.4	7.4	28.0
24.7	23.7	22.4	27.9	38.7	28.1	7.4	26.3
29.2	20.5	25.6	23.5	37.0	26.7	7.2	27.0
42.8	24.6	20.5	22.3	35.6	25.7	6.8	26.3
49.8	21.5	22.3	26.4	37.8	27.0	7.5	27.8
54.2	21.1	31.6	27.4	33.5	28.4	5.5	19.2
70.9	19.5	27.9	25.7	37.7	27.7	7.5	27.2

**Appendix 5-5 Sensor response for Tray 1 (cooked whelk-on-shell samples stored in the fridge)**

**Sensor Response to Cooked Whelk-On-Shell - Sample Tray 2**

<b>Time (Hours)</b>	<b>Sensor 1 (au)</b>	<b>Sensor 2 (au)</b>	<b>Sensor 3 (au)</b>	<b>Sensor 4 (au)</b>	<b>Ave Response (au)</b>	<b>STDev</b>	<b>%CV</b>
0.0	0.0	0.0	0.0	0.0	0.0	0.0	0.0
1.8	7.2	-0.6	11.9	11.2	7.4	5.7	76.9
3.6	12.7	11.3	17.9	20.8	15.7	4.4	28.3
5.4	14.0	11.0	16.3	20.9	15.5	4.2	26.9
7.6	22.2	14.1	21.0	27.0	21.1	5.3	25.3
9.3	21.5	17.7	23.8	28.3	22.8	4.5	19.6
12.1	23.4	20.3	25.1	28.1	24.2	3.3	13.5
18.7	13.9	7.1	27.7	24.4	18.3	9.5	52.0
21.7	13.5	12.0	24.2	25.5	18.8	7.0	37.4
24.7	12.5	17.6	31.0	26.6	21.9	8.4	38.2
29.2	17.6	15.2	22.5	25.4	20.2	4.6	22.9
42.8	15.3	13.7	24.9	17.6	17.9	5.0	27.9
49.8	24.4	18.1	25.6	27.2	23.8	4.0	16.7
54.2	30.0	18.2	27.1	28.8	26.0	5.4	20.7
70.9	28.5	26.6	25.0	29.5	27.4	2.0	7.3

**Appendix 5-6 Sensor response for Tray 2 (cooked whelk-on-shell samples stored in the fridge)**

**Sensor Response to Cooked Whelk-On-Shell - Sample Tray 3**

Time (Hours)	Sensor 1				Ave Response		
	(au)	Sensor 2 (au)	Sensor 3 (au)	Sensor 4 (au)	(au)	STDev	%CV
0.0	0.0	0.0	0.0	0.0	0.0	0.0	0.0
1.8	3.1	15.3	8.0	17.5	10.9	6.6	60.7
3.6	11.2	13.5	18.9	17.4	15.2	3.5	23.2
5.4	11.1	13.7	19.2	21.9	16.5	5.0	30.2
7.6	10.1	14.2	27.3	22.0	18.4	7.7	42.0
9.3	15.7	20.6	29.4	18.6	21.1	5.9	28.2
12.1	12.1	17.1	28.9	20.9	19.8	7.1	35.9
18.7	10.1	14.1	11.1	16.3	12.9	2.8	22.0
21.7	12.3	15.4	32.6	26.9	21.8	9.6	43.9
24.7	15.1	16.8	18.8	26.5	19.3	5.0	26.1
29.2	10.4	12.5	25.8	22.1	17.7	7.4	42.1
42.8	9.8	19.2	27.0	23.6	19.9	7.4	37.4
49.8	10.8	17.9	32.9	37.0	24.7	12.4	50.1
54.2	10.5	15.4	33.1	24.0	20.7	10.0	48.0
70.9	10.5	20.0	31.3	35.5	24.3	11.3	46.6

**Appendix 5-7 Sensor response for Tray 3 (cooked whelk-on-shell samples stored in the fridge)**

**Sensor Response to Cooked Whelk-On-Shell – Average of 3 Sample Trays**

Time (Hours)	Tray 1			Tray3 (au)	Ave Response		
	(au)	Tray 2 (au)	(au)		(au)	STDev	%CV
0.0	0.0	0.0	0.0	0.0	0.0	0.0	3
1.8	12.2	7.4	10.9	10.2	2.5	24.3	3
3.6	14.8	15.7	15.2	15.2	0.5	3.0	3
5.4	16.1	15.5	16.5	16.0	0.5	2.9	3
7.6	19.1	21.1	18.4	19.5	1.4	7.1	3
9.3	22.9	22.8	21.1	22.3	1.0	4.6	3
12.1	24.1	24.2	19.8	22.7	2.5	11.2	3
18.7	23.3	18.3	12.9	18.2	5.2	28.7	3
21.7	26.4	18.8	21.8	22.3	3.8	17.1	3
24.7	28.1	21.9	19.3	23.1	4.5	19.6	3
29.2	26.7	20.2	17.7	21.5	4.6	21.5	3
42.8	25.7	17.9	19.9	21.2	4.1	19.3	3
49.8	27.0	23.8	24.7	25.2	1.7	6.6	3
54.2	28.4	26.0	20.7	25.1	3.9	15.7	3
70.9	27.7	27.4	24.3	26.5	1.9	7.1	3

**Appendix 5-8 Average sensor response for 3 Trays (cooked whelk-on-shell stored in the fridge)**

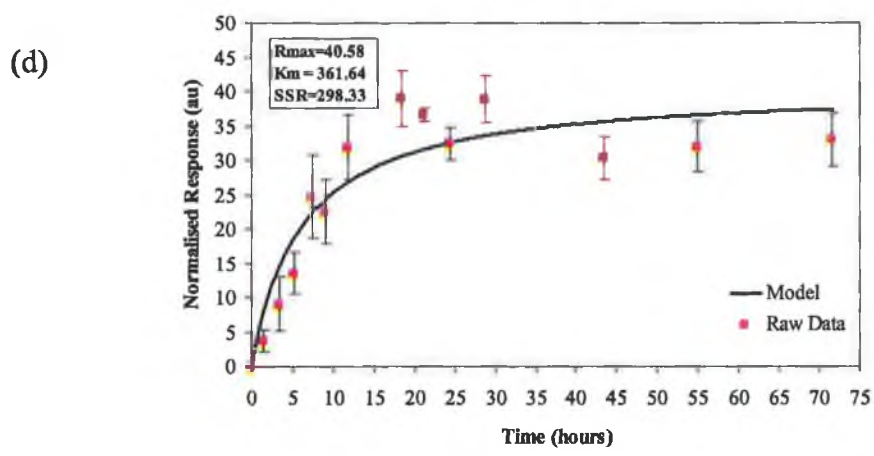
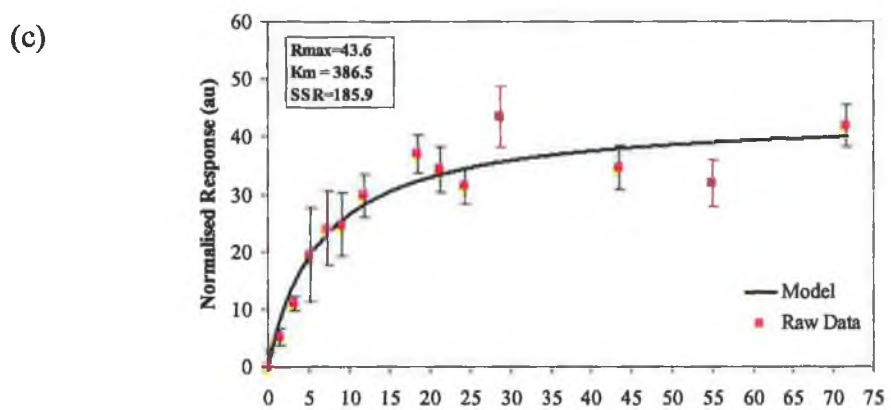
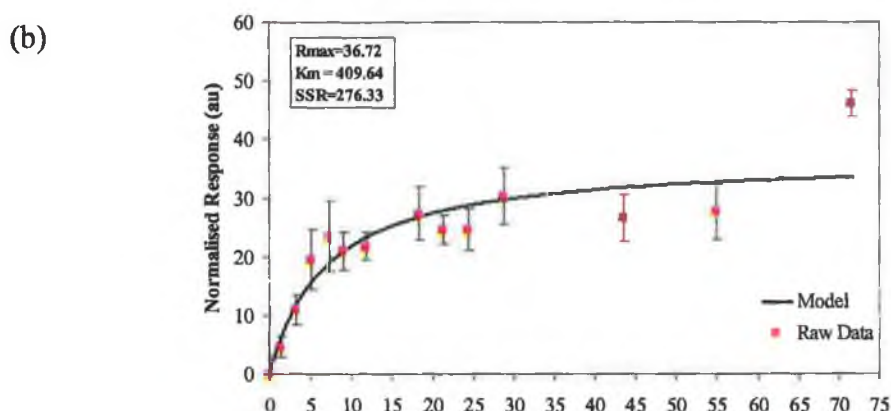
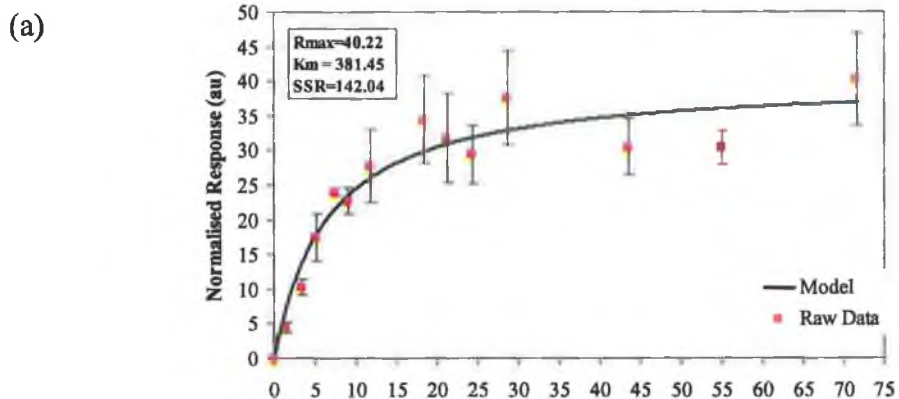
<b>TVC (CFU/g)</b>				
<b>Time</b>	<b>Room Temperature Samples</b>		<b>Fridge Samples</b>	
	<b>Sample 1</b>	<b>Sample 2</b>	<b>Sample 1</b>	<b>Sample 2</b>
<b>(h)</b>	<b>(CFU/g)</b>	<b>(CFU/g)</b>	<b>(CFU/g)</b>	<b>(CFU/g)</b>
0.0	-	-	-	-
2.8	81 x 10 <sup>2</sup>	59 x 10 <sup>2</sup>	-	-
3.9	-	-	75 x 10 <sup>2</sup>	68 x 10 <sup>2</sup>
5.8	70 x 10 <sup>2</sup>	90 x 10 <sup>2</sup>	-	-
7.8	65 x 10 <sup>3</sup>	75 x 10 <sup>3</sup>	-	-
8.9	-	-	91 x 10 <sup>2</sup>	119 x 10 <sup>2</sup>
10.8	16 x 10 <sup>4</sup>	17 x 10 <sup>4</sup>	-	-
11.9	-	-	87 x 10 <sup>2</sup>	105 x 10 <sup>2</sup>
19.0	70 x 10 <sup>5</sup>	63 x 10 <sup>5</sup>	-	-
20.1	-	-	22 x 10 <sup>3</sup>	25 x 10 <sup>3</sup>
23.5	34 x 10 <sup>6</sup>	29 x 10 <sup>6</sup>	-	-
45.1	-	-	80 x 10 <sup>4</sup>	90 x 10 <sup>4</sup>

**Appendix 5-9 Total Viable Counts for samples stored at room temperature and in the fridge**

<b>TVB-N (mg Nitrogen/100g)</b>		
<b>Time</b>	<b>Room</b>	
	<b>(h)</b>	<b>Temperature</b>
	<b>Samples</b>	<b>Fridge Samples</b>
0.0	-	-
1.3	14.0	-
1.4	-	14
5.5	16.8	-
7.5	18.2	-
8.6	-	16.8
10.5	16.8	-
11.6	-	17.5
18.8	19.6	-
19.9	-	16.8
23.5	35.0	-
32.6	-	27.0
37.1	-	25.5
57.6	-	34.3

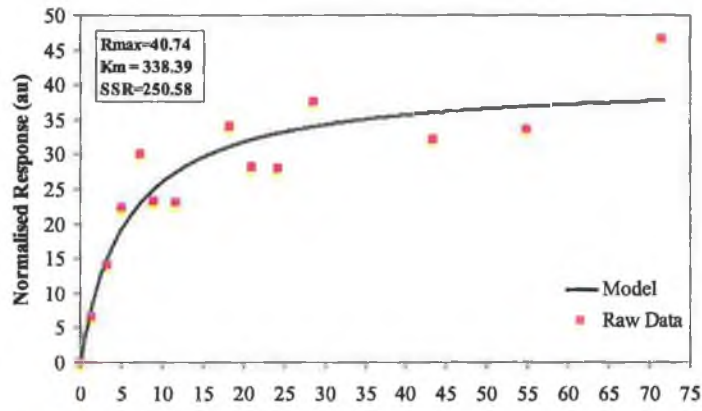
**Appendix 5-10 TVB-N results for samples stored at room temperature and in the fridge**



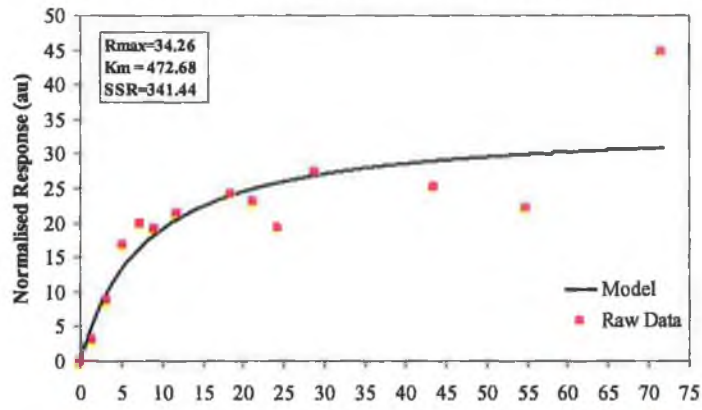


**Appendix 5-11 Average sensor response of (a) all 3 trays n=12 (b) tray 1 n=4 (c) tray 2 n=4 (d) tray 3 n=4 for samples stored at room temperature**

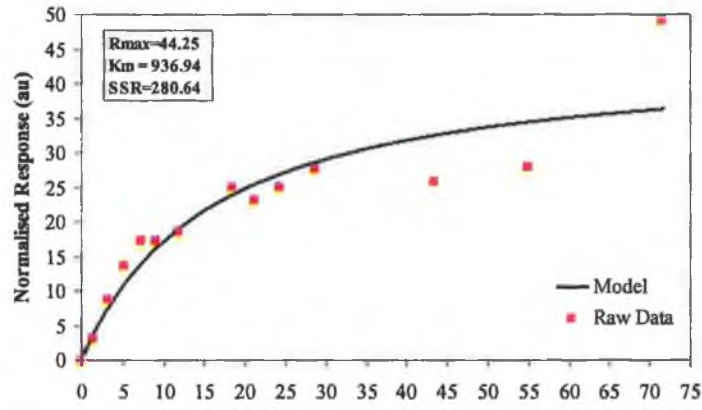
(a)



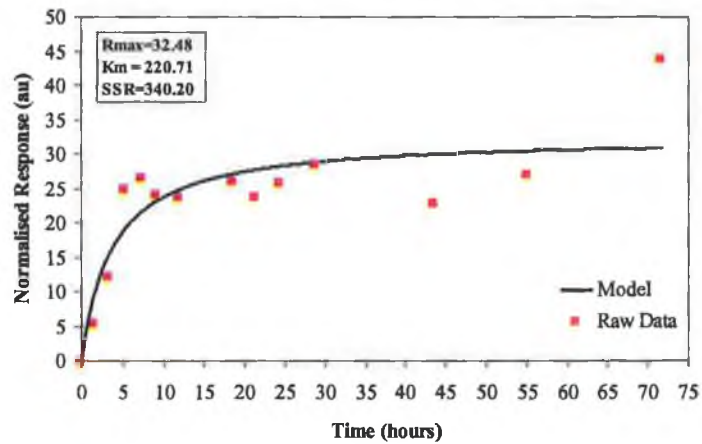
(b)



(c)

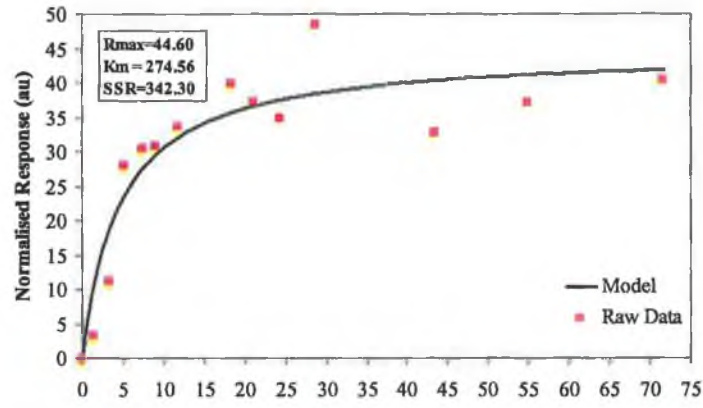


(d)

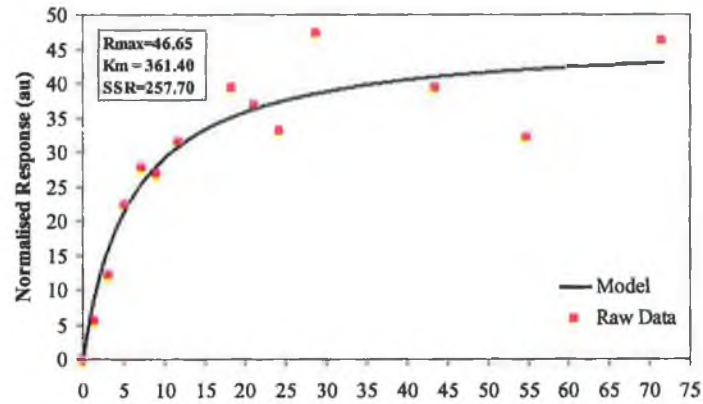


Appendix 5-12 Sensor response for tray 1 (a) sensor 1 (b) sensor 2 (c) sensor 3 (d) sensor 4 for samples stored at room temperature

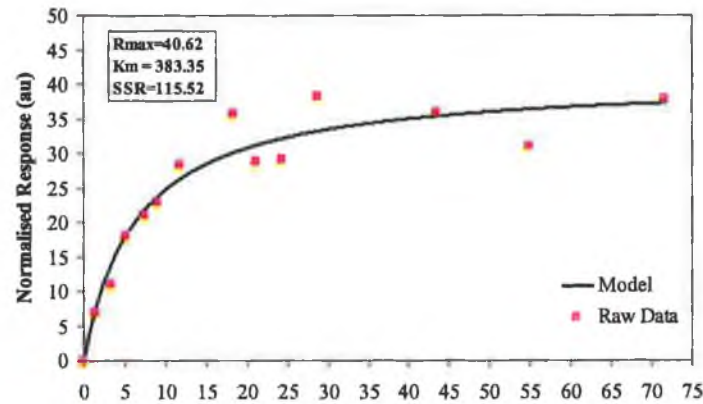
(a)



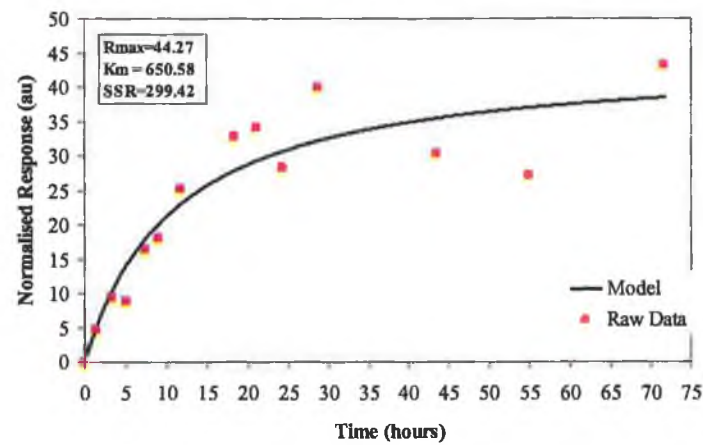
(b)



(c)

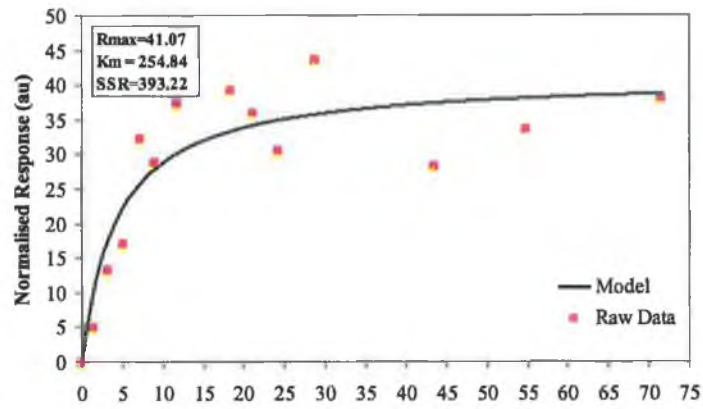


(d)

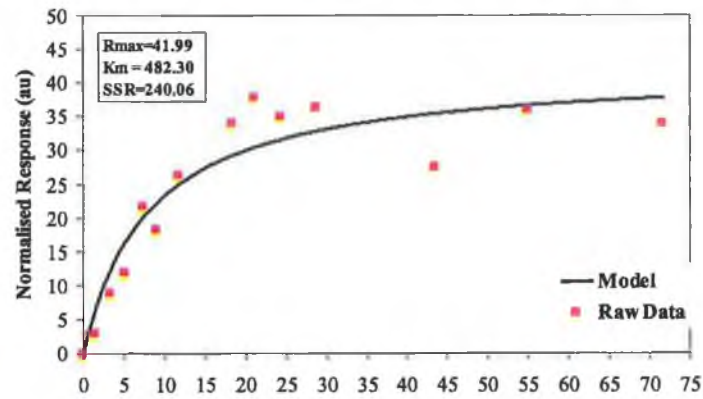


Appendix 5-13 Sensor response for tray 2 (a) sensor 1 (b) sensor 2 (c) sensor 3 (d) sensor 4 for samples stored at room temperature

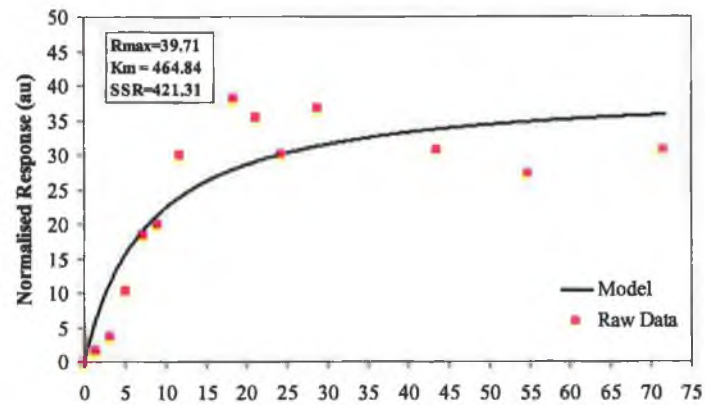
(a)



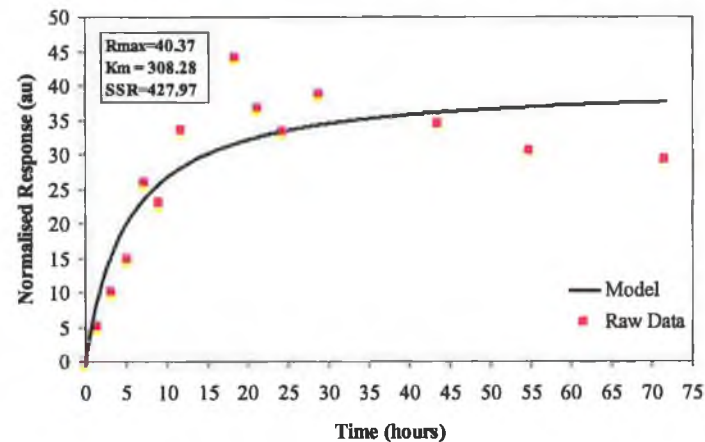
(b)



(c)

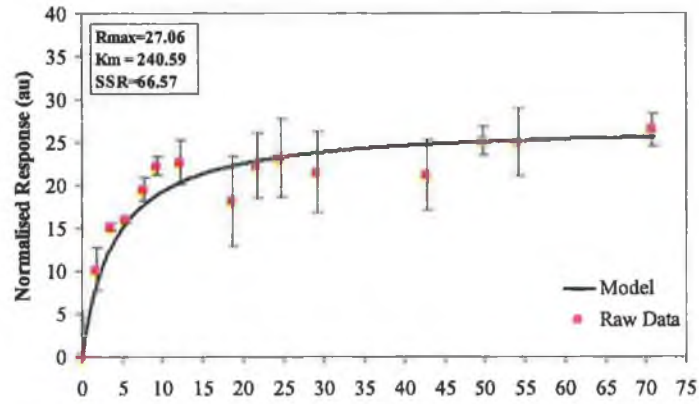


(d)

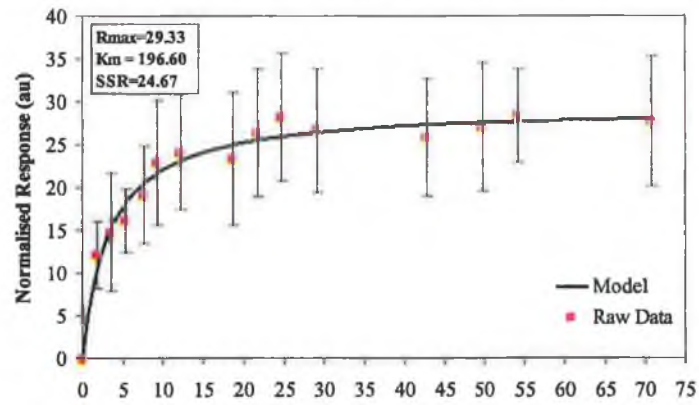


Appendix 5-14 Sensor response for tray 3 (a) sensor 1 (b) sensor 2 (c) sensor 3 (d) sensor 4 for samples stored at room temperature

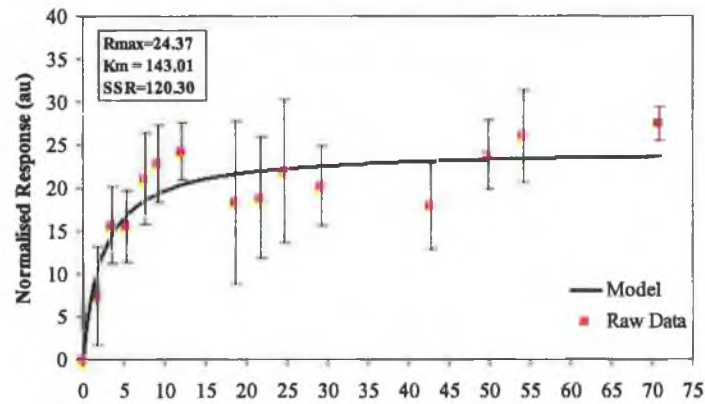
(a)



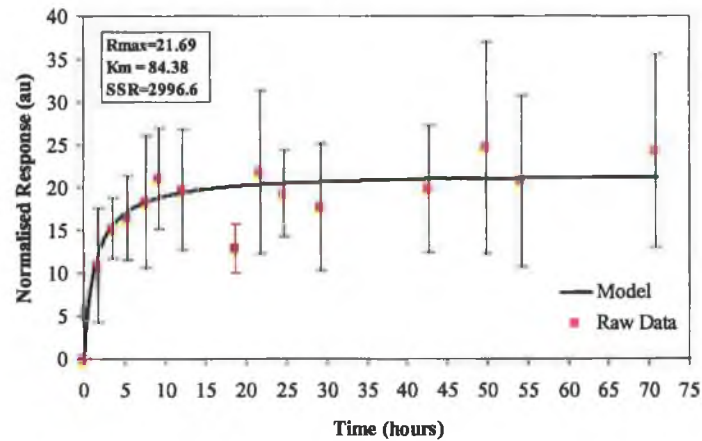
(b)



(c)

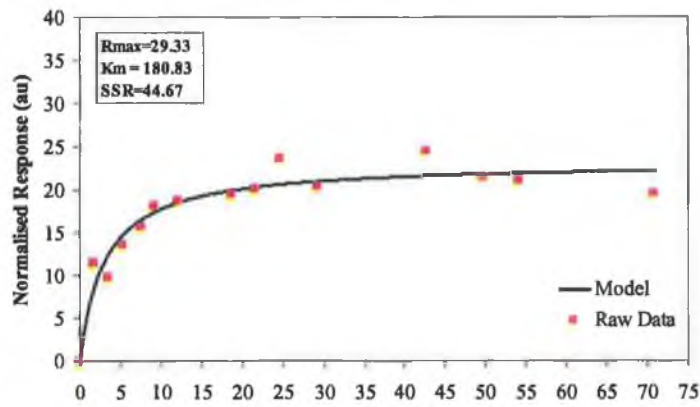


(d)

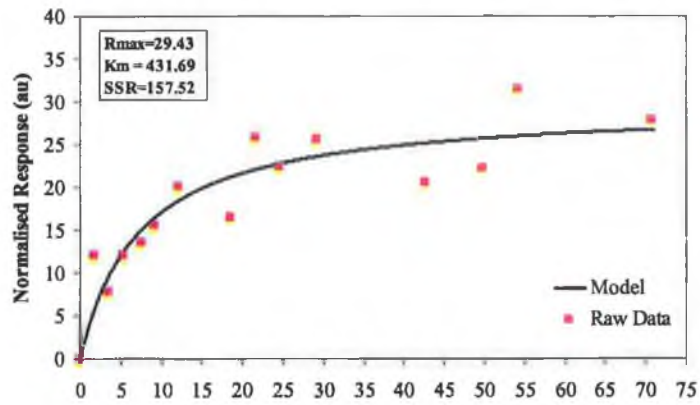


Appendix 5-15 Average sensor response for (a) all 3 trays n=12 (b) tray 1 n=4 (c) tray 2 n=4 (d) tray 3 n=4, for samples stored in the fridge

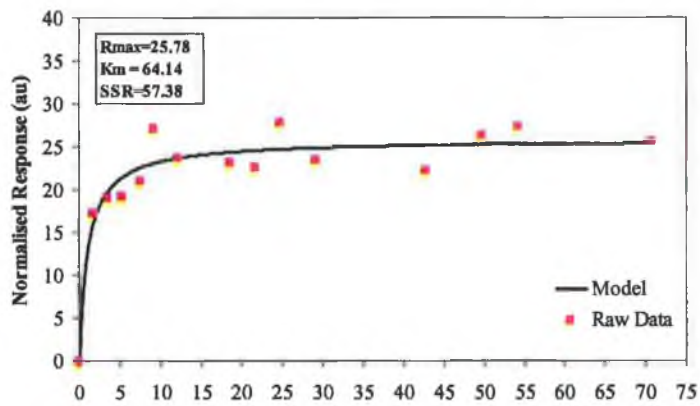
(a)



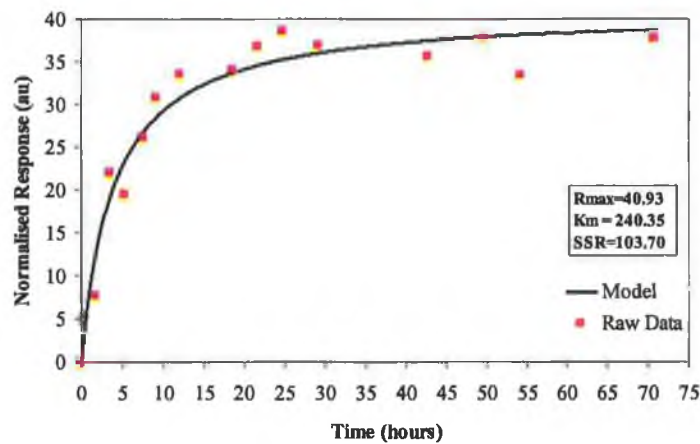
(b)



(c)

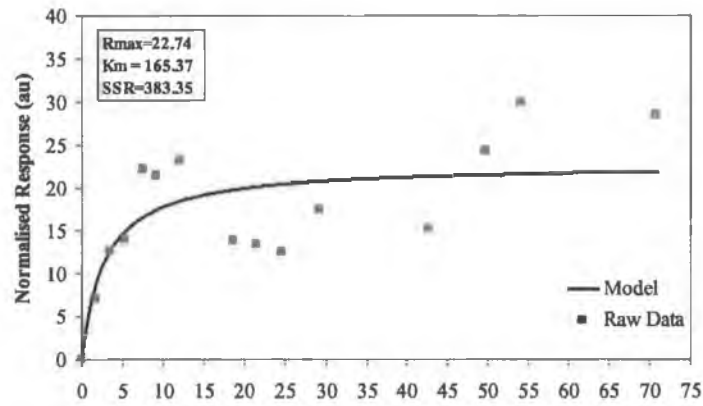


(d)

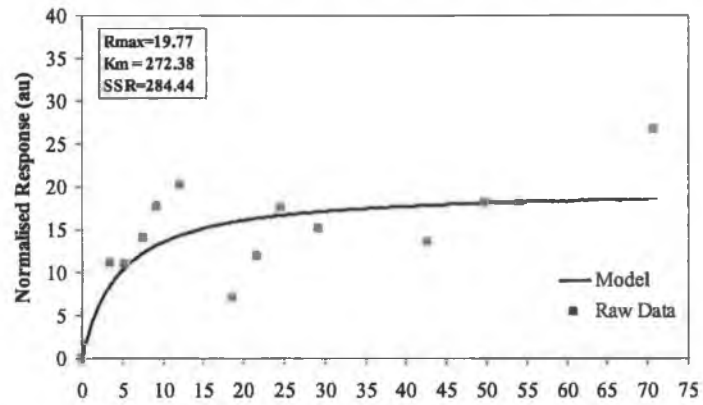


Appendix 5-16 Average sensor response for tray 1 (a) sensor 1 (b) sensor 2 (c) sensor 3 (d) sensor 4, for samples stored in the fridge

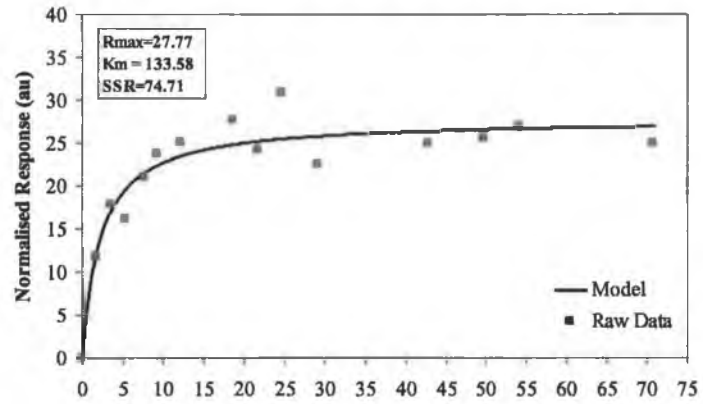
(a)



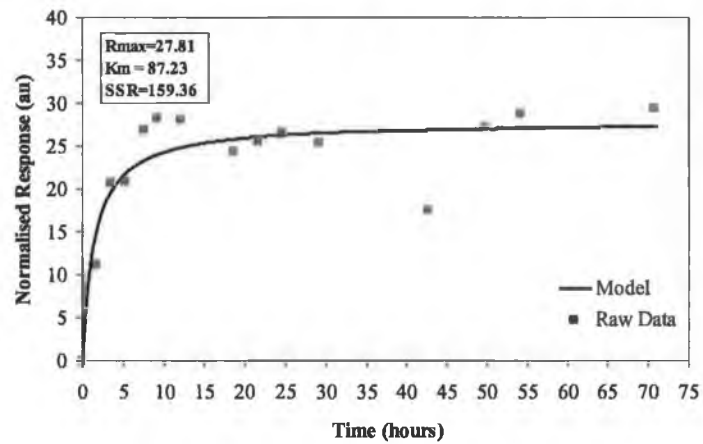
(b)



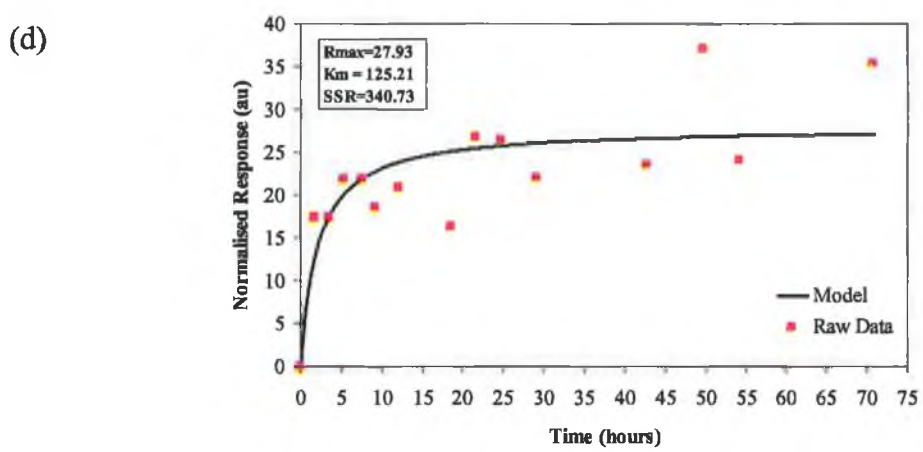
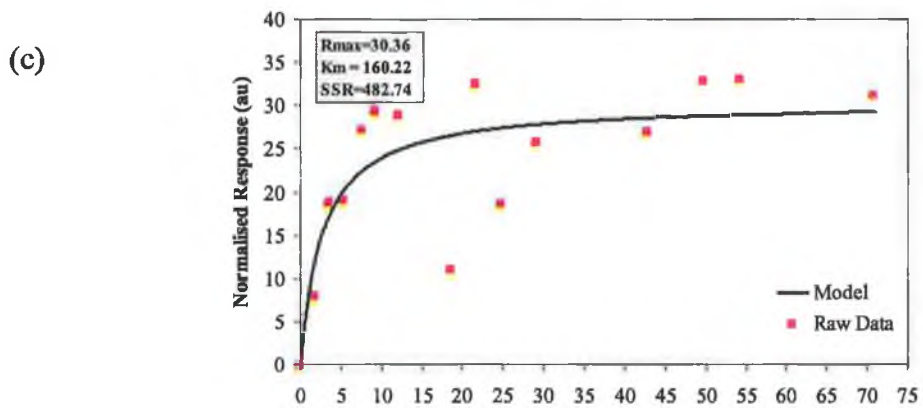
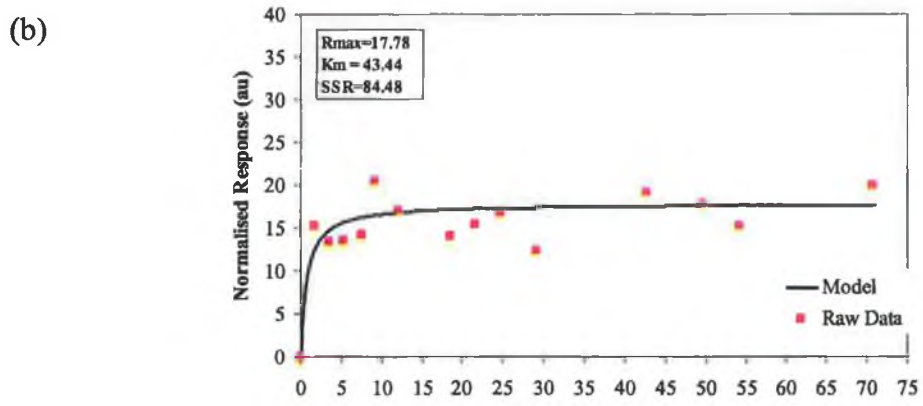
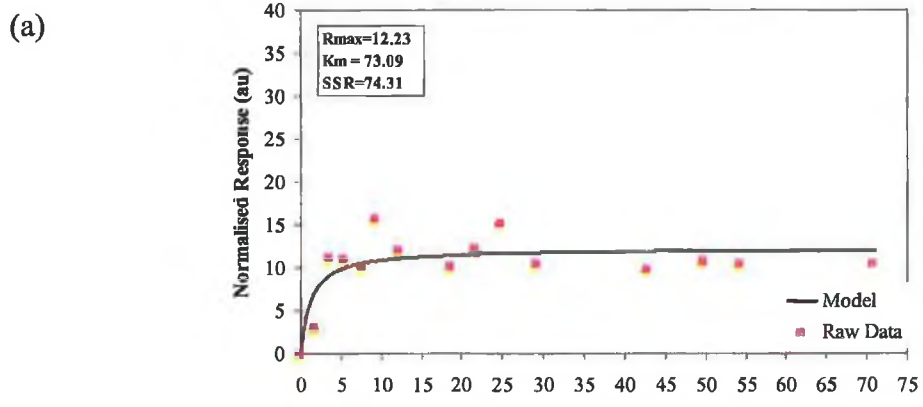
(c)



(d)



Appendix 5-17 Sensor response for tray 2 (a) sensor 1 (b) sensor 2 (c) sensor 3 (d) sensor 4, for samples stored in the fridge



Appendix 5-18 Sensor response for tray 3 (a) sensor 1 (b) sensor 2 (c) sensor 3 (d) sensor 4, for samples stored in the fridge



